GDANSK UNIVERSITY OF TECHNOLOGY
FACULTY OF OCEAN ENGINEERING AND SHIP TECHNOLOGY
SECTION OF TRANSPORT TECHNICAL MEANS
OF TRANSPORT COMMITEE OF POLISH ACADEMY OF SCIENCES
UTILITY FOUNDATIONS SECTION
OF MECHANICAL ENGINEERING COMMITTEE OF POLISH ACADEMY OF SCIENCE

ISSN 1231 – 3998
ISBN 83 – 900666 – 2 – 9

Journal of

POLISH CIMAC

DIAGNOSIS, RELIABILITY AND SAFETY

Vol. 2 **No. 2**

Gdansk, 2007

Science publication of Editorial Advisory Board of POLISH CIMAC

Editor in Chief: Jerzy Girtler Editorial Office Secretary: Jacek Rudnicki

Editorial Advisory Board

J. Girtler (President) - *Gdansk University of Technology*
L. Piaseczny (Vice President) - *Naval Academy of Gdynia*
J. Adamczyk - *University of Mining and Metallurgy of Krakow*
J. Błachnio - *Air Force Institute of Technology*
L. Będkowski - *WAT Military University of Technology*
C. Behrendt - *Maritime Academy of Szczecin*
P. Bielawski - *Maritime Academy of Szczecin*
J. Borgoń - *Warsaw University of Technology*
T. Chmielniak - *Silesian Technical University*
Romuald Cwilewicz - *Maritime Academy of Gdynia*
T. Dąbrowski - *WAT Military University of Technology*
Z. Domachowski - *Gdansk University of Technology*
C. Dymarski - *Gdansk University of Technology*
M. Dzida - *Gdansk University of Technology*
J. Gronowicz - *Maritime University of Szczecin*
V. Hlavna - *University of Žilina, Slovak Republic*
M. Idzior – *Poznan University of Technology*
A. Iskra - *Poznan University of Technology*
A. Jankowski – *President of KONES*
J. Jaźwiński - *Air Force Institute of Technology*
R. Jedliński - *Bydgoszcz University of Technology and Agriculture*
J. Kiciński - *President of SEF MEC PAS, member of MEC*
O. Klyus - *Maritime Academy of Szczecin*
Z. Korczewski - *Naval Academy of Gdynia*
K. Kosowski - *Gdansk University of Technology*
L. Ignatiewicz Kowalczuk - *Baltic State Maritime Academy in Kaliningrad*
J. Lewitowicz - *Air Force Institute of Technology*
K. Lejda - *Rzeszow University of Technology*
J. Macek - *Czech Technical University in Prague*
Z. Matuszak - *Maritime Academy of Szczecin*
J. Merkisz – *Poznan Unversity of Technology*
R. Michalski - *Olsztyn Warmia-Mazurian University*
A. Niewczas - *Lublin University of Technology*
Y. Ohta - *Nagoya Institute of Technology*
A. K. Oppenheim – *University of California, Berkeley*
M. Orkisz - *Rzeszow University of Technology*
S. Radkowski - *President of the Board of PTDT*
Y. Sato - *National Traffic Safety and Environment Laboratory, Japan*
M. Sobieszczański - *Bielsko-Biala Technology-Humanistic Academy*
A. Soudarev - *Russian Academy of Engineering Sciences*
M. Ślęzak - *Ministry of Scientific Research and Information Technology*
W. Tarełko - *Maritime Academy of Gdynia*
W. Wasilewicz Szczagin - *Kaliningrad State Technology Institute*
F. Tomaszewski - *Poznan University of Technology*
J. Wajand – *Lodz University of Technology*
W. Wawrzyński - *Warsaw University of Technology*
E. Wiederuh - *Fachhochschule Giessen Friedberg*
K. Wierzcholski - *Maritime Academy of Gdynia, Gdansk University of Technology*
B. Wojciechowicz - *Honorary President of SEF MEC PAS*
M. Wyszyński - *The University of Birmingham, United Kingdom*
M. Zablocki – *V-ce President of KONES*
S. Żmudzki - *Szczecin University of Technology*
J. Żurek - *Air Force Institute of Technology*

Editorial Office:

GDANSK UNIVERSITY OF TECHNOLOGY
Faculty of Ocean Engineering and Ship Technology
Department of Ship Power Plants
G. Narutowicza 11/12 80-952 GDANSK POLAND
tel. +48 58 347 29 73, e – mail: sek4oce@pg.gda.pl

This journal is devoted to designing of diesel engines, gas turbines and ships' power transmission systems containing these engines and also machines and other appliances necessary to keep these engines in movement with special regard to their energetic and pro-ecological properties and also their durability, reliability, diagnostics and safety of their work and operation of diesel engines, gas turbines and also machines and other appliances necessary to keep these engines in movement with special regard to their energetic and pro-ecological properties, their durability, reliability, diagnostics and safety of their work, and, above all, rational (and optimal) control of the processes of their operation and specially rational service works (including control and diagnosing systems), analysing of properties and treatment of liquid fuels and lubricating oils, etc.

All papers have been reviewed
@Copyright by Faculty of Ocean Engineering and Ship Technology Gdansk University of Technology
All rights reserved
ISSN 1231 – 3998
ISBN 83 – 900666 – 2 – 9

Printed in Poland

CONTENTS

DIAGNOSTIC RELATIONS BETWEEN STATE PARAMETERS AND OPERATIONAL PARAMETERS OF MARINE GAS TURBINE ENGINE

Andrzej Adamkiewicz

Szczecin Maritime Academy
Wały Chrobrego 1-2, 70-500 Szczecin, Poland
tel.: +48 91 4809384, fax: +48 91 4809575
e-mail: a.adamkiewicz@am.szczecin.pl

Franciszek Tomaszewski

Poznan University Of Technology
Piotrowo 3, 60-965 Poznań, Poland
tel.: +48 61 6652570, fax:+48 61 6652204
email: franciszek.tomaszewski@put.poznan.pl

Abstract

This article presents the basis of construction of diagnostic relations between the technical condition of the object and diagnostic symptoms. Terms: "relation" and "functional relations" describing diagnostic relations were defined. Using a one-rotor gas turbine engine as an example, construction of diagnostic relations for chosen operational parameters and the state of the engine, described by its power, has been shown.

Keywords: *ships, power plant, gas turbine engine, diagnosis*

1. Introduction

The term "relation", according to Wikipedia, the free encyclopaedia may refer to: a relation - a person to whom one is related, a generalization of arithmetic relations, such as "=" and "<", international relations and many others [1, 4].

The term "diagnostic relations" generally applied in diagnostics refers to relationships between the states of an object, *X,* and parameters of a diagnostic signal, *Y.* The state of the object may be defined as a set of structure parameters (eg. parameters describing operational or regulation tear) or in the sense of reliability: fit for use or unfit (faulty). Diagnostic relations can be determined on the basis of results from experiments carried out on real object/objects or basing on simulation research, when there is a model that well represents chosen states of the objects.

The aim of this paper is to study the relations between chosen state parameters and diagnostic parameters (signals) of marine gas turbine engines operating in a ship power plant.

2. Meaning of a relation

Any subset of a cartesian product of n sets is called a relation with n arguments. These sets have to be identical. A relation means a connection between elements of a set. If a relation is denoted as ρ, than $\rho \subset X_1 \times X_2 \times .... \times X_n$. Relations included in the n-th cartesian power of one set are a special case [1, 4]:

$$\rho \subset X \times X \times .... \times X = X^2, \tag{1}$$

In practice one-argument relations, i.e. subsets of the X set, are more common. However the most common relations are the binary ones. They are the sets of ordered pairs of the $\langle x, y \rangle$ type. If $\langle x, y \rangle \in \rho$ than we write $x \rho y$ (where x is in ρ relation with y). In mathematics one can encounter the following special relations:

- mathematical function,
- partial ordering,
- accurate ordering,
- transitive relation,
- symmetric relation,
- ant symmetric relation,
- equivalence relation,
- reflexive relation

and many others. Diagnostic relations usually appear in the form of function relations (mathematical function). Functions as relations of two sets X (states) and Y (symptoms) are defined as in [3]:

If a binary relation $\rho \subset \mathrm{X} \times \mathrm{Y}$, fulfils the condition that for each $x \in X$ there is exactly only one element $y \in Y$, then $x \rho y$ is called a function.

It relates to one element x of the X exactly one element of the Y set, so it is a function reflecting the X set into the Y set according to the definition of a function. Moreover the X set (states) and the Y set (symptoms) should meet the requirements of equivalence, symmetric and transitive relations which allows using in the simulation diagnostic research the reverse task i.e. simulating different states of the object and obtaining their symptoms.

In technological diagnostics, relations between the states of the object X and the diagnostic parameters (symptoms) Y, are most frequently studied using regression. It is a functional relation between the random variable X (states as a describing variable) and the variable Y (symptoms as a described variable) with the accuracy equal to a random error ε whose expected value is zero. Formally it is represented in the following way:

$$Y = f(X) + \varepsilon, \tag{2}$$

where:

Y – random variable,
$f(X)$ – regression function,
X – any variable (or a set of variables),
ε – random disturbance, $E(\varepsilon)=0$.

Regression is used to study the relations between parameters (qualities) X and Y. In diagnostic practice a relation between a describing variable X (states) and a described variable Y (diagnostic signal) is searched for. To determine the intensity of the relation between real parameters of a diagnostic signal Y and the estimated values $\hat{Y}$, a determination coefficient
$R^2 = R^2(Y, \hat{Y})$ given as:

$$R_i^2(Y, \hat{Y}) = \frac{\left[\sum_{k=1}^{n}(Y_k - \overline{Y})(\hat{Y}_k - \overline{Y})\right]^2}{\sum_{k=1}^{n}(Y_k - \overline{Y})^2 \sum_{k=1}^{n}(\hat{Y}_k - Y)^2} \tag{3}$$

is used.

The determination coefficient, as a standarised measurement of intensity of linear relation between the diagnostic signal and the states of units of which the object is comprised, makes the basis for the choice of equations. Equations with determination coefficient values closest to one should be chosen. A small value of the determination coefficient indicates a poor relation between the real parameters of the diagnostic signal, Y and its estimated values, $\hat{Y}$.

3. The object of the research

An auxiliary one-rotor gas turbine engine of the GTU-6A type, whose cross-section is shown in Fig.1., was chosen as the object of the research.

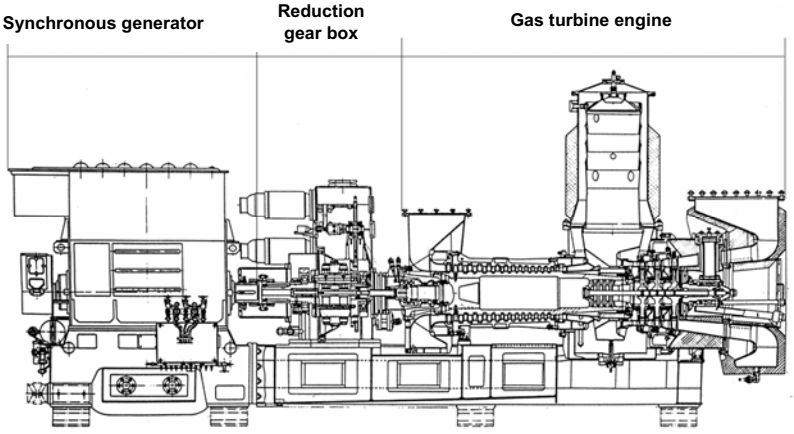

Fig. 1. A cross-section of a one-rotor gas turbine engine of the GTU-6A type in an auxiliary power unit

The GTU-6A engine, through a planetary reduction gear drives a synchronic generator of the MSK 750/1500 type. On a ship there are four engines of this type, placed in separate machine compartments, which cooperate with the ship power system through a sectioned bar. Designed properties of the GTU-6A gas turbine engine are shown in Tab. 1.

Tab.1. Designed properties of the GTU-6A gas turbine engine

Parameter/ Symbol	Unit	Load range					
		Idle run	0,5	0,7	0,8	1,0	1,1
P_e	kW	–	300	430	480	600	660
T_3	K	791	870	930	970	1033	1097
T_4	K	508-538	608-638			708-738	>793
π_C	–	3,2-3,5	3,8-4,1			4,1-4,4	5,35
n	min^{-1}	12150	12150	12150	12150	12150	12150
p_{fuel}	MPa	4,5-5,2	4,8-5,5			5,1-5,8	
p_{oil}	MPa	0,28-0,3	0,28-0,3			0,28-0,3	
$\dot{m}_{air}$	kg/s					6,64	

4. Operational studies

Operational studies on a one-rotor gas turbine engine were carried out according to a passive diagnostic experiment in which engine operational parameters are studied while state parameters (structure parameters) are unknown. There is a possibility of regulating the control vector. The choice of passive experiment was due to technical considerations connected with the tasks performed by the ship during its operation.

Specifics of gas turbine engine operation in marine conditions leads to representing the diagnosed engine states by discreet sequences of diagnostic signals, recorded in uneven time periods. These signals comprise the measurements representing [2]:

- effective energy flow,
- energy state of the engine,
- energy flaxes driving the engine.

Operational parameters considered as measurable ones, were the input and output observable variables of engine subunits, which due to technical conditions could have been measured and recorded during the engine operation. On-line controlled operational parameters of the main and auxiliary gas turbine engines in ship power systems of chosen vessels are presented in Tab. 2.

Tab. 2. Observed operational parameters of auxiliary gas turbine engines of the GTU-6A type

Subunit	Operational parameter	Symbol	Accessibility
Air inlet duct	Atmospheric air pressure	p_0	1
	Atmospheric air temperature	T_0	1
	Air pressure loss on the filter	Δp_F	1
Compressor	Rotor speed	n	1
	Air temperature at the compressor	T_1	1
	Air pressure behind the compressor	p_2	1
Combustion chamber	Exhaust gas temperature behind the combustion chamber	T_3	0
Compressor turbine	Exhaust gas temperature behind the turbine	T_4	1
Control system	Fuel pressure at the burner	$p_{fu.at.burn}$	1
	Overflow fuel pressure	$p_{fuel.overfl}$	1
	Oil pressure behind the regulator	$p_{ol.contr.}$	1
	Fuel pressure behind the supply pump	p_{fuel}	1
	Fuel pressure loss on the filter	$\Delta p_{fuel.F}$	1
Oil and cooling system	Oil pressure at the engine inlet	$p_{ol.eng.I}$	1
	Oil temperature behind the cooler	$t_{ol.eng.I}$	1
	Compressor bearing temperature	$t_{bearingC}$	1
	Turbine bearing temperature	$t_{bearingT}$	1
	Water temperature behind the oil cooler	$t_{w.ol.CO}$	1
	Oil pressure at the reduction gear	$p_{ol.R}$	1

1 – measured parameters,
0 – parameters experimentally inaccessible

Measured and recorded, by the subsystems of the 61 MP "SLAN" control network, were the average values of the operational parameters at stationary random energy states of engines. The measurements were carried out for random engine loads at the atmospheric air parameters, p_0, T_0 and the relative air humidity, ϕ_0. During one observation, at a single time sequence, from more than 10 to over 20 recordings of diagnostic signal parameters were taken, trying to include the possibly widest range of loads, from idle run to the possibly biggest powers.

5. Diagnostic relations

For the parameters presented in Tab. 2, relations of a function type were established, where for the set of states, X, engine power was used (describing variable) and as the set Y (symptoms) the measured parameters (Tab. 2) were taken. To determine the relation between the X and Y sets the least squares method was applied and as the criterion of the best relation (the strength of the relation) R^2. In Fig. 2. and Fig. 3. exemplary relations for exhaust gas temperature T_3 and T_4 and fuel mass flow $\dot{m}_{fuel}$, supplied to the combustion chamber are given.

The presented relations show that there are diagnostic relations between the measured operational parameters of marine gas turbine engines and the parameters characterizing their technical condition. Such relations allow, after performing the reverse task, to estimate the condition of the engine (in this case expressed as the power) basing on the recorded parameters of engine operation.

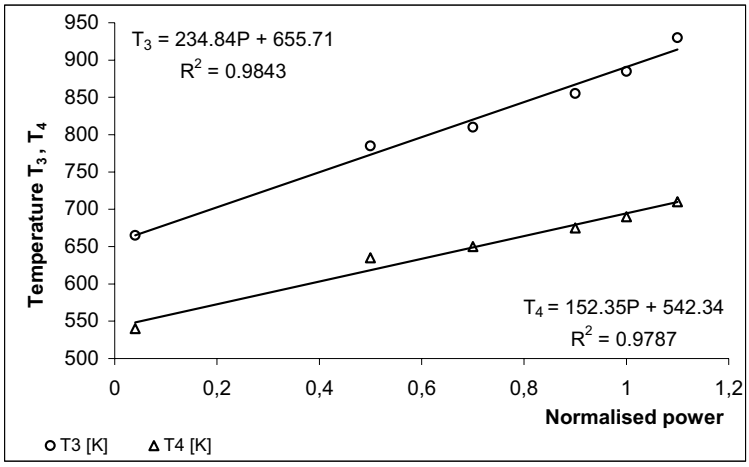

Fig. 2. Diagnostic relations between the exhaust gas temperature behind the combustion chamber and the turbo-compressor and the engine power

6. Summary and conclusions

This study presents the essence of constructing diagnostic relations between diagnostic parameters and state parameters. Basing on literature, the meaning of a relation has been presented. Special relations applied in pure mathematics were listed. In diagnostics the term "diagnostic relation" means the relation between the states of the object, X, and the parameters of the diagnostic signal Y. Example of established diagnostic relations have been presented for chosen operational parameters of marine gas turbine engines and their technical condition. Diagnostic relations have been constructed applying regression analysis and the least square method.

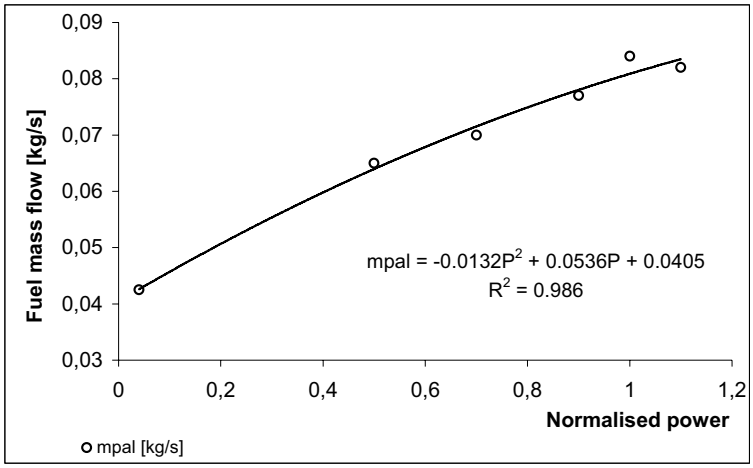

Fig. 3. Diagnostic relations between the mass of fuel supplied to the combustion chamber and the engine power

The exemplary diagnostic relations presented in this study and the method of constructing such relations can be applied to:

- establishing the strength of relations between the state of the object and diagnostic parameters,
- the choice of diagnostic parameters which best represent the state of the object,
- diagnosing the object basing on a model.

References

[1] Adamkiewicz, A., *Relacje diagnostycznew okrętowych turbinowych silnikach spalinowych*, Problemy Eksploatacji, 3/2001 (42), Instytut Technologii Eksploatacji, Radom 2001, s. 9 –19.

[2] Adamkiewicz, A., *Study Of The Applicability Of Operational Parameters For Diagnosing Marine Gas Turbine Engines,* Naval University of Gdynia, 2004, Reserch Proceedings Nr 158 A, Gdynia, (in Polish).

[3] Rasiowa, H., *Wstęp do matematyki współczesnej,* PWN Warszawa 1979.

[4] http://pl.wikipedia.org/wiki/Relacja, January, 2007.

MONITORING SYSTEM FOR GRINDING MACHINE OF TURBINE-ENGINE BLADES

Wojciech Batko, Witold Cioch, Ernest Jamro

University of Science and Technology (AGH-UST)
al. Mickiewicza 30, 30-059 Kraków, Poland
tel.: +48 12 6173622, fax.: +48 12 6332314
e-mail: cioch@agh.edu.pl

Abstract

Monitoring operation of grinders of aviation-turbine blades is especially vital for the demanded product quality and economic expenses associated with defected products and production stoppages. In technological process of grinding, not always even wear of tools occurs and machine tools work definitely in non-stationary conditions. Self-induced vibrations are often observed. Therefore monitoring system of module structure was designed, dedicated to non-stationary signal processing. The system is composed of modules for recording and preliminary hardware signal processing, database servers and user's terminals.

Keywords*: monitoring, diagnostics, grinding machine,*

1 Introduction

Despite varied production technologies, machining is still commonly applied nowadays. It is the result of the fact that it provides a very high accuracy, high efficiency and could be easily automated. Perfect examples of devices carrying out machining process are grinding machines for aviation turbine blades.

Problems regarding grinders operations can have various causes. They can be associated with machine-tool defect, wear process of a tool or self-induced vibrations [2]. Hence it is advisable to diagnose machine-tool condition not only before machining process but also during the actual process. The condition of machine tool is vital for the product quality and for continuity of production process, the stoppage of which would bring significant economic losses.

Monitoring systems enable to detect changes in condition or operation parameters of machine tools [1]. Based on data collected, it is also possible to project the technical condition, which is important for production-process planning. It is of great significance in aviation industry, where manufactured elements are of high quality and precision. Therefore their production is expensive and loss of the whole batch of product is not acceptable.

Machine tool condition and machining process characteristics are vitally affected by dynamic phenomena. Hence vibration is a basic quantity measured in a monitoring process. Vibration is also measurement quantity bringing the most valuable diagnostical information [5]. Monitoring tool condition and self-induced vibrations is still an unsolved problem.

The most significant features, determining functional properties of monitoring systems are according to [4]:

- purpose (machine tool, machining type),
- type of selected diagnostical signals and their measurement manner,
- signal transformation methods,
- method of determining boundary values,

- diagnostical inference methods,
- maintenance characteristics, interfaces.

Having those items in mind, an innovative monitoring system for grinder machine of aviation turbine blades has been designed.

2. Monitoring system

The monitoring system for grinding machine includes methods and algorithms for signals acquisition, pre-processing, transmission and data processing and storage. Consequently, the whole system consists of the following modules:

- Programmable Unit for Diagnostic (PUD)
- Dedicated Server for data collection and processing
- Dedicated server for data storage with limited access for users.
- External users terminals for diagnostic signals analysis.

The block diagram of whole system is presented in Fig. 1.

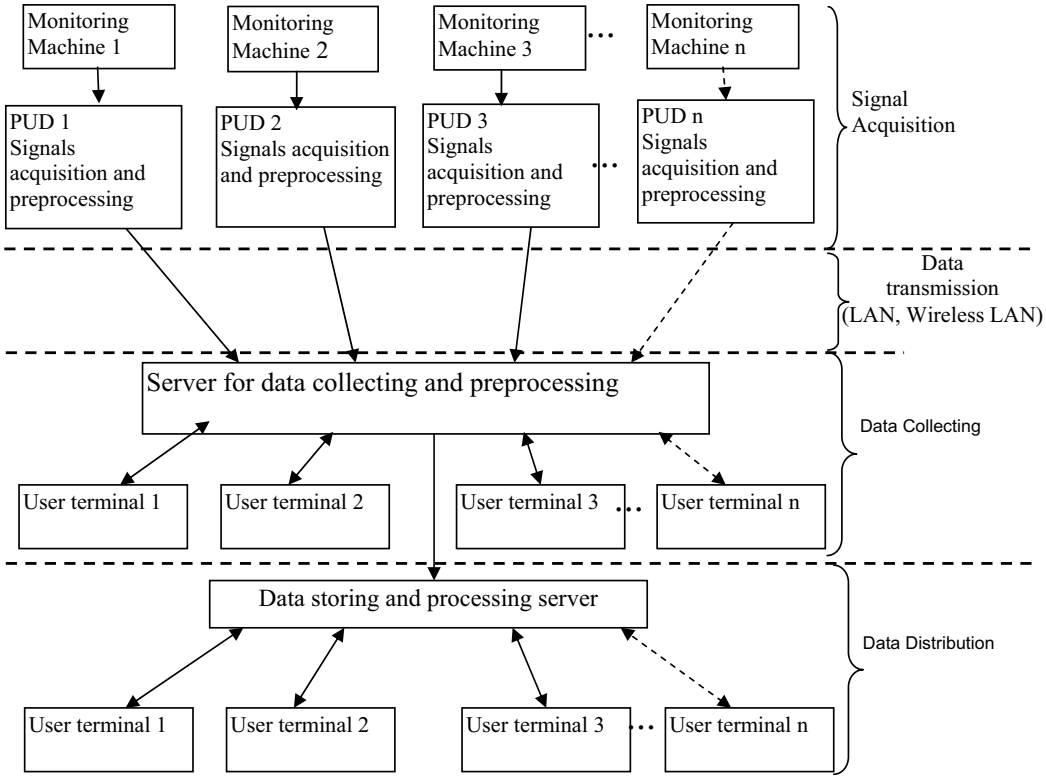

Fig. 1. The monitoring system block diagram

3. Signals acquisition and preprocessing

Electronic implementations of signals acquisition and preprocessing are often disregarded in academic considerations. Nevertheless they often determine the diagnostic procedure and final results. Therefore in this section the electronic solutions for high-speed diagnostic devices will be considered.

Usually three different electronic solutions are considered:

1) General-purpose processors or digital signal processors (DSP)
2) Dedicated VLSI chipset – Application Specific Integrated Circuit (ASIC)
3) Field Programmable Gate Arrays (FPGAs)

General-purpose processors (e.g. Pentium) or DSPs are very flexible, easy to be programmed and relatively cheap, nevertheless the signal sampling frequency and signal processing speed is relatively small. Consequently this solution is suitable for relatively slow diagnostic systems, for which signal-sampling frequency is roughly below 100kHz. The given threshold frequency differs for different algorithm complexity, number of channels, processor computing power and so on, therefore it should be regarded only as a rough number.

Dedicated (ASIC) solution is the best solution for mass-production devices for which the solved problem and algorithm is stable. This holds as device designing time and initial costs are high, but device per unit price is relatively low. Unfortunately, diagnostic devices are usually used only by specialists and therefore are produced in low-volume. Besides, the diagnostic algorithms are often adapted to different problems. This causes that this solution has rather only historical significance.

For diagnostic systems for which data sampling frequency is above roughly 100kHz the FPGAs (Field Programmable Gate Arrays) solution is the best one. FPGAs can be programmed by an end-user in similar way as microprocessors, nevertheless they employ different design procedures, which causes that they can be designed only by electronics engineers. For FPGAs, sampling frequency is up to roughly 500 MHz; similarly data processing speed is also very high.

The most important feature of FPGAs is programmability, i.e. logic or arithmetic functions performed by FPGAs can be programmed according to user requirements. Therefore FPGAs resemble microprocessors. The most important difference is that microprocessors fetch instructions from external memory, and FPGAs have built-in configuration memory. Consequently, microprocessors waste time for fetching and decoding instructions, which limits their speed and level of parallelism; nevertheless the executed program can be relatively easily changed. Conversely, FPGAs can execute user functions relatively quickly and in parallel, as they do not waste time for fetching and decoding instructions.

The main disadvantage of FPGAs is that they can execute a limited number of logic (instructions) at a time and changing logic functionality (reconfiguring FPGAs) is time consuming. For microprocessors, the size of a machine instruction is usually about 1-8 Bytes. Conversely, for FPGAs configuration size is e.g. roughly 50 kB (Xilinx XC3S50) ÷ 1.5MB (XC3S5000). Consequently, FPGAs reconfiguration requires relatively large amount of time (about 10-1000 ms) when FPGAs cannot execute any logic. Besides storing many different FPGA configurations is also difficult to be obtained because of large memory size. Summing up, FPGAs execute very quickly (in parallel) a limited number of instructions, but branching to another set of instructions (reconfiguring the FPGAs) is usually unacceptable. Consequently, it is recommended that FPGA perform only instructions that are executed in loop millions of times. Usually this is satisfied for data-driven algorithms, for which the same relatively simple algorithm is executed for a great number of times for different data.

Hardware software co-design

FPGAs and microprocessors complement each other, i.e. usually the most computationally intensive algorithms are data-driven algorithms, therefore they can be speed-up by FPGAs. On the others hand, program-driven algorithms, i.e. complex algorithms processed a limited number of times, cannot be easily implemented in FPGAs. Usually these algorithms are not computationally intensive and therefore are well suited for microprocessors. Partitioning an algorithm into software part (executed by microprocessors) and hardware part (executed by logic incorporated in FPGAs)

is denoted as hardware-software co-design [49]. As hardware-software co-design is very efficient, FPGAs are often connected with microprocessors, i.e. two different chips (FPGA and microprocessors) are incorporated on the same PCB (Printed Circuit Board). Furthermore, FPGAs often incorporate microprocessors in the same chip, therefore combining hardware and software is more effortless.

Embedded Development Kit (EDK)

FPGA design cycle is relatively difficult and time consuming. Almost every engineer can program microprocessors employing C/C++ or other high-level programming languages. Unfortunately, FPGAs can be designed only by limited-number of electronic engineers. Besides design cycle is difficult, error-prune and time-consuming. And last but not least, finding errors (debugging) FPGA designs is a major drawback, which is often overlooked. Therefore a dedicated Advance Programmable System Interface (APSI) [26] was employed in the developed system.

In order to speed-up FPGA design cycle, modular design is often adopted. Modules, denoted as Intellectual Property (IP) cores, which functions are well defined and tested, are supplied by different vendors and connected with each other. Each module is in charge for different tasks, e.g. external SDRAM memory interface, Analog Digit Converter (ADC) interface. To speed-up modular design Xilinx Embedded Development Kit (EDK) was employed. This software packet allows connecting different modules graphically. Consequently adding a microprocessor and employing hardware/software co-design is significantly quicker and easier. An example of a Huffman compression system design in EDK is given in fig. 2.

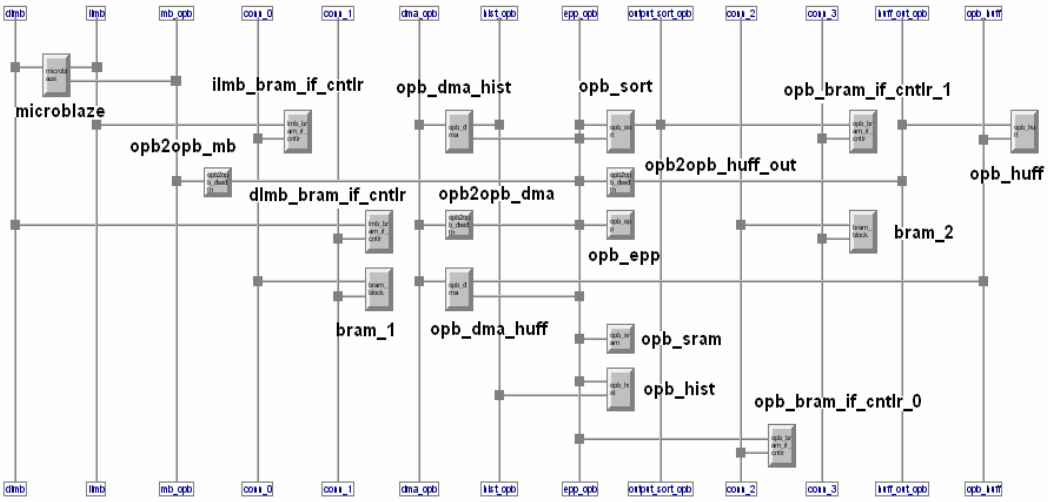

Fig. 2. An example of EDK design [27]

Programmable Diagnostical Unit (PDU)

Programmable Diagnostical Unit (PDU) is a device which core is FPGA device [6]. The block diagram of the PDU is shown in Fig. 3 and it incorporates the following parts:

- Four independent analog / digital modules on separate PCB.
- Two independent SDRAM memory banks, 64MB each, employed to store acquired data from analogue / digital modules and other temporal data.

- CPLD (Xilinx XC95144XL device) – module employed to configure FPGA and to control the PUD in power stand-by mode.
- Flash memory (4MB) to store FPGA configuration, MicroBlaze program and other non-volatile data.
- Hard Disk Drive (HDD) to store high volume data
- LCD display employed to visualise the state of the device and results for acquired data.
- Keyboard – allows user to control the PUD and to start / stop data acquisition.
- PC computer communication by Parallel or Serial Ports.

Besides, the PDU incorporates some optional devices: Compact Flash memory, VGA display, PC keyboard, and Ethernet and Radio Communication modules.

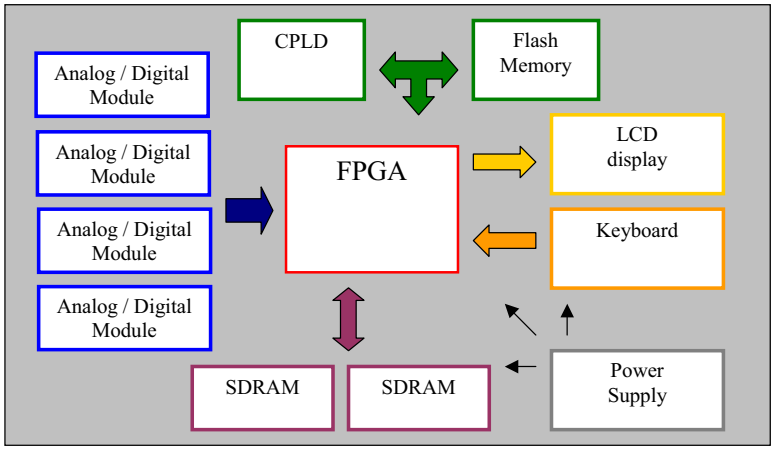

Fig. 3 Block diagram of the PDU

The PDU incorporates four independent analog / digital boards. These boards include Analog Digital Converters (ADC), input signal amplifiers with digitally controlled level of amplification and ICP sensor interface. Each analog board incorporates 2 channels 16-bit 500kS/s each or 4 channels 16-bit 250kS/s each, consequently up to 8 (16-channels) can be acquired by the PUD. It should be noted that changing analog / digital board requires FPGA configuration to be changed. Fortunately modular design in EDK significantly reduces designing time.

Data servers

To increase data security and to improve data visualization, data are stored on two independent servers. On the first server, data coming directly from the signal acquisition unit are collected. Then they may be preprocessed in order to decrease the data volume and to select only important diagnostic estimates. Then preprocessed data are stored in a local database and are transferred to the second server. The main task of the second server is data backup and data distribution as a database or by HTTP protocols on WWW. As a result end users can access data by users terminals, which need not advance diagnostic programs. This solution allows controlling data access to a limited number of users. Besides any data access or modification can be recorded in the system.

In the database apart from acquired signals some additional information, as acquisition time, sampling frequency and amplifier settings may be stored. The database allows also storing some additional information as an exact place of signals acquisition, grinding machine information and

users comments. The database allows to group selected signals as a result of acquisition time, data processing type, etc. It allows also to process recorded signals by externals programs such as MATLAB.

5. Conclusions

Application of Programmable Diagnostical Unit into preliminary signal processing system enable to record data with high frequency and data hardware processing [7]. Using programmable FPGAs brought the possibility of non-stationary signal analysis in real time. The applied PDU module enabled, apart from measuring diagnostical signals, also to record parameter signals, especially rotation speeds of spindles.

Application of two servers for data collecting and for data distribution separately improved the safety of database.

It also gave the vast possibilities of processing (implementing Matlab suite) and surveying of collected signals by authorised users. Thanks to this solution, classifying grinding-machine condition and diagnosing operational process can be carried out by means of:

- numeral measures,
- functional measures,
- neural networks,
- parametrical models.

The modular construction of the monitoring system allows the whole system to be easily extended or modified to new grinding machines and acquisition points.

6. References

[1] Batko, W., Korbiel T., *System monitoringu diagnostycznego przekładni planetarnej pracującej w warunkach zmiennego obciążenia,* Diagnostyka nr 1, 2006.

[2] Pod red. Batko, W., Dąbrowski, Z., *Procesy wibroakustyczne w technice i środowisku,* Wydawnictwo Wydziału Inżynierii Mechanicznej i Robotyki, AGH, 2006.

[3] Bodnar, A., *Vibration Monitoring on a Milling Machine Using the Analysis of Stochastic Features of Generated Noise,* Ninth World Congress on the Theory of Machines and Mechanisms, August 29/September 2, 1995, Milano, Vol. 4, s. 2910-2914.

[4] Bodnar, A., *Diagnostyka i nadzorowanie drgań obrabiarek***.** Materiały Sekcji Podstaw Technologii Komitetu Budowy Maszyn PAN z 50 posiedzenia w dniu 24.06.93 w Szczecinie, W: Prace Inst. Technologii Mechanicznej Politechniki Szczecińskiej, 1993, s. 5-16.

[5] Cempel, Cz., *Diagnostyka wibroakustyczna maszyn*, Wydawnictwo Politechniki Poznańskiej, Poznań, 1985.

[6] Jamro, E., Adamczyk, A., Krzyworzeka, P., Cioch, W., *Programowalne urządzenie diagnostyczne stanów niestacjonarnych pracujące w czasie rzeczywistym*, XXXIII Ogólnopolskie Sympozjum Diagnostyka Maszyn, Węgierska Górka, 8.-11.03. 2006 r.

[7] Krzyworzeka, P., Adamczyk, J., Cioch, W., Jamro, E., *Monitoring of nonstationary states in rotating machinery,* Instytut Technologii i Eksploatacji, Radom 2006.

This work has been executed as part of research project at KBN no 6T0720005C/06545.

A NON-DESTRUCTIVE METHOD TO ASSESS A DEGREE OF OVERHEATING OF GAS TURBINE BLADES

Józef Błachnio

Air Force Institute of Technology
ul. Księcia Bolesława 6, 01-494 Warszawa, Poland
tel.: +48 22 6851982, e-mail: jozef.blachnio@itwl.pl

Mariusz Bogdan

Bialystok University of Technology
ul. Wiejska 45c, 15-351 Białystok, Poland
tel.: +48 85 7469237, e-mail: marbog@pb.bialystok.pl

Abstract

The paper has been intended to propose an objective, non-destructive method to assess a degree of overheating of gas turbine blades material. The method has been based on the opto-electronic recognition of images of blade surface layers to extract characteristics thereof for both overheated and serviceable blades. Any image of a blade surface layer is analysed within the Fourier plane by means of a computer-generated version of a matrix of ring-wedge detectors. A ring-wedge detector enables good effects when used to assess health/maintenance status of gas turbine blades. Results of examining microstructures of both overheated and serviceable blades are the confirmation. Findings can give grounds for a method of diagnosing to what degree blades in operation suffer overheating.

Key words*: turbine blade, diagnosing, visual method, microstructure*

1. Introduction

The diagnostic examination is usually aimed at determining health/maintenance status of an engineering object. In the case of complex structures, the diagnostics plays an important part in the assessment of real time of failure-free operation. Extremely varying operating conditions of particular components and sub-assemblies of engineering objects are factors of great importance that affect operating conditions. While operating a turbine engine, no matter whether an aircraft, a marine or a traction one, various failures to engine assemblies occur. The most common ones are the blade's material overheating and thermal fatigue. Elimination of this kind of failures is always carried out as a major engine repair, which results in tremendous cost [1, 5].

A decision on whether the repair is necessary is taken by a diagnostician who can diagnose condition of individual components with a visual method, using e.g. a videoscope (Fig. 1). The recorded image of the surface layer of a component under examination gives grounds for the assessment of the component's condition. It is compared to standard images of similar components, both fit and unfit for use, e.g. turbine blades.

This kind of condition assessment proves very subjective, since it depends on the diagnostician's knowledge and vision. Light that falls on the surface is reflected and, therefore, objects can be observed. Shapes and colours of surfaces of metal objects become distinguishable. Although a skilled and efficient diagnostician can distinguish over a wide range of colours (ones within the scope of 400 through 700 nanometers, starting with violet to dark red), any mistake due to his subjective assessment can result in acknowledging an unserviceable (overheated) blade for a fit-for-use one, and vice versa. In the first case, an engine failure may happen in a short time, in the

second one – an expensive major repair of the engine may be effected. Therefore, the diagnostician's decision is verified with a destructive method. The component under examination is subjected to analysis of microstructure of the microsection [5, 7].

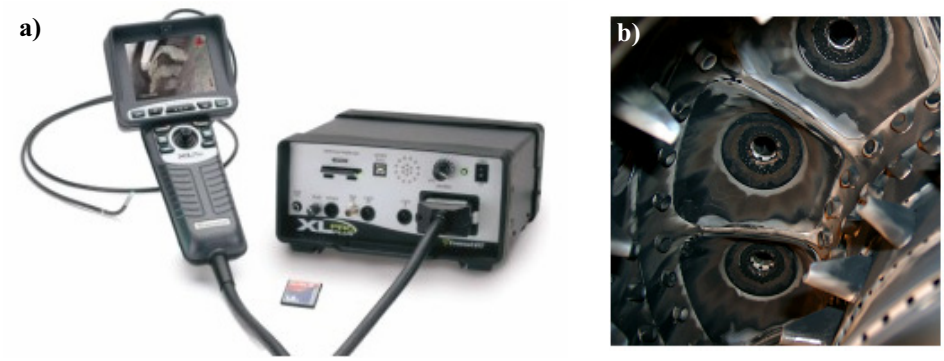

Fig. 1. A commercial videoscope (a), and a jet engine combustor on the videoscope screen (b)

In the case illustrated with Fig. 2, one cannot explicitly determine whether the surface of at least one of the presented blades indicates the material overheating. Furthermore, according to criteria in force until now, nothing can be said about the degree of overheating. No objective criteria have been determined to explicitly and in a non-destructive way assess the degree of the blade's material overheating [3, 4].

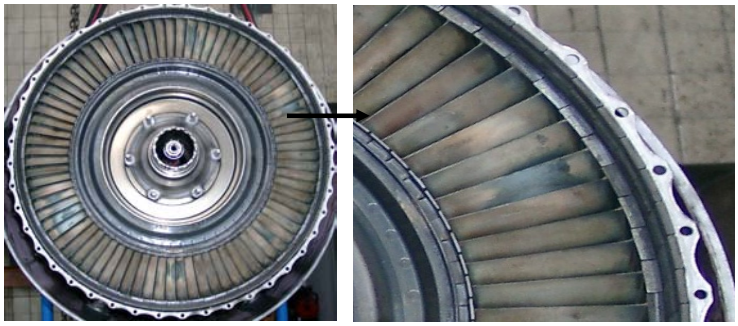

Fig. 2. A gas turbine with visible changes of colours on blades surfaces [4]

2. Methods of analysis of light signals reflected from a metallic object's surface

Dynamic development of technique of acquiring images, both monochromatic and colour ones, facilitates extensive and easier use of information included in recorded images to satisfy needs of the diagnostics. From the diagnostician's point of view, the correct colour assessment proves of great significance in many cases [4, 6]. It is often used in numerous diagnostic procedures in areas such as cartography, chemical industry, aviation. A decision is made by comparing a standard colour with that/those of recorded images. In [12], an advisory system has been suggested to assist objective colour assessment as a method to determine petroleum products that affect corrosion of metals. In the postulated system, methods of fuzzy logic are used to assess and classify colours. Authors of [10 - 12] present also methods of calculating a membership function of the analysed point of a colour image to determine colour (area) according to the classification of colours based on the CIE chromaticity diagram, the so-called colour triangle.

In the present-day diagnostics, integrated image analysers (image matrices) are more and more common. They are used in various image recording/analysing techniques aimed at acquisition of the quantitative and qualitative information on investigated states and phenomena represented by means of images [10]. Among various assisting methods, morphological methods of image conversion are of particular interest. They are among the most significant methods in the computer-image analysis, since they are a preliminary step to create more complex operations connected with analysing shapes of objects and their positioning to each other.

Images of uniform structures, commonly called 'textures', build up a characteristic group. They are of great importance in many areas of science and technology, e.g. metallography, crystallography, tribology, etc. Extraction of their characteristics (e.g. statistical parameters, Haralick's parameters) would enable to classify them and then to infer on characteristics of materials, objects, and processes represented with texture images [9].

A method that makes use of laser technology [2] is an interesting non-destructive solution to assess (diagnose) condition of rotor blades that do not rotate. Properties of laser radiation are used in the course of investigation. Examined are differences between the incident and reflected radiations. The diagnostic testing work with dynamic excitation engaged provides interferograms that determine forms of blade vibration at different resonance frequencies. This is a source of information on the blade's dynamics, and hence, on mechanical properties, design condition, etc. of this blade.

Sarnecki J. [8] applied a ring-wedge detector to recognise images of tribological-wear-effected products to diagnose types of wear of bearing systems.

3. Methodology of image acquisition – of luminance (brightness) and chrominance (colour) of surface layers of gas-turbine blades

The jet's gas-turbine rotor blades made of the ŻS6 alloy (Fig. 3) are subject to tests. The blades have been covered with alitised layers (consisting of aluminium and other elements) for protection against high-temperature gas affecting them.

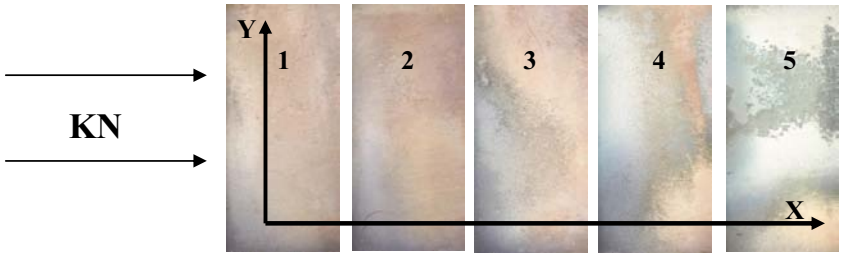

Fig. 3. Surface layers of gas-turbine blades in service (KN – edge of attack)

Colour and intensity feature light – the visible radiation (a part of the electromagnetic spectrum), which are recorded with human organ of sight. In case of a digital camera it is the built-in optics that focuses light rays and plays a part of the 'organ of sight', and the electronics, i.e. a light-sensitive sensor. An image in front of the camera lens is mapped against surface of matrix provided with detectors furnished with tri-colour RGB filters (RGB – three primary colour constituents, i.e. red - R, green - G, blue - B) which enable detection of particular colours.

To simplify, the acquired information on the intensity of colour distribution in case of colour images, and of shades of grey (grey scale) in case of monochromatic images is recorded on a memory card in the form of points called pixels, which form an image [9].

Modern methods of image analysis have found applications in broadly understood technical diagnostics. As a primary advantage of this type of diagnosing one should mention the non-

destructive nature of the method to acquire information on health/maintenance status of a given object. The described non-destructive method enables determination of the condition of a given surface, i.e. of a surface layer discerned as luminance (brightness) and chrominance (colour) that reach a recording device, i.e. a camera. The photographing and the recording of images were both carried out on a test stand (Fig. 4).

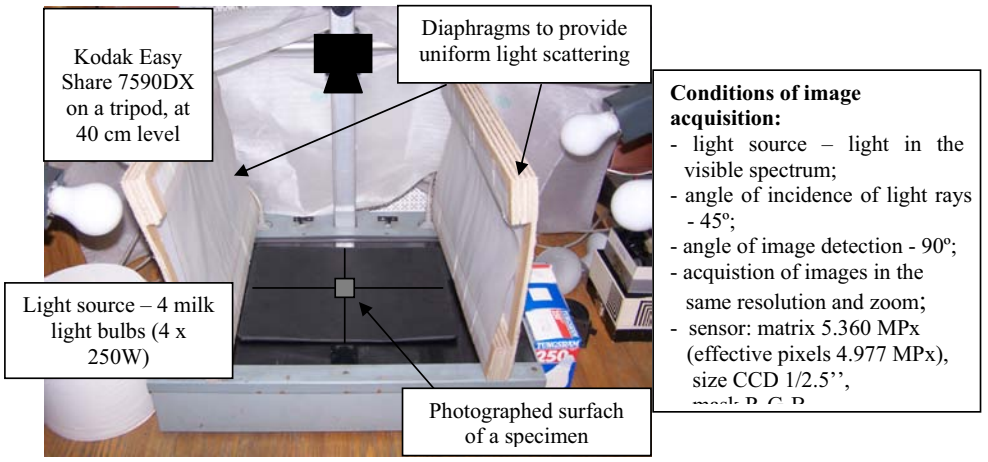

Fig. 4. Test stand to acquire images of surface layers of turbine blades

Repeatability of results was proved by photographing blades under the same conditions, with suitably matched parameters of the digital camera. Application of diaphragms ensured uniform reflection of light from the metal surface to provide uniform light scattering. The diaphragms eliminated light reflections that cause over-exposure of obtained images. Identical photographing conditions enabled comparisons of changes in colours of surface layers of blades showing different health levels. The image recording format was adjusted to satisfy needs of image compression according to Exif 2.2 standards. In order to maintain as much information about the recorded image as possible, compression was set to the lowest level acceptable.

4. Analysis of images of turbine blade surfaces

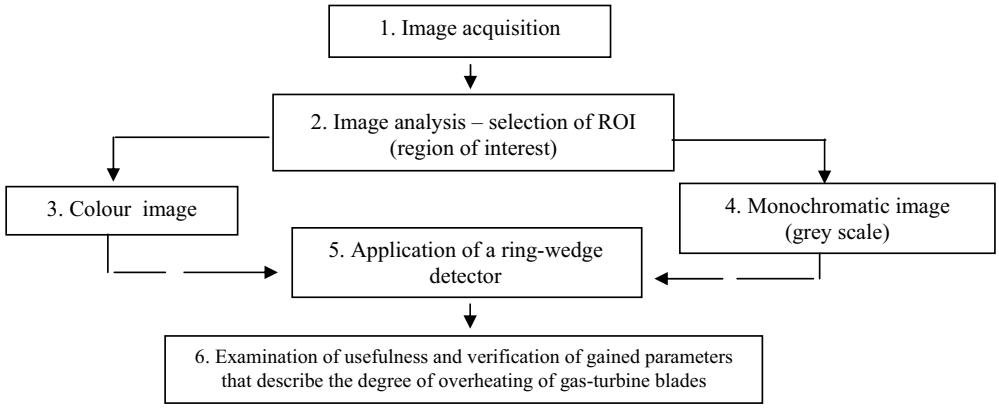

Fig. 5. Acquisition, and computer colorimetric and spectral analyses of signals from blade surfaces – a diagnostic model

Some representative regions of blade surfaces (averaged ROI – regions of interest) were chosen to explicitly describe the blades. The RGB colour image is a model that results from receptive properties of the human eye and is based on the fact that the sensation of almost all colours by the eye can be effected by mixing - in some pre-set proportions – only three selected light beams of some suitably matched spectral bandwidths. In the RGB model of colour identification there are only three constituents: R - red, G - green, and B - blue. Therefore, it is an additive model, where each colour is obtained by means of combining three primary colours. Hence, each channel is analysed separately. Colour images were analysed using the Matlab software (Image Processing Toolbox).

A colour image was converted into a monochromatic one, i.e. one, for which information on colour distribution is negligible. Using the Matlab software (Image Processing Toolbox), a colour image was converted into one representing the grey scale (256 grey levels). It was investigated whether the 'black-and-white' information is sufficient to describe changes in colours due to high temperature affecting the blades.

A ring-wedge detector was used to analyse images. It is a circle-shaped instrument, which comprises two parts: the first one includes concentric-located rings, whereas the second one is formed with wedges that join in a common vertex in the middle of the detector. Each of the regions is a surface photodetector that transforms intensity of the incident light into a signal proportional to intensity of this light. A computer-generated hologram (CGH) shows shape identical to that of the ring-wedge detector, and is also composed of areas of rings and wedges. Therefore, the CGH acts as an extractor of features (characteristics) from images in the domain of frequency. Results of analyses of colour images of turbine blades, and those within the grey scale are presented in Fig. 6. Values of rings and wedges for blades no. 4 and 5 evidently stray from those for the remaining blades.

5. Microstructure of turbine blades

Mechanical and technological properties of any alloy are closely related to its microstructure, which in turn strongly depends on the sort of heat treatment applied. Affected with multiple temperature fluctuations, the alloy is subject to thermal fatigue. High temperature affects also the surface layer. The turbine blades are made of high-temperature nickel-base alloy ŻS6. They are covered with alitised layers to increase their high-temperature creep resistance.

Metallographic microsections of blade specimens were prepared with standard methods to be then etched with a reagent of the following chemical composition: 30 g $FeCl_2$ + 1 g $CuCl_2$ + 0.5 g $SnCl_2$ + 100 ml HCl + 500 ml H_2O. The microstructure was observed by means of a light microscopy, and SEM - the scanning electron microscopy.

Examination of microstructures of the alitised layer and the ŻS6 alloy shows that the effect of exhaust gas of high temperature on turbine blades under examination resulted in decohesion of the alitised layer and modification of the strengthening phase γ' (Figs 7 and 8). Fig. 7 shows regular (correct) structures of the alitised layer and the ŻS6 alloy of turbine blade no. 1 (see Fig. 6), where as Fig. 8 shows overheated microstructures of the alitised layer and the ŻS6 alloy of turbine blade no. 5 (see Fig. 6). The alitised layer suffered swelling, pop-offs also occurred, and even worse, cracks were initiated due to thermal fatigue (Fig. 8a). The image of microstructure of the ŻS6 alloy shows secondary precipitates of fine-dispersion phase γ' (Fig. 8b), effected with exhaust gas of high temperature. The phase γ' morphology proves that after having exceeded critical temperature, the alloy suffers overheating and any turbine blade cannot be considered serviceable (fit for use) any more.

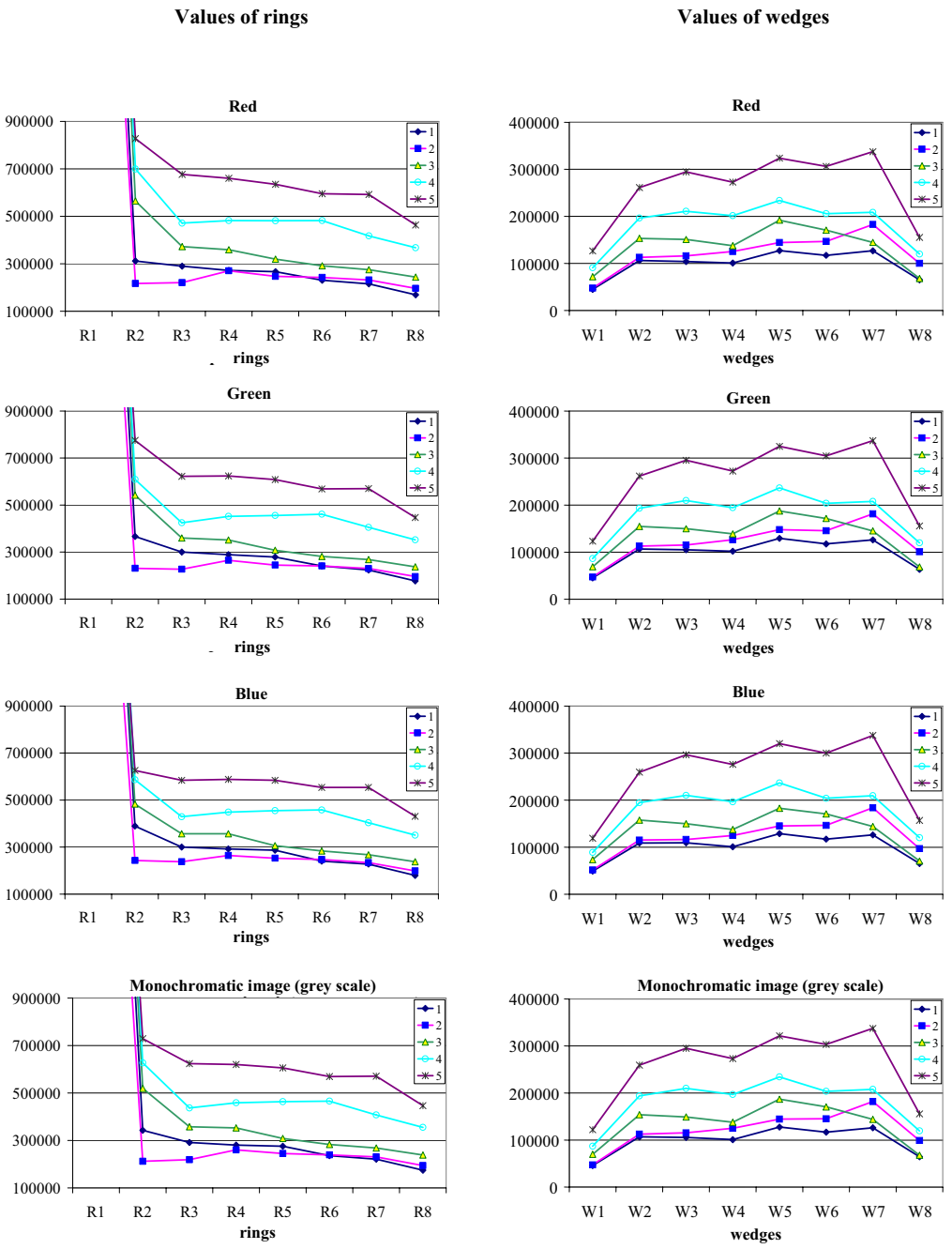

Fig. 6. Values of rings and wedges for particular turbine blades

According to A. Dudziński [5] and A. Poznańska [7], any modification of this kind of the strengthening phase γ' proves susceptibility to brittle cracking. Furthermore, A. Dudziński states in [5] that any blade made of a very similar alloy EJ-929, subjected to a creeping test should be recognised overheated after exceeding temperature 1188 K. The acquired images of microstructure of blade no. 5 can give good grounds to assess a degree of overheating of gas-turbine blades made of the ŻS6 alloy.

a) b)

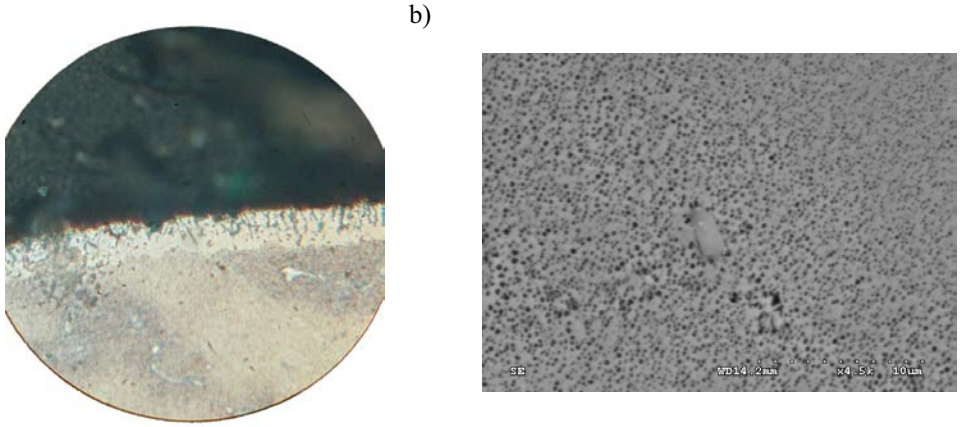

Fig. 7. Regular (correct) microstructure of a turbine blade: a) of the alitised layer, x 450, and b) the ŻS6 alloy, x 4500

a) b)

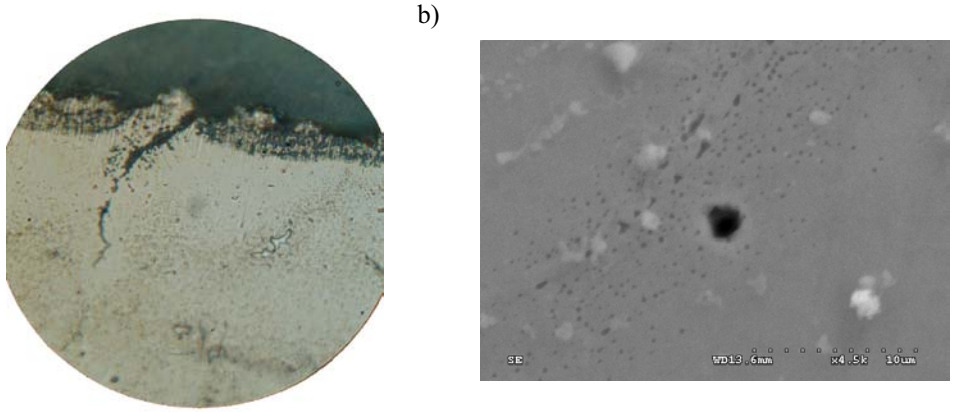

Fig. 8. Overheated microstructure of a turbine blade: a) of the alitised layer, x 450, and b) the ŻS6 alloy, x 4500

6. Summary

Findings of experimental work on high temperature affecting gas-turbine blades made of the ŻS6 alloy have been presented in the paper. The operated blades of aircraft jet engine were subject to examination. A ring-wedge detector was used to analyse images of surfaces of blades showing different health levels. Results of blade-microstructure examination have entitled a statement that blade no. 1 shows regular (correct) structure, whereas blade no. 5 – the overheated one. Comparing these results to those of analysing images of blade surfaces, the following can be stated: blades no. 1 to 3 show correct condition, since values of rings and wedges remain comparable. On the other hand, blades no. 4 and 5 are overheated, because values of rings and wedges differ considerably

from those for blades mentioned above. Therefore, correlation has been shown between the blade-surface image and condition of microstructure of turbine blades made of the ŻS6 alloy and covered with the alitised layers.

The intended aim of applying both a visual non-destructive method used in the diagnostics of engineering objects and the methodology of analysing blade-surface images acquired in visible light spectrum was to gain some cognitive information of great importance. In practice, this information could be used to assess changes in the microstructure, i.e. the overheating and thermal fatigue of components and sub-assemblies of engineering objects affected with variable high-temperature heat loads.

References

[1] Błachnio, J., *Non-destructive testing methods as applied to the diagnosing of turbine engine,* IV International Scientific – Technical Conference, Gdańsk - Kopenhaga 2005.

[2] Bieńczak, K., Lewitowicz, J., *Zastosowanie laserów w diagnostyce lotniczej*, Problemy badań i eksploatacji techniki lotniczej, Tom 2, Wyd. ITWL, Warszawa 1993.

[3] Bogdan, M., Błachnio, J., *Badanie rozkładu temperatury zespołów statków powietrznych,* 8th International Conference, „Airplanes and helicopters diagnostics AIRDIAG'2005", ss. 31÷38, Warszawa 2005.

[4] Bogdan, M., Błachnio, J., *Analiza sygnału świetlnego odbitego od powierzchni w diagnostyce obiektów technicznych,* VI Krajowa Konferencja, „Diagnostyka techniczna urządzeń i systemów DIAG'2006", Diagnostyka Nr 2/38/2006, ss.175÷186, Ustroń 2006.

[5] Dudziński, A., *Analiza rentgenostrukturalna stopu EJ-929 poddanego długotrwałemu wygrzewaniu*, Rozprawa doktorska, WAT, Warszawa 1987.

[6] Kolek, Z., *Właściwości optyczne a wrażenia barwne*, Materiały VII Krajowego Sympozjum Kolorymetrycznego, Wyd. Politechniki Białostockiej, Kielce - Ameliówka 2005.

[7] Poznańska, A., *Żywotność łopatek silników lotniczych ze stopu EJ -867 w aspekcie odkształcenia niejednorodnego i zmian strukturalnych*, Rozprawa doktorska, Politechnika Rzeszowska, Rzeszów 2000.

[8] Sarnecki, J., *Model procesu zużywania elementów układu łożyskowania silnika lotniczego,* Rozprawa doktorska, ITWL, Warszawa 2006.

[9] Tadeusiewicz, R., *Komputerowa analiza i przetwarzanie obrazów*, Wyd. Fundacji Postępu Telekomunikacji, Kraków 1997.

[10] Wiaderek, K., *Badanie funkcji przynależności w analizie obszarów barwnych,* Problemy Eksploatacji, Nr 1, ITE, ss. 207-219, Radom 2000.

[11] Wiaderek, K., *Wykorzystanie trójkąta chromatyczności CIE do ograniczenia liczby barw w cyfrowym obrazie barwnym,* Problemy Eksploatacji, Nr 2, ITE, ss. 213-225, Radom 2002.

[12] Wojutyński, J., Wiaderek, K., *Komputerowe diagnozowanie stopnia skorodowania na podstawie oceny barw,* Materiały IV Krajowej Konferencji „Diagnostyka Techniczna Urządzeń i Systemów DIAG '98", Gdańsk 1998.

DIAGNOSTIC MODEL OF COMPRESSION-IGNITION ENGINE SLIDE BEARINGS FOR CONTROLLING THE CHANGES OF THEIR STATE

Piotr Bzura

Gdansk University of Technology
ul. Narutowicza 11/12, 80-950 Gdansk, Poland
tel.: +48 58 3472181
e-mail: pbzura@pg.gda.pl

Abstract

The paper presents a conception allowing to control the processes of changes of the engine operating states based on a diagnostic model of slide bearings. A topological diagnostic model was adopted as a slide bearing model, which allows to use fully the lubricating oil as one of the information carriers about the technical state of bearings. Presented is also interpretation. of the bearing operation states and it has been found that the slide bearing operation state change process is one of important parameters influencing the engine operation state control process.

Keywords: *diagnostics, model, slide bearing*

1. Introduction

In order to be able to use diagnostic tests for control of the slide bearing operation process, it is necessary to build a diagnostic model defining the slide bearing states in the engine operation phases.

The paper presents a possibility of using diagnostic tests describing the technical states of slide bearings in the compression-ignition engine operation in order to control the changes of their state. An optimum engine operation may be effected through controlling those changes of the slide bearing state.

At first, the slide bearing principle of operation is presented, with the parameters necessary for the bearing technical state diagnostic information. Those diagnostic observations allow to construct a transformed topological diagnostic model, taking into account the lubricating oil and other diagnostic signals helpful in determining the technical state of a slide bearing.

In the second part, from an interpretation of the operation states of slide bearings [3], an example has been worked out of a slide bearing operation state change process in the engine time between overhauls.

Finally, a possibility is shown of the practical application of both models to the slide bearing operation control process.

2. Possibilities of identification of the slide bearing states

In order to be able to construct a diagnostic model, an identification procedure of the slide bearing technical and energy state must be known.

Such a procedure is presented in the diagram of slide bearing, where a continuous flow of energy and information as well as diagnostic observation are shown. However, all sorts of diagnostic information distortions (interferences) should also be taken into account when a bearing state is identified.

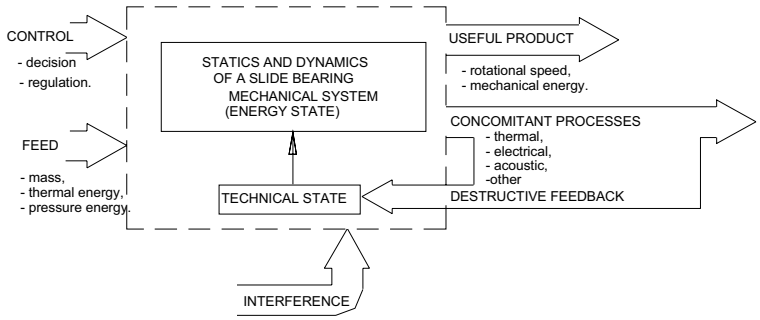

Fig.1. Diagram of a slide bearing as a system with flow of energy and information as well as with a possibility of diagnostic observation

A slide bearing diagnostic model allowing to determine the changes of technical states in the main engine operation process can be constructed mainly in connection with parameters of the concomitant processes which are an inherent part of the slide bearing operation. These are thermal, chemical, electric, acoustic and other processes. Measurements of those parameters allow to estimate the technical condition of a slide bearing without dismantling it, during its normal work.

3. Transformed topological diagnostic model of slide bearings

The transformed topological model (Fig. 3) allows to present general but more complete relations between selected technical states of slide bearings and the distinguishing diagnostic parameters. It allows also more precise analysis, by means of the graph theory and the Lorenz curve [1], of the technical states determining the slide bearing proper functioning. In the operational practice, the change of technical states of a slide bearing is a random process of a continuous positive and restrained realization. Discretization of that process leads to generating an (adequate to reality) set of technical states $S = \{s_1, s_2, s_3\}$, which may be considered a set of the stochastic process values $\{W(t): t \geq 0\}$ with constant intervals and the right-hand-side continuous realizations.

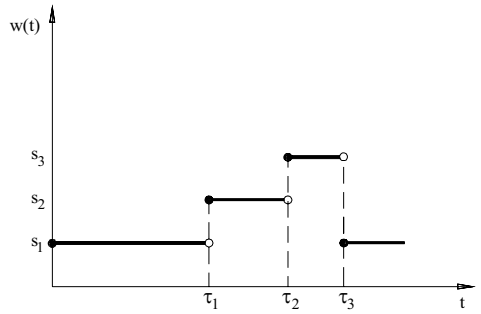

Fig. 2.. Example of realization of an engine slide bearing {W(t):t≥0} process, where: s_1 - state of full ability, s_2 - state of partial ability, s_3 - state of inability;[0, τ_1), [τ_1, τ_2), [τ_2, τ_3) – state duration intervals.

As determination of the technical state of a slide bearing is connected with a high level of disturbances of the diagnostic signals, the reliability of diagnosis is essential for decision taking. Therefore, the diagnostic signals should be treated in the categories of probability and the use of a probabilistic diagnostic matrix is advisable.

The three-element set of technical states S= {s_1, s_2, s_3} consists of a sum of the following three diagnostic matrices:

- State of full ability s_1

$$M_p^{s_1} = \begin{array}{c} \\ s_{11} \\ \vdots \\ s_{15} \end{array} \begin{array}{c} \begin{array}{cccccc} k_1^{(1)} & & k_2^{(1)} & & k_3^{(1)} & \ldots & k_{15}^{(1)} \end{array} \\ \begin{bmatrix} p(k_1^{(1)}|s_{11}) & p(k_2^{(1)}|s_{11}) & p(k_3^{(1)}|s_{11}) & \ldots & p(k_{15}^{(1)}|s_{11}) \\ \ldots & & & & \\ p(k_1^{(1)}|s_{15}) & p(k_2^{(1)}|s_{15}) & p(k_3^{(1)}|s_{15}) & \ldots & p(k_{15}^{(1)}|s_{15}) \end{bmatrix} \end{array} \tag{1}$$

where: $k_1^{(1)}, k_2^{(1)}, k_3^{(1)}, \ldots, k_{15}^{(1)}$ - the s_1={s_{11}, …, s_{15}} state defining diagnostic parameters.

From the probabilistic diagnostic matrix expressed in the form of formula (1) the probability of occurrence of states $s_{1i} \in s_1$, $i = \overline{1,5}$, may be determined by means of formula [2]:

$$p\left(s_{1i} \middle| k_{1i}^{(1)}, k_{2i}^{(1)}, k_{3i}^{(1)}, \ldots, k_{15i}^{(1)}\right) = \frac{p(s_{1i}) \cdot p\left(k_{1i}^{(1)}, k_{2i}^{(1)}, \ldots, k_{15i}^{(1)} \middle| s_{1i}\right)}{p\left(k_{1i}^{(1)}, k_{2i}^{(1)}, k_{3i}^{(1)}, \ldots, k_{15i}^{(1)}\right)} \tag{2}$$

where: $k_{1i}^{(1)}$ - value of parameter $k_1^{(1)}$ meaning the existence of state s_{1i}.

- State of partial ability s_2

$$M_p^{s_2} = \begin{array}{c} \\ s_{21} \\ \vdots \\ s_{24}^* \end{array} \begin{array}{c} \begin{array}{cccccc} k_1^{(2)} & & k_2^{(2)} & & k_3^{(2)} & \ldots & k_{15}^{(2)} \end{array} \\ \begin{bmatrix} p(k_1^{(2)}|s_{21}) & p(k_2^{(2)}|s_{21}) & p(k_3^{(2)}|s_{21}) & \ldots & p(k_{15}^{(2)}|s_{21}) \\ \ldots & & & & \\ p(k_1^{(2)}|s_{24}) & p(k_2^{(2)}|s_{24}) & p(k_3^{(2)}|s_{24}) & \ldots & p(k_{15}^{(2)}|s_{24}) \end{bmatrix} \end{array} \tag{3}$$

where: $k_1^{(2)}, k_2^{(2)}, k_3^{(2)}, \ldots, k_{15}^{(2)}$ - the s_2={s_{21}, …, s_{24}} state defining diagnostic parameters.

Probability of occurrence of states $s_{2i} \in s_2$, $i = \overline{1,4}$, by means of formula [2]:

$$p\left(s_{2j} \middle| k_{1j}^{(2)}, k_{2j}^{(2)}, k_{3j}^{(2)}, \ldots, k_{15j}^{(2)}\right) = \frac{p(s_{2j}) \cdot p\left(k_{1j}^{(2)}, k_{2j}^{(2)}, \ldots, k_{15j}^{(2)} \middle| s_{2j}\right)}{p\left(k_{1j}^{(2)}, k_{2j}^{(2)}, k_{3j}^{(2)}, \ldots, k_{15j}^{(2)}\right)} \tag{4}$$

where: $k_{1j}^{(2)}$ - value of parameter $k_1^{(2)}$ meaning the existence of state s_{2j}.

- State of inability s_3

$$M_p^{s3} = \begin{array}{c} \\ s_{31} \\ \vdots \\ s_{33} \end{array} \begin{array}{c} \begin{array}{cccccc} k_1^{(2)} & & k_2^{(2)} & & k_3^{(2)} & \ldots & k_{15}^{(2)} \end{array} \\ \begin{bmatrix} p(k_1^{(3)}|s_{31}) & p(k_2^{(3)}|s_{31}) & p(k_3^{(3)}|s_{31}) & \ldots & p(k_{15}^{(3)}|s_{31}) \\ \ldots & & & & \\ p(k_1^{(3)}|s_{33}) & p(k_2^{(3)}|s_{33}) & p(k_3^{(3)}|s_{33}) & \ldots & p(k_{15}^{(3)}|s_{33}) \end{bmatrix} \end{array} \tag{5}$$

where: $k_1^{(3)}, k_2^{(3)}, k_3^{(3)}, \ldots, k_{15}^{(3)}$ - the s_1={s_{31}, …, s_{33}} state defining diagnostic parameters.

Probability of occurrence of states $s_{3l} \in s_3$, $i = \overline{1,3}$, by means of formula [2]:

$$p\left(s_{31} \middle| k_{1l}^{(3)}, k_{21}^{(3)}, k_{31}^{(3)}, ..., k_{15l}^{(3)}\right) = \frac{p(s_{31}) \cdot p\left(k_{1l}^{(3)}, k_{21}^{(3)}, ..., k_{15l}^{(3)} \middle| s_{31}\right)}{p\left(k_{1l}^{(3)}, k_{21}^{(3)}, ..., k_{15l}^{(3)}\right)} \tag{6}$$

where: $k_{1l}^{(3)}$ - value of parameter $k_1^{(3)}$ meaning the existence of state s_{3l}.

The presented topological model may be treated as a diagnostic model (MD) of slide bearings in a compression-ignition engine including a probabilistic diagnostic matrix:

$$MD = M_p^{s_1} \cap M_p^{s_2} \cap M_p^{s_3} \tag{7}$$

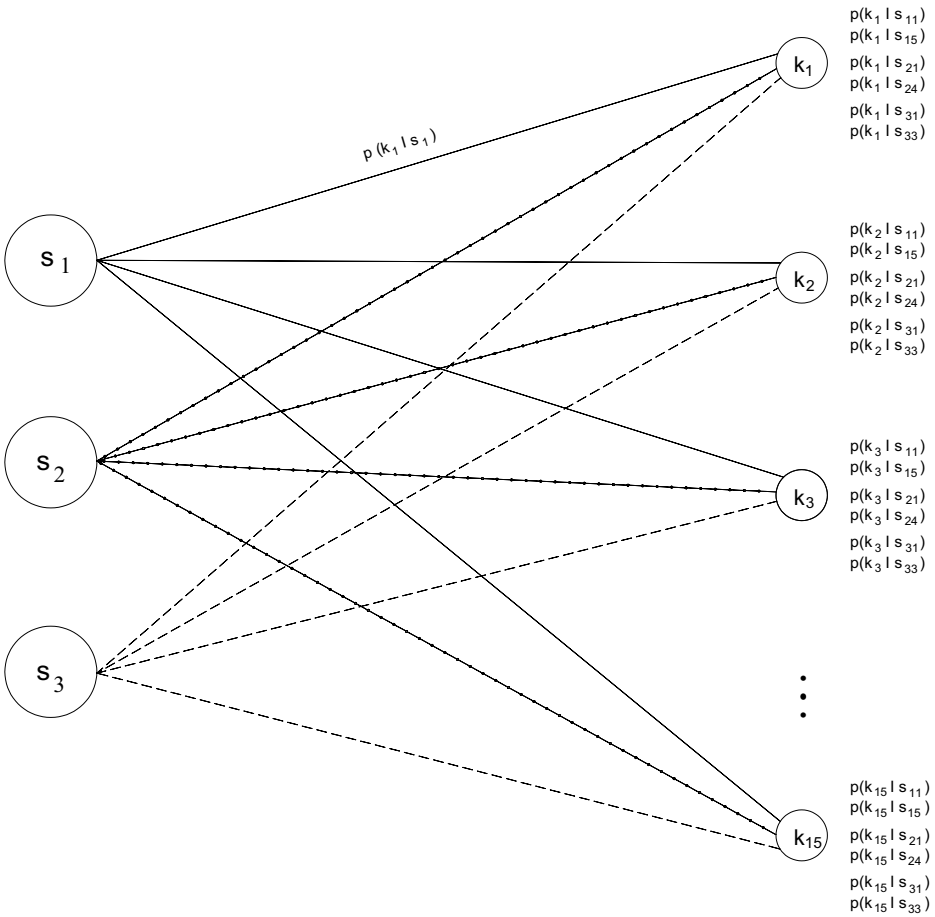

Fig.3. Examples of relations necessary to construct a transformed topological diagnostic model, where: k_1 – kinematic viscosity; k_2 – absolute viscosity; k_3 – base number; k_{15} – thickness of oil film; s_1 – state of full ability; s_2 – state of partial ability; s_3 – state of inability, s_{11} – fresh lubricating oil; s_{15} – less than admissible bearing slackness, the bearing shell and crank pin surfaces without significant traces of wear; s_{21} – lubricating oil with content of water within the range from admissible to limiting; s_{24} – lubricating oil with physical and chemical properties not worse than those admissible; s_{31} - excess linear wear, i.e. bearing slackness greater than the limiting value; s_{33} – lubricating oil with physical and chemical properties not meeting the requirements; $p(k_1|s_{11})$ – the probability of a change of the k_1 parameter value when the s_{11} state occurs.

The processes of changes of the slide bearing technical states are closely connected with the process of changes of their operational conditions.

4. Process of changes of a slide bearing operational states

Proper use of a compression-ignition engine with due attention given to the durability and reliability of slide bearings means that certain rules and principles have to be observed. An example of the interpretation of a slide bearing operational states e_1, e_2, e_3, e_4 may be the following:

State of an active use (e_1)

- introducing a constant oil centrifuging process to all the ship compression-ignition engine lubricating systems,
- using oil filters of the purifying accuracy corresponding to the bearing bushing type and checking those filters in connection with the oil pressure drop value.

State of non-operation (e_2)

- turning the crankshafts and lubricating the idle engine bearings at least once a day,

State of a planned maintenance (e_3)

- periodic checking of the oil physical and chemical properties, including solid impurities,
- periodic checking of journal smoothness and cleanness of the assembly during the preventive maintenance services.

State of forced maintenance (e_4)

- replacement of damaged crank bearing shells,
- replacement of a damaged lubricating oil pump.

The set of operation states $E=\{e_1, e_2, e_3, e_4\}$, as well as the set of technical states, may be treated as a set of the stochastic process $\{X(t):t\in T\}$ values with constant intervals and the right-hand-side continuous realization.

Fig. 4 presents an example of realization of a process of the slide bearing operation state changes in the time between overhauls.

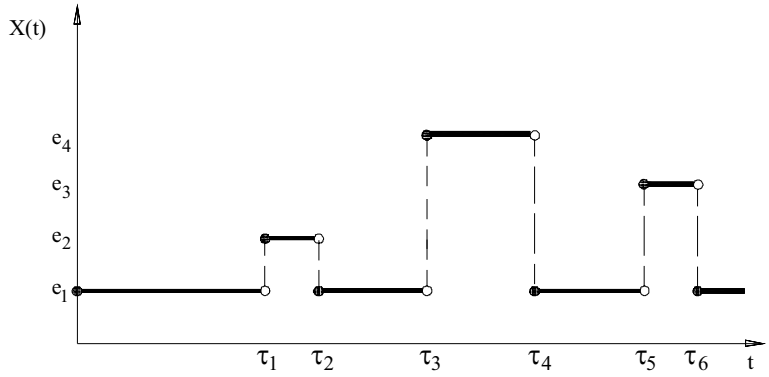

Fig. Example of realization of a slide bearing {X(t): t≥0} process

5. Slide bearing operation process

Realization of the {W(t):t≥0} process (Fig. 2) and the {X(t): t≥0} process (Fig. 4) are interdependent realizations, therefore, like in [2], a two-dimensional process should be considered with the W(t) and X(t) processes as its components. A process in the form of a Cartesian product

of the S and E states has been used. The combined use of both sets of states, which may occur simultaneously, allows to create a set of the slide bearing operation states:

$$Z = S \times E = \{(s_1, e_1), (s_1, e_2), (s_1, e_3), (s_2, e_1), (s_2, e_3), (s_3, e_4)\} \tag{8}$$

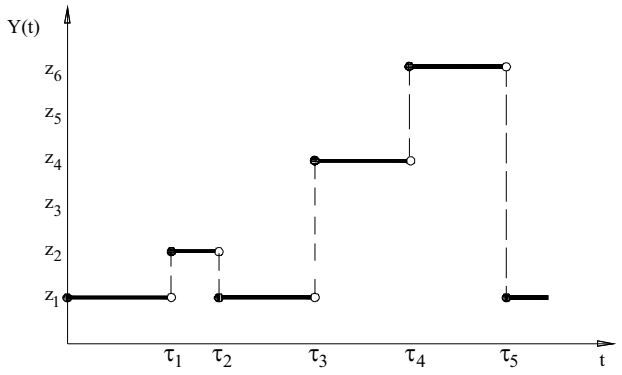

Fig.5. Example of a slide bearing {Y(t): t≥0} process realization, where: {Y(t): t∈T} – the slide bearing operation process $z_1 = (s_1, e_1), z_2 = (s_1, e_2), z_3 = (s_1, e_3), z_4 = (s_2, e_1), z_5 = (s_2, e_3), z_6 = (s_3, e_4)$

The slide bearing s_1 state will last from $\tau_0 = 0$ to τ_3. In the $[\tau_0 = 0, \tau_1)$ time interval the slide bearing was in the e_1 state. At the τ_1 instant the slide bearing found itself in the e_2 state (the engine stopped) and after restarting the engine it returned to the (s_1, e_1) state at the τ_2 instant. Then in the $[\tau_2, \tau_4)$ time interval the bearing was in the e_1 state and at the τ_4 instant it was damaged. Earlier, at the τ_3 instant the slide bearing technical state underwent a change s_2 (partial ability) and the engine load was not changed, which caused a damage in the $[\tau_3, \tau_4)$ time interval. At the τ_4 instant the s_3 state (inability) occurred and lasted during the $[\tau_4, \tau_5)$ time interval, i.e. as long as the e_4 operation state when the s_1 state was restored.

6. Concluding remarks

The analysis presented in this paper suggests that it may be worthwhile to use the transformed topological diagnostic model of slide bearings in the combustion engine operation control process.

References

[1] Bzura, P., *Topological diagnostic model of the main slide bearings of a compression-ignition engine,* (in Polish), XXVII Sympozjum Silowni Okretowych, Szczecin 2006, p.145-152

[2] Girtler, J., *Control of the ship combustion engine operation process by a decision diagnostic model,* (in Polish), ZN AMW, nr 100A, Gdynia 1989.

[3] Kicinski, J., *Selected problems of the construction and operation of large-size slide bearings in combustion engines,* (in Polish), Instytut Maszyn Przepływowych PAN, Gdansk.

MARINE AUXILIARY DIESEL ENGINE TURBOCHARGER DAMAGE (EXPLOSION) CAUSE ANALYSIS

Leszek Chybowski, Zbigniew Matuszak

Maritime Academy of Szczecin
ul. Wały Chrobrego 1-2, 70-500 Szczecin, Poland
tel. +48 01 48 09 412; +49 91 48 09 414
e-mail: lchybowski@am.szczecin.pl; zbimat@am.szczecin.pl

Abstract

In the paper causes of a container ship auxiliary engine turbocharger self damage during its service at sea have been analyzed. The damaged turbocharger working elements have been presented. The direct reason of the turbocharger damage was its explosion. The damage cause analysis takes into consideration the possibility of stimuli accumulation leading to the damage as well as damage causes overlapping and the influence of quality of fuel feeding the auxiliary engine. Eventually the turbocharger damage has been attributed to fuel quality. Probability of fuel seeping into exhaust manifold and scavenge air receiver due to injector needle suspension as well as ignition and combustible properties of fuel feeding the auxiliary engine have been focused on. Injector testing results achieved on trial stand and fuel quality analysis carried out by means of FIA-100/3 analyzer have been presented.

Keywords*: marine engine turbocharger, fuel oil quality, combustion properties, stress accumulation, damage*

1. Introduction

A turbocharger damage cause of a container vessel combustible auxiliary engine during the regular engine room service at sea has become the subject of the following analysis. Before the damage occurred growing whistle denoting the turbocharger revolutionary speed increase significantly exceeding the range of normal revolutionary speeds achieved during its service (28 000-34 000 rpm), which was followed by explosion. The turbocharger suffered total destruction which made the auxiliary engine further exploitation impossible .There were no casualties among the crew members. The engine was stopped and the place protected against possible fire.

In Fig.1. basic turbocharger working components after the explosion have been presented (rest of the compressor rotor, turbine rotor and the broken shaft) by means of marking their location in the broken turbocharger. The turbocharger shaft got divided into two parts as a result of twisting. Its crack occurred near the labyrinthine sealing on the exhaust gas side.

In Fig. 2. main components condition seen from the turbine side and the compressor side have been presented (A - closing cover of exhaust gas side, B - parts of the turbine rotor wheel, C - the gas inlet casing with rest of the nozzle ring of turbine side, D - parts of the compressor casing, parts of the compressor wheel, F - the nozzle ring of compressor side).

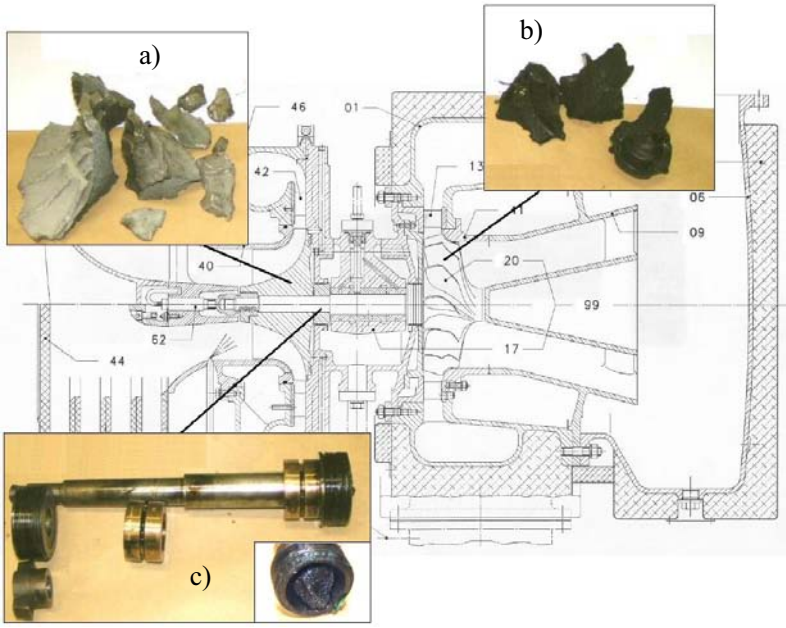

Fig. 1.Rest of the turbocharger working elements after the failure: a) – compressor rotor, b) – turbine rotor, c) – propeller shaft, bearings, and labyrinth sealing

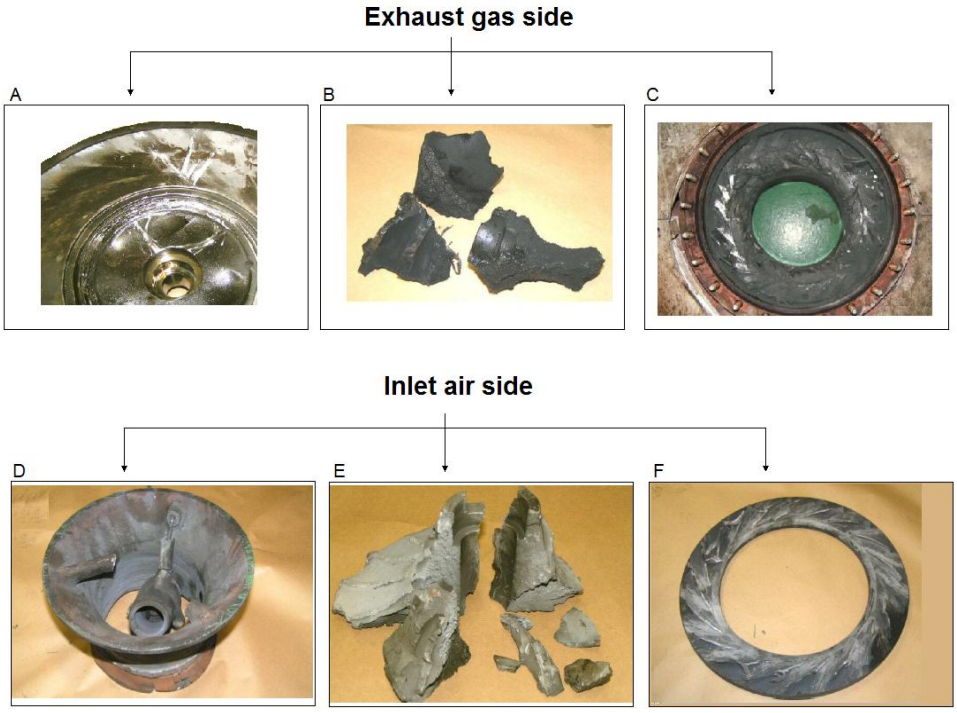

Fig. 2.Damage of working components on both sides of the turbocharger

The components inspection pointed out fuel accumulation in the outlet installation. The turbine casing was covered with a significant amount of carbon deposit and asphalt (Fig. 3.).

Fig. 3. Carbon deposits / asphalts taken from the exhaust gas outlet casing

When analyzing the turbocharger failure causes two cases were taken into consideration:

- -possibility of stimuli accumulation resulting in the damage [5, 6, 7, 18, 21] as well as damage
  causes overlapping [9, 10, 12, 13, 16, 17];
- -influence of the quality of fuel feeding the auxiliary engine.

2.Fuel oil quality and the damaged components of the engine

Physical-chemical fuel oil properties certainly influence correct and failure free working of combustible engines [19, 20, 22]. Fuel oil composition may influence faster wear of fuel injection systems precise pairs as well as forming of sediment and carbon deposits on the components of load exchange system and the engine combustible spaces. Most important characteristics of fuel oils and its effects for diesel engine components are given in Tab. 1.

Combustion quality is an essential indicator for engine fuel oils, however, so far there is no common, standard method of combustion evaluation. One of the calculated indexes defining the property may be *Calculated Carbon Aromaticity Index* (*CCAI*). In the case analyzed above value of *CCAI* was high. It is generally assumed that if *CCAI* value does not exceed 860 during regular service the fuel possesses acceptable combustible quality, there may occur problems with right engine exploitation for fuel oils of *CCAI* between 860-880, exploitation problems including engine damage within a short time shall be caused by fuel oils of *CCAI* beyond 880. Apart from *CCAI* sometimes *Calculated Ignition Index* (*CII*) is used. *CII* gives values for residual fuels in the same order as the cetane index for distillate fuels. However, it should be pointed out that *CCAI* as well as *CII* as indicators are calculated on the basis of fuel viscosity and density according to formulas:

$$CCAI = \cdot\rho_{15} - 141 \cdot \log\log(\nu_{50} + 0{,}85) - 81\,, \tag{1}$$

$$CII = (270{,}795 + 0{,}1038 \cdot T_r) - 254{,}565 \cdot \rho_{15} + 23{,}708 \cdot \log\log(\nu + 0{,}7)\,, \tag{2}$$

where:

ρ_{15} – density at 15ºC [kg/m^3]
υ_{50} – viscosity at 50 ºC [cSt]
υ – viscosity at temperature T_r [cSt]

Tab. 1. Characteristics of engine fuel oils influencing engine work and fuel systems

Quality criteria	Fuel oil characteristics	Main effects
Combustion quality	Conradson Carbon Asphalteness	Ignition ability. Combustion condition. Fouling of gas ways.
Impurity content	Sulphur	Corrosive wear.
	Vanadium Sodium	Formation of deposits on exhaust valves and turbochargers. High temperature corrosion.
	Water	Disturbance of combustion process. Increased heat load of combustion chamber components. Fouling of gas ways. Mechanical wear and cavitation of fuel injection system components.
	Ash Catalyst fines	Mechanical and corrosive wear of combustion chamber components. Formation of deposits. Mechanical wear of fuel injection system, cylinder lines and piston rings.
Handling properties	Viscosity Density Pour point	Temperatures, pressures and capacities of fuel oil systems for storage, pumping and pre-treatment.
	Flash point	Safety requirements.

These measures may be applied only for initial fuel combustible quality evaluation because the indexes do not take into account the influence of fuel chemical composition on the combustion process. In the case above *CCAI* was 850 which means that it ranged within the recommended limits. Combustion process may be defined with the use of combustion analyzers. *DNV Petrolium Services* offers combustion quality tests carried out with the use of *FIA-100/3* analyzer [11]. *FIA – 100/3* establishes the ignition quality of diesel engine fuel oils based on an ignition delay measured on an actually measured ignition delay. A fuel oil sample that is injected into the combustion chamber of *FIA-100/3*, self ignites and burns as in real engine. Start of Main Combustion process is used in order to establish the ignition quality of a fuel oil tested as a *FIA CN* (Cetane Number). For heavy fuel oils the ignition properties are typically ranging from *CN*=18.7 to above *CN*=40. Fuel ignition quality depends on *FIA CN* for different fuel oils is given in Tab. 2.

Tab. 2. Ignition quality of the fuel oil tested as a FIA Cetane Number (FIA CN) (Depends on engine type, engine condition and load) [11]

FIA Cetane Number	Heavy Fuel Oil	Marine Diesel Oil
< 20 to 25	Very bad ignition properties	Unfit for use
25 ≤ FIA CN <28	Bad ignition properties	Very bad ignition properties
28 ≤ FIA CN <35	Acceptable ignition properties	Bad ignition properties
35 ≤ FIA CN <40	Good ignition properties	Acceptable ignition properties
40 ≤ FIA CN <45	Very good ignition properties	Good ignition properties
FIA CN ≥ 45	Very good ignition properties	Very good ignition properties

The basis for *FIA CN* is a reference curve for the instrument in question, showing the ignition properties for mixtures between the reference fuels *U15* and *T22* from *Phillips Petroleum International*. On the basis of these data the mean value for ignition delay, start of main combustion, pressure trace, *FIA CN* and *Rate of Heat Release* (*ROHR*) are established

After the turbocharger had broken down fuel combustible properties were tested by *DNV Petroleum Services*. For the case in question the fuel analysis results obtained with the use of *FIA–100/3* analyzer have been presented in Fig.4.

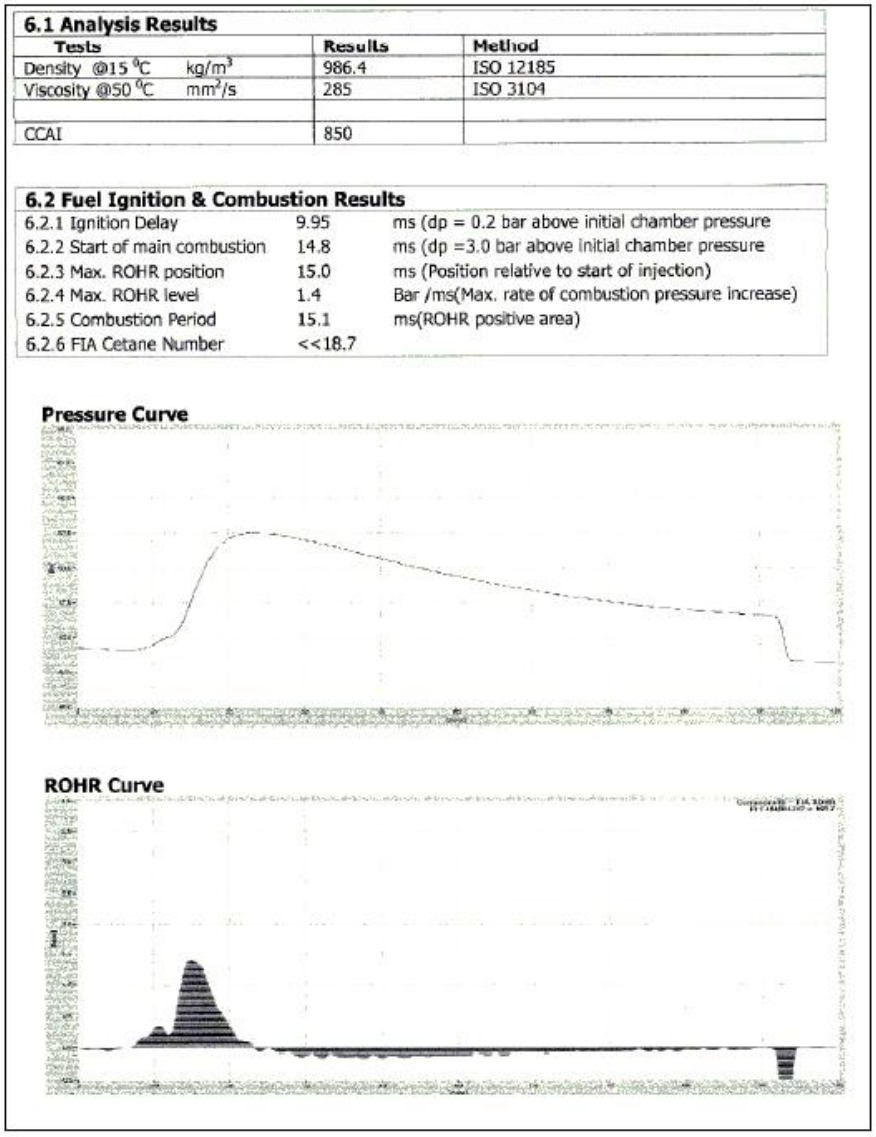

6.1 Analysis Results

Tests	Results	Method
Density @15 °C kg/m³	986.4	ISO 12185
Viscosity @50 °C mm²/s	285	ISO 3104
CCAI	850	

6.2 Fuel Ignition & Combustion Results

6.2.1 Ignition Delay	9.95	ms (dp = 0.2 bar above initial chamber pressure
6.2.2 Start of main combustion	14.8	ms (dp =3.0 bar above initial chamber pressure
6.2.3 Max. ROHR position	15.0	ms (Position relative to start of injection)
6.2.4 Max. ROHR level	1.4	Bar /ms(Max. rate of combustion pressure increase)
6.2.5 Combustion Period	15.1	ms(ROHR positive area)
6.2.6 FIA Cetane Number	<<18.7	

Fig. 4. Combustion tests results carried out by FIA

Value of the *CCAI* being 850, the *Fuel Ignition Analyzer test* results indicate a fuel with very bad ignition quality, *FIA CN*<<18.7. Combustion properties of this fuel are very poor, being below the values of an average intermediate fuel oil. Fuel oils with poor combustion and ignition properties are likely to contribute to high pressure peaks and thermal overload of combustion chamber.

3.Consolidation

The analysis of the described turbocharger damage points out that the main cause of its explosion was leak and not burnt fuel oil accumulated in exhaust manifold and/or scavenge air receiver. The fuel may have leaked into the mentioned spaces due to injection needle suspension, which may have been caused by the adverse effect of sodium contained in the fuel. Then the fuel ignition took place which caused blow-by of vast amount of exhaust gases into the turbine and eventually led to its damage. This cause, however, seems to be unlikely and it has not been explicitly confirmed.

Another cause may have been poor ignition properties and poor combustion quality of the applied fuel. Generally fuel with high *CCAI* ignites very late after injecting it into the combustion chamber and in extreme cases self ignition may not take place at all. Then the not burnt fuel leaks into the charging air spaces and exhaust manifold, and after some time it burns leaving a thick layer of coke. The coke as well as the fuel may cause jamming of valve stems in guides which helps fuel to enter the described spaces.

After testing the injectors of the engine in question performed on the trial stand the first cause was eliminated. Exhaust valves were jammed on two cylinder systems of the engine in question and left in open position during the whole cycle of the engine work. This fact confirms the latter mentioned causes. Presumably the series of events leading to serious damage [1,2,3,4] of auxiliary engine components most probably took place due to very poor combustible property of fuel which was later confirmed by combustion quality tests.

In the discussed above case an engine room fire did not take place, which often happens in such situations (e.g. 13.09.1999 on a Singapore container vessel *X-Press Jaya* the fire broke out as a result of main engine turbocharger explosion [15].

References

[1] Borysiewicz, M., Furtek, A., Potempski, S., *Poradnik ocen ryzyka zwiego z niebezpiecznymi instalacjami procesowymi*, Instytut Energii Atomowej, ZPZiOŚ, IEA Świerk 2001.

[2] Brandowski, A., Grzybowski, P., *Procedura analizy wpływu uszkodzeń na bezpieczeństwo systemu okrętowego (CPBR 9.5)*, Wydawnictwo INPT-WSM, Gdynia 1989.

[3] Chybowski, L., *Analiza pracy systemu energetyczno-napędowego statku typu offshore z wykorzystaniem metody drzew uszkodzeń*, Materiały XXII Sympozjum Siłowni Okrętowych SymSO 2001, WTM Politechnika Szczecińska, pp. 83-88, Szczecin 2001.

[4] Chybowski, L., *Auxiliary installations' fault tree model for operation analysis of vessel's power plant unit*, Балттехмаш – 2002, KGTU, pp. 299-301, Kaliningrad 2002.

[5] Chybowski, L., Matuszak, Z., *Symulacja niegotowości systemu siłowni okrętowej oparta na drzewie niezdatności*, Zeszyty Naukowe nr 1 (73) Akademii Morskiej w Szczecinie, Explo-Ship 2004, Akademia Morska, pp. 145-159, Szczecin 2004.

[6] Chybowski L., Matuszak Z., *Simulation of unavailability of the offshore unit's power plant system with use of selected algorithms*, Problems of Applied Mechanics, International Scientific Journal no 2 (15)/2004, IFToMM of Georgia, pp. 33-47, Tbilisi 2004.

[7] Czajgucki, J. Z., *Metoda realizacji postulatu wymaganej niezawodności spalinowych siłowni okrętowych w procesie ich projektowania*, Wydawnictwo Uczelniane WSM Gdynia, Gdynia 1991.

[8] Esary, J. D., Proschan, F., *The reliability of coherent systems in Redundancy Techniques for Computing Systems*, red. R. H. Wilcox, W. C. Mann. Spartan Books, pp. 47-61, Washington 1962.

[9] Girtler J., *Niezawodność silnika w przypadku wyeliminowania uszkodzeń pochodzących od bodźców kumulujących się*, Zagadnienia Eksploatacji Maszyn Nr 1/1992, pp.75-80.
[10] Gniedenko, B.W., Bielajew, J.K., Sołowiew, A.D., *Metody matematyczne w teorii niezawodności*, WNT, Warszawa 1968.
[11] *Introduction to FIA-100/3*, Materials of Ship Operations Cooperative Program, http://www.socp/projects/completedproj/BunkerFuelOil/Introduction_to_FIA.pdf. 25.10.2006.
[12] Jaźwiński, J., Ważyńska-Fiok, K., *Niezawodność systemu z nadmiarem funkcjonalnych w aspekcie bezpieczeństwa,* Zagadnienia Eksploatacji Maszyn Nr 12/1984, pp. 191-199.
[13] Karpiński, J., Korczak, E., *Metody oceny niezawodności dwustanowych obiektów technicznych*, Omnitech Press, Instytut Badań Systemowych PAN, 1990.
[14] Łuczak, A., Mazur, T., *Fizyczne starzenie elementów maszyn*, WNT, Warszawa 1981.
[15] *Maritime Case Histories*, International Maritime Fire and Rescue Information, FireNet Maritime, http://fire.org.uk/marine/incidents.htm. 05.11.2006.
[16] Matuszak, Z, *Modeli otkazow i prinadleżnost dannych ob otkazach k generalnoj sowokupnosti na primierie sudowych energeticzeskich ustanowok*, Kaliningradskij gosudarstwiennyj techniczeskij uniwersytet, Kaliningrad 2002.
[17] Matuszak, Z., *Badania niezawodności i rozkładów uszkodzeń systemów siłowni okrętowych*, Zeszyty Naukowe Politechniki Śląskiej Nr 22 (seria Organizacja i Zarządzanie), pp. 313-323, Gliwice 2004.
[18] *Niezawodność okrętowych siłowni spalinowych. Sformułowanie problemu i propozycja jego rozwiązania*, Raport techniczny Nr RT-95/T-01, Centrum Techniki Okrętowej, Gdańsk 1995, maszynopis.
[19] Piaseczny, L., *Technologia napraw okrętowych silników spalinowych*, Wydawnictwo Morskie, Gdańsk 1992.
[20] Piotrowski, I., Witkowski, K., *Okrętowe silniki spalinowe*. Trademar, Gdynia 1996.
[21] *System gromadzenia i przetwarzania informacji dotyczących niezawodności i bezpieczeństwa instalacji okrętowych*, Raport techniczny Nr NN96/T-041. Centrum Techniki Okrętowej, Gdańsk 1997, maszynopis.
[22] Wajand, J.A., Wajand, J.T., *Tłokowe silniki spalinowe (średnio- i szybkoobrotowe)*, WNT, Warszawa 1993.
[23] Włodarski, J.K., *Tłokowe silniki spalinowe - procesy trybologiczne*, WKiŁ, Warszawa 1982.

DIAGNOSTICS SYSTEM OF CURRENT GENERATING AGGREGATE OF DIESEL LOCOMOTIVES

Andrzej Erd

Politechnika Radomska
Ul. Malczewskiego 29, 26-600 Radom, Poland
Tel.+48 48 3617743
e-mail a.erd@pr.radom.pl

Abstract

The significance of existence train communication network for diagnostic purpose is described in this paper. It provides background for modern stand for power transmission system in diesel locomotives implemented at the beginning of 2006. Diagram of diagnostic stand for diesel-locomotive is presented. The main diagnostic tests are listed. Tests are divided in two groups: no-load tests and under-load of current aggregate. The last part of paper characterizes software specially created for described object and divided in three parts: software for control of test running, database software and auxiliary software.

Keywords: *diagnostics, current generating aggregate, diesel locomotives*

1. Introduction

Railway manufacturers who are in possession of modern railway vehicles largely avail themselves of on-board diagnostics, due to the actual technical state recognition.

In majority vehicles are provided with the network TCN(Train Communication Network) which consists of two control buses: train bus – WTB (Wire Train Bus) and vehicle one – MVB (Multifunction Vehicle Bus), connected through Gateway (GW) of structure as on fig.1.

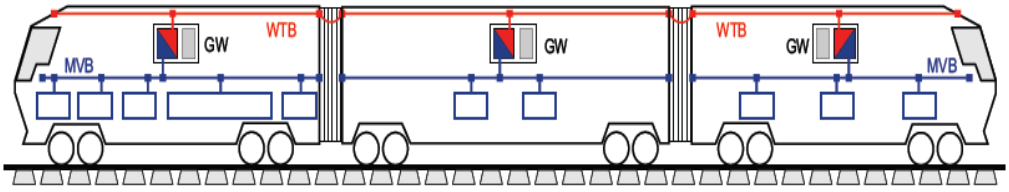

Fig. 1. Basic device of networks communication in UIC Trains.

Presence of these two buses is normalized accordingly to the charter of UIC – the organization of the majority of carries by train in Europe and also in US, China and Japan.

The vehicle network MVB has connectivity up to 255 separate controllers and 4095 individual measurements points. Thus continuous watching performance of all main vehicle units is possible. Presence of diagnostic-oriented controllers allows to record probable action errors or worsening work parameters.

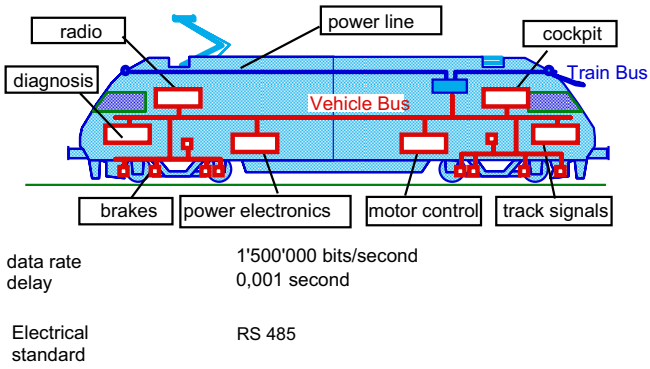

Fig. 2 MVB - Standard communication interface for all kind of on-board equipment in locomotive

Unfortunately, the situation in Poland is quite different for complete lack of rolling-stock electronization.

The whole diagnostics has to be founded on periodical surveying effected on Railway Rolling Stock Works. Stand testing has to ensure the determination of technical condition for main vehicle units. In case of diesel locomotives the base block configuration of the vehicle is shown in fig. 3.

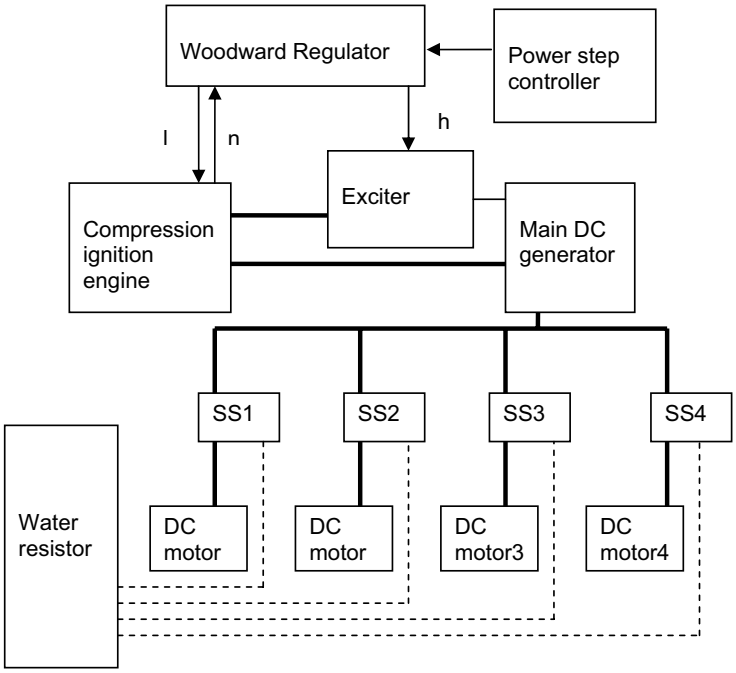

Fig 3. Block diagram of diesel-locomotive, SS1..4 - Motor contactors

2. Stand for power transmission system test

The idea of diagnostic stand testing of diesel locomotives consists in disconnecting electrical driving motors and switching on the water resistor with power selected accordingly. Changes of a resistance of the water resistor allow to vary a quantity of load for current-generating aggregate which is the basic element of power transmission system being examined.

2.1. Stand construction

In this paper one presents the stand being PKP CARGO property located on ground of Railway Rolling Stock Works in Warsaw. The stand is designed for diagnostic testing and adjustment of diesel locomotives.

With the object to make diagnostic investigations, driving motor contactors are disconnected. Instead, load leads are connected through high voltage cubicle and joined to the water resistor. Beside this a locomotive is equipped with additional sensors which allow to measure a number of nonelectric quantities.

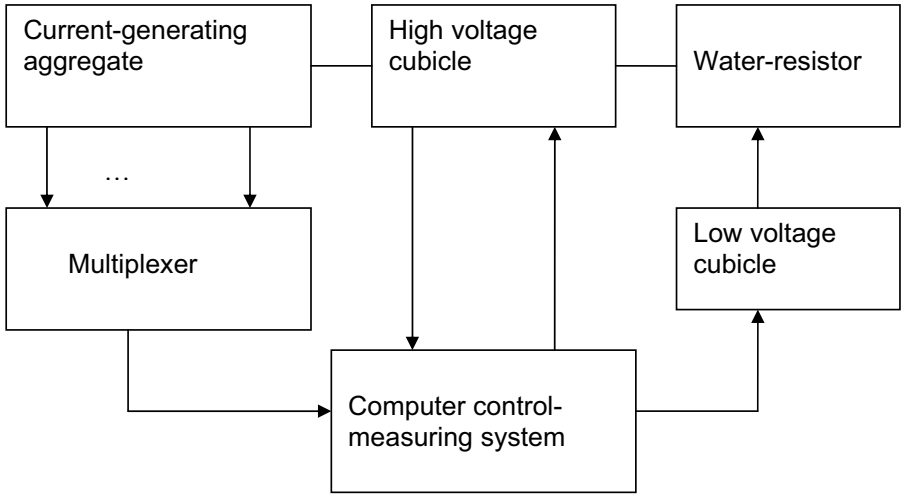

Fig.4. Diagram of diagnostic stand for diesel-locomotive

The sensors are multiplexed by a portable auxiliary cubicle and then directly joined to the measuring system. The sensors indicate, among other things, values of temperature of : ex-haust gas in cylinder, water, oil, fuel; rotational speed of : diesel engine shaft, turbo-compressor, fan; position of fuel charge controller, fuel charge quantity. For proper state evaluation, command of a number of electric quantities is required.

These quantities are first of all the following ones: main generator current and voltage, excitation current of main generator, exciter voltage, voltage of Woodward regulator.

Main parameters of data processing system are presented in tab.1

Tab. 1. Main parameters of computer measuring system

Computer measuring system			
	Number of analog channels		80
	AD converter resolution		16 bits
	Maximal frequency		250 kS
	Insulation voltage		5 kV
Measuring converters			
	Number of voltage channels		4
		Producer of converter	Knick Varitrans
		Model of converter	P27000
	Number of current channels		12
		Producer of converter	LEM
		Model of converter	PR 20, 200, 2000
	Number of pressure channels		32
		Producer of converter	ZEPWN
		Model of converter	CL1, CL5
	Number of temperature channels		19
		Producer of converter	ZEPWN
		Model of converter	CL61, CL62
	Number of displacement channels		2
		Producer of converter	ZEPWN
		Model of converter	CL70
	Number of rotational speed channels		3
		Producer of converter	OPTOM
		Model of converter	S50-PA-5C01-PP (PNP)

2.2. Diagnostic tests

The basic task of diagnostic station software is to regulate the diagnostic test run. However because of practical considerations the station acts also as a regulation stand. In the case of unsuitable work detection of system, as for as it is possible, setting correction of regulating elements is done.
Locomotive tests are divided into following groups:

- No-load tests
  a) control of main generator excitation
  b) control of stepping excitation
  c) control of disconnected-motor voltage

- Under-load tests:
  a) outer characteristic control
  b) shunter characteristic work control
  c) regulation of shunting control
  d) overload relay control
  e) earth fault relay control
  f) transient state characteristic
  g) cooling system control regulation
  h) diesel engine starting test
  i) compression pressure measurement
  j) fuel injection measurement
  k) peak firing pressure measurement
  l) measurement of exhaust gas emission
  m) motive-power battery evaluation

Before carrying out proper tests of power transmission system it is necessary to check the excitation of main generator; no-load test units provide this purpose.

Among the under-load tests the most important are (a) and (f). If improper characteristics or suspicious as to wrong diesel engine work are found then tests (j) and (k) are concluded. The residual tests are conducted in purpose to see auxiliary locomotive systems work properly.

2.3. Database software

Test execution should be proceeded by the vehicle and test files. In this purpose station diary is kept. The diary contains general data about the vehicle, and service staff. During basic data input it is possible to reload vehicle data with results of "hand-made" measurements scheduled for periodical surveying. Exemplary of such data are: results of insulation resistance measurement of main circuit and generator R_{15} and $R_{60,}$ also standard required R_{15}/R_{60} coefficient. Moreover, with the purpose of recording, one loads data of water and oil analyses.

2.4. Auxiliary Software

Measuring computer system takes out data from sensor units in voltage form and processes them with analog-to-digital converters. In the object to demanded accuracy assurance it is possible to calibrate respective measuring channels by change of voltage gain and also characteristic shift in zero. For this purpose, unit of program aid of calibration was built up in system. For servicing and screen display it is possible to make configuration of particular channels, in the meaning of availability, during measuring processes.

Protocol listing of particular tests is necessary element of investigation. Formatting procedure is determined in pattern sheets modified by system administrator.

Because of importance of measuring data operating, process has to be protected against unauthorized access with the aid of individual passwords for each system operator and administrator.

3. Summary

The presented system was implemented at the beginning of 2006. It is modern treatment and allows to improve operating quality of diesel locomotives. Precise control of power transmission systems permits to obtain significant economical effects in fuel consumption.

References

[1] *Train Communication Network IEC 61375* International Electrotechnical Committee, Geneva http ://www.iec.tcn.org

[2] Kirchmann Hubert, *The ICC/IEE Train Communication Network*, ABB Corporate Research and P.A. Zauber Daimler Chrysler Rail Systems, http://lamspeople.epfl.ch/kirchmann/Pubs/m2kirr.lo.pdf.

[3] Plint Michael, Martyr Anthony, *Engine Testing Theory and practice,* Butterworth Heineman, Oxford Boston Johannesburg 1999.

[4] *Dokumentacja Techniczno Ruchowa. Urządzenie do diagnostyki agregatu prądotwórczego lokomotyw*. Zakład Elektroniki Pomiarowej Wielkości Nieelektrycznych, Marki, Unpublished Issue, 2006.

THE DIAGNOSTIC OF TECHNICAL CONDITION OF TURBINE ENGINE'S BEARING BY MEANS OF METHOD OF ALTERNATOR FREQUENCY MODULATION

Andrzej Gębura, Tomasz Tokarski

Instytut Techniczny Wojsk Lotniczych
ul. Księcia Bolesława 6, 01-494 Warszawa, skr. poczt. 96
tel. 0-22 - 6856510
e-mail: andrzej.gebura@itwl.pl

Abstract

The paper has been intended to discuss an application of a diagnostic method based on measurements and analyses of frequency modulation.

The method has been developed at Instytut Techniczny Wojsk Lotniczych – ITWL (Air Force Institute of Technology, Warszawa, Poland). It has been based on measurements of pulse-frequency modulation of a DC generator or that of an AC alternator. The method has been intended to determine the usual wear-and-tear of a subassembly under examination and to locate defects, both of them in the course of normal operation of an aircraft power plant. The diagnostic system is connected to any terminal supplied with DC[1] or AC[2] voltage.

Results of performance tests of the turbine engine have been presented. An airborne D.C. generator and a three-phase rate A.C. alternator were used as generators-observers.

Subsequent stages of the wear-and-tear of rolling bearings, the turbine unbalance, and the misalignment were observed while taking measurements during both flight and bench tests. What was observed first was some increase in the amplitude of braking the bearing induced by the increasing resistance to motion due to the wear-and-tear of the bearing's components. Then, the amplitude was observed to decrease due to the wearing-in of the bearing's components. At the beginning of operation, the rolling-friction coefficient was 0.4, then this value kept increasing with time until some rapid decrease beyond any mathematical meaning. This decrease resulted from the extension of radial clearances.

Such being the case, the bearing's operation had to be stopped to avoid intense destructive effects.

Key words*: distortion, frequency, modulation, characteristic set, power-plant diagnosing*

1. Introduction

Power plants often suffer premature wear-and-tear, which means complications to the operational-use/maintenance schedule and sometimes even a real hazard to human life.

Most maintenance systems in Poland have been based on calendar/hourly-rated schedules. In case of repairs/overhauls within such systems, it quite often appears that a given power plant under treatment doesn't, in fact, require any renewal and can be operated further on to the benefit of its operator. The on-condition maintenance enables, with reliable technical means and methods employed, the monitoring of any item's health/maintenance status and the withdrawing it from operation as soon as the recorded symptoms prove the object may be hazardous.

In the Author's opinion, the presented FAM-C method can become a precious tool of the interference-free monitoring of health/maintenance status of power plants for example turbine

[1] The method has been labelled 'FDM-A' (F - frequency, M - modulation, D - direct current, A - level of the method's advance)
[2] The method has been labelled 'FAM-C' (F - frequency, M - modulation, A - alternating current, C - level of the method's advance, here: C means that the system finds application as an automatic tester)

engine's ball bearings. Some applications discussed further on have already proved some maintenance-dedicated advantages of this method. These are as follows:

- no need to use any sensors – a regular built-in alternator assembly plays this role,
- measurements can be taken at any point of the electric network, even far away from the object under examination,
- easy automation of the diagnostic process,
- high speed of acquiring diagnostic information.

The FAM-C method has been based on measuring the alternator's frequency modulation. It has been used for many years in aviation to diagnose, e.g.: one-way clutches, motor-generator sets, gear boxes, etc.

2. Description of the FAM-C diagnostic method

The method was thoroughly described in [2,6÷13]. However for better understanding the subject's context some its more important elements are highlighted below.

With every assembling or wear fault e.g. skew of transmission splined couplings, a modulation of the output rotational speed is associated. Period of the modulation is proved to be a characteristic parameter for the fault type and rated rotational speed of a given kinematic pair. Where as the modulation amplitude is proportional to size of a given fault. The modulation effects are transferred through the transmission system to the rotor of the alternator. The aircraft alternator, being a synchronous machine, reflects changes of the instantaneous angular speed as a modulation of the output voltage frequency. By measuring the time increments between successive zero-level crossing points and applying the inverses of their doubled values on the plane of the rectangular coordinates (t , f_i) a set can be obtained which reflects, in a discrete way, a course of speed changes of the alternator's rotor. Two parameters can be assigned to every i-th deviation, as follows:

- the deviation time Δt_i,
- the deviation amplitude ΔF_i.

The deviation time Δt_i can be replaced with the process frequency fp according to the formula:

$$f_{pi} = 1/(2\Delta t_i) \tag{1}$$

Every such deviation can be represented on the plane (f_p , ΔF). During many investigations it was observed that the set of such points tends to gather into clusters. They were called the characteristic sets as they characterised wear state of particular subassemblies.

It was observed that they had different shapes, heights and locations relative to the abscissa axis. It was also stated that the greater the fault magnitude the greater height of a given cluster, $\{/\Delta F_{max}+\Delta F_{min}/\}$, and the bound accommodated by the cluster relative to the abscissa axis 0-fp was characteristic for a given subassembly type. During many applications of the method it was stated that the representations realised in the form of the characteristic sets have been applicable for a thoroughly recognised object, i.e. that of known relations between change of magnitude of a mechanical fault and that of depth of modulation amplitude. Use of such representations has many advantages:

- easiness of diagnostic process automation,
- easiness of observation, on one plane, of arbitrarily long time courses, which is especially important in the case of occurrence of stochastic signals,
- easiness of pulse component separation out of highly modulated signals, free from drawbacks of partial Fourier's analysis.

However, in spite of the advantages of the representation method in question, its use is not recommended for the objects not recognised in the earlier given sense, and direct using the functional courses f_i = f(t) is instead advised for diagnostic purposes. The experienced

diagnostician is able to make use of it effectively for assessment of technical state of an object, however in a more time consuming way.

3. Description of the diagnose object as well as the meter circuit

The single-shaft turbine engine has been an object of examinination (Fig. 1). The motion shaft has been sectional (compresor's shaft turbine's shaft) and connected in the centre by means of a splined coupling. It has been supported on three rolling bearins. The fore bearing had 12 rolling components. The central (midle) and rear bearings had 22 components. Their charcteristic sets have been easily distingnished by means of FAM-C method. The central bearing is pressed into a spring sleeve, which is fastoned by its splines with engine frame. Sometimes during engine's overhauls the traces of bearing's circut rotation in the sleeve (slides) become visible. The craks of the sleeve also occur.

The internal bearing's ring is pressed on the compressor's pin. The tear of that point is in danger of crash, because it causes the tear of link with the power turbine – stops drives of pomps and other units nesessary for running of engine. The point is submitted multivector stresses. Skews often arise in that point. They introduce dynamic load. Additional forces arise in that point.They are caused by bearing's assembly errors and radial clearances. Distinct levels under small radial clerance of the central support are dangerous from point of view of the pin's loads – strong loads occur and bend the pin. Slides of internal ring of the bearing on the pin are the most threatening operating conditions. They cause dynamic excesses and increase the level of thermal field.

Considering engine construction it is very important to secure the bearing mountings to be coaxial. Theoreticaly, all three bearings should be in one axis with small tolerance. Changes in the coaxial geometry lead to troubles in bearing operation.

Condition of the bearing separator, which separates bearing's rolling components, is very important component of every bearing. Smothness of bearing montion ensures corrctness of reeling rolling components.

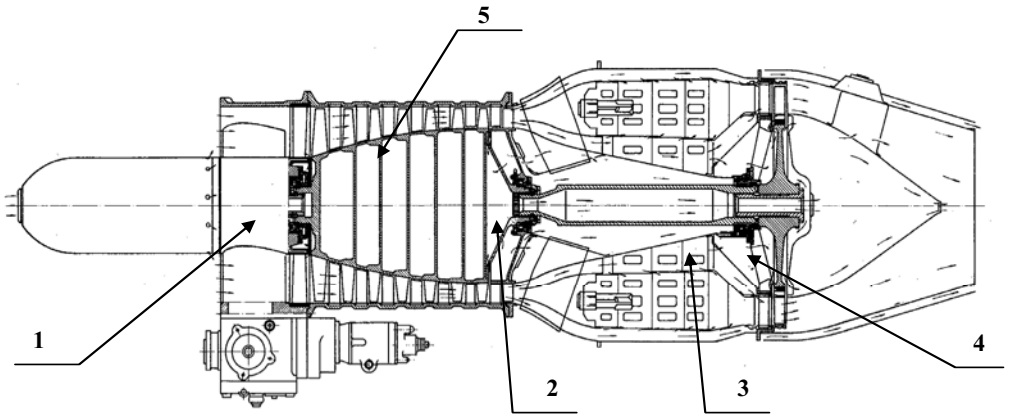

Fig. 1. Investigated turbine engine: 1 – fore bearing, 2 – central bearing, the point of coupling both parts of the shaft (turbine's shaft, compressor' shaft), 3 – rear bearing, 4 – turbine, 5 - compressor

The investigation has been executed differently – Fig.. 2. Signals from the genrator DC and the three-phase rate generator AC have been used for the investigation. Both channels have been complementary to one another.

The three-phase rate generator AC "has afforded" information about faults relevant to the slowly unstable processes:

a) technical condition of the gear box,
b) unbalance of the main motion shaft (with compressor and turbine) as well as the size of the radial clerance in bearing support (Fig. 3),
c) skew of the main shft – it can be evaluated, if skew of the compressor's shaft increases. It can be also evaluated, if the skew does not exceed permissible value specified by manufacturer of the bearing,
d) crack of the sleeve fastering the control bearing.

Generator DC "has afforded" information about fast – changing processes. The fallowing can be observed and diagnosed:

a) the main shaft co-operation with the vibration damper of the lateral vibration (central support) - Fig. 5,
b) extended friction force of the force bearing caused by longitudinal montion of the compressor's shaft ($h \geq 12\cdot$, $p_s \geq 0{,}4$),
c) blocking of the front bearing separator – 12 th harmonic of the rotational speed of the main shaft appers (h=12),
d) blocking of the central bearing separator – 22 nd harmonic of the rotational speed of the main shaft appers (h=22) - Fig. 6,
e) total level of the wear of the wear of the bearing kinematic pair.

4. Succeeding typical stages of the wear of bearings by means of FAM-C method

According to the bibliography there are three succeeding stages of the wear of bearing [5]: noisy, vibrating, thermal.

In the subject engine bearing separator is covered with the galvanic layer of silver. In the first period of operating (i.e. noisy) spalling of the silver follows. In this cause more heavy operation of bearings is observed. This height of characteristic sets (Fig. 3) of bearings systematical increases – Fig. 4. The coefficient[3] of reeling of the central bearing, which is determined from the proportion of total band with frequency of N harmonic (where N – number of rolling components, also increases during this time – bearing separator rotates with difficulty.

In the second stage – vibrating – the height of characteristic sets systematically decreases – in view of coming to an end of spalling of galvanic layer and rinsing out previous spalling products by circulation of lubricating oil. The coefficient of reeling also decreases. In this stage considerable clerances in the bearing occur. The process of wear goes on, but the wear is a result of dynamic forces influencing moveable components of the bearing in the environment of increasing clerances. During the investigation value of the reeling coefficient below mathematical sense has been mentioned. It can mean, that not all-rolling components of the bearing reel themselves on the bearing race. In the stage of vibrating wear cracks of the sleeve which fastens the external bearing race with the engine's frame. This crac has been detected in the circuit of the three-phase rate generator by means of the first harmonic of the main shaft for all rotational speeds, except the speed approximate maximal decreases almost – 10 times – Fig. 7. Sometimes symptoms of a mechanical resonance occur characteristic set or sets decrease of their frequency band. Sometimes the height of characteristic set increases – so-called mechanical quality factor of a kinematics pair increases (Fig. 3 – point 2). This stages, as it appears from experiences of authors, sometimes signal advanced level of kinematics pair destruction (Fig. 7).

[3] the bearing factor – a proportion of an average angular velocity of the main symmetry axis of the bearing component and a velocity of the main shaft

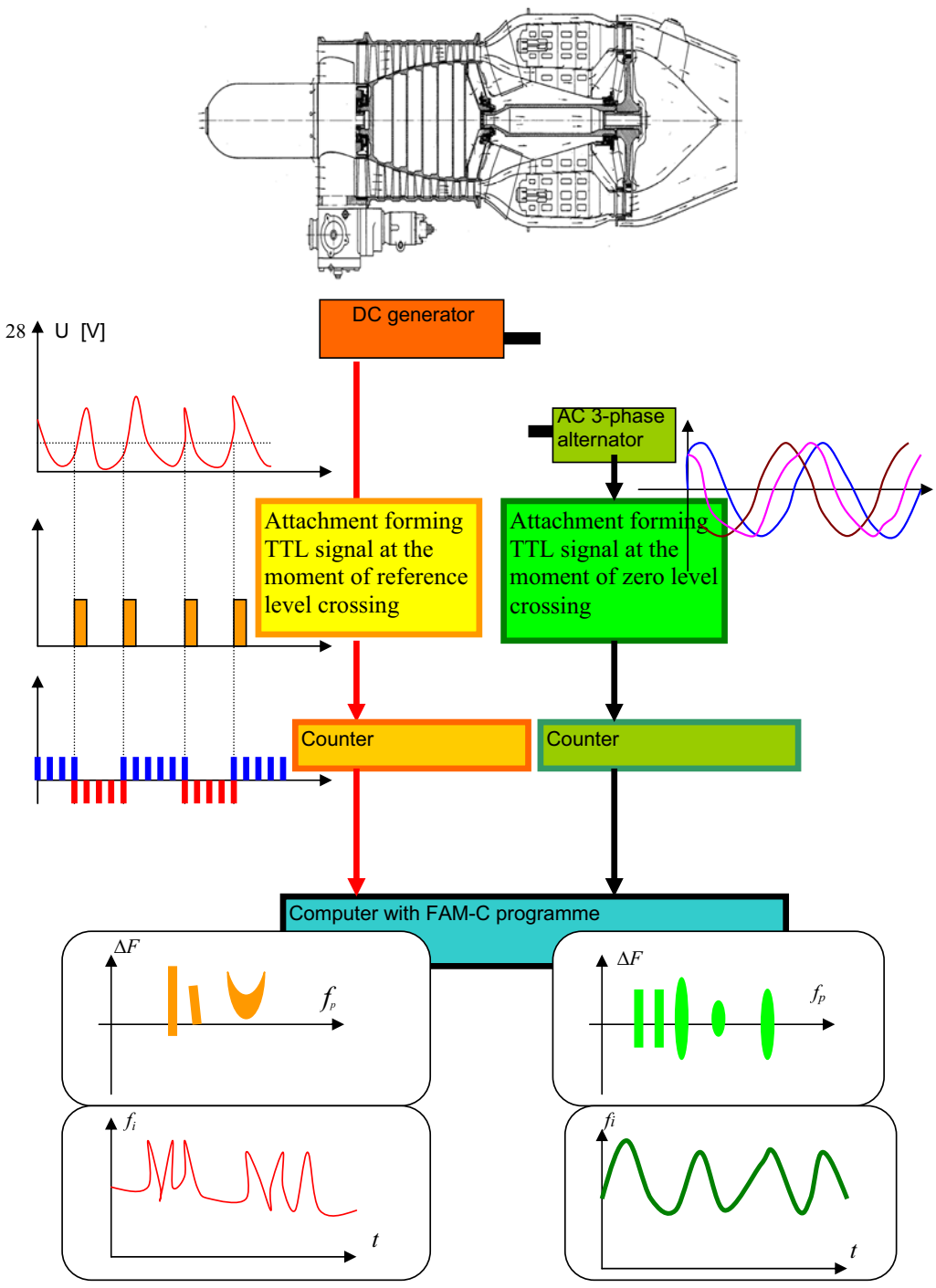

Fig. 2. The method of gaining of diagnostic signal from the engine investigated by means of FAM-C method

During intensifying of occurrence of rolling components reeling along the bearing race, total disappearance of rotation of most rolling components – the stage of thermal wear begins. Considerable amount of heat emits in the bearing. By now oil circulation does not secure an off take of heat in the bearing. As a result of increased temperature a reduction of strengths of material structure of bearing's components follows (e.g. intensive working of window width in the bearing separator even an interruption of separation – Fig. 7). Groups of pulses which number is proportional to number of interrupted windows are generated. The shape and parameters of generated groups are repeated. As a result of direct action of rolling components, groups of pulses can be observed in alternating current channel for a momentary frequency in time f_i = f (t). Simultaneously a pulsation amplitude increased from level about 10% to 160%. As a result of increased temperature a thermal deformation of central bearing's ring follows. The bearing loses a clamp on the pin and slides. Using FAM-C method in a direct current DC generator channel, an angle of those slides as well as their frequency can be precisely defined. To this and a duration as well as a repeat time of dissipated pulses of the momentary frequency in time f_i = f (t).

5. Assembly errors observing by means of FAM-C method

Assembly errors of bearing supports should be distinguished independently on wear processes. They can influence acceleration or deceleration of the duration of particular wear stages. Errors are as follows:

- radial clearances particular bearings,
- increased backlashes,
- coaxial error of three bearing supports – Fig.8,
- unbalance error of the turbine or the compressor,
- ovalization error of the bearing mounting,
- skew error of couplings of both parts of shafts,
- perpendicularity error of the compressor pin,

Increased radial clearances appear as a increase of the characteristic set amplitude (presentation of ΔF = f(f_p) central bearing for the channel generator. The increase of circuit clearances in the channel of AC generator appear as a particular undercuts of diagram f_i = f(t).

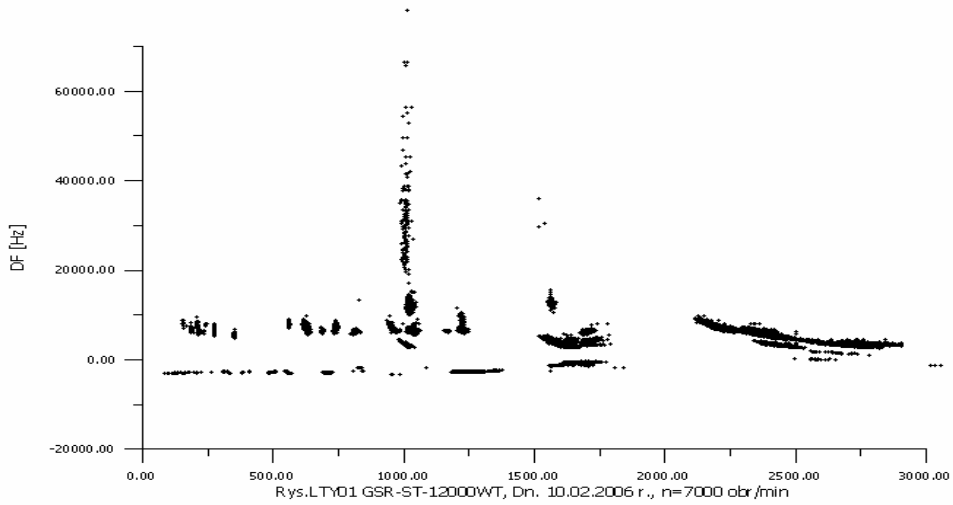

Fig. 3 Characteristic sets obtained from DC generator channel

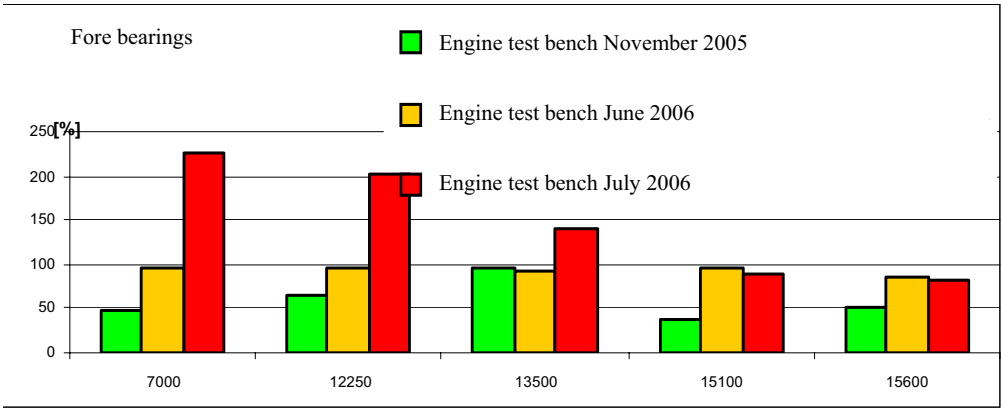

Fig. 4. The graph of the characteristic set height of the fore bearing for three succeeding observation periods of the rolling bearing in the stage of noise wear

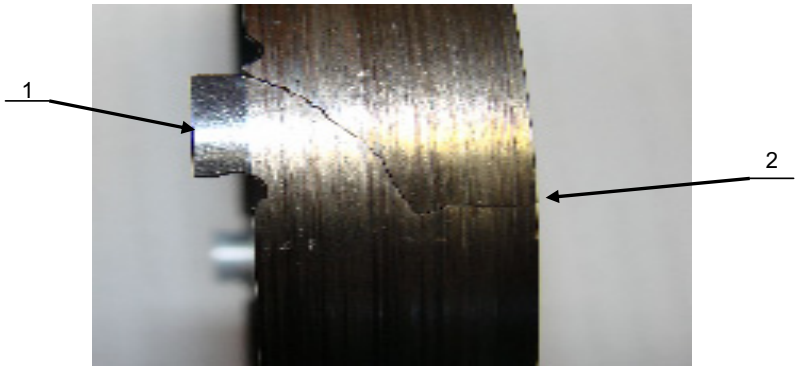

Fig. 5. The cracked sleeve fastening the internal bearing race to the engine frame: 1 – the component protecting the sleeve against rotation, 2 – the point of sleeve crack

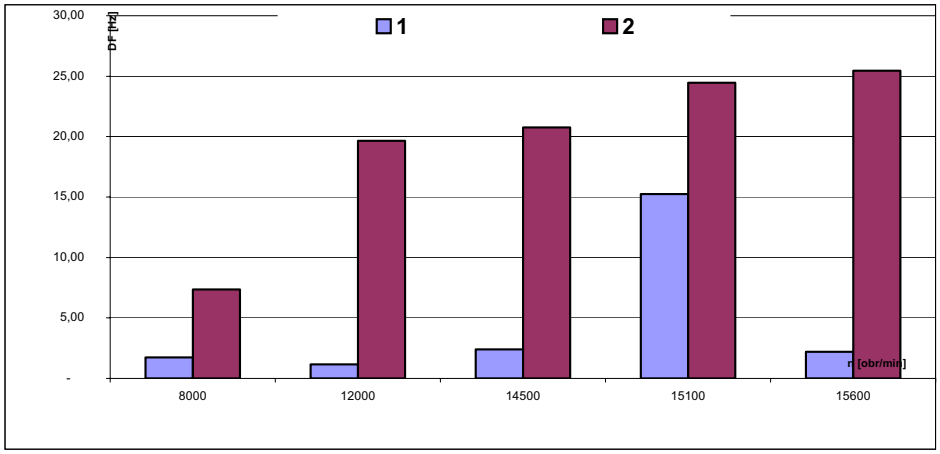

Fig. 6 Changes of the characteristic sets height of the first harmonic after the crack of the sleeve fastening internal bearing race to the engine frame: 1 – after the crack of the sleeve, 2 – before the crack of the sleeve

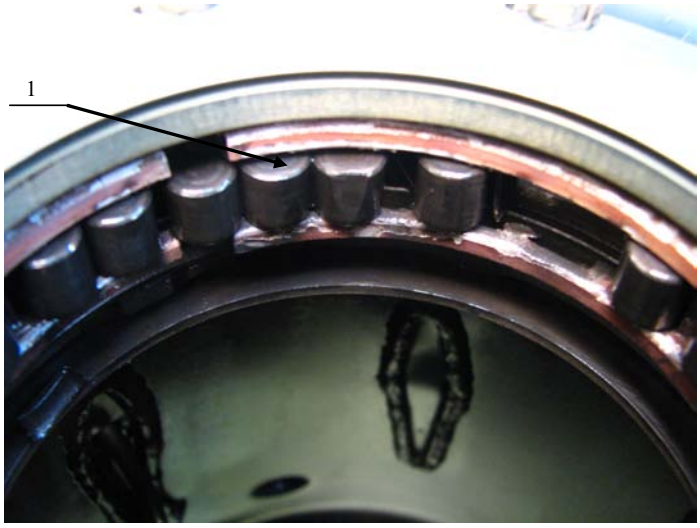

Fig. 7. The damaged central bearing diagnosed by means of FAM-C method: 1- interrupted ring of the spacer-separator

Generally all characteristics of reeling coefficient are inversely proportional to rotational speed. Increased hydrodynamic forces can easily explain it with decrease resistance of rolling friction. Long- drown observations supported by mechanical measurements have enabled a statement, that if minimum appears on the reeling characteristic, considerable value of non-coaxial bearing supports occurs.

An unbalance error of the turbine or the compressor appears as a increase of the characteristic set amplitude in the channel of AC generator (presentation $\Delta F = f(f_p)$ first harmonic of rotational speed of the main shaft as well as an extension of the band width). If the error of an ovalization of the bearing mounting appears the characteristic set disintegrates as a two vertical characteristic sets. A skew of the coupling of both shaft parts appears as a increase of the characteristic sets height of the first subharmonic.

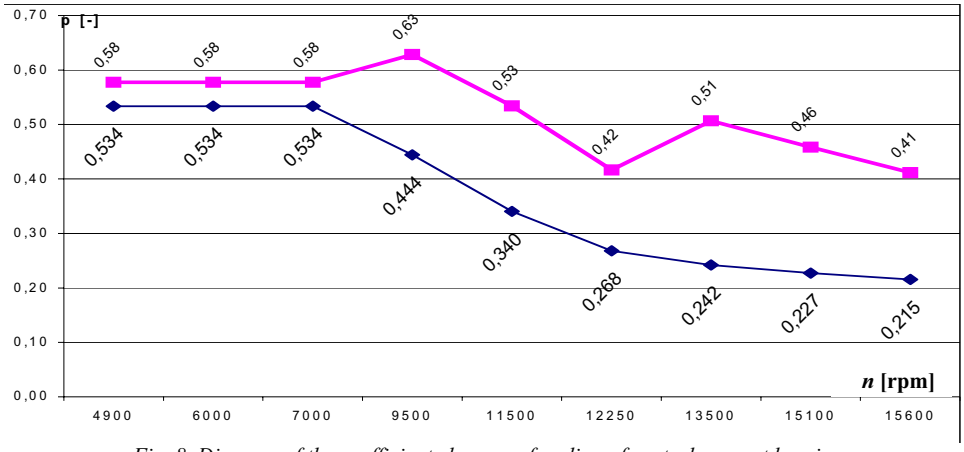

Fig. 8. Diagram of the coefficient changes of reeling of central support bearing:
- *top diagram – under negative coaxial,*
- *bottom diagram under positive coaxial.*

A perpendicularity error of the compressor's pin can be determined by means of a measurement of amplitude modulation depth on the presentation $f_i = f(t)$.

Summary

In the paper theory and application of the diagnostic FAM-C method have been described. This method is based on analysis of frequency modulation parameters of output voltage used for diagnosis of technical condition of turbine engines bearing supports. The application of FAM-C method enables prior detection of subassembly failure, before the failure is danger for flight safety. It is possible to detect various assembly errors as well as monitor of wears effects occurring in bearing supports.

Bibliography

[1] Abramov, B. I., *Waddle wheel with tooth primary form,* Charków, 1968

[2] Biarda, D., Falkowski, P., Gębura, A., Kowalczyk, A., *Opis patentowy PL 175664B1. Sposób diagnozowania technicznego elementów sprzęgających silnik, a zwłaszcza lotniczy silnik spalinowy, z prądnicą prądu przemiennego,* Zgłoszenie 08.07.1996, udzielenie patentu 29.01.1999

[3] Borgoń, J., Stukonis, M., Szymczak, J., *Czy uszkodzenia połączeń wielowypustowych w silnikach lotniczych mogą spowodować wypadki lotnicze,* Informator wewn. ITWL nr 311/93, [w:] Materiały konferencji "Techniczne problemy eksploatacji i niezawodności wojskowych statków powietrznych", Kiekrz 1993

[4] Bułgakow, E.B., Gałobanow, W.W., Klimow, A.W., *Informacionno -izmieritielnaia sistiema kontrolia sostojania aviacionnych i obszczziemaszinostroitielnych rieduktorov, privodov i korobok pieriedacz* „Informacionnyj matieriał", Centralny Lotniczy Instytut Konstrukcji Napędów im. P. I. Baranowa, Moskwa 1990

[5] Cempel, C., *Podstawy wibroakustycznej diagnostyki maszyn,* WNT, Warszawa 1982

[6] Gębura A., Falkowski P., Kowalczyk A, Lindstedt P., *Diagnozowanie skrzyń napędowych,* Zagadnienia Eksploatacji Maszyn, zeszyt 4/97(120)

[7] Gębura, A., Falkowski, P., Kowalczyk, A., *Airborne generators as diagnostic sensors of a power transmission system,* 5-th International Conference Aircraft and Helicopters Diagnostic AIRDIAG'97, Warsaw 1997

[8] Gębura, A., *Związki modulacji częstotliwości napięcia wyjściowego prądnicy z wybranymi wadami układu napędowego,* [w:] monografia pod redakcją naukową prof. M. Orkisza p.t. „Turbinowe silniki lotnicze w ujęciu problemowym"; Polskie Naukowo-Techniczne Towarzystwo Eksploatacyjne, Lublin 2000, ss. 75-93

[9] Gębura, A*., Przekoszenia połączeń wielowypustowych a modulacja częstotliwości prądnic,* Zagadnienia Eksploatacji Maszyn, zeszyt 4/99(120)

[10] Gębura, A., *Diagnostic of aircraft power transmission track based on the analisys of generator's frequency*, Journal of Technical Physics, No. 1/2002

[11] Gębura, A., Radoń, T., Tokarski, T., *Diagnozowanie zespołów napędowych na podstawie obserwacji zmian częstotliwości napięcia wyjściowego prądnic,* II Międzynarodowa Konferencja N-T „Explo-Diesel&Gas Turbine'01", Gdańsk-Międzyzdroje-Kopenhaga 2001

[12] Gębura, A., *Pulsacje napięcia wyjściowego prądnicy pokładowej prądu stałego źródłem informacji diagnostycznej o stanie układu napędowego,* Zagadnienia Eksploatacji Maszyn, zeszyt 1 (133) 2003

[13] Gębura, A., *Possibilities of FAM-C method in diagnosting ship power plants*, Polish Maritime Research No 2 (36) 2003 Vol 10

STATISTIC AND PROBABILISTIC MEASURES OF DIAGNOSIS LIKELIHOOD ON THE STATE OF SELF-IGNITION COMBUSTION ENGINES

Jerzy Girtler

Politechnika Gdańska
Wydział Oceanotechniki i Okrętownictwa
80-951 Gdańsk, ul. G. Narutowicza 11/12
tel. +48 58 347-2430, tel./fax: +48 58 347-1981, fax: +48 58 341-47-12
e-mail: jgirtl@pg.gda.pl; sek4oce@pg.gda.pl

Abstract

The paper presents the reasons for the need to differ the notions of: diagnosis likelihood and diagnosis rightness at making operating decisions. The formula of probability for formulating the right diagnosis, as the measure of diagnosis likelihood, has been herein derived. For deriving this formula the theory of semi-Markov processes and the Bayes' formula of conditional probability have been applied. Other probabilistic measures of diagnosis likelihood have also been provided. These measures have been referred to technical state of such important systems as e.g. main engines of sea-going ships. However, they can be useful for determining the technical state of other transport means.

1. Introduction

The diagnostic inference [1] enables, in the stochastic decision situation, formulating a diagnosis at determined likelihood. The knowledge of the diagnosis likelihood is necessary for taking a rational operating decision – this is such operating decision which has been worked out by using the optimum calculus [4, 7]. It is also known that each arbitrary decision should be taken only after analyzing the results of its performance. Deciding of which the result is the decision, should be understood as making a non-random choose at work, although, up to the moment of taking the decision, there are used probabilistic and stochastic measures of phenomena, events and processes which occur in the phase of operating the self-ignition combustion engines as e.g. main engines of sea-going ships, and measures of the diagnosis likelihood, too [3, 4, 5]. These measures are necessary to work out decision information which enables making the decision, e.g. the decision on whether determined self-ignition combustion engines such as main engines of sea-going ships can be used to realize a given task or whether their states need prior renovation after which they can be used to realize the task.

The diagnosis likelihood is determined in different ways [5]. It can be accepted that the diagnosis likelihood is:

- *in the descriptive meaning*, a characteristic of a diagnosis which describes the degree of identification of the real (past, actual, future) state (technical, energy – more generally, operating) of a self-ignition combustion engine acting as a diagnosed system (DNS), made by a diagnosing system (DGS).
- *in the valuing meaning,* a characteristic of a diagnosis which is determined by values of essential, in particular cases, indexes that describe the degree of identification of the state of a the self-ignition combustion engine (DNS) by the DGS.

The identification consists in that the DGS classifies the real state of DNS to the known class of diagnostic model states. Such action equals taking a diagnostic decision and in consequence of that – an operating decision.

The indexes that describe the degree of identification of the state of self-ignition combustion engines (DNS), are:

- probability of taking the right diagnostic decision (DG),
- ratio of the expected number of identified (in the fixed time) states of the DNS by the DGS to the expected number of really occurred DNS' states of the same kind (in the same time interval),
- expected value of relative frequencies of working the right diagnosis out.

Accepting that the essential index describing (determining) the degree of identification of the real state of the DNS by the DGS is the mentioned probability of working the right DG out, the diagnosis likelihood can be defined (in the value meaning) as follows: *"diagnosis reliability" is the probability of formulating a right diagnostic decision (the probability of formulating the right diagnosis), so the probability of classifying the supposed real state of the DNS (the state being identified by the DGS) to the class of model diagnostic states, which this real state belongs to and which it should be classified by the DGS to.*

2. Formulating the problem

In the operating practice, decisions concerning the operation of self-ignition combustion engines as main engines of sea-going ships are taken by a user of a diagnosis (a decision-maker) during different phases of the process of diagnosing. This results from the work of the DGS which, in case of the same type of self-ignition combustion engines, can be differently fitted to diagnostic inference. Among operated diagnosing systems (DGS), that are fitted to diagnosed self-ignition combustion engines (DNS) there are such ones which can be named: complex and local [5]. In the both cases the diagnostic inference consists of measuring, symptomatic, structural and operating inferences [1]. In each kind of the inference there are made mistakes which influence the diagnosis likelihood negatively.

From the mentioned reasons it follows that after making n-diagnostic tests and inferences with formulated n-diagnoses on the state of self-ignition combustion engines (e.g. the technical state) by using the proper DGS, the right diagnoses can be obtained (so, it can be rightly stated that the state of the supposed self-ignition combustion engine is the same as its real state or belongs to the given class of the model states) in the quantity: $m < n$. The other quantity: $k = n - m$ tells that the diagnoses are not right. It means that the measure of formulating right diagnosis (the measure of likelihood), can be accepted as the following quantity:

$$h = \frac{m}{n} = 1 - \frac{k}{n} \tag{1}$$

Considering that at the known number n of expected (planned) diagnostic tests and inferences value taken by m is unknown, that's why the randomness of receiving the right diagnosis about the state of the self-ignition combustion engines should be taken into account while determining the likelihood. Therefore, it can be admitted that elaborating of the right diagnosis is a random event because during realization of a test and the diagnostic inference in determined conditions it may appear but it doesn't have to. When the event of formulating the right diagnosis was often observed in the past, one can assume that it exists a great chance of appearing it in the future (in the same conditions). This chance can be defined with help of the probability of taking the right diagnostic decision (formulating the right diagnosis) which can be, therefore, accepted as a measure of the diagnosis likelihood.

Considering the possibility of formulating the right diagnosis on the state of self-ignition combustion engines in the time interval [0, t] there can be tested two random variables: $N(t)$ which determines the number of possible-to-perform tests and diagnostic inferences, and $M(t)$ which determines the number of possible-to-formulate right diagnoses.

In case of such tests the expected values $E\{N(t)\}$ and $E\{M(t)\}$ can be defined, as well. Thus, the measure of the diagnosis likelihood can be also the quantity which can be called a likelihood index and defined by the formula:

$$w = \frac{E\{M(t)\}}{E\{N(t)\}} \tag{2}$$

The presented measures of the diagnosis likelihood do not reflect clearly the fact that identification of the state S of the self-ignition combustion engines by the DGS is done in the consequence of observing the adequate vector K of values of diagnostic parameters – being generated by the self-ignition combustion engines acting as DNS. They also do not reflect the fact that the DGS can, just like the DNS, be in different states which the diagnosis likelihood depends on. Thus, such a formula determining the probability $P(S/K)$, should be derived in way that would reflect these mentioned facts.

3. Solving the problem.

The process of using the diagnosing system (DGS) is the process $\{W(t): t \geq 0\}$ of which the values can be the elements of the set:

$$D = \{d_1,\ d_2,\ d_3\} \tag{3}$$

with interpretations as follows:

d_1 – state of active using (u) of the DGS (the state of this system's work), which is when the DGS is in the state of the full ability (s_1), thus, d_1 means diagnosing of the DNS state with the help of the DGS when the DGS is in the state s_1, so $d_1 = (u, s_1)$;

d_2 – state of active using (u) of the DGS, which is when the DGS does not stay in the state s_1, but in the state $\sim s_1$, so in the state of partial ability (s_2) or in the state of disability (s_3), that means the state which makes formulating the right diagnosis impossible, so the state $d_2 = (u, \sim s_1)$;

d_3 – state of active using (u) of the DGS, which is when the DGS stays in the state s_1 and in the same time it occurs the state s_0 of the self-ignition combustion engines (DNS), which has not been considered during diagnostic task performance, so it is the state which cannot be identified by the DGS, so $d_3 = (u, s_1, s_0)$.

It can be accepted that the work time of a DGS being in arbitrary state $d_i \in D$ (i = 1, 2, 3) is a random variable with the distribution $F_i(t) = P\{T < t\}$, continuous density $f_i(t)$ and positive expected value $E(T_i)$. It can be assumed that variables $T_i = (i = 1, 2, 3)$ are mutually independent [5]. In the time T_1 the DGS stays in the state d_1 from which, after finishing the time T_{12}, it can transform to the state d_2 at the probability p_{12} or after finishing the time T_{13} – to the state d_3 at the probability p_{13}. The state d_2 exists in the time T_2 and d_3 – in T_3. The diagnosing system (DGS) can change the state d_2 into the state d_1 in the case when a user finds that the DGS is damaged and immediately makes repairing on it. This change follows after the end of the time T_{21} at the probability p_{21}. The DGS can change from the state d_3 into the state d_1 when a user finds

occurrence of the state s_0 of the self-ignition combustion engines as DNS (not identified earlier by the DGS) and immediately makes repairing on it. This change follows after the end of the time T_{31} at the probability p_{31}. In the time of the process $\{W(t)\colon t \geq 0\}$realization different random variables can be observed, that determine the moments $\tau_0 = 0$, τ_1, τ_2 ..., in which changes of the states of the process take place. At the known state of the process $\{W(t)\colon t \geq 0\}$ in the moment τ_n ($n = 1, 2, ...$), the time of lasting the current state and the state occurring in the moment τ_{n+1} can be identified as stochastically independent from the process states appeared in the moments τ_0, τ_1, τ_2, ... τ_{n-1} and of the time intervals of their duration.

Therefore the process $\{W(t)\colon t \geq 0\}$ can be accepted as the semi-Markov process.

According to [3]:

$$P_1 = \mathrm{E}(T_1)M^1 \tag{4}$$

in which: $M = \mathrm{E}(T_1) + p_{12}\mathrm{E}(T_2) + p_{13}\mathrm{E}(T_3)$

where:

p_{ij} – probability of changing the process $\{W(t)\colon t \geq 0\}$ from the state d_i into the state d_j ($d_i, d_j \in D$; $i, j = 1, 2, 3$; $i \neq j$),

$\mathrm{E}(T_j)$ – expected value of duration of the state $d_j \in D (j = 1, 2, 3)$.

The probability P_1 is of the following interpretation:

$$P_1 = \lim_{t \to \infty} P\{W(t) = d_1\} \tag{5}$$

The probability P_1 can be considered as the probability of occurring the event A_1 which determines using a diagnosing system (DGS) in the time of lasting the state d_1 of the process $\{W(t)\colon t \geq 0\}$, so $P_1 = P(A_1)$; $A_1 = \{d_1\}$.

Any state of self-ignition combustion engines (which belongs to the set of the states enclosed in a diagnostic task) can be identified by the DGS when:

- the event A_1 occurs, being the event: when "the state d_1 of the process $\{W(t)\colon t \geq 0\}$is lasting";
- the event K occurs, which determines appearing of a vector of values of diagnostic parameters;
- occurrence of the event K is a consequence of occurrence of the event S which determines occurrence of an important (for a user) state of self-ignition combustion engines, enclosed in the diagnostic task and should be classified to the class of the model diagnostic states

Therefore, the diagnosis likelihood can be defined by the probability of occurrence of the events: A_1, S, K in the same time, according to the following dependences [5]:

$$P(A_1 \cap S \cap K) = P(A_1)P(S \mid A_1)P(K \mid A_1 \cap S) \tag{6}$$

$$P(A_1 \cap S \cap K) = P(K)P(S \mid K)P(A_1 \mid K \cap S) \tag{7}$$

From the equations: (6) and (7) it results that the probability P(S/K) as a diagnosis likelihood measure, can take the following form:

$$P(S|K) = \frac{P(A_1)P(S|A_1)P(K|A_1 \cap S)}{P(K)P(A_1|K \cap S)} \tag{8}$$

Occurrence of the event A_1 doesn't influence the probability of occurring the event S, what is obvious because the events: S and A_1 are independent. That means: $P(S \mid A_1) = P(S)$. If the DGS is reliable (if the process $\{W(t)$: $t \geq 0\}$ is always in the state $d_1 \in$ D), it always occurs the event which consists in occurring the event K, at the assumption that the event A_1 had occurred. In this situation the dependence: $P(K/A_1 \cap S) = P(K \mid S)$ is obtained. Apart from that, having reliable DGS, the event A_1 can be always observed at the assumption that the events: K and S have occurred at the same time. Therefore, it becomes obvious that, in the case of reliable DGS (such the DGS for which $P(A_1) = 1$) it should be taken into account, that $P(A \mid K \cap S) = 1$ and $P(K \mid A_1 \cap S) = P(K \mid S)$. Thus, at the assumption that $P(A_1) = 1$, the formula (8) can be reduced to the following form:

$$P(S|K) = \frac{P(S)P(S|K)}{P(K)} \tag{9}$$

what brings the diagnosis likelihood measure [2].

Assuming that the diagnosing system (DGS) worked without any failure while diagnosing the states of self-ignition combustion engines being diagnosed systems (DNS), the diagnosis likelihood measures can be also expressed by quantities of dependences: (1), (2) and (8).

3. Diagnostic inference and diagnosis likelihood

In the operating practice it exists the necessity of formulating diagnoses on the states of self-ignition combustion engines (e.g. main engines of sea-going ships), as inferences which can be logically deduced from the premises being the values of diagnostic parameters which create the vector K, are recorded by the diagnosing system (DGS) and suggest existing (or just occurrence of) the state S of the mentioned self-ignition combustion engines being diagnosed systems (DNSs). This kind of inference (diagnostic inference) is called the non-deductive inference. Thus, significant becomes the answer to the questions*: in what degree can one trust the inferences being results of a non-deductive inference?, in what degree such inferences can be accepted as reliable and used for taking operating decisions*?

During formulation of the diagnosis (inference) on the state S of the DNS the sentence K is taken for a completely reliable premise. The sentence says that not any other but this vector (in this case, the vector K) of values of diagnostic parameters was recorded by the DGS. The sentence S says that that not any other but this DNS state (in this case, the state S), is the inference formulated on the basis of the sentence K, being the result of the finished non-deductive inference. In that case, the inference is the reductive one [5] which runs in the following schematic way: if the implication $S \Rightarrow$ K is true and its direct successor (K) is true, direct predecessor (S) of the implication is also true. It means that the presumed state of the DNS is taken for S because the vector K of values of diagnostic parameters has been recorded by the DGS.

In case, when the sentence S is the inference formulated on the basis of the sentence K (considered as a completely granted presume) in the process of the non-deduction inference it can be accepted that the sentence S is made probable by the sentence K. The measure of the probability can be the logical probability [8] of the sentence S for the sake of the sentence K. Accepting the sentence $K^*(n)$ as the following sentence: *K^* is the set of n – results of tests and diagnostic inferences of the state S of a diagnosed system,* and $S^*(m)$ - as the sentence: *S^* is confirmed by m- results of tests and diagnostic inferences*, the logical probability of the state S, considering the vector K, can be determined as:

$$P_L(S|K) = \frac{m}{n} = h; \; m \leq n \tag{10}$$

One can easily noticed that the formula (10) is the same as the formula (1) which determines the frequency of a random event. From the formula (12) it results that the degree of likelihood at which the diagnosis is accepted as reliable, can be bigger than the value of the logical probability *h* of the inference saying that the DNS is in the state *S* on the basis of the presume which is the observed vector *K* taken for completely right because of occurrence of (or existing) the state *S*. In case when $n \to \infty$, the determined by the formula (1) frequency of a random event tends to the statistic probability [8] that. in this case, can be determined by the formula:

$$P_S(S|K) = \lim_{n\to\infty} \frac{m_S}{n} \tag{11}$$

Determining the both probabilities: logical (P_L) and statistic (P_S), it should be taken into consideration that they concern the repeating events: *S* (that the state *S* has appeared) and *K* (that the vector *K* has appeared), which can occur only together. It means that, it is assumed, that the event *S* appears only when *K* occurs.

From the considerations above it results that the frequency *h* determined by the formula (1), can be considered as the logical probability (P_L) when the tests and diagnostic inferences are repeated many times, and when lots of tests and inferences (in the theory $n \to \infty$) are made it can be considered as the statistical probability (P_S).

Formulating the diagnosis about the state *S* of the SDN, the sentence *S* (which says that the DNS is in the state *S*) is a hypothesis and the sentence *K* is a result of a diagnostic test. The sentence *K** is the set of sentences *K* (the set of results of diagnostic tests), from which all are the tests confirming *m* – times or not confirming (falsifying) *n–m* - times the hypothesis *S*. The hypothesis about the state of the DNS can be, in this case, formulated in the following way: *the SDN is in the state S because the vector K of values of diagnostic parameters is observed.*

The suggested measures of the diagnosis likelihood are objective. When the measures cannot be applied because of different reasons (e.g. technical, economic, organizing) the diagnosis likelihood can be determined with the help of a psychological (subjective) probability [8]. The probability determines the degree of conviction (certainty) of the user of the diagnosis about the chances of coming such expectations true, that the state of the DNS, according to the formula included in the diagnosis, is the state *S*. Acceptance of the diagnosis as a reliable or not reliable one, by using this probability, is subjective because depends on the knowledge of the person who formulates (works out) the diagnosis. It differs from the objective probability at the fact that it reflects the subjective estimation of the SDN state, according to the relation: this state of the DNS is more probable than each other one or – this state of the DNS is the most probable, or it is the most probable that DNS stays in the state *S*, etc. The probability is indeed graduated but deprived of number measures which would determine the particular degree of acceptation. The diagnosis on the state *S* of the DNS can be considered only as more or less reliable. Therefore, the psychological probability (subjective) is not a good measure of diagnosis likelihood. From this reason, for operating practice, this should be of a limited application in case of technical kinds of transport, just like sea-going ships and aircrafts.

4. Summary

Occurrence of the event $A_1 = \{d_1\}$ is the necessary (but not sufficient) condition to be able to identify the state *S* of the given DNS. In case of using a complex DGS, the all states which the SDN can be in are considered at the diagnostic task and then $A_1 = \{ d_1, d_3\}$. Thus in the practice, the diagnosis likelihood (in case of employing the local DGS) can be bigger than $P(A_1) = P_1 < 1$, what follows from the formula (4).

The formula (8) which enables determining the diagnosis likelihood, has been formed by using the limiting distribution of the semi-Markov process $\{W(t): t \geq 0\}$ and the Bayes' formula.

The presented semi-Markov model of the process $\{W(t): t \geq 0\}$ is of the essential practical meaning because of the easiness of determining estimators of the probability p_{ij} as well as simply estimation of expected values $E(T_j)$ of random variables T_j, stating for the time of state duration $d_j \in D$ ($j = 1, 2, 3$) [7].

The presented measures of diagnosis likelihood are readable because in the extreme cases they can be assigned to by:

– the value 1 when the diagnosis is completely reliable,

– the value 0 when the diagnosis is completely unreliable.

In the cases, when it can be only stated that the diagnosis is reliable at a certain degree, this degree is needed to be précised by assigning a value from the non-negative real numbers interval $R_+ = (0, 1)$ to its likelihood.

References

[1] Bękowski, L., *Elementy diagnostyki technicznej*, Wyd. WAT Warszawa, 1992.

[2] Cempel, C., *Diagnostyka wibroakustyczna maszyn*, Wyd. Politechnika Poznańska, 1985.

[3] Girtler, J., Girtler J.: *Probabilistic measures of diagnosis' likelihood about the technical state of transport means*, Archives of Transport, Quarterly of Committee of Transport of Polish Academy of Sciences, vol. 9, iss. 3-4, Warsaw, 1997, pp.33-42.

[4] Girtler, J., *Zastosowanie bayesowskiej statystycznej teorii decyzji do sterowania procesem eksloatacji urządzeń*, XXII Zimowa Szkoła Niezawodności, Wyd. SPE KBM PAN – ITE, Szczyrk, 1994, s.55–62.

[5] Girtler, J., *Diagnostyka jako warunek sterowania eksploatacją okrętowych silników spalinowych*, Wyd. WSM, Studia Nr 28, Szczecin 1997.

[6] Girtler, J., *Zastosowanie wiarygodności diagnozy do podejmowania decyzji w procesie eksploatacji urządzeń,* Materiały V Krajowej Konferencji „Diagnostyka Techniczna Urządzeń i Systemów" DIAG'2003. WAT, PAN, Warszawa-Ustroń 2003, s.100-109.

[7] Grabski, F., *Teoria semi–markowskich procesów eksploatacji obiektów technicznyc*h, ZN WSMW (AMW), Nr 75A, Gdynia 1982.

[8] Pabis, S., *Metodologia i metody nauk empirycznych*, PWN, Warszawa 1985.

PRELIMINARY RESEARCHES OF INFLUENCE OF DIFFERENT LOADS ON WORKING CONDITIONS AND PERFORMANCES OF THE PISTON COMBUSTION ENGINE WITH DIRECT FUEL INJECTION

Barbara Jankowska-Sieminska

Institute of Aeronautics
Al. Krakowska 110/114 02-256 Warsaw, Poland
tel.+48 22 846 0011, fax: +48 22 846 4432
e-mail: kones@ilot.edu.pl

Antoni Jankowski

Institute of Aeronautics
Al. Krakowska 110/114 02-256 Warsaw, Poland
tel.+48 22 846 0011, fax: +48 22 846 4432
e-mail: kones@ilot.edu.pl

Marcin Slezak

Motor Transport Institute
ul. Jagiellonska 80, 03-301 Warsaw, Poland
tel.: +48 22 6753058, fax: +48 22 811 0906
e-mail: marcin.slezak@its.waw.pl

Abstract

The most of research works with reference to piston engines with the direct fuel injection concentrate on two basic systems . One system is a homogeneous system and refers to high engine loads both from the point of view of torque and rotational engine speed. The second system refers to small loads and rotational engine speeds which usually do not exceed 50 % of the maximum allowable loads and the rotational speed.
These systems were an object of the analysis and research with use of the laser-equipment , mostly the PDPA and LDV. For the comparison only the PIV research were brought over. In brought over analysis one returned the special attention on stratified combustion, homogeneous combustion, water injection and water fuel emulsions, heat exchange.

In particular research injectors, the combustion space of the constant of the volume with 3D laser equipment (PDPA, LDV), results of researches of fuel spray concerning droplet diameters, results of researches of fuel spray concerning droplet distribution of lineal and volume, and dependences Rosin-Rammler, results of researches of fuel spray concerning distribution of 3D droplet velocity, results of the analysis of combustion rate and impulse for fuel spray are presented in the paper. The obtainment of small droplet dimensions is possible in the way increasing of the injection pressure. However high increasing of the pressure unfavourably bears on life of fuel equipment. From other methods one can mention methods mechanical improvements of spraying of the fuel. One of mechanical methods stayed put-upon in research of the ignition process.

Keywords: *combustion engines, direct fuel injection , mixture preparation* processes *, homogeneous strategy , heterogeneous strategy, laser-methods*

1. Introduction

The most of research works with reference to piston engines with the direct fuel injection concentrate on two basic systems . One system is a homogeneous system and refers to high engine

loads both from the point of view of torque and rotational engine speed. The second system refers to small loads and rotational engine speeds which usually do not exceed 50 % of the maximum allowable loads and the rotational speed (Fig. 1). This system is a heterogeneous system. Ideas relating to two names are speculative ideas and Ideas relating to two names are speculative ideas and essential conditions occurring in an engine significant differ from homogeneous conditions and heterogeneous ones, where also homogeneous areas are visible.

The first system, the homogeneous system, is also characterized that it can be applied both with reference to Diesel and a spark-ignition engines. This system is characterized with the early fuel injection, usually during the intake stroke. So there is a lot of time for proper (homogeneous) preparation combustion mixture which should be homogeneous. However even uniform distribution of the fuel in combustion chamber does not give the full view of qualitative and quantitative preparation of the mixture. The quality of injected fuel spray has a very big meaning for obtainment of correct work parameters of the engine referring to torque, fuel consumption and emission level of exhaust gases. Preliminary researches showed that the quality of injected fuel spray having very essential importance for the obtainment of suitable parameters engine work was name only homogeneous spray, and practically her homogeneity refers to the macro scale. Such approach for the problem is a strong simplification. Such approach for the problem is a large reduction, if the accepted name of the homogeneous charge has to be applied. Uniform fuel distribution in combustion chamber differs only this system from second one, where fuel can be not uniform distributed in combustion chamber and can also appear areas where there is not fuel at all.

In the second work system, the heterogeneous system, fuel is heterogeneously distributed in combustion chamber. In this system of engine work, fuel injection occurs close to end-point phase of compression stroke. So, there is a little time for combustion mixture preparation . However in the zone of the mixture ignition should be homogeneous, and fuel spray should be characterized with small dimensions of fuel droplets. This refers especially for so called "the cold" ignition which at the heterogeneous mixture can not appear or miss fire will appear, what negatively affects on engine economic parameters and emission level of exhaust gases. In this second system the exchange and thermal conditions have essential influence on the correct process run of the combustion and emission level of exhaust gases.

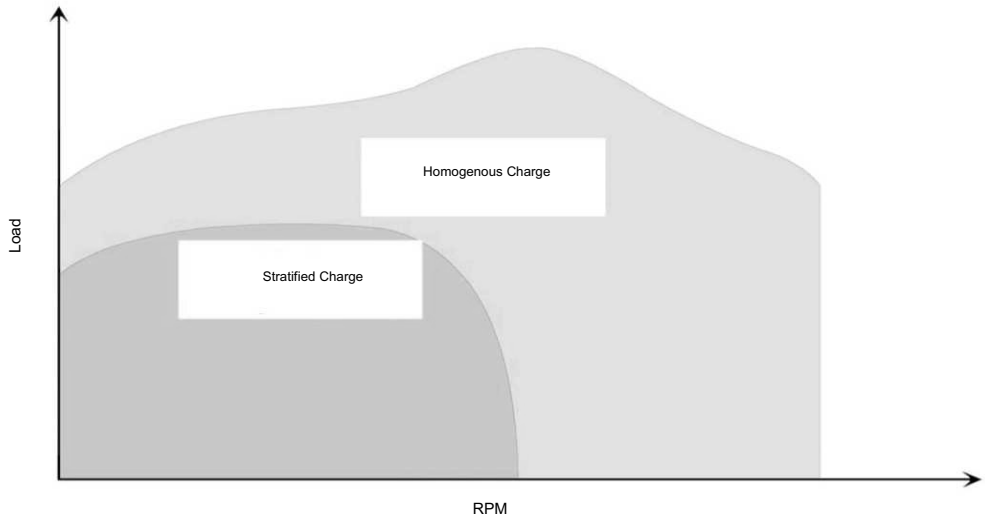

Fig. 1. Two strategies of the power supply of with the spark-ignition engines with the direct-injection: the stratified charge at small loads and rotational speeds and the homogeneous charge at big loads and rotational speeds of the engine

The heat flux passes from charge across a boundary layer of thermal resistance on the wall of combustion chambers (cylinder liner, cylinder head and piston crown), itself wall, the boundary layer of thermal resistance on the outer side of combustion chamber to cooling fluid cylinder wall and head, and on a other piston side, an oil-layer from a oil sump. Heat lost in cooling system of the walls is the row of 15 - 20 % heat supplied in fuel, and with reference to the rated power of the engine it takes out of 40 - 50 % and even more. The temperature on boundary surfaces of the layers spreads according to thermal resistances of these layers. From the point of view of the cycle of the highest efficiency, the charge temperature should be the maximal (but on the walls not higher than acceptable one of the wall material; novel materials, eg. ceramic, let on application of high temperatures). On the other side the temperature cooling fluid is settled automatically on several degrees below boiling heats cooling fluid. The barrier layer of cool charge on internal walls of combustion chambers is so advantageous from point of view of engine efficiency. Charge is swirled, what provides charge exchange and restore of the barrier layer. Too intensive swirl influences however unfavorably on combustion processes and besides the high temperature bears on the NO_x emission level. On conditions of heat exchange in combustion chamber of the piston-engine, and what to these is going run of combustion processes, engine performance and level emission of combustion gases influences the water injection and exhaust gases recirculation (EGR), what one ought to take into account in analysis of present-day combustion engines.

Explored experimental included derivation of homogeneous fuel spray for the homogeneous system , estimation of the fuel spray homogeneity by means of special analytical methods, the mathematical description of experimental data by means of different dependences, and determination of the best description of the fuel spray quality. In reference to different fuel sprays, the best qualitative description according to brought over research has been obtained by means of the Herdan diameter (D_{43}).

2. Stratified combustion

In ideal case the engine is operated without throttle and with lean overall mixture. The direct injection for SI engines with stratified operation combines the improvement of charge cycle and thermal efficiency (Fig. 2.). Therewith the direct injection is the most promising engine-related measure regarding fuel efficiency. However stratified operation in early stages was limited on a small area in the engine map. The stratified engine map is limited to small engine speeds and low loads because of the dependency of the mixture process on the piston position and because of unreliable inflammation under some conditions. Consequently the benefit in fuel consumption is limited on this small engine map which is hardly used in the real drive cycle. Further the fuel consumption benefits are reduced by extended wall wetting on the piston surface leading to considerable energy loss. Another difficulty of all lean burn engines is the exhaust gas aftertreatment with regard to the reduction of NOx emissions. Therefore the NOx storage catalysts are used mostly in combination with an intermittent lean-rich engine operation. While the engine is running lean the NOx is stored in the catalyst until the storage capacity is reached. Then the engine is switched to rich operation to enable a regeneration of the catalyst. Especially at higher loads high NOx raw emissions occur at stratified operation so that switching from stratified to homogeneous mode achieves a higher overall efficiency. To allow a reduction of the regeneration frequency of the catalyst and to enable stratified operation at higher loads, the engine development should be focused on the reduction of the NOx emissions. These engines achieve a benefit in fuel efficiency mainly by downsizing effects while using the very efficient 3-way catalyst technology. A lot of investigations shown that the stratified operation map may be larger for the next generation of direct injection engines. These engines are realized with a spray guided idea. Due to a narrow arrangement between spark plug and injector the mixture process is not supported by the piston surface. The mixture process is nearly independent of the piston motion. This leads to a

significant reduction of piston wall wetting. Further the ignition and combustion timing can be adjusted regarding thermal efficiency concerns instead of mixture process requirements.

Fig. 2. The strategy of the power supply of engines with the spark-ignition direct-injection: the stratified charge at small loads and rotational speeds of the engine

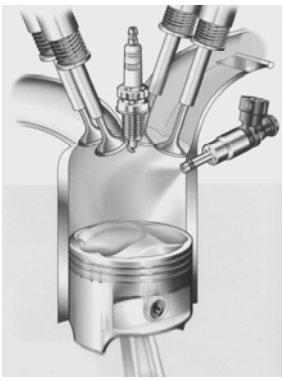

Fig. 3. The strategy of the power supply of engines with the spark-ignition and direct-injection: the homogeneous charge at big loads and rotational speeds of the engine

The advantage is that no defined charge motion is required to enable the mixture transport as necessary for air-guided concepts. Consequently charge motion strategies can be involved to support the combustion and fuel evaporation specifically. The advantages of the spray guided combustion concept can be enhanced further with the combination of turbo charging and increased injection pressure. Further the direct injection allows a comparatively high compression ratio even for turbocharged engines because the knock tendency is reduced. Compared to natural aspirated engines the increased air-mass in case of the turbocharged engines allows an extension of the stratified engine map leading to a benefit in fuel economy. Another advantage of turbo charging is the increase in power at full load operation.

3. Homogeneous combustion

The homogenous combustion strategy has potential to reduce NOx, PM emissions and improve part load engine efficiency. It is suitable for a variety of fuel types (Fig. 3.). However, to achieve a successful application, problems such as control of ignition timing and heat release rate over the entire engine operation range, have to be solved. Homogenous combustion needs an essential ignition temperature. The methods used to achieve such a temperature have to be able to manage the rate of heat release followed by ignition and avoid extreme sharp pressure increases.

The results obtained from experimental investigations and theoretical simulation studies have indicated that the control over homogenous combustion can be achieved with lean mixtures in a limited range ($\lambda > 2$) by using various engine control strategies and air/fuel mixture modifications. Variable Compression Ratio and valve timing technologies are potential control technologies for homogenous combustion. Late fuel in cylinder direct injection can be an ideal strategy for homogenous combustion with heavy fuels, such as diesel at low loads. Since the main ignition of homogenous combustion occurs at a certain temperature, which is independent of fuel types, modification of the air/fuel mixture by fuel blending or using various additives can only control homogenous combustion via their effects on the heat release rate during first stage ignition. The selection of additives should be in agreement with the fuel type and its octane number.

Future experimental investigations should focus on variable valve timing, late in-cylinder injection for heavy fuel in particular, and supercharging. These potential technologies can be

applied individually or combined in various forms. Most calculations have so far been done using closed cycles. The impact between intake and exhaust flows has serious effects upon the temperature time history of the charge inside the combustion chamber. Therefore, it is anticipated that such an impact may have a serious effect on homogenous combustion as well, since homogenous combustion is very sensitive to charge temperature time history. Using a lean air/fuel mixture or diluting a richer mixture largely with EGR can control the heat release rate of homogenous combustion, but it will result in poor power output. SI offers a high power output density. A hybrid homogenous-SI strategy can therefore operate the engine with homogenous at low loads to improve emission and efficiency, without sacrificing the high load performance where SI strategy can be used. For engines utilising heavy fuels, homogenous has the potential to significantly reduce PM and NOx emissions without sacrificing fuel efficiency. However, this benefit can only be considered when the engine load is low. At high load, fuel enrichment would largely increase the heat release rate of homogenous combustion and result in an extremely high cylinder pressure increase, due to the nature of simultaneous combustion throughout the entire combustion chamber. At high load, conventional Diesel engine may still have to be employed.
Compared to SI, high compression ratios are preferred by CAI combustion due to its self-ignition nature. Therefore a higher thermal efficiency can be obtained. Values of CR may reach 21:1 for Diesel engine and 12:1 for SI engine. Fuel rich zones are the main source of PM emissions in conventional Diesel engine. However, with CAI strategy, air and fuel mixture are premixed before combustion starts, and thus very low PM emissions can be achieved.

Homogenous combustion is a combustion process which utilises homogeneous air/fuel mixture, but combustion is initiated by fuel self-ignition. It therefore combines features of both SI and Diesel engine combustion. During the compression process, different parts of the charge mixture have different heat capacities due to local in-homogeneities which results in non-unified temperature distribution throughout the combustion chamber. When the hotter parts overcome their threshold energies, ignition of these zones is initiated. The energy exothermal warms and compresses the remainder of the charge, increasing the temperature, until full-scale ignition is established after a short time delay. Therefore, homogenous combustion is a thermal environment related auto-ignition process, but ignition itself is controlled by the chemical kinetics of the mixture with relatively little influence of turbulence and mixing.

4. Water injection

Water can be incorporated into diesel fuels in two forms: micro emulsions (10^{-10} m) and macro emulsions (10^{-6} m). Micro emulsions are especially suitable for if the fuel stability and acceptability by the distribution system. However, they require higher surfactant concentrations and consequently they have a cost/effectiveness challenge, especially at high water concentrations. On the other hand, macro emulsions are specially suited for applications where fuel cost acceptance is a major consideration, since they require lower surfactant concentrations for preparation. Macro emulsions, however, have a white distinctive color because water is distributed in micron range droplets. This characteristic also poses a stability challenge, because water tends to settle over time, when the fuel is kept quiescent.

Water introduction causes NO_x reduction, PM reduction, variability of the addition of water, effects on cold start, lubricating oil dilution, and expenditure. As the main portion of NO_x is formed by highly temperature-dependent reactions, it has been tried for a long time to utilize the heat of vaporization of water for reducing the combustion chamber temperatures. For that reason but not only there is a good idea to apply of exhaust gases recalculations (EGR). Other methods are: water injection into the inlet manifold, water injection directly into the combustion chamber by means of a separate nozzle, injection of a pre-mixed diesel fuel-water emulsion, injection of a diesel fuel-water-diesel fuel sequence by means of a particularly modified nozzle. For obtaining a maximum NO_x reduction from a minimum of water, it has to be brought to the right spot at the

right time, namely to those spaces in the combustion chamber where the highest temperatures prevail for considerable periods of time, i.e. the post flame areas. For this reason it is essential to introduce the water by help of the nozzle used for injecting the diesel fuel, as is the case when diesel fuel-water emulsions are injected as well as with the stratified diesel fuel-water. In this regard, the other methods, namely inlet manifold water injection and direct water injection with a separate nozzle, are unfavourable as they supply water also to areas where it is ineffective or even harmful in other respects. Thus, the amount of water required for a certain NOx reduction is twice as great as with water injection by means of the diesel fuel injection nozzle. This excessive quantity of water reduces the temperature level all over the combustion chamber to the extent that soot oxidation is impeded and HC emission increased, resulting in an increased PM emission. In addition, lubricating oil dilution corrosion, and increased wear are observed with these methods. Inlet manifold water injection yielded NO_x reduction rates of 30 percent, in combination with EGR up to 50 percent. Next method, diesel fuel-water emulsion, which lowers the combustion temperatures, which is undesirable at the beginning and end of combustion and results in increased ignition delay, engine noise, and retarded combustion. Thus, at the beginning and end of injection only diesel fuel is introduced into the combustion chamber, to the effect that the aforementioned disadvantages are prevented. In this way, 15 percent lower NOx emissions are measured when the same amount of fuel as with diesel fuel-water emulsion is introduced. Compared to the use of diesel fuel water emulsions, the most import property of the DWD system is that the amount of water injected can be quickly varied dependent on engine load and speed, which is of highest importance in view of transient operating conditions and cold start. The exhaust gas opacity is considerably reduced with diesel fuel-water emulsions too, reportedly by 80 percent. Improved mixture formation due to the increased injection quantity and, therefore, higher injection pressure as well as micro explosions may play a part, and the same might apply to improved soot oxidation by H. and OH. Radicals resulting from partial dissociation of the water. When using diesel fuel-water emulsions, the opacity reduction does not correspond to a comparably large PM reduction, as this is affected by a marked increase in HC emission.

5. Laser researches

Experimental laser researches (PDPA, LDV, PIV) allowed to determine basic spray parameters of atomized fuel including droplet dimensions and velocity field. The view of research injectors for SI engines for research of atomization process, from left worked out injector research with air assist is presented in Fig. 4 and view of combustion chamber of the constant volume with laser equipment 3D (2 transducers and 1 receiver) - in Fig. 5.

Fig. 4. Research injectors, on the left experimental injector with air assist

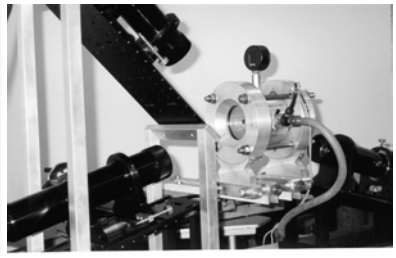

Fig. 5. The combustion space of the constant of the volume with 3D laser equipment (PDPA, LDV)

Researches were concentrated on measurement of droplet dimensions, their dispersion in spray by determination their substitutive diameters and velocity fields in combustion chamber of

constant volume. The substitutive diameter is definite by the general dependence expressed by equation:

$$(D_{ab})^{a-b} = \frac{\int_{D_o}^{D_{max}} D^a (di/dD) dD}{\int_{D_o}^{D_{max}} D^b (di/dD) dD}, \quad (1)$$

where:

D_{ab} – substitutive diameter of droplets in spray order a+b,

D – diameter of droplet in spray,

D_o – minimum-diameter of droplet in spray,

D_{max} – maximum-diameter of droplet in spray,

i – droplet number.

If the spray is homogeneous with reference to droplet dimensions , then all kinds of diameters are equal. Thus a measure of the homogeneity of fuel spray are differences among each diameters. Self-evident is that clear homogeneous spray are possible only theoretically.

The modelling spray fuel dispersion o is possible with many dependences. A most widespread method is the method Rosin-Rammler d described by dependence:

$$1 - Q = \exp\{-(D/X)^q\}, \quad (2)$$

where:

Q –volume droplet part of smaller diameter than D,

D – droplet diameter,

X – parameter describing stipulated droplet diameter,

q – parameter describing degree of droplet dispersion.

Results of laser researches are presented in Fig. 6, 7 and 8.
In Fig. 9 data for determining of the relative velocity of combustion in constant chamber volume and impulse charge are presented

6. Conclusions

The obtainment of small droplet dimensions is possible in the way increasing of the injection pressure. However high increasing of the pressure unfavourably bears on life of fuel equipment. From other methods one can mention methods mechanical improvements of spraying of the fuel. One of mechanical methods stayed put-upon in research of the ignition process.
Similar connected results with increasing of the pressure one can obtain by means of other methods from which most known is air assist for the process of fuel atomization. This method has however certain due limitations with the necessity of usage of the air-compressor. Other methods concerning improvements of the process of spraying are an object of numerous research works, in this also carried by authors of the paper.

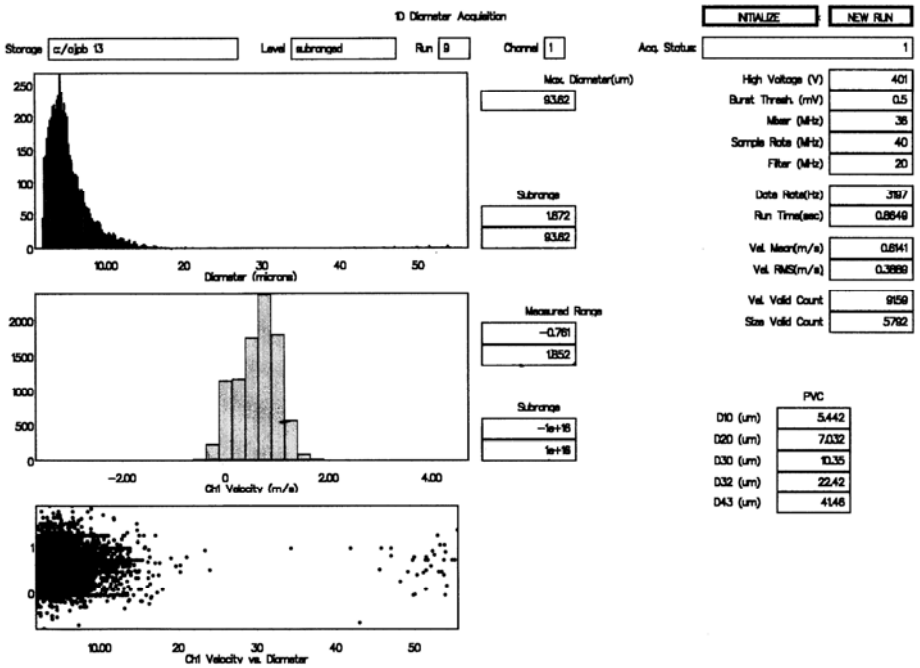

Fig. 6. Results of researches of fuel spray concerning droplet diameters for two kinds of principle dimensions small within the range about 10 μm and greater - within the range about 50 μm

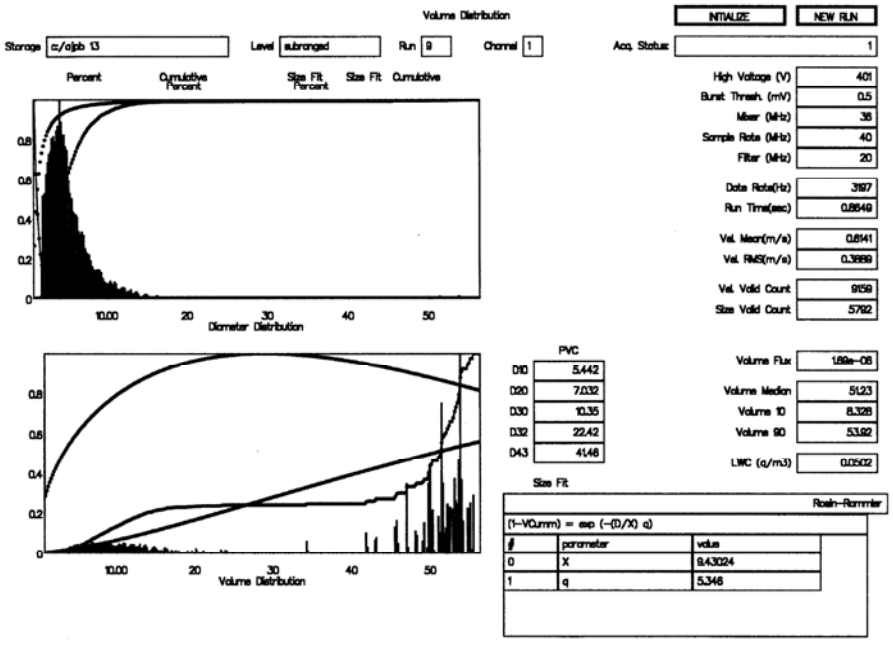

Fig. 7. Results of researches of fuel spray concerning droplet distribution of lineal and volume, and dependences Rosin-Rammler for two kinds of principle dimensions small within the range about 10 μm and greater - within the range about 50 μm

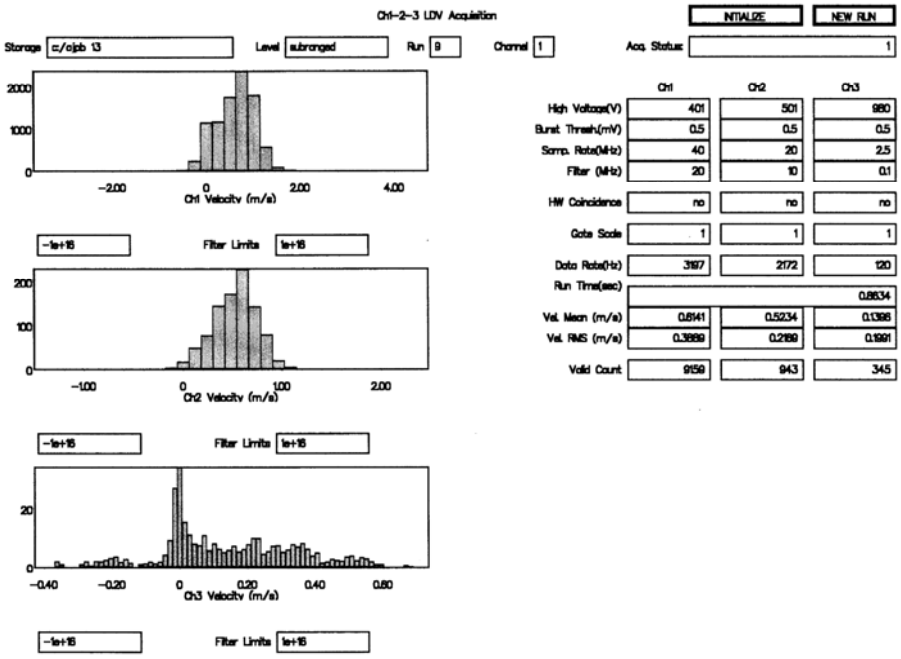

Fig. 8. Results of researches of fuel spray concerning distribution of 3D droplet velocity for two kinds of principle dimensions small within the range about 10 μm and greater - within the range about 50 μm

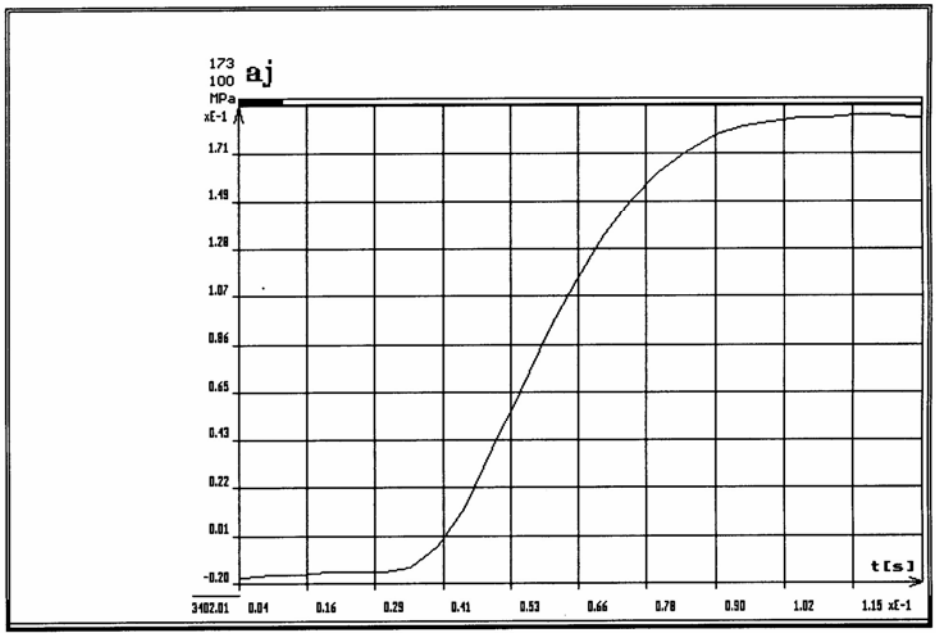

$t_{min}(t_1)$ [s]	$p_{min}(p_1)$ [MPa]
0,0356	0,002
$t_{max\,r}(t_r)$ [s]	$p_{max}(p_r)$ [MPa]
0,085	0,19
Δt [s]	Δp [MPa]
0,0494	0,188
$\frac{\Delta p}{\Delta t}$ [$\frac{MPa}{s}$]	3,806
$\int_{t_{min}}^{t_{max}} p\,dt$ [kPa s]	4,644

Fig. 9. Results of the analysis of combustion rate and impulse for fuel spray of D_{43} 28,8 μm, λ=2,8

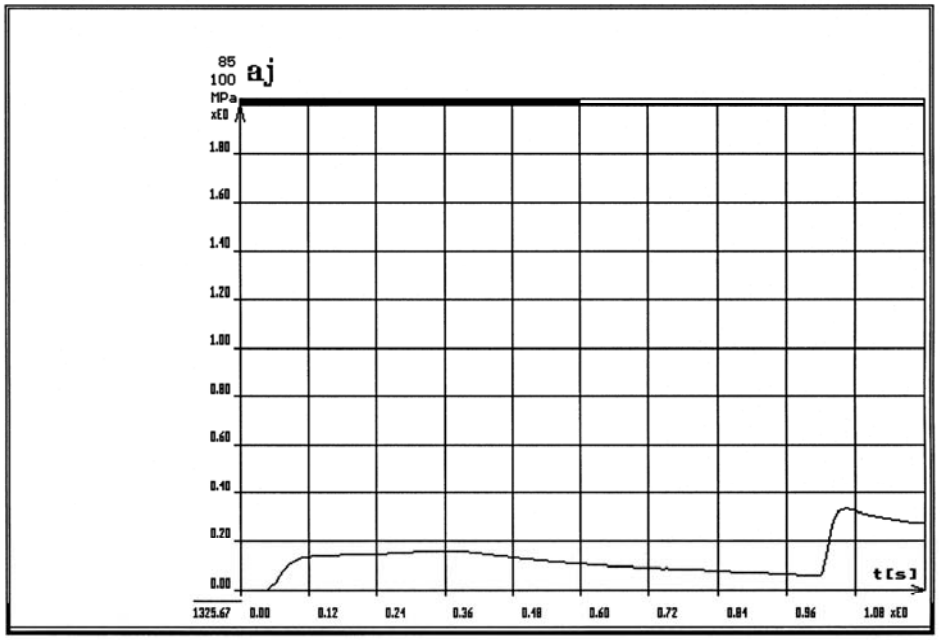

Fig. 10. Run of the combustion process in constant volume chamber for the heterogeneous fuel spray (λ=2,5)

Applied fuels can differ with the value viscosity and the surface tension what can have the essential influence at additives for fuels having different proprieties than gasoline (ethanol). It leads for considerable differences in process of the fuel/air mixture preparation.

The PIV research method lets on definition of the structure and distribution of velocity in stream. It lets on quality rather evaluation than quantity one. Laser-methods PDPA and LDV let on the qualification of diameters of droplets, their velocities and dispersion.
From brought over research the combustion process in the constant volume chamber about the constant of the volume results that the ignition and the correct combustion are possible, when the fuel spray is characterized with small measurements of the diameter D43 which does not exceed the value of 30 μm.

If in the fuel spray she appears droplets of dimensions exceeding 30 μm, but also the sufficient number small droplets of the D_{43} diameter of 30 μm, is the ignition and the combustion are also possible, though the combustion be characterized with different rate during durations of the all process.

During research of the ignition process of the and the combustion at higher pressure in the constant chamber volume (for the value of 1 MPa) appointed that, at large dimensions of droplets, when D_{43} is greater than 30 μm the ignition is not possible, even at the essential growth of the pressure in combustion chamber. Critical influence on the ignition in conditions of the cold combustion chamber has a fuel atomization.

The essential atomization of the fuel influences favourably on the emission level of toxic components of exhaust fumes gases, in this especially on the level the emission of hydrocarbons because of eliminating of misfires and on the level the emission of nitrous oxides on account the short time staying droplet of the fuel in burning zone.

The PDPA laser method can be prosperously applied for the diagnostics of the injection's apparatus of engines with the spark-ignition, diesel, as well as of turbine-engines.

Most injurious are drops in the stream of the fuel about large dimensions. Even several such droplets firmly change the process of the combustion and the emission of components of toxic combustion gases, mostly (NO_x). The process of spraying from the point of view processes of combustion and ignition, as well as of the level the emission characterizes the best supplementary diameter D_{43} which the value is nearing for the volume median.

References

[1] Ambrozik, A., Jankowski, A., Kruczynski, S., Slezak, M., *Researches of CI engine fed with the vegetable fuel RME oriented on heat release,* FIFSITA Paper F2006P256, 2006.

[2] Ambrozik, A., Jankowski, A., Slezak, M., *Some problems using of vegetable fuels in diesel engines,* Journal of KONES Powertrain and Transport, Vol. 13, No. 4, Warsaw, 2006.

[3] Jankowski, A., Sieminska, B.*, Slawinski, Z., *The resistance on thermal shocks of combustion engine pistons,* FIFSITA Paper F2006M232, 2006.

[4] Kim, H., Lai, M.-C., Yoon, S., Quelhas, S., Kumar, N., Yoo, J. S., *Correlating Port Fuel injection to Wetted Fuel Footprints on Combustion Chamber Walls and UBHC in Engine Start Processes,* SAE Paper 2003-01-3240 2003.

[5] Klein, D., and Cheng, *W. K., Spark Ignition Engine Hydrocarbon Emissions Behaviors in Stopping and Restarting,* SAE Paper 2002-01-2804, 2002.

[6] Kruczynski, S. W., Danilczyk, W., Ambrozik, A., Jankowski, A.*, Slezak, M., *Performance of three way catalytic converter containing magnesium oxide for SI engines with lean mixtures,* FISITA Paper F2006P237, 2006.

[7] Landsberg, G. B., Heywood, J. B., and Cheng, W. K., *Contribution of Liquid Fuel to Hydrocarbon Emissions in Spark Ignition Engines,* SAE Paper 2001-01-3587, 2001.

[8] Lee, S, Tong, K., Quay, B. Q., Zello, J. V., and Santavicca, D., *Effects of Swirl and Tumble on Mixture Preparation During Cold Start of a Gasoline Direct-Injection Engine,* SAE Paper 2000-01-1900 2000.

[9] Santoso, H., and Cheng, W. K., *Mixture Preparation and Hydrocarbon Emissions Behaviors in the First Cycle of SI Engine Cranking,* SAE Paper 2002-01-2805, 2002.

[10] Schock, H., Shen, Y., Timm, E., Stuecken, T., and Fedewa, A., *The Measurement and Control of Cyclic Variations of Flow in a Piston Cylinder Assembly,* SAE Paper 2003-01-1357, 2003.
[11] Shin, Y., Cheng, W., and Heywood, J. B., *Liquid Gasoline Behavior in the Engine Cylinder of a SI Engine,* SAE Paper 941872 1994.

RELIABILITY OF THREE-STATE RESTORABLE SYSTEMS WITH REGARD TO THE UNRELIABILITY OF THE SAFETY IN THE RESTORABLE STATE

Jerzy Jaźwiński

Air Force Institute of Technology
ul. Księcia Bolesława 6, 01-494 Warszawa, PO BOX 96, Poland
tel.: +48 22 6852161, fax: +48 22 6852163
e-mail: jjur@wp.pl

Abstract

A model of a three-state system has been considered in the work. The system can pass from the state of full ability into the state of safety unreliability (irreversible state) or into the state of efficiency unreliability (reversible state). From this state the system can also pass to the state of safety unreliability. To the system's modeling Kołmogorov-Chapman differential equation has been used. The obtained results have been presented with an example. Analysis with the obtained equations has been done.

Keywords: *Systems reliability, restorable systems, restorable state, nonefficiency failure rate, danger failure rate, recurrence rate*

1. Introduction

The contemporary systems are characterized by a large surplus in the reliability sense. The failures of such systems cause not very important effects for the realization of a task, but the effects for safety are of course very important. Then the analysis of the system must take into account the safety factors. The author considered problem of safety in many works devoted to models of un restorable systems.
In this paper I would like to present a model of restorable system in safety aspects.

The system in which two kinds of failures can occur. The first kind of failures causes system efficiency unreliability and in this case the system is restorable. This restoration can be dangerous and the system can pass to safety unreliability. The second kind of failures causes system safety unreliability. In this case I assume that the system is not restorable.

To describe such models of the systems, the reliability and safety factors will be formulated.

2. Basic concepts and definitions

Taking into account that this field of knowledge is very young and the terminology is not fully unificated, that is up to now the object of discussion.
Due to limited length of this paper, only basic concepts used in this work, are presented.

$R(t)$ - Function of the system reliability - the probability of fulfilling requirements from the point of view of safety and reliability of the system;

$Q_B(t)$ - Function of the system safety unreliability - the probability of occurrence of event causing a dangerous situation.

$Q_S(t)$ - Function of the system efficiency unreliability - the probability of occurrence of event causing an unreliable inefficient work of the system.

Of course for all these quantities both the exploitation conditions (in a broad sense) and exploitation time interval must be strictly defined.
In practice we have most often dealt with systems which can be in the fitness-for-use state or in the efficiency unreliability state or in the safety unreliability state, In the case when the system passes to the efficiency unreliability state, it is restorable but can be dangerous.

Let us denote the additional reliability factors as follows:

λ_S - intensity of the passing from the ability state to the unreliable efficiency state;
λ_B - intensity of the passing from the ability state to the safety unreliability state;
μ_S - intensity of the passing from the state of efficiency unreliability to the ability state;
μ_B - intensity of the passing from the unreliability efficiency state to the unreliability of the safety state.

3. The system with restorable state of efficiency unreliability

The graph of the system is shown in fig. 1.

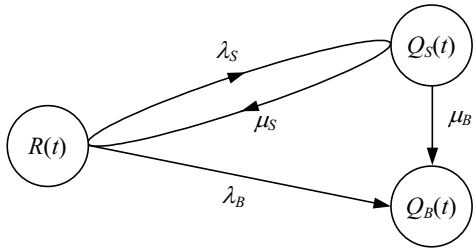

Fig. 1. The graph of the system with restorable efficiency unreliability state with regard to the safety unreliability with the restorable state

The system may be described by the Kołmogorov-Chapman differential equation set:

$$\begin{aligned} R'(t) &= -(\lambda_S + \lambda_B) R(t) + \mu_S Q_S(t), \\ Q_S'(t) &= \lambda_S R(t) - (\mu_S + \mu_B) Q_S(t), \\ Q_B'(t) &= \lambda_B R(t) + \mu_B Q_S(t), \\ R(0) &= 1;\ Q_S(0) = Q_B(0) = 0, \\ R(t) &+ Q_S(t) + Q_B(t) = 1. \end{aligned} \tag{1}$$

The Laplace transforms of equation set (1) are:

$$\widetilde{R}(p) = \frac{\mu_S + \mu_B + p}{p^2 + p(\lambda_S + \lambda_B + \mu_S + \mu_B) + \mu_S\lambda_B + \mu_S\mu_B + \lambda_B\mu_B} = \frac{\mu + p}{p^2 + pA + B}, \tag{2}$$

$$\widetilde{Q}_S(p) = \frac{\lambda_S}{p^2 + pA + B}, \tag{3}$$

$$\widetilde{Q}_B(p) = \frac{1}{p}\left[\lambda_B R(p) + \mu_B Q_S(p)\right], \tag{4}$$

where:

$\mu = \mu_S + \mu_B$,
$A = \lambda_S + \lambda_B + \mu_S + \mu_B$,
$B = \mu_S\mu_B + \mu_S\lambda_B + \lambda_B\mu_B$.

Solving the equation:

$$p^2 + pA + B = 0, \tag{5}$$

we obtain:

$$x_{1/2} = \frac{1}{2}(-A \pm C), \tag{6}$$

$$C = \sqrt{A^2 - 4B}. \tag{7}$$

Taking Laplace reciprocal transforms, after simple modifications we have got formulae as follows:

$$R(t) = \frac{1}{C} e^{x_1 t}\left[(x_1 + \mu_S) - (x_2 + \mu)e^{-Ct}\right], \tag{8}$$

$$Q_S(t) = \frac{\lambda_S}{C} e^{x_1 t}\left(1 - e^{-Ct}\right), \tag{9}$$

$$Q_B(t) = 1 - R(t) - Q_S(t). \tag{10}$$

The mean time of work of the system to the occurrence of its safety unreliability is given by the formula:

$$\overline{T}_B = -\left.\frac{d\left[p\widetilde{Q}_B(p)\right]}{dp}\right|_{p=0} = \frac{\mu + \lambda_S}{\mu_S\,\lambda_B + \mu_B\,\lambda_S + \mu_B\,\lambda_B}. \tag{11}$$

Example
In fig. 2 the relation of the mean time of work T_B has been shown to the occurrence of the safety unreliability state from the intensity μ_S at different values of μ_B=0, 0.1, 0.2, 0.5; λ_S=0.1; λ_B=0.01.

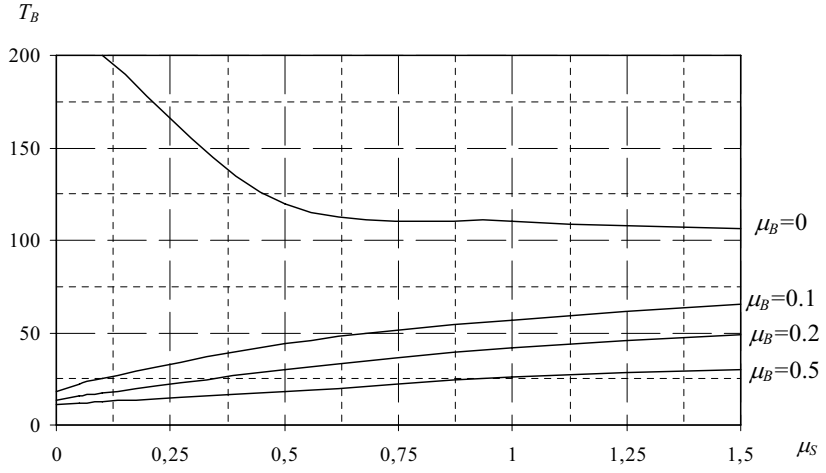

Fig. 2. Diagram of relation of $T_B = f(\mu_S)$ for the three state restorable system

The following conclusions result from the presented graph:

- when $\mu_B = 0$ - then with the increase of μ_S, T_B decreases;
- when $\mu_B \neq 0$ - then with the increase of μ_S, T_B increases and with the increase of μ_B - T_B decreases.

The equivalent danger failure rate of the whole system is given by:

$$\lambda_B(t) = \frac{\lambda_B R(t) + \mu_B Q_S(t)}{R(t) + Q_S(t)}. \tag{12}$$

Taking into account (8) and (9) we can determine $\lambda_B(t)$. Analysing this function we can show that:

$$\lambda_B(0) = \lambda_B$$

$$\lambda \lim_{t \to \infty} \lambda_B(t) = \frac{\lambda_B(x_1 + \mu) + \mu_B \lambda_S}{x_1 + \mu + \lambda_S}. \tag{13}$$

We can see that in consequence, $\lambda_B(t)$ is the decreasing function and the time $\overline{T}_B$ depends on the ratio λ_S / μ_S.

4. Conclusion

A dangerous restoration can essentially reduce the system's safety.

To apply in practice safety and reliability factors proposed in this paper, the investigations to obtain credible data for their calculation are necessary.

References

[1] Jaźwiński, J., *Reliability and safety of restorable systems*, Journal of Explo-Diesel & Gas Turbine'05, IV International Scientifically-Technical Conference, Gdańsk – Międzyzdroje – Kopenhaga 2005.

[2] Jaźwiński, J., Grabski, F., *Niektóre problemy modelowania systemów transportowych,* Biblioteka Problemów Eksploatacji, Warszawa-Radom 2003.

[3] Jaźwiński, J., Ważyńska-Fiok, K., *Bezpieczeństwo systemów czterostanowych z odnawialnym stanem zawodności sprawności*, Zagadnienia Eksploatacji Maszyn, z. 2.1, 1971.

[4] Jaźwiński, J., Ważyńska-Fiok, K., *Bezpieczeństwo systemów*, WNT, Warszawa 1993.

[5] Jaźwiński, J., Ważyńska-Fiok, K., *Niezawodność systemów transportowych*, PWN, Warszawa 1990.

[6] Jaźwiński, J., Ważyńska-Fiok, K., *Problems of System Safety with Functional and Time Surplus*, Second European Simposion on System Safety, La Baule, France 1982.

[7] Jaźwiński, J., Ważyńska-Fiok, K., *Reliability and Safety of Transport Systems*, 8 Zuverlassig-keitstagung, Leipzing – DDR 1987.

ENDOSCOPY AND THERMOGRAPHY IN THE PROCESS OF MAINTENANCE OF AUTOMOTIVE VEHICLES

Ryszard Jedliński

University of Technology and Life Sciences in Bydgoszcz
Faculty of Mechanical Engineering
Department of Thermal Technology and Metrology
85-796 Bydgoszcz, tel/fax: (052) 3408654, e-mail: jedlin@utp. Bydgoszcz.pl

Abstract

The process of automotive vehicles maintenance requires thorough assessment of the state of the vehicle and its systems. This is necessary for every day monitoring of changes of the vehicle technical state which, in turn, is the basis for scheduling and performing necessary operations involving repair or replacement of the parts whose fatigue life have come to an end. Detection of the reasons of inefficient operation of interacting systems and subsystems is also of great importance. Traditional methods and tools are often ineffective for providing the right diagnosis. The author discusses the possibilities of endoscopy and thermovision when used for assessment of the vehicle technical state

1. Technical Endoscopy

1.1. Introduction

Endoscope is an optical tool used for examining closed, inner spaces. Endoscopy technique developed, first of all, for medical purposes, where its application is undoubtedly irreplaceable (avoidance of use of invasive therapy and diagnostic methods) In case of technical objects this technique, involving introduction of the endoscope end into the cylinder through an opening left after unscrewed sparkling plug or an injector, allows examinations of the engine working surfaces (valves, cylinder bearing surface, combustion chamber, an assembly of crankshaft piston and connecting rods, and the piston bottom) thanks to very bright halogen lighting.
Two kinds of endoscopes find practical application: stiff –probe made in the form of a metal rod [1] and elastic ones making use of a beam of fibers. The elastic probe is featured by much better capabilities of reaching hardly available places. The stiff probe is characterized by certain restrictions in reaching these hardly available places. However, the latter one has a picture of higher quality, and a lower price. The basic assumption of the tool operation is the possibility of diagnosing the vehicle technical state without a necessity to disassemble (no invasion) its structure, thereby not causing any damage or change of the object. All examination methods involving accompanying assemble-dissemble methods introduce hazard of disruption in machine parts cooperation which, in turn, may appear to be very costly and time consuming. These disruptions result from disarrangement of elements and seals, which often involves a necessity of running them in, again. Simple workshop endoscopes of American make have been available on the Polish market since 2005. These are endoscopes with a high picture resolution 7500 pixels. They are capable of remembering the shape, and an attachment enabling observation at an angle. The discussed endoscopes can be purchased at the price below 200 PLN. Therefore, it is possible for car service stations, associations of experts, and even private persons to buy these devices.

1.2. Practical Aspects of Using Endoscopy in Engineering

As far as evaluation of diagnostic susceptibility of automotive vehicles is concerned, it should be noted that they are not adjusted to being examined with the use of endoscopy. Constructors did not design appropriate ways of access to basic engine subassemblies or drive systems of vehicles. In practice only openings designed for the sparkling plug and injectors are used, this being the only way to see the head from the side of the cylinder, the piston surface or the valve head. Fig.1 presents a view of an open exhaust valve recorded by means of an endoscope (carbon deposit visible on the valve walls).

Fig. 1 View of an open exhaust valve recorded by an endoscope (carbon deposit visible on the walls of the valve)

As for the remaining sets of automotive vehicles assemblies, apart from applicability for identification of the engine and chassis numbers it can be widely employed for assessment of the vehicle body state using its technological openings. It is the only way of looking into closed profiles as well as exposure and assessment of the metal plate corrosive wear. (fig.2).

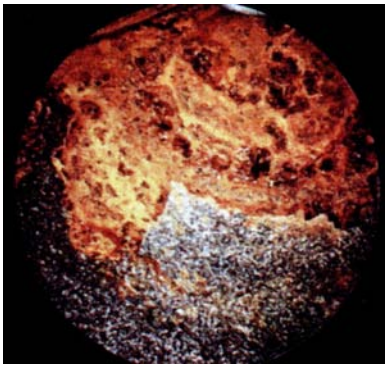

Fig. 2 View recorded by an endoscope: corroded surface of metal plate of a closed profile of an automotive vehicle door

Possibilities that are provided by endoscopy could be largely extended if constructors took into consideration design of proper ways of access to 'inner organs' of an engine. This refers mainly to the valve system and the assembly of crankshaft piston connecting rods (fig.3).
In order to demonstrate the possibilities of endoscopy, when applied in vehicle technical service, we can refer to one case when a transport company applied with a request to explain some unserviceability. It was about finding reasons of inefficient work of an engine. The symptoms were: difficulties to start the engine, decreased power, black exhaust fumes and knocks coming from the crankshaft-piston area.

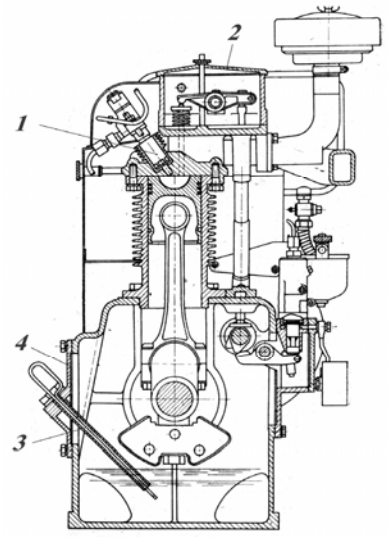

Fig.3 proposed places of the endoscope access to the engine inside: 1-opening of the injector or the ignition spark, 2- blinded opening in the valve cover, 3- bayonet opening of the oil level meter, 4- opening for introducing endoscope in order to assess the state of the crankshaft - piston system

After getting familiar with the engine maintenance course (work cards, damage register, service register) a measurement of compression pressure was carried out in particular chambers of the engine in question.

The measurement result (fig.4) showed unmistakably too low compression pressure in one of the cylinders. Before having this measurement performed the owner of the car had made several attempts to repair it, including injection pump regulation, replacement of fuel filters and high pressure cycle.

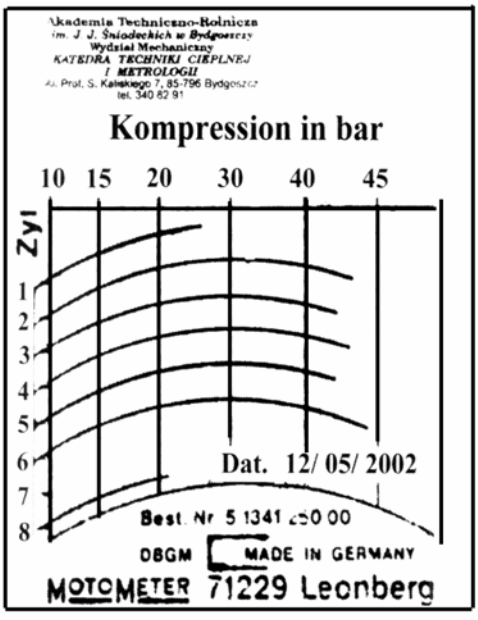

Fig 4 Results of compression pressure measurement in cylinders

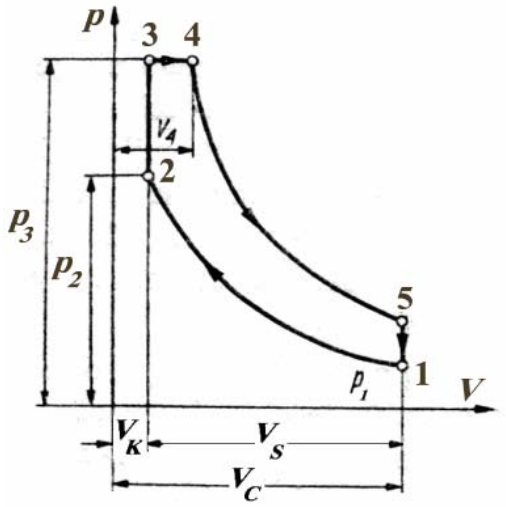

Fig.5 Comparative cycle of a self ignition engine

Before starting activities connected with disassembly of the engine, an attempt was made to determine analytically real parameters characterizing the engine in question. Thus, the pressure at the end of the compression weld p_2 can be calculated [4] from the dependence:

$$p_2 = p_1 \cdot \varepsilon \quad (1)$$

hence, the compression degree value $\varepsilon = \sqrt[n]{\frac{p_2}{p_1}}$. Using the calculated compression degree value the temperature of the compressed air, in point 2 of the comparative cycle, was determined from the formula:

$$T_2 = T_1 \cdot \varepsilon^{n-1} \quad (2)$$

Calculation results are set up in Table 1.

Table 1 Setting up of calculations of compression degrees and temperatures

Specification	Compression degree	Temperature at the end of the compression stroke
Cylinder II…VI	21,8	947
I cylinder	14,1	780

As the calculations show the compression degree in cylinder 1 varies significantly from the values in the remaining cylinders.
In result of decreased compression pressure at the end of the compression stroke, temperature in cylinder 1 did not reach the required value of about 900 K [4]. It was the cause of disruption of the combustion process in this cylinder which resulted in inducing less power and black exhaust fumes. In result of carried out disassembly it was revealed that the cause of the problem was a twisted connecting rod, and in consequence damage of the cylinder sleeve in cylinder 1 (fig.6).

Fig. 6 View of damaged: a) connecting rod, b) cylinder sleeve

A conclusion can be drawn that reasons of the engine inefficiency could be found out much earlier if there had been possibilities of using an endoscope for examinations of the crankcase interior. Also, the costs connected with the vehicle demurrage and other indispensable service activities.

2. Using Thermography in the Process of Vehicle State Monitoring

2.1. Introduction

Each body with temperature higher than absolute zero is the source of radiation in the band of infrared IR, and its intensity depends on the body surface temperature and features. Thermovisual apparatus is a variety of television sensitive to a fragment of infrared radiation range. Creation of a thermo-visual picture consist in recording radiation emitted by a given object by a camera, and next processing it into a colored map of temperatures. While measuring infrared radiation emitted by a given body also the body temperature is being measured in an indirect way. For a perfectly black body the correlation of temperature with infrared radiation intensity is presented in the following way:

$$T = \sqrt[4]{\frac{E_O}{C_O}} \cdot 100 \qquad (3)$$

where:

Eo - thermal radiation intensity, W/m2

Co- radiation constant of a perfectly black body is equal to 5.77 $\frac{W}{m^2 \cdot K^4}$

T – absolute temperature of K surface.

Thermovision system enables measurement of temperature in a non contact way, and in many points at the same time. However, it must be remembered that temperatures can be compared directly only within one material. The body radiation power depends on its temperature, therefore, warmer places are brighter in the visible picture. Thermovion measurement of temperature makes it possible to define distribution of temperatures on the whole surface of the examined object. Thermovision examination results can be used for assessment of heat losses from power engineering devices and other objects as well as for localization of their occurrences.

Thermovisual measurements enable detection of potential hazards early enough to schedule service and repair activities, thereby, avoiding costs connected with demurrage or unexpected failures. Application of thermovision in scientific research improves significantly the quality of gained information on thermodynamic processes, heat exchange or cooling conditions.

2.2. Practical aspects of thermo-vision in the process of vehicle maintenance

Thanks to the fact that this kind of examination enables making a temperature map of the whole engine, the analysis of values for particular components of thermal balance for different fuels and parameters of the engine work has become easier. As it is known [4] the heat gained from fuel combustion can not be exchanged fully into mechanical work. In the combustion engine the amount of heat exchanged into practical work is equal merely to 25-40% of the heat generated in result of fuel combustion. The remaining heat, in the amount of 60-75 %, escapes with exhaust gases, or is carried away by a cooling factor or is included in other thermal losses. In order to assess utilization of the heat supplied to the engine a thermal balance is made.
General equation of the outer balance has the form:

$$Q = Q_e + Q_{ch} + Q_w + Q_n + Q_r, \quad {}^{J}\!/_{h} \qquad (4)$$

where:

Q - heat supplied to the engine in J/h
Qe- usable heat (changed into usable work) in J/h
Q_{ch}- cooling losses
Q_w –outlet losses in J/h
Qn – losses of incomplete combustion in J/h
Qr – the rest of balance in J/h

Energy losses increase the temperature of the engine parts and elements After reaching proper temperature of the engine work, the cooling and lubrication systems carry away the excess of thermal energy. The amount of carried away energy can not be too big. This is supposed to maintain the engine temperature within the required range. High temperature is also very dangerous for the engine and here thermo-vision makes it possible to reveal this fact early including the cause of such a situation. In turn, in result of too low temperature of the engine the process of fuel combustion and evaporation is disturbed. Part of not combusted fuel goes to the exhaust system where frequently occurs its firing accompanied by increase in temperature of the exhaust system elements which is also recorded by the thermovision camera.

In the Department of Thermal Technology and Metrology initial thermographic examinations of a combustion engine were performed with the use of thermograph V-20. The examined object was a high-pressure, four-stroke, 6-cylinder combustion engine S-359M.The engine is cooled by a liquid with a cycle forced by a pump. Thermograph V-20 (thermo-graphic camera) that was used, is a device designed for non contact representation of the temperature distribution on the examined area, on the basis of infrared radiation power measurement emitted by particular elements of this surface.

Fig.7 Thermo-graphic camera V-20

Results of the measurement are presented in the form of a colored thermogram Thermographic pictures were obtained in result of scanning the engine heated surfaces.. Some of them are presented in this article.(fig.8, 9,10). The engine heads, exhaust collector, exhaust pipe, the engine body, oil sump - right after starting and after a certain time of work, were important places to examine. It allowed evaluation of the engine rise dynamics, during its work both without and with service load.

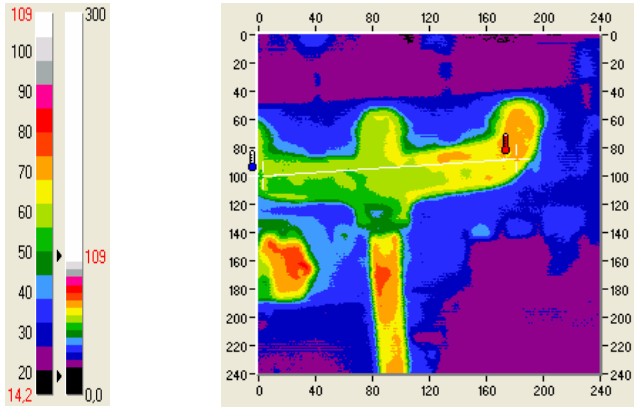

Fig.8 Thermograph of exhaust collector of an engine without service load made after 5 min. from the engine start

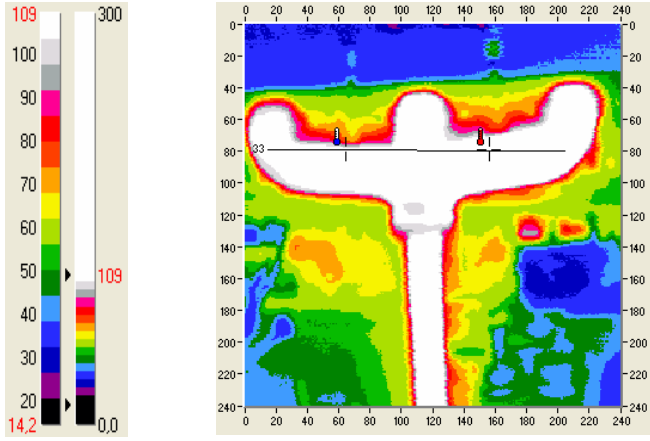

Fig. 9. Thermograph of an exhaust collector of an engine working without service load made after 20 min. from the start

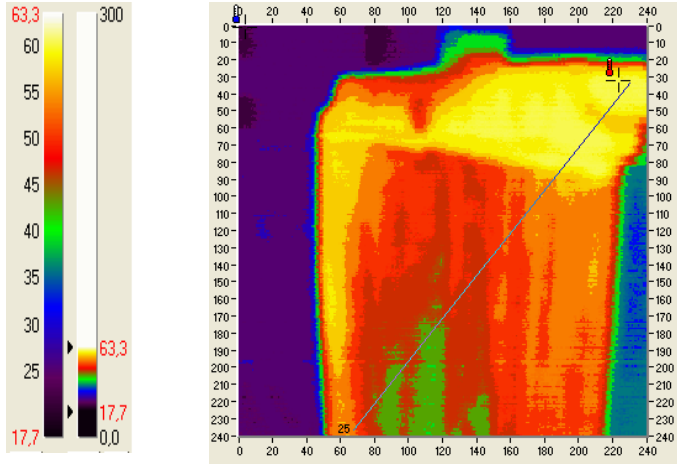

Fig.10. Thermographic picture of an engine radiator made after 40 min. from the engine start.

On the basis of observation of thermographs of water coolers (fig.10) it can be seen that bright colors on the cooler liquid inlet transform into cold colors on the outlet, which means sufficient cooling of the coolant .

As the information gained from the analysis of the thermographs shows, examinations of an engine by a thermovision camera should be recognized as one of diagnostic methods. This method makes it possible to obtain information about the examined object in a non invasive way, that is, without a necessity of its disassembly. Undoubtedly, a big advantage of this method is a possibility of examining the engine working with and without service load. Thermographic analysis provides information on temperature distribution on the whole surface of the examined object, in a given moment, thanks to which it gains advantage over other diagnostic methods. Using equations of thermal balance and additional measurements concerning masses and flow of media (liquid, gas) as well as tests results from the engine test house, one can venture to make a complex evaluation of the examined object thermal balance, its efficiency, and indication of areas where temperature anomaly occur which can be the cause of the engine failures.

3. Summary

Due to the publisher's restrictions the article presents only some aspects of application of endoscopy and thermography in assessment of the vehicle technical state. It should be emphasized that some objective obstacles resulting from high purchase costs have been overcome recently, and currently thermographs can be purchased at the price of about 40 thousand pln, whereas, endoscopes for 1200 thousand pln.

References

[1] Bogdański, J., *Endoskop warsztatowy*, Auto Moto Serwis – 1/2002.

[2] Jedliński, R., *Diagnostyka w procesie wyceny wartości pojazdów samochodowych i ustalaniu przyczyn oraz następstw uszkodzeń*; XII Międzynarodowa Konferencja „Diagnostyka Maszyn Roboczych i Pojazdów", ATR Wydział Mechaniczny, Bydgoszcz – Borówno 23-25.06.2005.

[3] Jedliński, R., *Zastosowanie termowizji w pojazdach samochodowyc;* III Konferencja nt.: Problemy jakościowe, energetyczne i eksploatacyjne w maszynach cieplnych, Duszniki Zdrój, 2006.

[4] Niewiarowski, K., *Tłokowe silniki spalinowe (tom1)*, WKiŁ, Warszawa 1983.

[5] Rudowski, G., *Termowizja i jej zastosowanie*, WKŁ Warszawa 1978.

FAILURES' IDENTIFICATION OF CYLINDER LINERS OF MARINE DIESEL ENGINES IN OPERATION

Zbigniew Korczewski

The Polish Naval Academy
ul. Śmidowicza 69, 81-103 Gdynia
tel: +48 58 6262635, fax: +48 58 6262681,
e–mail: Z.Korczewski@AMW.Gdynia.pl

Abstract

Within this paper there have been presented selected issues concerning the endoscopic diagnostics of cylinder liners of marine diesel engines. The considerations have been focused on theoretical bases of normal wear and tear process of the cylinder liners in the aspect of identification, localization and genesis of the well known and recognizable operational unserviceable states. There have been also demonstrated selected results of endoscopic exams carried out on marine engines operated on the Polish Navy warships, concerning cylinder liners' failures.

Keywords: *marine diesel engines, cylinder liners, operational wear and tear process, endoscopic diagnostics*

1. Introduction

A rational operation of a marine diesel engine requires precise knowledge of the degradation process's course within construction structure of functional systems. The process intensity is determined, among the others, with an alteration character of mechanical and thermal stresses in structural of the engine become during conversion of the chemical and thermal energy into mechanical work. The product of mean effective pressure and average piston's velocity represents a measure of dynamical stresses. The higher is the product's value the earlier an acceleration of the wear and tear process of the engine structural elements is expected [9]. The engine lifespan and reliability being expressed with, respectively: time and time's probability of the work correctness.

Many research workers all over the world and our country deal with the issue of wear and tear kinetics of the structural elements during engine usage [1,4,6,7]. The achievements in this domain of L. Piaseczny are well known in the environment of diesel engines engineers. He published widely results of operational examinations of the limiting and permissible wear and tear of the structural elements and an impact of operation condition in the very wide meaning [5]. Research elaborations of A. Niewczas and A Sitnik are also very vital from the point of of marine diesel engine operation. The elaborations are concentrating on mathematical modeling the wear and tear kinetics of combustion engine elements [4,6].

A very important conclusion results from the worked out reliability examinations. The usage potential of the contemporary marine engines is determined with limited wear and tear of crankshaft and its bearings as well as structural elements of the piston-cylinder system, timing gear system of the working medium and precise pairs of the fuel fed system. A process of the structural elements wearing for all the above mentioned systems represents a complex physical-chemistry process considering fricion, impact of high and quick changeable pressures and temperatures, non-uniform temperature distribution, considerable velocities of mutual movement of the friction pairs and changeable lubrication conditions [9].

The main aim of diagnostic research taken over by the author is to determine a dominant form of the wear for the vulnerable structural elements of the marine engines operated in the Polish

Navy. More than twenty years of operational examinations confirm that cylinder liners of medium and high speed engines are characterized with considerable intensity of wear and tear as well as occurrence of failures [11]. The application of endoscopic methods for their searching and recognition prevents further development of serious secondary failures of the engine's functional systems leading usually to the engine's total operational unserviceability.

2. Forming mechanism of cylinder liners' failures

During valve's running its structural elements are subject to the considerable mechanical and thermal loads talking about a value and changeability in terms of time. The mechanical stresses caused by gas forces becoming as a result of thermodynamic processes worked out in cylinders as well as inertial forces of the masses of a piston-crank system's elements carrying out rotational and reciprocating motion, are especially essential from the kinetic cylinder liner wear's point of view.

Taking into consideration the forces' system reacting on the cylinder liner sliding surface during cooperation between the liner, piston and piston rings there could be concluded that a dominant wear and tear process would be the non-reversible wear of the abrasive elements making by normal forces (crosswise) on the liner's sliding surface as well as friction forces occurring in the contact points of the sliding surface and piston rings. There also must be considered a fact the system represents the dynamical forces' system where a load changes in constant way. The proceeded processes of micromachining metal particles loosening (as a result of multiple plastic strain) as well as a deep pulling metal particles caused by the friction connection (so called friction welding) are mainly dependent on intensity (conditions) of the cylinder liner lubrication in the way of piston's moving. The loss of required surface state and geometric shape as well as required dimensions of internal liner diameter represent the consequences of cylinder liner sliding surface's wear. A defection research carried out on four-stroke engines shows that the biggest intensity of a wear takes place at the upper parts of a cylinder liner in the plane of crank's rotation – fig. 1a [5,9]. As a consequence, a characteristically shaped, elliptic wear threshold occurs, mostly in the top dead centre (TDC) in the region of contact between the cylinder liner sliding surface and the first two sealing piston's rings – fig. 6d. This is usually caused by a friction action of the carbon deposits layering on the walls of the combustion chamber, as a result of incomplete fuel burning. Carbon particles, getting into radial clearance between a cylinder liner and piston, disturb a layer of lube oil, causing an intensive attrition of the tip layer in the places of their biggest concentration. Besides carbon deposits other deposits occur on the walls of internal spaces of a cylinder liner. They have the form of lake layer of the dense and viscous substance getting into points piston gas rings and making difficult their free movement in the piston's grooves. It is also possible rings "hanging up" in the grooves. This phenomenon remains typical lengthwise attrition traces on the cylinder liner sliding surface – fig. 7f. Other reasons deepening destructing effects of friction and enlarged intensity of a wear of the cylinder liner sliding surface on the upper parts are mentioned below:

- high unitary pressure in the space limited with the first pair of piston's gas rings and cylinder walls, while the piston takes position of TDC at the end of compression stroke and beginning of discharge stroke – compressed air and gaseous combustion products being forced through ring clearances in the pistons grooves cause rings' expanding, what increases a side thrust on the sliding surface;
- high temperature of the combustion chamber walls – during engine running a temperature of the upper part of a cylinder liner achieves 523 – 533 K [1,9]. Hence, metal particles of cylinder liner's material demonstrate increasing mobility. This phenomenon is loaded in favour of a plastic deformation of the tip layer because of friction forces' reaction;
- unfavourable lubrication conditions – in the close vicinity of the combustion chamber lube oil evaporates and burns out making hard carbon particles along with combustion products;

- corrosion impact of the combustion products on the cylinder liner sliding surface at high temperature.

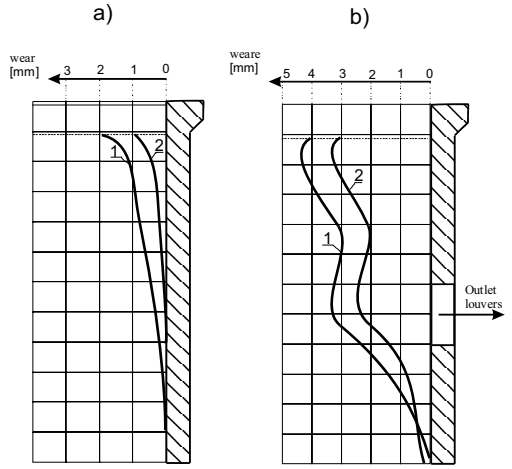

Fig.1. Wear and tear of IC engine's cylinder liner: a) four-stroke engine, b) two-stroke engine
1 – wear curie in the plane of crank's rotation, 2 – wear curie in the plane walking through the crank shaft axis

Defect research has shown that threshold occurs on the upper part of cylinder liners of the marine engines M400 type made of nitroalloy steel after working lifespan hours guaranteed by the producer. This is tightly connected with the considerable decreasing a thickness and hardness of the nitric layer [1]. Additionally observed defect of the cylinder liner sliding surface resulting from the loss of plasticity of the tip layer (nitrided) consists in its spalling in the form of characteristic areas close-fulfilled with minute erosion pits, so calle "rush" – fig. 5a. The producer of M400 engines adjusts a limiting value on the cylinder liner sliding surface on the level of 0,4 mm. After its exceeding, because of an inadmissible, critical decrease of nitric layer. There might be expected the accelerated, very intensive abrasive wear and tear process of the liner [1].

There also might be concluded, on the basis of numerical data presenting the wear character of two-stroke engines' cylinder liners (fig. 1b) that the application of louver timing gear introduces some singularities into this process [9]. Well, there might be observed that an intensity of the wear of the cylinder liner sliding surface in the vicinity of outlet louvers increases and in the extreme case a wear might exceed the wear in the liner's upper part. Such a specifity of the wear character explains following factors:

- corrosion impact of the hot outlet exhaust gas,
- high temperature of the cylinder liner's walls which are not cooled in this areas,
- unfavourable lubrication conditions of the cylinder liner sliding surface,
- cylinder liner's deformation.

Very practical, operational conclusions result from statistic data of the defect research have been carried out. Well, an average wear of the cylinder liner sliding surface of the marine medium and high speed engines achieves 0,02 – 0,21 mm per 1000 running hours, depending on achieved speeding and intracylinder pressures [1]. But the number of carried out start-up processes and transient processes has got a deciding significance for the wear intensity of cylinder liners. In such processes a chemical corrosion, activated with acid vapors as well as unsteady process of hit exchange and associated with – thermal deformation of cylinder liner's walls represent the main factors [1]. The corrosion appears as a consequence of vapors condensation on the cylinder liner's walls at the temperature below the daw point.

The loss of required surface smoothness caused by the piston attrition in the cylinder liner stands for other failure of the cylinder liner which is met very often in the engines' operation. In the extreme situation it is also possible the piston's material rolling on the cylinder liner sliding surface. This phenomenon usually leads to total piston's seizing in the cylinder liner and self lay-out process of the engine [5,9]. During routine endoscopic examinations of the marine diesel engines the alterations within the "honing" structure of the cylinder liner sliding surface (a depth of "honing" scratches equals from 0,01 mm up to 0,1 mm depending on the diameter and structural material of the cylinder liner) and presence and depth of corrosion-erosion defects as well as surface scratches (admissible depth is 0,5 mm, width – 1,0 mm and length – not more than 80 – 100 mm, depending on the engine's type) [5]. The overall level of a cylinder liners' degradation, intensity of the cylinder liner sliding surface's wear as well as a trend of its development are evaluated on the basis of the research, endoscopic results [1].

Cylinder liner's cracks are the most dangerous failures for the engine's reliability. They are usually caused by exceeded mechanical and thermal stresses occurring within the walls creating the combustion chamber – fig 7c and 7d. The covering cylinder liner's external walls with boiler scale disturbing hit abstraction from cylinder liners and pistons represents the most frequent reason of the cracks existence for the cylinder liners cooled with water. As a consequence the considerable thermal gradients within cylinder walls and excessive thermal deformations occur. Additionally, lubrication conditions get worse what causes cracks of structural material [5]. Thermal deformations of cylinder liner in the vicinity of TDC achieve more than 100μm [8].

Strength features weakening of the applied structural material and even its perforation caused by intensive erosion and corrosion processes of the cylinder liner's external surface represent other reason of cylinder liners' cracks, which quite usually occur during marine diesel engines operation. This kind of primary failures develop very quickly and being not detected in the right time usually lead to so called water hammers in the engine's cylinders, endangering widespread destructions.

3. Cylinder liners' examinations of the marine engines in operation

Modern diagnostic examination methods are more and more common in marine diesel engines operation. Endoscopy, earlier used only in medical practise, dynamically develops and represents very useful and even irreplaceable diagnostic tool for assessing the technical state of marine machines.

Endoscopy is a disassembling – free method of visual – optical examination of internal spaces of machines and facilities with the use of speculum devices called endoscopes.

In order to carry out endoscopic examinations of the engines operated in the warships of the Polish Navy the endoscopic equipment is provided. The equipment consists of OLYMPUS IF8D4-15 fiberoscope and boroscope set that differs each other with the length, diameter and observation angel of the optics: 90cm/8mm/90^0, 55cm/8mm/90^0, 45cm/8mm/90^0, 50cm/6mm/90^0, 30cm/4mm/0^0, 30cm/10mm/120^0 - fig. 2. This apparatus enables visual inspection and working out fotodocumentation internal engine's parts through the inspection holes at the diameter more than 5 mm. A special digital OLYMPUS photo camera Camedia C–2500L typ is applied to perform dimension analysis of the detected failures, their visualization and storage in the computer data base. This camera is connected to the boroscopes and fiberoscope by means of special adapters (couplings).

The fiberoscope can be introduced through the inspection holes of the diameter greater than 8 mm. Its elastic light-pipe is 1500 mm long. It has the replaceable ends, which enable observation within 60^0 and 80^0 face sectors and 80^0 side sectors. Thanks to this features the manual possibilities of the inspection, through the internal spaces of the air and exhaust flow passages within the engine and turbocharger, considerably increase.

Boroscopes having different length of the stiff lens system enable carrying out observation at side and face sectors, within wide range of visual angle alterations. The optics of 30cm/10mm/120^0 represents especially useful tool in diagnostic investigations of the engines' combustion chambers in the region of valve seats mounted on the low board of the cylinder's head. Boroscopes are also very useful tool during inspections of the guide and rotor blades' edges of the turbocharger. In order to perform inspection every one of rotor blades, the inspection should be carried out simultaneously with turning the rotor around – by hand or by means of compressed.

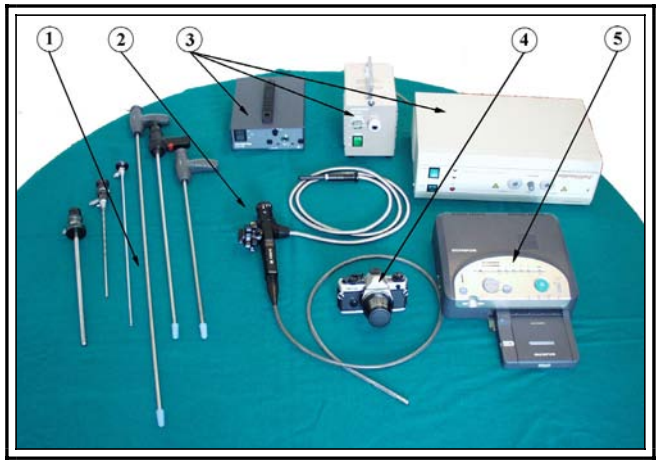

Fig. 2. OLYMPUS diagnostic endoscope set: 1 – boroscope set, 2 – fiberoscope, 3 – light sources, 4 - photo camera, 4 – light source, 5 – photo printer

In figure 3 there is presented the way of performing diagnostic examinations of the marine engine's cylinder systems by means of boroscopes and fiberoscope. Figure 4 demonstrates how to get access and introduce optics through the inspection holes into internal spaces of the cylinder liner during endoscopic inspections of the marine engines M401A-1(2) and Detroit Diesel 16V149TI type.

a)

b)

Fig. 3. The way of introducing boroscope and fiberoscope endings into cylinder space
a) M401A-1 engine- through the holes after removing fuel injectors,
b) Detroit Diesel engine 16V149TI type – through the inlet air slots on the cylinder liner.

A fiberoscope (boroscope), after fuel valve removing, gives an operator opportunity to look trough the flexible optic system on the piston crown, cylinder liner, cylinder head and other parts within one, such as fuel valve nozzle, inlet and exhaust valves, starting air valves and others (fig. 4). This method plays important part in multi-block and multicylinder engines. For example in "star-shape" engines M503A and M520A series, lower monoblocks and lower parts of reduction-reversing gear are not easy accessible in small ship's compartments. So, during overhauls engines together with gears must be uncoupled with propeller shaft, bind up, take up and sometimes even turn up in engine room to get access to the first or seventh monoblock. From our operation experiences results that a fiberoscope with elastic and long enough optic system allows avoiding some of these difficult and dangerous inconveniences hence, allows saving time and money even by 25-30% [7].

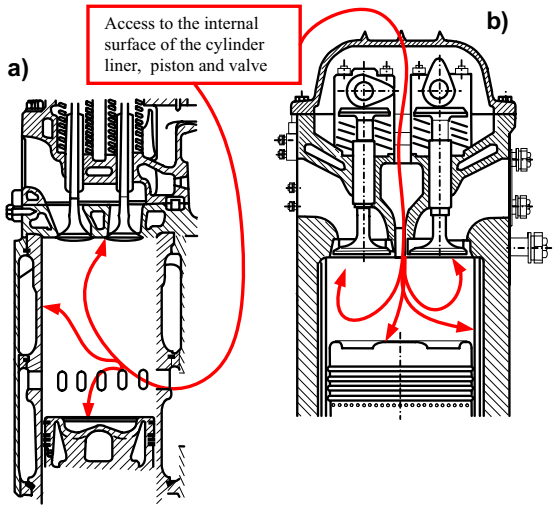

Fig. 4. Endoscopic examinations of the marine engine – access to the internal spaces of the cylinder liner: a) Detroit Diesel engine 16V149TI type b) M401A-1(2) engine

4. Failures of the marine engines' cylinder liners

The systematic periodical endoscopic investigations of the engines operated in the Polish Navy should be carried out in the following situations:

- ⇒ during prophylactic surveys (at least once a year),
- ⇒ during assessment of engine technical state when extension of between – repair period is necessary,

⇒ in the case of excessive vibrations, metal filings detected in lube oil, deviations of the trend line of the average indicated pressure's values (indicated power) from the cylinder, excessive exhaust temperature, drop of power, excessive smoking, etc., when disassembling the engine heads is difficult and time consuming.

On the basis of perennial endoscopic examinations of the marine engines there have been elaborated methods of the technical state evaluation in the operation conditions. The methods include the range and chronology of the performing internal space inspections enabling defects detection of the engine functional systems' parts. There have been also elaborated detailed guidelines for the diagnostic research performance with the usage of fiberoscope and boroscope set. The detected defects are photographically recorded to file them in a computer data base and establish their trends. The most frequent defects of the cylinder liners of the examined marine diesel engines are presented in fig. 5, 6 and 7 [2,3,11].

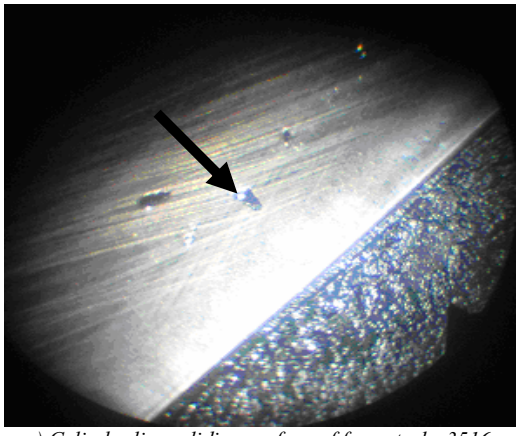

a) Cylinder liner sliding surface of four-stroke 3516 CATERPILLAR engine – erosion pits so called „rush" on the nitric layer in the TDC

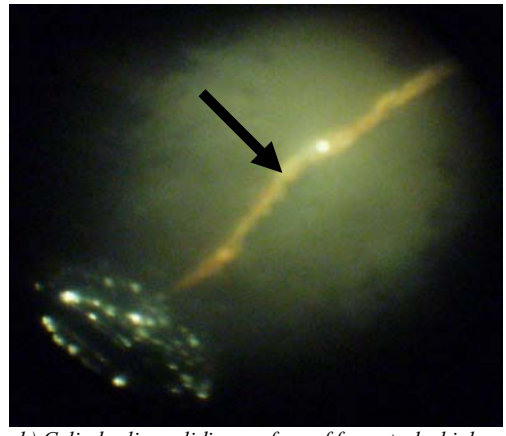

b) Cylinder liner sliding surface of four-stroke high-speed M503A ZVEZDA engine – cylinder liner cracks

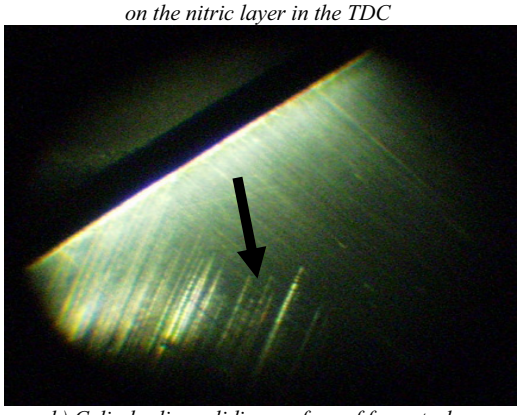

b) Cylinder liner sliding surface of four-stroke 6AR25/30 SULZER engine – insignificant friction wear traces, clear visible "honing" boundary

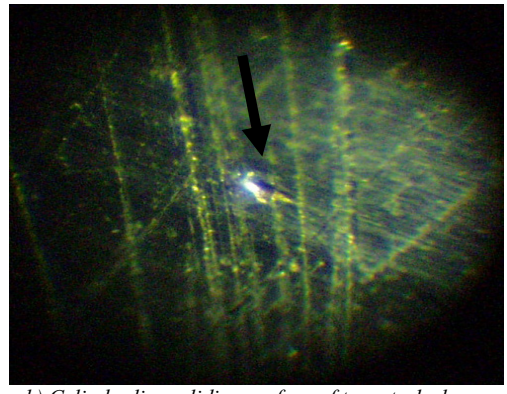

b) Cylinder liner sliding surface of two-stroke low-speed 6TD48 SULZER (ŚWIĘTOCHOWICE) engine – a local corrosion source

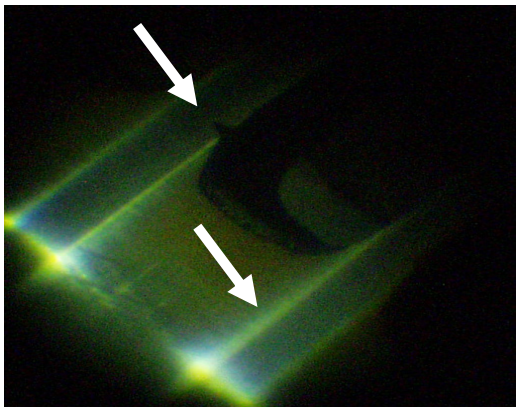

e) Outlet louver of timing gear system of two-stroke low-speed 6TD48 SULZER (ŚWIĘTOCHOWICE) engine – material dent on the louver's edge as well as visible friction traces

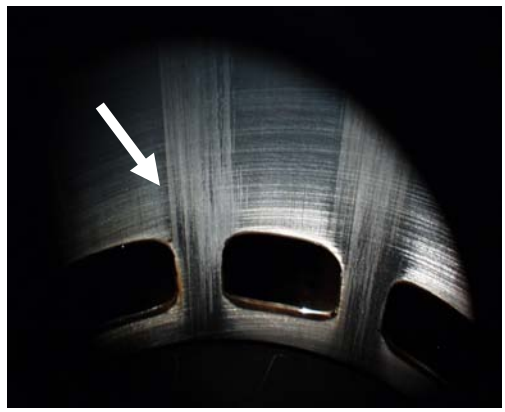

f) Cylinder liner's lower part of two-stroke low-speed 6TD48 SULZER (ŚWIĘTOCHOWICE) engine, in the vicinity of timing gear louvers – clearly visible friction traces on the cylinder liner sliding surface

Fig. 5. Marine engines' cylinder liner defects identified during endoscopic inspections

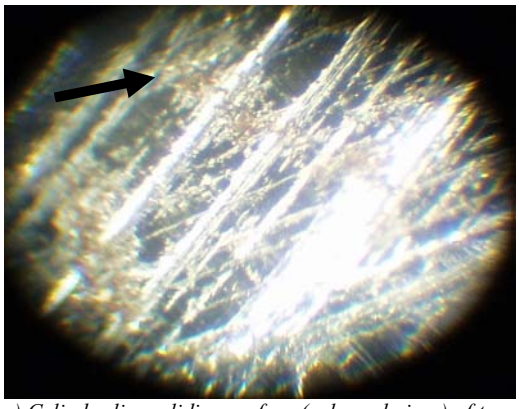

a) Cylinder liner sliding surface (enlarged piece) of two-stroke low-speed 6TD48 SULZER (ŚWIĘTOCHO-WICE) engine – remained products of friction wear (leading rings made of copper alloy), rubbed into „honing" traces

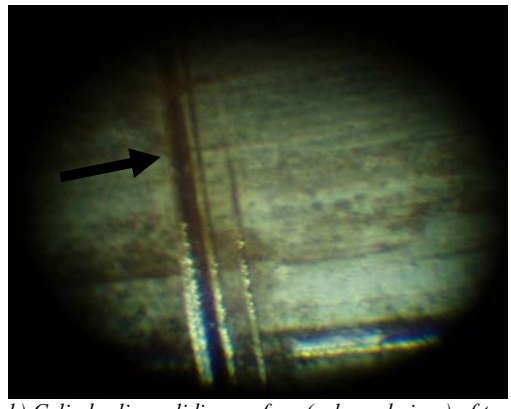

b) Cylinder liner sliding surface (enlarged piece) of two-stroke low-speed 6TD48 SULZER (ŚWIĘTO-CHOWICE) engine in the upper part – deep scratch in the plane of crank's rotation

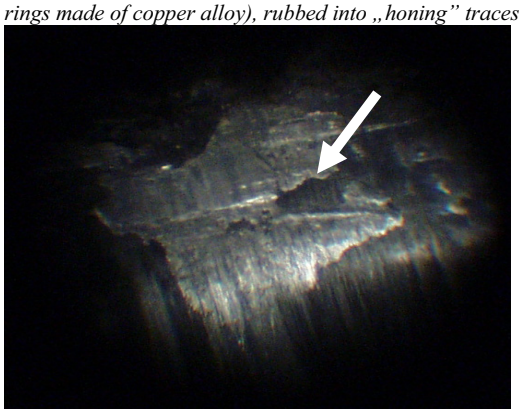

c) Cylinder liner sliding surface of four-strokeM401A2 ZWIEZDA engine e- traces of piston's seizing in the cylinder liner

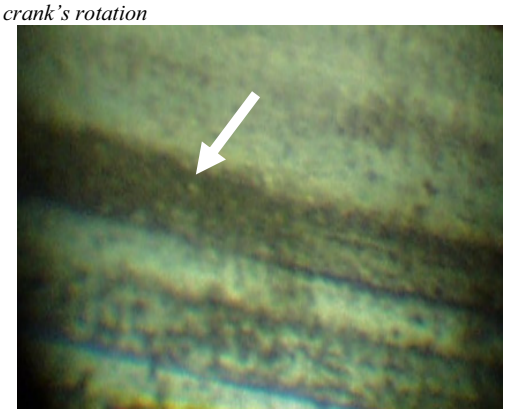

b) Cylinder liner sliding surface (enlarged piece) of two-stroke low-speed 6TD48 SULZER (ŚWIĘTOCHO-WICE) engine in the upper part –piston ring wear traces

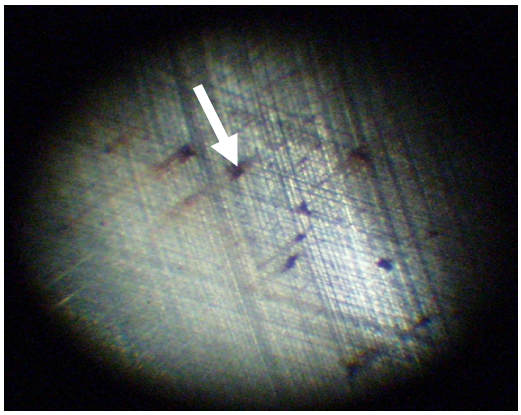

e) Cylinder liner sliding surface of four-stroke 4.400E/ESC NANNI DIESEL engine – local corrosion sources

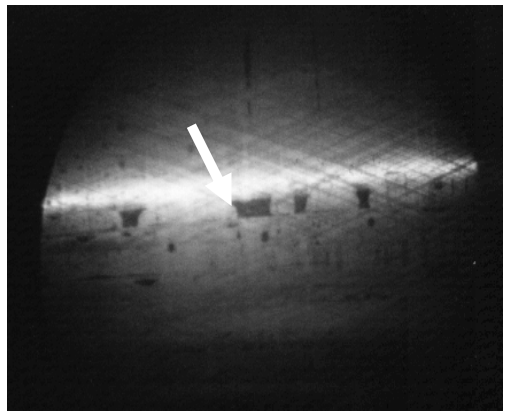

f) Cylinder liner sliding surface of four-stroke 6ATL25/30 SULZER engine – corrosion and erosion scars

Fig. 6. Marine engines' cylinder liner defects identified during endoscopic inspections

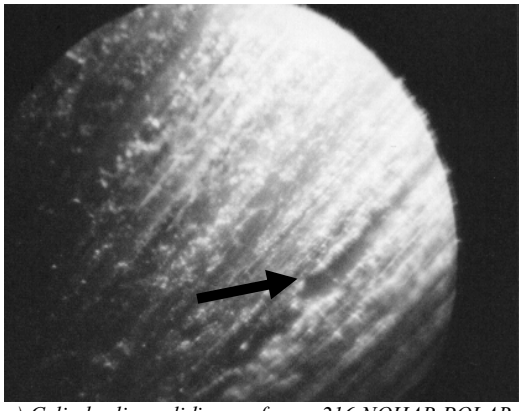

a) Cylinder liner sliding surface – 216 NOHAB POLAR engine – catastrophic friction traces

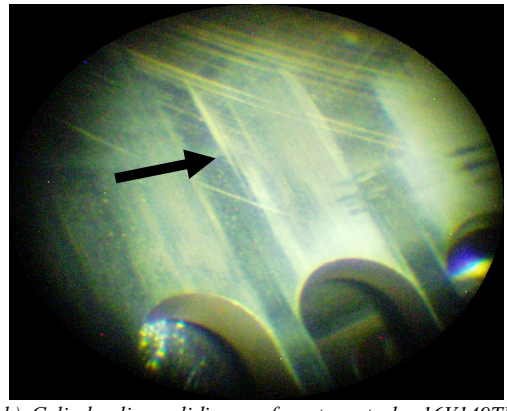

b) Cylinder liner sliding surface two-stroke 16V149TI DETROIT DIESEL engine in the vicinity of air louvers – the wane of "honing" traces

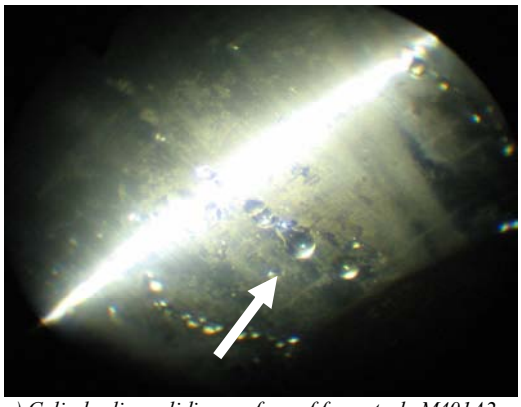

c) Cylinder liner sliding surface of four-strokeM401A2 ZWIEZDA engine – a presence of water drops testifying the cylinder liner's crack

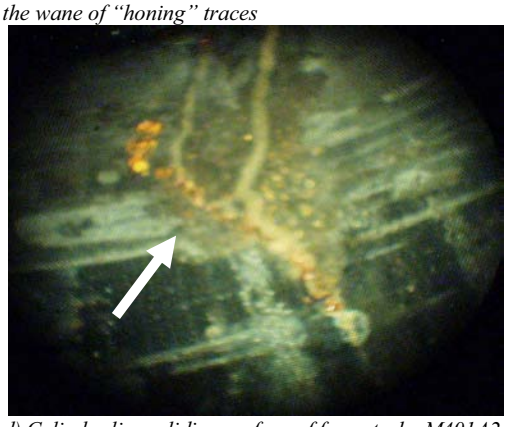

d) Cylinder liner sliding surface of four-stroke M401A2 ZWIEZDA engine – cracked cylinder liner

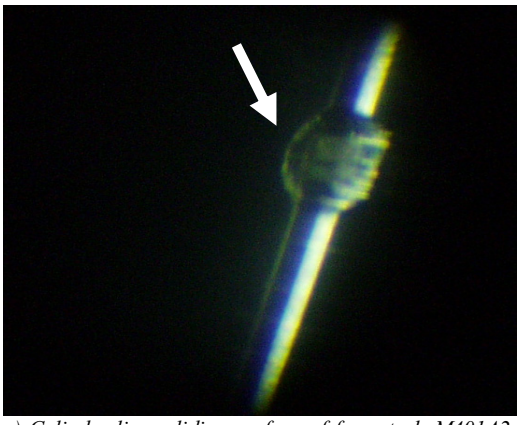

e) Cylinder liner sliding surface of four-strokeM401A2 ZWIEZDA engine – visible friction wear traces

f) Cylinder liner sliding surface of four-strokeM401A2 ZWIEZDA engine – a lengthwise friction wear trace originated by the piston ring being "hung up" in groove

Fig. 7. Marine engines' cylinder liner defects identified during endoscopic inspections

5. Conclusions

The endoscopic investigations carried out during almost 15 years periodical prophylactic surveys of naval diesel engines demonstrated that the method was very effective and usage of the applied instruments was relatively easy. Many material defects of the structural elements, which could be dangerous for the engine in the case of their uncontrolled growing, were identified in result of the examinations. Detail description of the detected defects can be found in the relevant annual reports [11].

The wane of the "honing" traces on the cylinder liner sliding surface represents the observable symptom of the marine diesel engines' wear and tear process. Endoscopic methods being introduced into routine diagnostic examinations of the engines operated in the Polish Navy give the possibility of wear and tear intensity evaluation and prognosis as well as failures' detection within combustion chambers (cylinder sets) in advance (in due time) which threaten the engine with a break-down. This advantage enables the engine's operator an efficient planning the usage according to the engine's actual shape, at considerable costs' diminishing even by 25-30%.

6. References

[1] Kondratiev, N.N., *Otkazy i defekty sudowych dizelej*, Izdatielstwo „Transport", Moskwa 1985.

[2] Korczewski, Z., Pojawa, B., *Diagnostyka endoskopowa silników okrętowych*, XXXII Ogólnopolskie Sympozjum „Diagnostyka Maszyn", Węgierska Górka, 28.02-05.03.2005.

[3] Korczewski, Z., Pojawa, B., *Diagnozowanie okrętowych silników spalinowych z zastosowaniem endoskopów*, VII Sympozjum Naukowo-Techniczne „Silniki spalinowe w zastosowaniach wojskowych" „SILWOJ'2005", Rynia, 26.10-28.10.2005. s. 183-192.

[4] Niewczas, A., *Podstawy stochastycznego modelu zużywania poprzez tarcie w zagadnieniach trwałości elementów maszyn*, Zeszyty Naukowe, Mechanika nr 19, WSI Radom 1989.

[5] Piaseczny, L., *Technologia naprawy okrętowych silników spalinowych*, Wydawnictwo Morskie, Gdańsk 1992.

[6] Sitnik, L., *Kinetyka zużycia*, Wydawnictwo Naukowe PWN, Warszawa 1998. ,

[7] Tartakovskij, I.B., *Korreliacionnyje uravnienia iznosa*, Vestnik Maszinostroenija nr 2. Moskwa 1968.

[8] Wajand, J.A., Wajand, J.T., *Tłokowe silniki spalinowe średnio- i szybkoobrotowe*, WNT Warszawa 2005.
[9] Wieszkielskij, S.A., Łukianczenko, B.S., *Techniczeskaja eskpłuatacja dwigatielej wnutriennowo sgoranija*, Maszinostronije, Leningrad 1978.
[10] *Dokumentacja techniczna i eksploatacyjna okrętowych turbinowych silników spalinowych typu M401A-1(2), M503, M520, Detroit Diesel.*
[11] Sprawozdania z badań diagnostycznych tłokowych silników spalinowych eksploatowanych na okrętach MWRP - *Prace badawcze AMW,* Gdynia 1992 ÷ 2006.

SURVEY OF DESIGN STRATEGIES INCREASING SAFETY OF SHIP POWER PLANTS

Tomasz Kowalewski, Antoni Podsiadło, Wiesław Tarełko

Gdynia Maritime University
ul. Morska 81-87, 81-225 Gdynia, Poland
tel.: +48 58 6901331, fax: +48 58 6901399
e-mail: tar@am.gdynia.pl

Abstract

There are many various sources of dissipated information supporting design of ship power plant from a safety point of view. As a rule, they have diverse forms and scopes and their use makes design of the operator's safety difficult for designers. Therefore, it is reasonable to collect and integrate all developing and existing design rules, taking into consideration the operator's safety, into one coherent system. This paper deals with the computer-aided system supporting design of the most dangerous zones for machinery operators. Its first module compares selected hazard zones from a danger point of view for operators. In depends on the obtained dangerous degree, the second module proposes various design strategies for the considered zones for example: withdrawing operators to more safe places, selection of suitable design features for machines, installations and their layouts, etc. In this paper, the examples of such strategies are presented as well.

Keywords: *ship power plant, computer-aided system, safety, hazard zone, design strategies*

1. Introduction

Effective ship power plant design that satisfies functional requirements and can be easily operated and maintained requires a vast amount of knowledge. Design, in turn, mainly depends on skills and possibilities of designers. As a rule, they specialize in designing different design properties (reliability, manufacturability, etc.) and they can apply design solutions proved in practice at the final design stage or present their proposals during so-called design reviews. More complexity of current ship power plants contests effectiveness of such design methods. This issue concerns such a design property like a safety as well.

One of the possible solutions for increasing the effectiveness of the design process is to build a computer-aided system supporting design process of safe ship power plants. Such the system has been developing in Gdynia Maritime University. It consists of two main modules:

- a system of hazard zones identification in ship power plants on a base of a their preliminary design,
- an expert system aiding design of the most dangerous zones from a safety point of view.

The main task of the first module is to compare selected hazard zones from a danger point of view for operators. The second module task is to propose detailed design solutions decreasing the impact of dangerous and harmful factors for operators of ship machinery. The concept of the first system is presented in [5]. The proposed paper deals with the second system that is the computer-aided system supporting design of the most dangerous zones from a safety point of view.

2. Assumptions of computer-aided system supporting the design of safe ship power plants

In the developed computer-aided system supporting a design process of ship power plants that should be safe for their operators, we have taken into consideration the following assumptions:

1. Design solutions taking into account the operator's safety can be 'built-in' into a ship power plant at any phases of the design process.
2. Scale of these solutions depends on the considered design phase of according to the rule: *the earlier design phase, the more general design solutions*.
3. Potential hazards appearing for operators of a ship power plant can came into being when the operators will be carried out any operational or maintenance activity involving the ship machinery.
4. The eventual design solutions have to be related to such ship power plant zones, in which can appear potential hazard situations for operators.
5. Identification of such hazard situations is carried out based on:
   - information concerning factors influenced the operator's safety can be received based on analysis of the design documentation developed for a given design phase of a ship power plant,
   - knowledge acquired from experts in the field of ship power plant design, operation and maintenance.
6. The set of operator's safety design strategies can be developed for each of the related design phases.
7. Such design strategies should allow to develop a set of detailed design solutions related to the related design phases.

The last two assumptions mean that we should not 'build-in' the detailed design solutions at the initial design phases and the general design solutions at the final design phases.

3. Design strategies increasing the safety of ship power plants operators

The first module of the developed computer-aided system makes possible carrying out the assessment of the potential hazard situations according to the rule: *the earlier design phase, the assessment more general*. In this assessment, both types of information distinguished in point 5 of assumptions are used. In depends on results of such assessment, we can take various design strategies into account during design of the considered zone with the potential hazard situations.

In order to develop such design strategies, we taken into account of so-called the operator's activity chain [7], which consisted of the following elements:

- an operator,
- an engine room component (part, unit, installation, etc),
- an operator's operational activity.

Combinations of these elements set up so-called the elementary hazard zones considered in the first module of the mentioned system. Moreover, they are potential sources of hazards for operators carrying operational or maintenance activities involving the ship machinery. Therefore, we can state that each of such elementary hazard zones can be more or less dangerous for the operators. Based on this statement, we could formulate the crucial design rules for the safety of ship power plant operators:

- to minimize time of carrying out operational or maintenance tasks by operators in the machinery room,
- to minimize impact of sources triggering hazards for operators carrying out operational or maintenance activities in the machinery room.

Next, to obtain a set of design strategies we associated all elements of operator's activity chain with the crucial design rules mentioned above. This way, we obtained a kind of a matrix contained

design strategies allowing to increase the safety of ship power plant operators. Such design strategies set up a kind of framework making possible to develop the detailed design rules, which could be used in design of the operator's safety. This framework is presented in Tab. 1.

In our opinion, the developed design strategies presented in Tab. 1 make possible to develop the detailed design rules, which could be used in design of the operator's safety. It is obvious that such design rules, taking into account the operator's safety, are applied in the most of design solutions in ship power plants of new built ships. However, the sources of information concerned these rules are dissipated.

Tab.1. The framework supporting to develop design strategies

Crucial design rules increasing the safety of ship power plant operators		**Elements of operator's chain activity**		
		Operator	Activity	Engine room component
Minimization of time of carrying out operational or maintenance tasks by operators	Exclusion of an operator from the machinery room hazard zone	Automation of operational or maintenance activities	Remote control of operational or maintenance activities	Withdrawing of engine room components to other zone
	Decreasing of time of operator's being in the machinery room hazard zone		Mechanization and grouping of operational or maintenance activities	Increasing of a maintainability level in the machinery room hazard zone
Minimization of impact of sources triggering hazards for operators	Exclusion of hazard sources from the machinery room hazard zone			Postponing of carrying out the required operation
	Decreasing of impact of hazard sources from the machinery room hazard zone		Reallocating of operational or maintenance activities to one zone with the less hazard level	Change of design properties of components situated in the machinery room hazard zone

Many of such rules can be found in domain books, for example in [1,6,8], in guidelines issued by International Maritime Organization (IMO) and classification societies, for instance [2,3]. Moreover, in many of new built ship power plants are applied design solutions taking into consideration the mentioned rules without any relations to the mentioned information sources [4]. In our opinion, the knowledge, intuition and experience of the designers have been employed in such cases. Therefore, it is reasonable to collect and integrate all developing and existing design rules, taking into consideration the operator's safety, into one coherent system. Such an approach does not exclude the possibility of devising and developing new design rules for the operator's safety. In order to do it, we could apply the presented fundamental design strategies increasing the operator's safety of ship power plants.

4. Survey of chosen design strategies increasing operator's safety in machinery room

4.1. Automation of operational or maintenance activities

Exclusion of an operator from the machinery room hazard zone can be carried out, for example by automation of:

- complement of cooling medium in gravity tanks,

- drainage of engine room bilges,
- activating boiler sootblowers (Fig. 1).

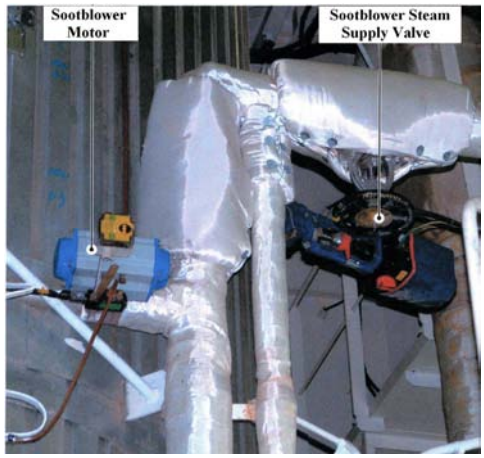

Fig.1. Automation of auxiliary boiler sootblowers

4.2. Remote control of operational or maintenance activities

In this design strategy, operators are withdrawing from hazard zones and their activities are carried out from a zone with the less hazard level by remote-controlled devices, for example:

- remote control of bilge, ballast or fuel valves (such control is realized most often by hydraulic power pack located in safety place in engine room) – of course the valves, besides the remote control, must have possibility of local control (Fig. 2a),
- remote control of fire dampers in ventilation systems (Fig. 2b).

a)

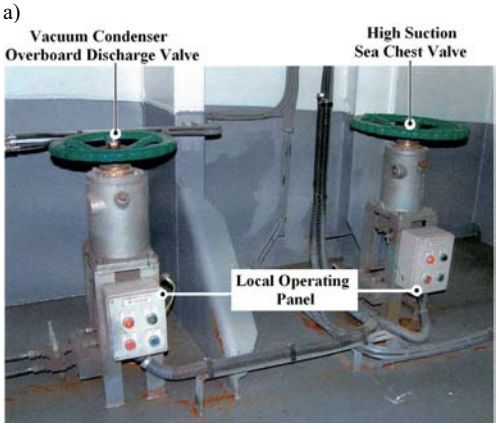

b)

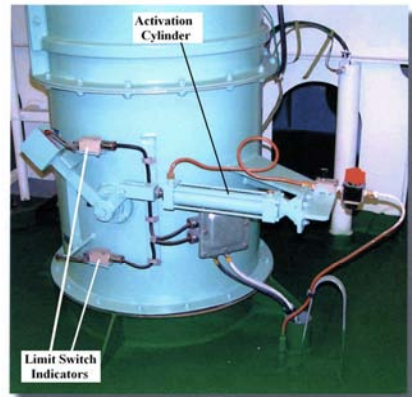

Fig. 2. Remote control of valves and fire dampers

4.3. Withdrawing of engine room components to other zone

In this design strategy, minimization of time of operational or maintenance tasks carried out by operators is realized by reallocating engine room components to machinery zones with the less hazards, for example grouping of engine room components in the separated spaces with the less

hazard level. It concerns systems like: hydrophore station of sanitary water, sewage treatment plant (Fig. 3), air condition plant, etc.

Fig. 3. Reallocating engine room components to machinery zones with the less hazards

4.4. Mechanization and grouping of operational or maintenance activities

In this design strategy, decreasing of time of operator's being in the machinery room hazard zone is realized by design of the compact manipulation spaces. Such spaces are presented in Fig. 4.

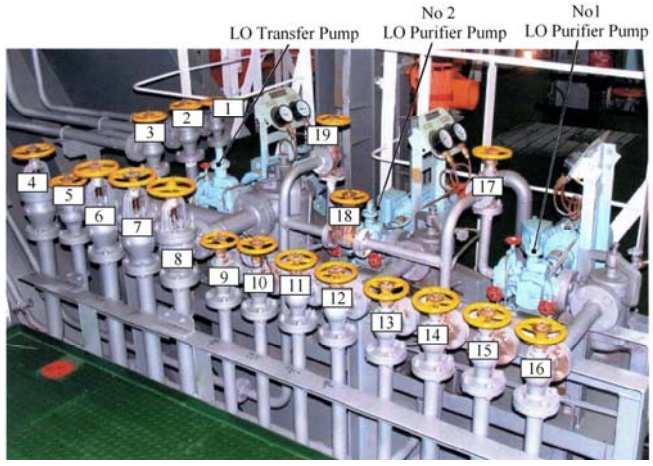

Fig. 4. Decreasing of time of operator's being in the machinery room by design of the compact manipulation spaces

4.5. Increasing of a maintainability level in the machinery room hazard zone

This strategy is realized by increasing of a maintainability level in the machinery room hazard zone, for example: increasing of operator's accessibility to places where is carried out a given operational or maintenance activity (Fig. 5).

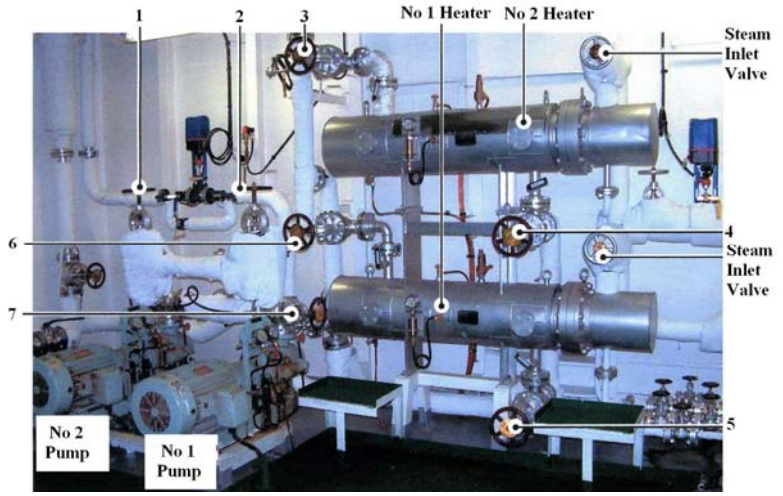

Fig. 5. A boiler fuel oil module with the high maintainability level

4.6. Postponing of carrying out the required operations until the operational stages of ship and/or her machinery permit their execution

In this strategy, decreasing of impact of hazard sources from the machinery room hazard zone is realized by applying of functional redundancy for ship machinery (pumps, heaters – Fig. 4, 5, coolers, tanks, compressors – Fig. 6, etc.).

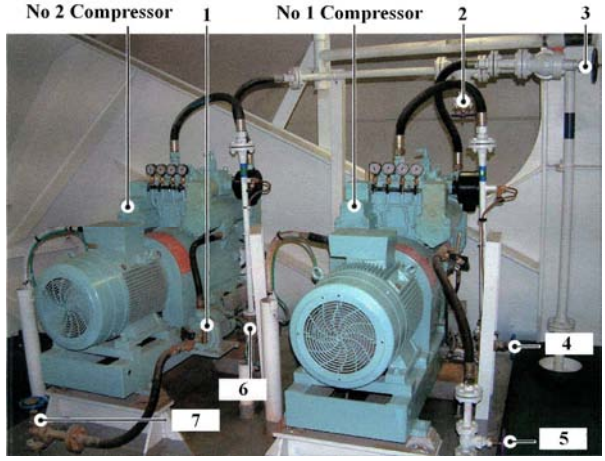

Fig. 6. Decreasing of impact of hazard sources by applying of functional redundancy

4.7. Reallocating operational or maintenance activities to one zone with the less hazard level

In this strategy, decreasing of impact of hazard sources from the machinery room hazard zone is realized by reallocating of operational or maintenance activities to one zone with the less hazard level (Fig. 7).

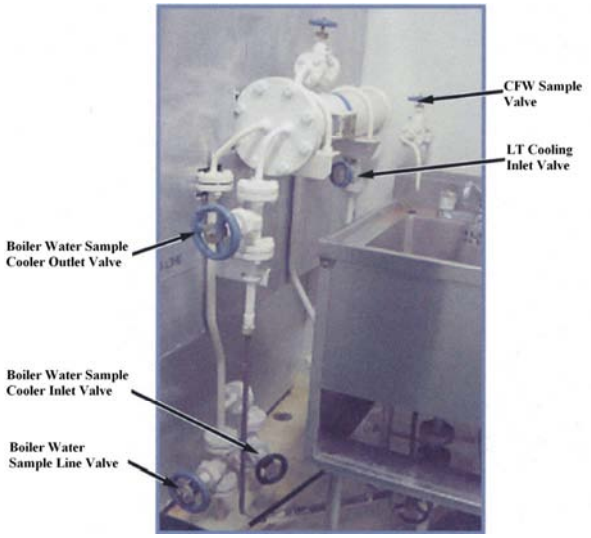

Fig. 7. Taking of water samples for the analyzing purpose from one place

4.8. Change of design properties of components situated in the machinery room hazard zone

In this strategy, decreasing of impact of hazard sources from the machinery room hazard zone is realized by changing of design properties of components situated in the machinery room hazard zone, for example:

- applying of thermal, acoustic and vibration isolations,
- applying of prevention screen, etc.

An example of thermal isolation of valves and pipes in the steam distributor is presented in Fig. 8.

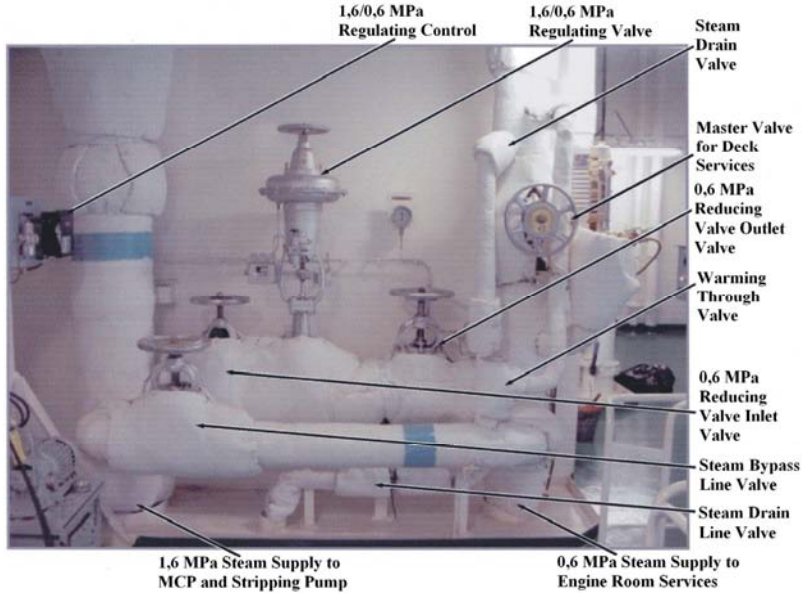

Fig. 8. Thermal isolation of valves and pipes in the steam distributor

5. Conclusion

The discussion about the information sources and the brief survey of chosen design strategies increasing operator's safety in machinery room allow us to state that:

- there are many various sources of dissipated information having diverse forms and scopes,
- their use makes design of the operator's safety difficult for designers of ship power plants.

Therefore, it is reasonable to collect and integrate all developing and existing design rules, taking into consideration the operator's safety, into one coherent system. Such an approach does not exclude the possibility of devising and developing new design rules for the operator's safety. In order to do it, we could apply the presented fundamental design strategies increasing the operator's safety of ship power plants.

In our opinion, the second module of the presented computer-aided system, that is an expert system aiding design of the most dangerous zones from a safety point of view, should meet such a requirement. As it was mentioned, such a system is developing in Gdynia Maritime University as the project funded by the Polish financial resources for scientific research.

References

[1] *Ergonomic design for people at work*, *Vol. 1 – Workplace, and environmental design and information transfer,* By: The Human Factors Section Health, Safety and Human Factors Laboratory, Eastman Kodak Company. Van Nostrand Reinhold, New York 1983, *Vol. 2 – The design of jobs, including work patterns, hours of work, manual materials handling tasks, methods to evaluate job demands, and the physiological basis of work.* By: The Ergonomics Group, Health and Environment Laboratories, Eastman Kodak Company, John Wiley & Sons Inc., New York 1986.

[2] *Guidance notes for the application of ergonomics to marine systems,* American Bureau of Shipping, Houston 2003.

[3] *Guidelines for engine room layout, design and arrangement*, International Maritime Organization, London 1998.

[4] *BP British Purpose Machinery Operating Manual,* Worldwide Marine Technology Ltd., Revision 1, October 2000.

[5] Podsiadło, A., Tarełko, W., *Modelling and developing a decision-making process of hazard zone identification in ship power plants*, International Journal of Pressure Vessels and Piping, 2006, No. 83, pp.287–298.

[6] Salvendy, G., *Handbook of human factors and ergonomics*, John Wiley & Sons Inc., New York 2006.

[7] Wojciechowicz, B., Ziemba, S., *Zadania nauki w budowie maszyn*, Zagadnienia Eksploatacji Maszyn, Zeszyt 3-4, 1986, s. 433-443.

[8] Woodson, W.E., Tillman, B., Tillman, P., *Human factors design handbook – Information and guidelines for the design of systems, facilities, equipment, and products for human use*, McGraw-Hill Inc., 1992.

Acknowledgement

This development is supported by the Polish financial resources for scientific research as the project no. 4 T07B 025 29.

MECHANISMS OF EROSION WEAR IN PIPES CAUSED BY A STREAM OF SOLID PARTICLES

Bazyli Krupicz

Bialystok Technikal University
ul. Wiejska 45C, 153-51 Bialystok, Poland
tel.: +48 85 7469015
e-mail: bazek@pb.edu.pl

Abstract

In the paper an analysis of pipe bend erosion was conducted. This erosion was compared to the erosion of flat samples. The function of particle velocity change: $v/v_o=e^{-cf}$ was assessed and contact stress caused by the centrifugal force of inertia of solid particles (diameter $d < 0,1$ mm) in the bend material was calculated.

Keywords: *erosion, pipe bend, contact stress*

1. Introduction

The contact of the jet of solid particles with the material surface causes its erosion. The magnitude of loss depends on three primary factors: 1) properties of the material exposed to erosion, 2) abrasive material, 3) the environment in which the erosion takes place. As far as erosion wear is concerned, only the material exposed to the impact of the particles is the subject of the analysis. In industrial practice, it concerns machine elements and installations that transport granular material. These are mainly: pump impellers, fans, turbines and pipe bends as well as Diesel engine elements [1]. General cause of the losses is common to all installations but each erosion case has its own characteristics. The magnitude of material loss may be different for different values of kinetic energy, glancing angles, shape, hardness and strength of granules of the abrasive material. The environment of the pipe bend is the most suitable for analyzing different glancing angles of impacting particles.

In this paper an analysis of erosion losses in the bend pipe covered with protection layer of polyurethane rubber was made

2. Analysis of particle motion in a pipe bend

The particle of the abrasive material slides on the surface of the bend. During this process friction force F_t influences the particle. The value of this force depends on the pressure of centrifugal force F_b and friction factor f, i.e.:

$$F_b = m\frac{v^2}{R}, \quad F_t = f m\frac{v^2}{R}, \tag{1}$$

where: m – mass of the particle. The resulting action of the force F_t is the decrease of the particle velocity. The friction force performs the work, which for elementary displacement *ds,* equals

$$dA = F_t ds = f m \frac{v^2}{R} ds. \tag{2}$$

Particle velocity on the way *ds* changes from value *v* up to *(v+dv)* and kinetic energy from $mv^2/2$ to $m(v+dv)^2/2$. The change of kinetic energy is equal to friction force F_t

$$\frac{mv^2}{2} - \frac{m(v+dv)^2}{2} = f \frac{mv^2}{R} ds . \tag{3}$$

After taking into account that $ds = v\,dt$ and value of $(dv)^2$ is negligibly small, equation (3) may be presented as follows:

$$dv = -\frac{fv^2}{R} dt \tag{4}$$

After integration with the initial conditions $t = 0$, $v = v_0$ particle velocity is equal to

$$v = \frac{v_0}{1 + \frac{fv_0 t}{R}} . \tag{5}$$

Derivative $\delta v/\delta t = a_t$ describes tangential deceleration of the particles which can be calculated from the equation

$$a_t = -\frac{v^2_0}{R} \frac{f}{(1 + \frac{fv_0 t}{R})^2} . \tag{6}$$

The path of the particle in the bend was calculated on the basis of equation (5) after its integration. Having taken into account the initial conditions of motion $s(t=0) = 0$, the following equations was obtained

$$s = \frac{R}{f} \ln(1 + \frac{fv_0 t}{R}). \tag{7}$$

Particle position in the bend in time *t* is described with angle α:

$$\alpha = \frac{s}{R} = \frac{1}{f} \ln(1 + \frac{fv_0 t}{R}) . \tag{8}$$

Equations describing velocity and tangential acceleration were obtained after eliminating of the variable *t* from equation (5) and (6)

$$v = v_0 e^{-\alpha f}, \quad a_t = -\frac{v_0^2}{R} \frac{f}{e^{2\alpha f}} = -a_n f e^{-2\alpha f} . \tag{9}$$

The decrease of relative velocity v/v_0 was calculated for several types of particles and different friction factor *f* on the distance $\alpha = \pi/2$. The decrease values are as follows:

- quartz sand (f = 0,2), $v/v_o = 0{,}73$,
- wood (f = 0,5), $v/v_o = 0{,}45$,
- wood with sand impurity (f = 0,3), $v/v_o = 0{,}62$.

The time which the particle remained in the bend ($\alpha = \pi/2$), was calculated from equation (8)

$$\Delta t = \frac{R}{f v_0}(e^{f\alpha} - 1). \qquad (10)$$

For R = 1,1 m, v_0 = 100 m/s, Δt_{sand} = 0,0094 s, Δt_{wood} = 0,011 s, $\Delta t_{sand+wood}$ = 0,0097 s. The change $v/v_o(\alpha)$ and $a_t/a_n(\alpha)$ is also presented in Fig. 1.

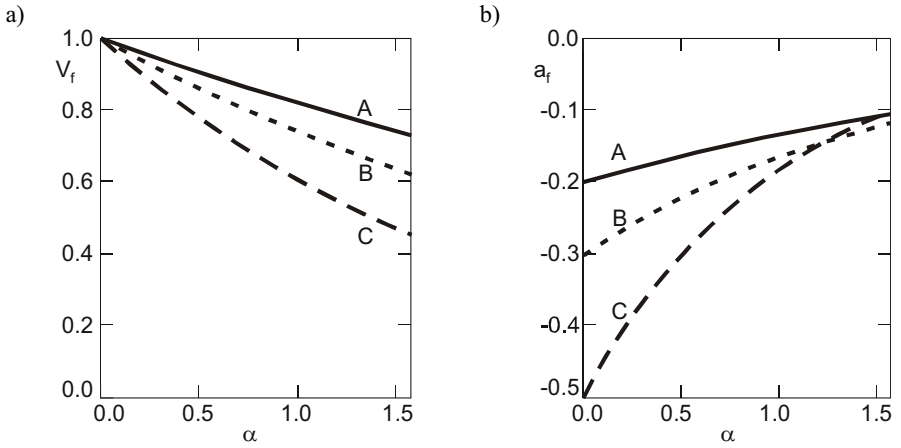

Fig. 1. Dependence between angle distance of the quartz particles (A), blend of quartz and wood particles (B), wood particles (C) : relative velocity v/v_o, b) acceleration a_t/a_n (α)

Several conclusions can be drawn from the analysis of Fig 1a. From the practical point of view, materials which guarantee large values of deceleration of the particles – i.e. materials with large friction factor – should be used in cyclones. On the other hand, the lowest possible velocity losses are required if pneumatic conveying is considered. Therefore, materials with very low friction factor are used in this case.

Erosion caused by particle impact, after which the particle rebounds, is another possible version of the erosion in the pipe bend. This mechanism concerning erosion of ventilator rotor blades is presented in [2,3] papers. Coefficient of velocity restitution after impact plays significant role in this wear mechanism [4].

3. Contact stress caused by inertia

Particle radius is very small compared to bend radius. Therefore a load model of sphere pressure on a flat surface was assumed for stress calculations [2]. In this case contact stress σ_H is equal to

$$\sigma_H = 0.62\sqrt[3]{\frac{F_0}{r^2}\left(\frac{1}{E_1}+\frac{1}{E_2}\right)^{-2}} = 0.62\sqrt[3]{\frac{mv^2}{Rr^2}\left(\frac{1}{E_1}+\frac{1}{E_2}\right)^{-2}} \cong \sqrt[3]{\rho\frac{r}{R}\left(\frac{1}{E_1}+\frac{1}{E_2}\right)^{2} v^2}, \qquad (11)$$

where: F_0 – centrifugal force of inertia, E_1, E_2 – Young's modulus of the particle and bend material, r – particle radius, m – particle mass.

In the case when the sand particle (r = 0,2 mm, E_1 = 400 GPa, density ρ = 4 g/cm^3) slides on the surface of a bend made of steel (E_1 = 208 GPa, R = 1,1 m) the value of contact stress is as follows:

$$\sigma_H = 10^{-6}\sqrt[3]{4\cdot 10^3 \frac{0.2\cdot 10^{-3}}{1.1}\left(\frac{1}{208\cdot 10^9}+\frac{1}{400\cdot 10^9}\right)^{-2} 100^2} = 514\,\text{MPa}.$$

Particle radius is much smaller r* = 1/20 r when particle has feather edges (even if the mass remained unchanged). In that case contact stress increases to $\sigma_H^* = \sqrt[3]{400}\,\sigma_H$ = 3787 MPa. This value of the stress can cause plastic strain and shearing in the upper layer of the material.

4. Bend and flat sample erosion

The analysis of the progressing wear of the pipe bend presented in Fig. 1 shows that the losses of protection layer started at point C described with the angle α = 15°. The shape and size of the crater changed during the experiment. The glancing angle of impacting particles at the edge of the crater approached 0, whereas at the bottom of the crater it approached 90 (point L). Curve CL in Fig. 1b shows the progressing erosion inside the material layer. The protection layer was completely destroyed in the place where α = 20° (point L in Fig. 2b). Particles impacting different parts of the pipe bend may fall at the angle $0 \le \alpha \le \alpha_{max}$. Contact angles correspond to points M and N (Fig. 2a) [1]. For the point N:

$$\cos\alpha_{max} = (R - d)/R; \quad \alpha_{max} \cong 66°.$$

A question arises why the erosion occurred in a particular place and not on the whole area of the bend. To answer the question, a research was conducted in order to show how different glancing angles effected the loss protection layer in the flat samples. The material analyzed was polyurethane PU-01. The experimental conditions were as follows: air pressure p = 0,5 MPa, intensity of flow of the particle abrasive amounted to 630 g/min, particles diameter r = 0,1 mm. The experiment was conducted on three samples..

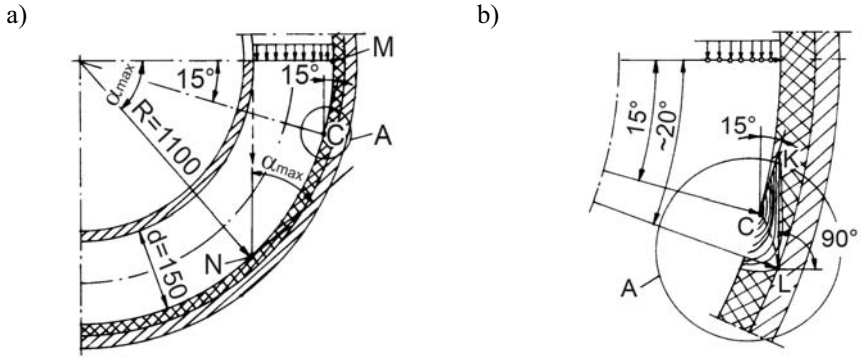

Fig. 2.The diagram of flow of the abrasive granules in pipe bend: a) α_{max} – maximum glancing angle of impacting particles on the pipe bend wall, b) location of forming losses in the layer of polyurethane rubber

The loss was measured in one minute intervals for each glancing angle of impacting particles. The obtained results were approximated with straight lines y = ax, presented in Fig. 3a. Fig. 3b shows the magnitude of wear of the polyurethane depending on the glancing angle of the abrasive. The most significant wear of the material was obtained for the angle which amounted to approx 15^O. This fact can be confirmed by analyzing the wear of the same material in the pipe bend (Fig. 2).

a) b)

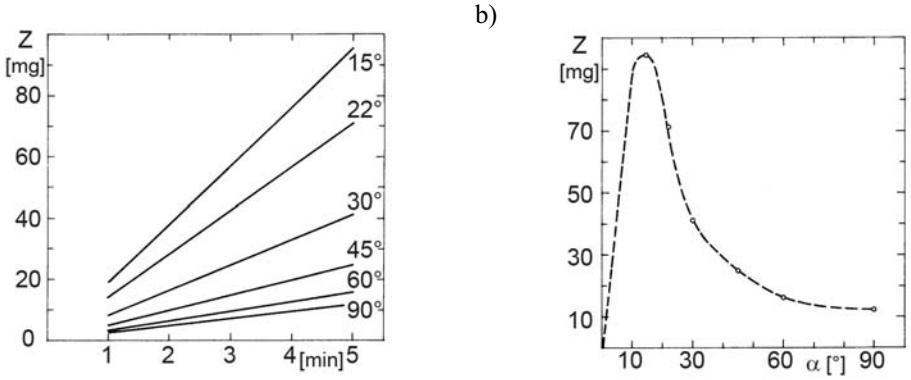

Fig. 3. Erosion of polyurethane PU-01 under the influence of abrasive jet depending on: a) time for different glancing angles, b) glancing angle.

As it is presented in Fig 2 and 3, maximal erosion velocity in a pipe bend and a flat sample is recorded at this same glancing angle of particles impacting on a flat sample and the angle formed by stream of particles and tangent to a pipe bend. Erosion is located only at this point which means that the particles rebound after they strike into a pipe wall. Rebounded particles protect further part of the bend from erosion. This mechanism leads to inventing a new bend construction [5] presented in Fig. 4. The pipe bend (7) has a caving (4) filled by material (3). This material can be easily replaced and refilled using a hole (5) in the bottom part of the caving. A stream of particles moving near the wall reduces velocity after impacting the material (3) and constitutes protection layer for other parts of the bend after it leaves the caving (6).

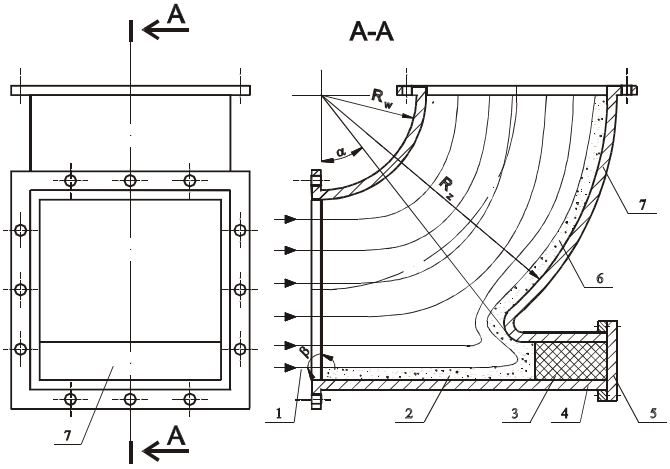

Fig. 4. Diagram of pipe bend construction with a replaceable element that is subject to erosion

5. Conclusions

1. Decrease of the particle velocity caused by centrifugal force of inertia depends on friction factor. Particle deceleration decreases with angular distance. Initially the deceleration is the greater the higher values of the friction factor there exist. After angular distance of $\pi/2$ the deceleration is practically independent of the friction factor.

2. Contact stress caused by centrifugal force of inertia of the particles may lead to plastic strain and shearing in the upper layer of the material
3. Maximum erosion velocity in a pipe bend and a flat sample takes place at the same glancing angle of impacting particles and the angle formed by a stream of particles and tangent to a pipe bend.

6. References

[1] Mechanisms of erosion wear in pipes caused by a stream of solid particles Pogodaew, P.I., Shewchenko, P.A., *Gidroabraziwnyj i kawitacionnyj iznos sudowogo oborudowanija,* Sudostroenie, Leningrad, 1984.

[2] Krupich, B., *Challenges in provision of the wear resistance of pneumatic transport parts,* Friction and wear, Vol.23, 2002, 5, 477-482.

[3] Barsukov, V.G., Krupich, B., Sviridenok, A.I., *Features in impact interations beween solid particles and fan vanes,* Friction and wear, Vol.25, 2004, 1, 41-47.

[4] Krupicz, B., *Rola współczynnika restytucji prędkości twardych cząstek w procesie erozyjnym wentylatorów*, Zeszyty Naukowe nr 10(82) Akademii Morskiej w Szczecinie, 299-307, IV Międzynarodowa konferencja Naukowo-techniczna EXPLO – SHIP 2006.

[5] Zgłoszenie patentowe P-329729 „Konstrukcja łuku rurociągu o zwiększonej odporności na działanie erozyjne strumienia cząstek stałych''.

Paper was written as a part of the Rector's project W/WM/01/03.

HARDWARE ABILITIES OF LINEAR DECIMATION PROCEDURE IN PRACTICAL APPLICATIONS

Piotr Krzyworzeka, Witold Cioch, Ernest Jamro

University of Science and Technology (AGH-UST)
al. Mickiewicza 30, 30-059 Kraków, Poland
tel.: +48 12 6173622, fax.: +48 12 6332314
e-mail: cioch@agh.edu.pl

Abstract

Procedure of Linear Decimation (PLD) has many practical implementations. The hardware implementation in FPGA (Field Programmable Gate Arrays) of the PLD significantly shortens computation time and allows increasing signal sampling frequency. As a result real-time signal analysis can be obtained which allows for e.g. rotating machine diagnostic during run-up phase. Examples of practical results for the PLD and novel Short-Time PLD are presented.

Keywords*: diagnostics, non-stationary signal, synchronism, decimation,*

1. Introduction

Diagnosing rotary-machine states in variable real-time conditions is vital for their operation safety. Early detection of conditions of incorrect operational processes, as well as of arising damage development can often prevent from failures or serious accidents. The Procedure of Linear Decimation (PLD) [4, 5, 8, 9] has been successfully tested in diagnostic systems for non-stationary cyclical machines. Appling the PLD offers the possibility to increase the energy contributions of time- and frequency- symptomatic components of the signal.

Early detection of failure is determined not solely by a proper detection procedure but also by electronic implementation of diagnostical device. Since the latter may significantly lengthen the calculation time, the failure-detection time may not be achieved within acceptable limits. Consequently, FPGAs (Filed Programmable Gate Arrays) implementation of the PLD is adapted. Hardware (FPGA) implementation of the PLD compared to microprocessors or Digital Signal Processors (DSP) can significantly reduce the calculations time. Furthermore, FPGA implementation of the PLD allows increasing signal sampling frequency, which results in more accurate spectra selectivity.

2. Procedure of Linear Decimation (PLD)

Procedure of Linear Decimation involves the dynamic signal resampling in accordance with rotation speed variations [2]. It assumes linear approximation of cycle variations curbed by values representing its beginning cycle time Θ_p and its end cycle time Θ_k. In other words, it involves the deletion of sample-cluster variations proportional to the cycle and maintaining the constant sample-per-cycle number. The resampling process is shown in fig.1

The key element is to define decimation coefficient Dc_K. This coefficient characterizes the increment of signal resampling [1]. It changes in accordance with the increase or decrease of the rotation speed, i.e. with the cycle variations. By adapting the final decimation coefficient we can determine its variations in accordance with linear signal trend. Selecting final decimation

coefficient enables to reduce the signal to the stationary form in the observation window for the last cycle, which is very convenient in real-time analysis.

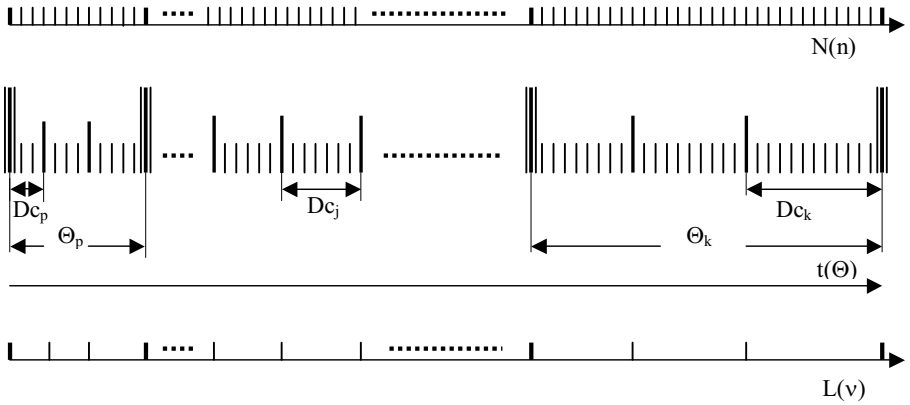

Fig. 1. Procedure of Linear Decimation: Θ - cycle time,(Θ) - observation time, N(n) - primary sample-cluster in the observation window , L(ν) - secondary sample-cluster in the observation window (after LDP), Dc_p - initial decimation coefficient, Dc_k - final decimation coefficient

By selecting a final-decimation-coefficient D_{Ck}, and assuming linear approximation of cycle variations, the decimation coefficient D_{Cn} for n-th sample can be obtained by the fallowing formula:

$$Dc_n = Dc_k \frac{N_{\Theta p}}{N_{\Theta k}} + \frac{n}{n_{Dk}}(Dc_k - Dc_p). \tag{1}$$

By applying the above formula, the secondary vector of the signal representing the constant number of samples-per-cycle is given by the formula:

$$w(\nu_k) = u(n_{Dk} + Dc_n) = u(n) \tag{2}$$

where:

u(n) – primary vector,
w(ν)– secondary vector (after resampling).

Fig.2 contains non-stationary signal representing the run-up phase for gear transmission. Cycle change and its linear approximation is shown in Fig. 3. Unfortunately for the given example, the linear approximation error equals 5.1%. Fig. 4 presents signal after applying the PLD. It features the significant improvement of spectrum quality in rotation frequency band. Unfortunately, distinct stripe selectivity in the frequency band of gear meshing and its harmonics was not achieved. It brings the conclusion that approximation by a linear function in the observation window is suitable only for signals with linear cycle-change trend. This made the authors search for new solutions extending the PLD abilities. For this purpose a Programmable Unit for Diagnostic (PUD) was constructed [6]. The PUD is dedicated to non-stationary signal analysis by means of the signal resampling method with a variable increment corresponding with reference cycle changes.

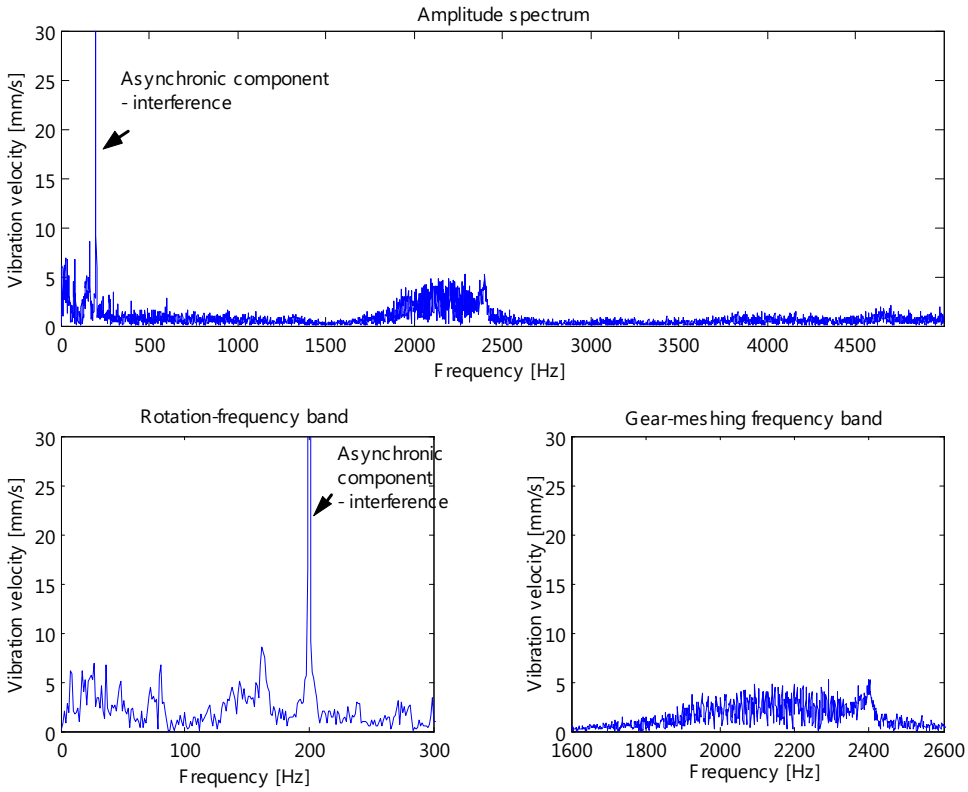

Fig. 2. Amplitude spectrum of vibration velocity of gear-meshing. Average rotational speed increase 0.38 % per cycle

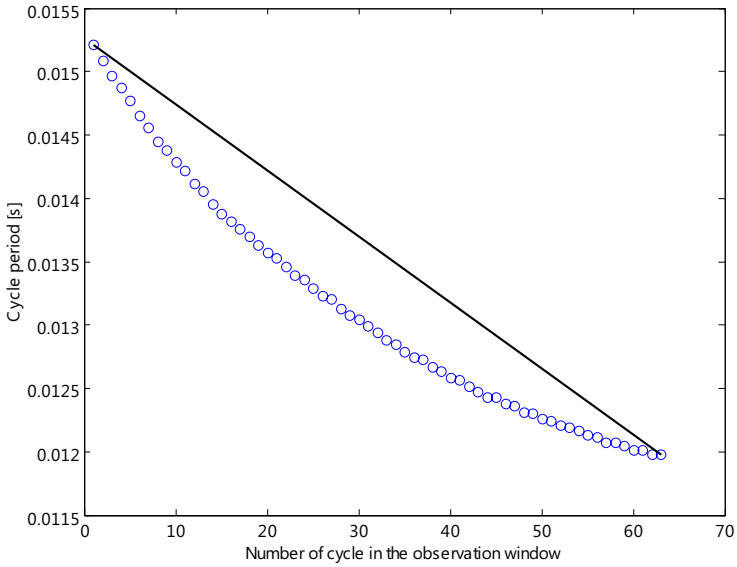

Fig. 3. Cycle length changes within the observation window and their approximation by linear characteristic

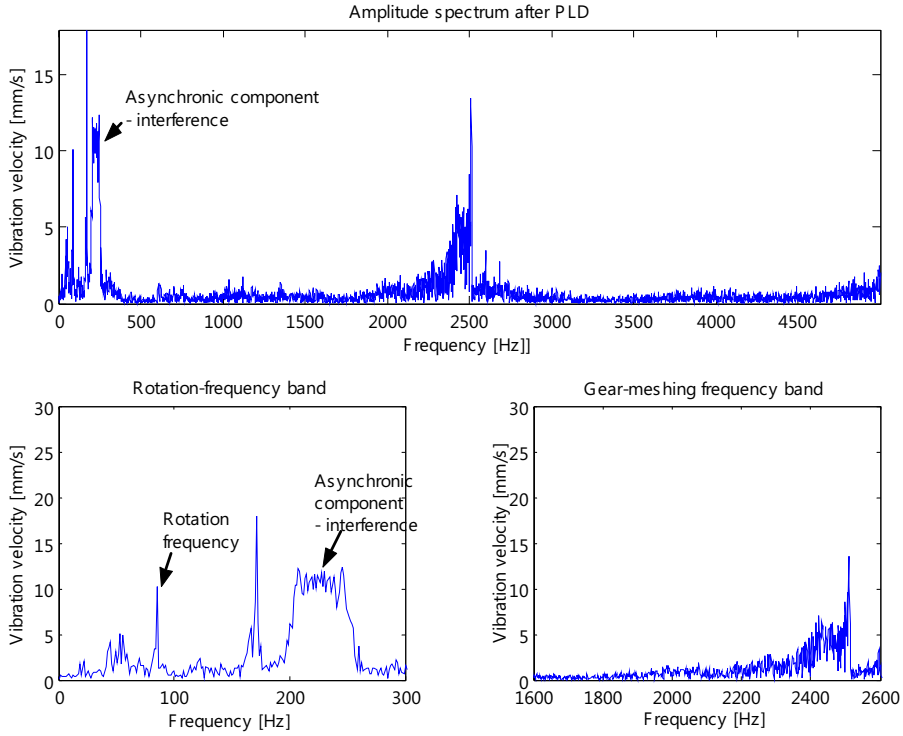

Fig. 4. Amplitude spectrum of vibration velocity of gear-meshing after applying of PLD. Average rotational speed increase - 0.38 % per cycle.

3. Hardware implementation

Electronic implementations of diagnostical procedures are often disregarded in academic discussions. Nevertheless, they can often determine a diagnostic procedure and final results.

The hardware implementation of the PLD can be divided into three separate tasks:

- Marker logic – rotation period indicator,
- Anti-aliasing filter,
- Linear decimation.

3.1 Marker Logic

One ADC channel is dedicated to marker logic (denoted also as rotation period indicator) whose purpose is to synchronise the acquired data with shaft rotation angle. Marker channel is a digital (binary) channel: the marker is detected or not. Nevertheless, the marker signal is usually acquired and transferred to memory as a standard ADC channel e.g. 14-bit channel. This results in inadequate utilization of the resources. Furthermore, in the PLD, the crucial information is not the state of the marker but time-slots between two successive markers. Calculating time periods in a software manner requires significant amount of time, firstly for reading marker state in the external memory and secondly for calculating the time slots by means of microprocessor. This would require tens of clock cycles per marker sample. As a result, dedicated (hardware) marker logic was designed in FPGA, consequently marker states are not transferred to external memory at all. The dedicated marker logic detects markers, then calculates and writes to external memory only time periods between two successive markers.

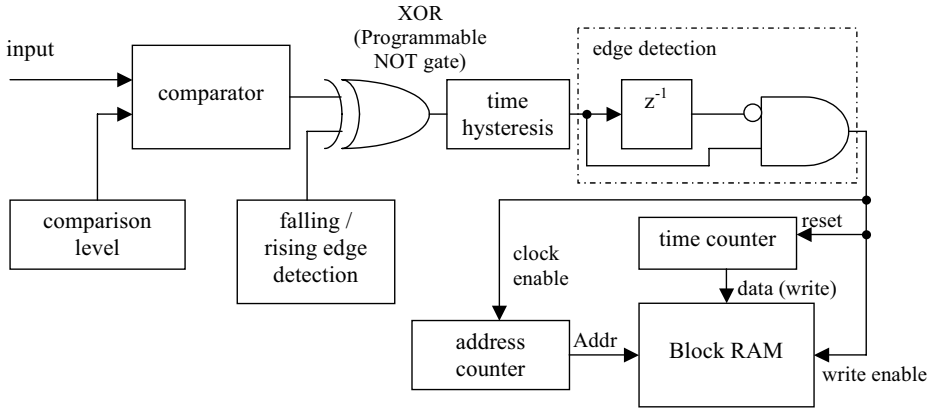

Fig. 5. Block diagram of the marker logic

The block diagram of the marker logic is given in Fig. 5. The input signal from ADC is compared with programmable comparison level (usually middle ADC range) to obtain the binary signal. An alternative solution is that the input signal is already binary, therefore the comparator can be skipped. The binary input is recommended as the number of analog ADC channels is often limited, and marker signal is binary by origin. Then the binary signal may be negated in a XOR gate to detect either rising or falling edge of the marker. Then a special time-hysteresis logic is employed to eliminate input signal glitches. The noise in the input signal is especially destructive when the input signal crosses the comparison level. The hysteresis logic is implemented as a simple up / down counter with saturation. The counter size (the maximum time of eliminated glitches) is programmable. After hysteresis logic, the input signal passes the edge detection logic which produces one clock impulse for every rising edge of the input signal. This impulse initialise the internal or external memory write.

3.2. Finite Impulse Response Filter

One of most remarkable example of employing FPGAs for Digital Signal Processing (DSP) is a FIR filter. Block diagram of FIR filter implemented in FPGAs is given in Fig 6.

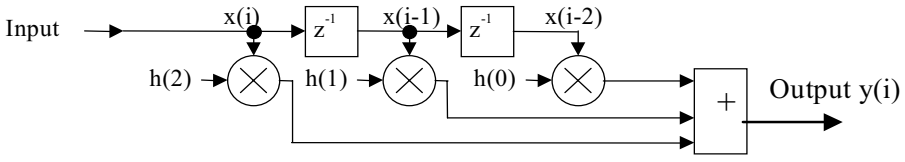

Fig. 6. Block diagram of FIR filter

In Fig. 6, the element z^{-1} denotes one clock delay element and is realized as a flip-flop. Multiplier ($n \times n$-*bit*) occupies less than n^2 Logic Elements (LE) of FPGA, for constant coefficient multipliers the number of occupied resources can be significantly reduced [7]. For example, Xilinx XC3S1500 contains 30 000 LEs. Besides FPGAs incorporate dedicated multipliers, e.g. XC3S1500 contains 32 18×18-bit dedicated multipliers. A n-bit adder occupies less than n LE. Consequently for symmetric (linear phase) FIR filters with constant coefficient multipliers (for constant FIR filter characteristic) and 12-bit inputs, the number of filter taps is larger than 1000

[7], which means that at least 1000 multiplications are carried out in a single clock cycle. Typical FPGA clock frequency is 50÷400MHz, which is roughly 10 times smaller than for microprocessors. Nevertheless, the number of operations carried out in parallel is significantly larger than that for microprocessors. Summing up, for selected operations, computation power of FPGAs is 10÷1000 (or even more) times greater than for microprocessors.

The above paragraph considered parallel FIR filters implementation which computation power is often far beyond required. Besides, great number of FPGAs resources is occupied by this parallel implementation, and FPGA should also carry out other functions. For example, for analog-digital converter sampling frequency f_S= *100kS/s*, employing parallel FIR filter which can be clocked by f= *100MHz* would be inefficient. In this case serial FIR architecture is recommended.

For serial FIR architecture only a single multiplication is carried out in a single clock cycle – a similar algorithm as for microprocessors is adopted (see Listing 1). Therefore, N clock cycles are required to calculate a single output value (where N - the number of filter taps). Consequently, serial architecture clocked by frequency $f= N*f_S$ is equivalent in achievements to parallel architecture clocked by frequency $f=f_S$. Nevertheless, the former occupies only a single multiplier – N times less than the parallel counterpart.

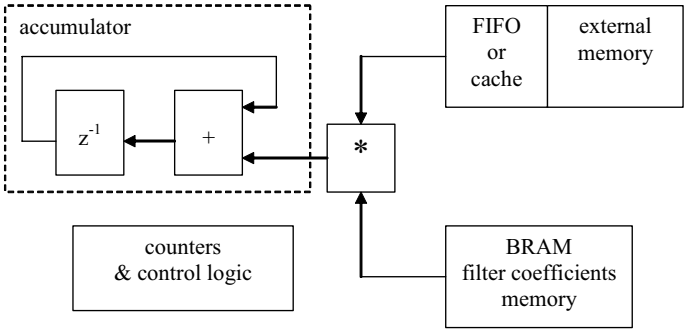

Fig. 7 Block diagram of serial FIR architecture

3.3. Decimation Procedure

In the first approximation, the PLD is a standard decimation procedure for which decimation ratio D is not constant. The crucial feature of PLD implementation is high decimation ratio D that is roughly $D\approx1000$.

In order to eliminate aliasing effect, a FIR filter is employed before decimation. Unfortunately, the number of the filter taps N must be several times greater than the decimation ratio D in order to properly filter the input signal. Implementation of such a large filter would require significant FPGA resources. Fortunately for FIR filters, filter calculations may be carried out only for output samples that are not ignored during decimation. This significantly reduces the calculation cost for such a large decimation ratio and is significant advantage of FIR filters over IIR filters.

The FIR filter is implemented employing serial architecture given in Fig. 7. The filter size and filter coefficients are programmable and can be easily changed. The FIR filter employs direct memory access (DMA) to read input data from external memory and to write the resultant data after decimation.

In PLD the decimation ratio D linearly increases / decreases as follows:

$$D= D_0 + c \cdot s \tag{3}$$

where:

D_0 – initial decimation ratio,
s – index of the input sample,
c – a constant value derived from the marker time slots.

The decimation ratio D is updated according to eq. (3) after each output sample (after decimation). The eq. (3) similarly like filter logic is calculated in hardware, without any co-operation with microprocessors. The microprocessor is only required to calculate values: D_0, c, and the total number of input samples. These values are then written to the hardware control registers.

4. Short-Time PLD

With the application of PUD and 10 MS/s sampling, the implementation of the method was created capable of adapting to non-stationary conditions. Furthermore, hardware signal processing enabled the real-time analysis of great number of samples.

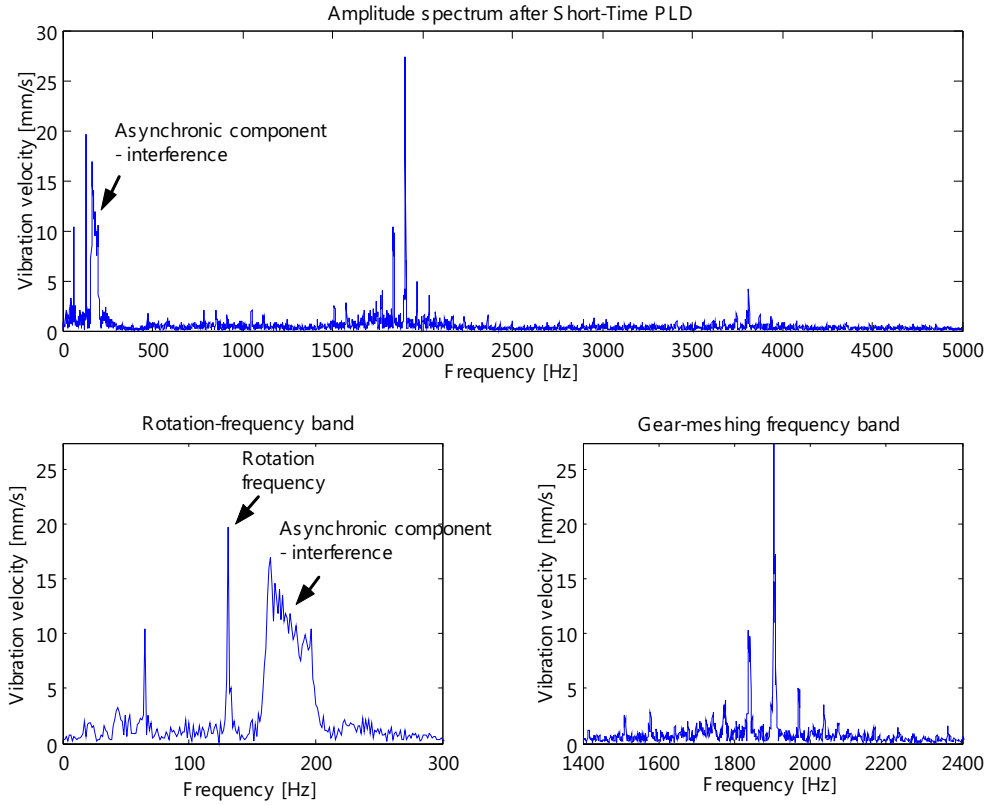

Fig. 8. Amplitude spectrum of vibration velocity gear-meshing after applying Short-Time PLD. Average rotational speed increase 0.38 % per cycle

After taking before-mentioned properties of newly designed device into consideration, a modified PLD was developed, also referred to as Short-Time PLD. Implementation results of the novel method involving the approximation adapting to cycle changes is shown in Fig. 8.

5. Conclusions

Hardware realisation of linear decimation procedure based on FPGA programmable systems gives the possibility of diagnosing cyclical machines at variable operating conditions in real time.

The benefit of applying the method of parallel signal processing is much shorter analysis time that with the processor implementations. It gives great advantage with filtration of signals of great number of samples (millions).

Designed and constructed device (PUD) contains analog-to-digital converters with sampling frequency of 10 MS/s, which enabled to test the developed procedures in high-frequency band at great variations of rotational frequencies. It should be noted that high sampling frequency is crucial for high-speed rotating machines, e.g. gas-turbine machines.

A novel Short-Time PLD method was developed, enabling to adapt the approximation to the cycle changes. This methods solves the problem of non-linear trend change and minimized the error resulted from the original PLD assumption of linear cycle trend in the observation window.

This solution has brought the method nearer to the order analysis without the necessity of applying interpolation filters.

6. References

[1] Adamczyk, J., Cioch, W., Krzyworzeka, P., *Wpływ interpolacji na procedurę liniowej decymacji,* Diagnostyka, vol. 27, 2002.

[2] Adamczyk, J., Cioch, W., Krzyworzeka, P., *Inżynieria Diagnostyki Maszyn. Elementy teorii diagnostyki technicznej* – praca zbiorowa, Roz. 14: *Metody synchroniczne w diagnozowaniu maszyn*, s. 264–278, Radom 2004.

[3] Cempel, Cz., *Diagnostyka wibroakustyczna maszyn*, Wyd. Politechniki Poznańskiej. Poznań, 1985.

[4] Krzyworzeka, P., Cioch, W., *Machine diagnostics in cycle-time scale using linear decimation procedure,* 1st Int. Conf. on Experiments/Process/System/Modelling/Simulation /Optimization, Univ. of Patras. LFME Athens 6–9 July 2005, Greece.

[5] Krzyworzeka, P., Cioch, W., *Dynamiczna kompensacja wpływu zmian długości cyklu na sygnał drganiowy*, Mat XXVII Sympozjum Diagnostyka Maszyn, z. 1, Z.N. Pol. Śl. Katowice 2000.

[6] Jamro, E., Adamczyk, A., Krzyworzeka, P., Cioch, W., *Programowalne urządzenie diagnostyczne stanów niestacjonarnych pracujące w czasie rzeczywistym,* XXXIII Ogólnopolskie Sympozjum Diagnostyka Maszyn, Węgierska Górka, 8.–11.03. 2006 r.

[7] Jamro, E., *Parameterised automated generation of convolvers implemented in FPGAs*, Ph.D. Thesis, University of Science and Technology (AGH-UST), Kraków, 2001.

[8] Krzyworzeka, P., *Wspomaganie synchroniczne w diagnozowaniu maszyn*, Instytut Technologii i Eksploatacji, Radom 2004.

[9] Krzyworzeka, P., Adamczyk, J., Cioch, W., Jamro, E., *Monitoring of nonstationary states in rotating machinery,* Instytut Technologii i Eksploatacji, Radom 2006.

This work has been executed as part of research project at KBN no 6T0720005C/06545.

RELIABILITY-BASED STRATEGY OF OPERATING TURBINE ENGINES, WITH CONSIDERATION TO SAFETY AND EFFECTIVENESS ISSUES

Jerzy Lewitowicz

Air Force Institute of Technology (Instytut Techniczny Wojsk Lotniczych)
01-494 Warszawa, 46, Poland; 6, Księcia Bolesława St., PO Box 96;
Tel.: +48 22 6852025, fax: +48 22 852017
e-mail: sekretariat.naukowy@itwl.pl

Abstract

The future strategy of operating engineering objects such as turbine engines could be sought in combining various strategies of operational use of engines with consideration to the issues of reliability, safety, and effectiveness. The strategy has been based upon tracking of variations in adequate parameters of reliability, safety, and effectiveness, where account is also taken of the risk to fail performing the assigned missions (*operational tasks*).

Keywords: *operation, reliability, engine, safety*

1. Introduction

The strategy of technical equipment operation requires permanent tracking of relevant parameters related to reliability, flight safety and performance effectiveness. This is the future-oriented strategy as it needs extremely high reliability level of subassemblies and structural components with the probability of fault-free operation nearly as high as one (1) over the entire lifetime of the equipment.

In order to select the adequate strategy for operation of such sophisticated technical object as turbine engines one has to be familiar with the following issues:

- methods and criteria for assessment of technical conditions for specific units,
- shape of the curve for the function of technical condition or the area where the curve runs with the presumed probability,
- interrelations between frequency and "depth" (overall scope) of prophylactic and maintenance operations on one hand and reliability and safety issues on the other one,
- interrelations between the historical records for the equipment exploitation and the stream of faults that is generated by the specific object (a set of objects) with consideration to the effects of these faults,
- physical phenomena that serve as reasons for alteration of technical condition, symptoms of defects and states that directly precede catastrophic breakdowns,
- interconnections between reasons and results where alterations to technical condition components and subassemblies lead to definition of the entire object operability.
- progress of destructive processes (1^{st}, 2^{nd}, 3^{rd} and 4^{th} degree [4]) alterations to technical condition of components and subassemblies as a function of operational condition, total time of service, schedule of maintenance operations, external disturbances, etc.,
- risk factors that may occur during exploitation of the equipment and that are conductive to defects and failures

2. The problem of reliability

The method of estimating the maximum permissible probability of extending the parameter value beyond the established thresholds with respect to the parameter that quantifies the adopted exploitation strategy is reduced to checking the reliability-related parameters that vary during the service lifetime (the value vs. time functions). A series of reliability factors can be used for that purpose, including the number of recorded failures (defects), numbers of components or subassemblies exchange operations, number of recorded so called specific cases of failures (that sometimes can be spontaneously converted into breakdowns or catastrophic disasters), etc. For a defined parameter, e.g. number of recorded failures, where the maximum value of the parameter is $n_{\max}$, the maximum acceptable probability of the parameter value can be expressed by the formula [7]:

$$P_{dop} = \sum_{n=0}^{n_d} \frac{(\omega \cdot a \cdot T)^n}{n!} \exp(\omega \cdot a \cdot T), \tag{1}$$

where:

ω – intensity of the stream of faults,
T – number of operation hours for the technical object (operation lifetime),
a – number of units under test,
n_d – number of failures that is allowed for the unit under test with no exceeding of adjustment limits for working parameters.

Monitoring of the reliability level with permanent checking of such threshold level when individual parts or subassemblies reveal symptoms of hazardous failures requires thorough examination of the entire population of such components under real operational conditions. Such examination makes it possible to be in control of the manufacturing process quality and tune up quality of the maintenance, repair and overhaul processes in order to achieve goals of efficient prophylactic for the equipment exploitation.

The parameters that are most frequently used for reliability analyses include the mean time to the first failure *MTTF*[1] and the mean time to the first exchange *MTTE*[2]. However, estimation of those parameters is quite difficult during the initial period of new aircraft exploitation. Trustworthiness of these parameters' estimation increases only as the lifetime of the equipment goes by. That is why during the initial period of technical equipment operation other reliability-related parameters are used as well, including probability of fault-free operation $P(t)$, fault intensity $\lambda(t)$, probability of the need for restoration (exchange, repair, overhaul) $P_{Od}(t)$, restoration intensity $\lambda_{Od}(t)$, the gamma-percent resource T_γ. The analysis is carried out for the specified time interval Δt, which is defined as $\Delta t_i = t_i - t_{i-1}$ for the series of products (parts, subassemblies) $N_S(t_i)$ that exhibit the time of fault-free operation $t \geq t_i$. For such presumptions the reliability indices can be calculated by means of the following formulas:

$$\lambda(\Delta t_i) = \frac{n_S(\Delta t_i)}{\left[N_S(t_i) - \sum_{j=1}^{i-1} n_S(\Delta t_j)\right]\Delta t_i}, \tag{2}$$

[1] *MTTF* : Mean Time To Failures.
[2] *MTTE* : Mean Time To Exchange.

$$P(t_i) = 1 - \frac{\sum_{j=1}^{i} n_S(\Delta t_j)}{N_S(t_i)}, \tag{3}$$

$$\lambda_{Od}(\Delta t_i) = \frac{m_S(\Delta t_i) + n_S(\Delta t_i)}{\left[N_S(t_i) - \sum_{j=1}^{i-1} n_S(\Delta t_j) - \sum_{j=1}^{i-1} m_S(\Delta t_j)\right]\Delta t_i}, \tag{4}$$

$$P_{Od}(t_i) = \frac{\sum_{j=1}^{i} m_S(\Delta t_j) + \sum_{j=1}^{i} n_S(\Delta t_j)}{N_S(t_i)}, \tag{5}$$

$$T_{\gamma i} = P(t_i) \cdot 100 = \left[1 - \frac{\sum_{j=1}^{i} m_S(\Delta t_j) + \sum_{j=1}^{i} n_S(\Delta t_j)}{N_S(t_i)}\right] \cdot 100, \tag{6}$$

where:

m_s (Δt_i) – number of products that had to be exchanged due to prophylactic reasons,
n_s (Δt_i) – number of products that exhibited failures during the time period of Δt_i, starting from the moment when the equipment was put into operation, counted by the calendar time of tests.

$$\tau = [t = 0 \text{ to } t = t_i]. \tag{7}$$

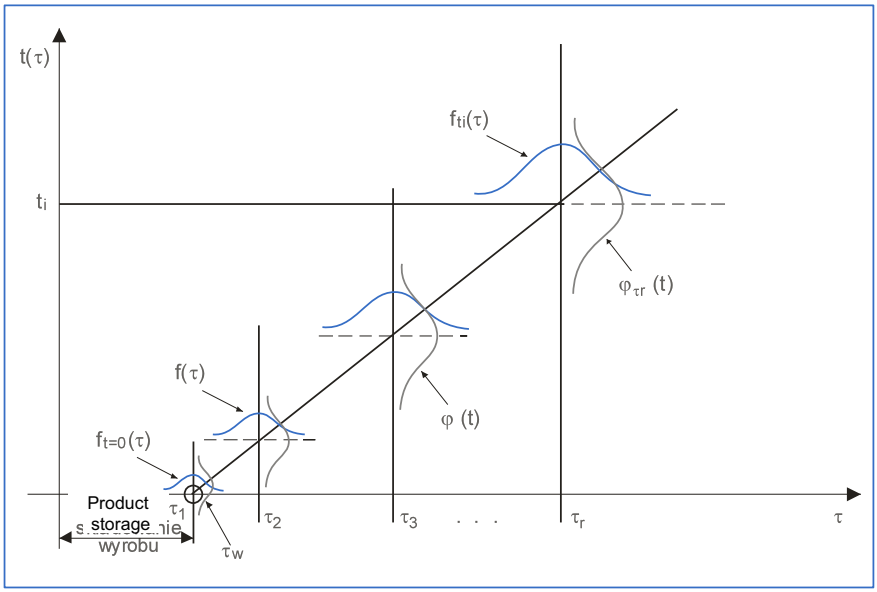

Fig. 1. Binomial process of the product operation time when the equipment is in service
t – operation time of the product; τ – calendar time; τ_w – moment when the product is put into operation

The above deliberations and analyses assume that the parameter of calendar time τ increases in a discrete manner with a specific increment and adopts the values of τ_1, τ_2, … τ_r. In general, variations of both t_i and τ_r are subject to random changes. In such a case they can be associated with the functions of densities $f_t(\tau)$ and $\varphi_\tau(t)$ that are shown on the example of the binomial process of the product operation when the equipment is in service (Fig. 1) [4].

3. Problem of safety

Basic safety parameters for the adopted strategy of the equipment exploitation include the safety untrustworthiness factor Q_B and the safety trustworthiness factor R_B along with the factor of transition (event) intensity for the system untrustworthiness λ_B, expressed as

$$\lambda_B = \frac{\mathrm{d}Q_B(t)}{\mathrm{d}(t)} \cdot \frac{1}{1-Q_B}. \tag{8}$$

The formula (8) can be transformed to calculate the following form of the R_B factor:

$$R_B(t) = R_{BO} \exp\left[-\int_0^t \lambda_B(\tau)\mathrm{d}\tau \right]. \tag{9}$$

The next two safety indices are represented by the leading distribution function of safety untrustworthiness Λ_B and the expected value (mathematical expectation) for the system lifetime until its transition to the state with untrustworthy safety $\mathbf{E}(T_B)$:

$$\Lambda_B(t) = \int_0^t \lambda_B(\tau)\mathrm{d}\tau, \tag{10}$$

$$\mathrm{E}(T_B) = \int_0^\infty R_B(\tau)\mathrm{d}\tau. \tag{11}$$

where:

T_B – the random variable of the system operation time until its transition to the state with untrustworthy safety.

4. Problem of effectiveness

The aircraft exploitation practices show that failures can occur during a flight and are detected either at flight or during earth maintenance but the failure occurrence does not interrupt progress of the assigned task. Alternatively, failures can both occur and be detected on the earth and the total effect thereof is proportional to the sum of flight intervals. For the above presumptions one of the methods dedicated to selection of efficiency indices takes account for the following postulations:

- an aircraft is in operation until its limit (terminal) state occurs,
- purchase costs of the aircraft are taken into account,
- operational downtime periods result from aircraft failures,
- every failure is immediately repaired, just after it has occurred,
- duration of each repair is a direct result of the totalized time of repair operations,
- aircraft downtime due to the lack of the need to its use is also considered,

- every aircraft can only be in one of the following operational states: operable or non-operable,
- operational effect due to the equipment exploitation is totalized for its entire lifetime,
- failures of an aircraft and related operational downtime lead to the loss caused by the lack of expected effects as well as connected with rectification of faults and indirect results thereof,

Therefore, the relation (12) is justified for the model of operation under the above conditions as it expresses the expected value of performance effectiveness [2, 3].

During the process of exploitation any technical object switches between various exploitation states with different operational and maintenance parameters. Let us assume that P_i denotes probability that the object is in the i^{th} state of a complex Markov chain whereas T_i - the mathematical expectation for time duration when the object remains in the i^{th} exploitation state with probabilities of $P(t_i)$, $P_{Od}(t_i)$ and fault intensities $\lambda(t)$, $\lambda_{Od}(t)$. Thus the system reaches the values of performance effectiveness equal to a_i (a_i can adopt both positive and negative values) for individual states of exploitation. The average performance effectiveness per unit of exploitation time for a specific technical object (a set of objects) $\left(\overline{E}_f\right)$ is defined by the following formula:

$$\overline{E}_f = \frac{\sum_{i \in S} P_i \overline{T}_i a_i}{\sum_{i \in S} P_i \overline{T}_i}, \tag{12}$$

where:

S – set of exploitation states for the specific object.

4. Conclusion

The described strategy of technical equipment operation requires conjunctive tracking of relevant parameters related to reliability, flight safety and performance effectiveness (formulas 1÷6 and 8÷11). The parameters can be calculated on the basis of historical information stored in data banks [7, 8]. However, estimation of the risk associated with the adopted strategy [5] and untrustworthiness limits [1] still remains an essential and a very difficult problem.

Wykonano w ramach granatu 4T12C02727.

Reference

[1] Bukowski, L., *Ocena niepewności w systemach logistycznych,* IX Konferencja Logistyki Stosowanej, Zakopane 2005 [in polish].
[2] Jamroż, J., *Economic criteria for optimal ship propulsion designs with low – speed diesel engines,* Conference EXPLO – DIESEL and GAS TURBINE'01. Kopenhaga 2001.
[3] Jaźwiński, J., Borgoń, J., *Niezawodność eksploatacyjna i bezpieczeństwo lotów,* WKŁ, Warszawa 1089. Konferencja EXPLO – DIESEL and GAS TURBINE'01. Międzyzdroje 2003 [in polish].
[4] Lewitowicz, J., *Podstawy eksploatacji statków powietrznych.* T.1. *Statek powietrzny i elementy teorii,* Wyd. ITWL, Warszawa 2001 [in polish].

[5] Lewitowicz, J., Kustroń, K., *Podstawy eksploatacji statków powietrznych.* T.2. *Własności i właściwości statku powietrznego,* Wyd. ITWL, Warszawa 2003 [in polish].
[6] Pigłas, M., *Kompleksowy system analizy i oceny bezpieczeństwa lotów lotnictwa Sił Zbrojnych RP „Turawa",* AKLOT ITWL, 3 (86), 2005 [in polish].
[7] Smirnow, N.N., Cziniuczkin, Ju.M., *Ekspłuatacjonnaja tiechnołogicznost' lietatielnych apparatow,* Wyd. Transport, Moskwa 1994 [in russie].
[8] Żurek, J., *Problemy bezpieczeństwa w lotnictwie,* Przegląd Wojsk Lotniczych i Obrony Powietrznej, Z. 12, 2001 [in polish].

INFLUENCE OF REDUNDANCY AND SHIP MACHINERY CREW MANNING ON RELIABILITY OF LUBRICATING OIL SYSTEM FOR THE MC-TYPE DIESEL ENGINE

Roman Liberacki

Gdansk University of Technology
ul. Narutowicza 11/12, 80-950 Gdańsk, Poland
tel.: +48 58 3471850, fax: +48 58 3472430
e-mail: romanl@pg.gda.pl

Abstract

Influence of redundancy and ship machinery crew manning on reliability of typical lubricating oil system for the MC – type diesel engine has been considered. The results of reliability calculations for the system with redundancy and without redundancy have been presented. Moreover, three training levels of crew have been taken account in those calculations: high, average and low.

Keywords: *reliability, redundancy, manning, lubricating system, diesel engine*

1. Introduction

Reliability of the main engine is extremely important for ship's safety. That's why the Ship Classification Societies like: Lloyd Register of Shipping, Det Norske Veritas, Germanischer Lloyd, American Bureau of Shipping, Polish Register of Shipping etc. require redundancy in the most important systems on ships. One of them is the lubricating oil system. In practical applications pumps and filters are doubled.

Lloyd Register of Shipping rules for lubricating oil pumps are [1]:

"Where lubricating oil for the main engine(s) is circulated under pressure, a standby lubricating oil pump is to be provided where the following conditions apply:
(a). The lubricating oil pump is independently driven and the total output of the main engine(s) exceeds 370 kW(500 shp).
(b). One main engine with its own pump is fitted and the output of the engine exceeds 370 kW (500 shp).
(c). More than one main engine each with its own lubricating oil pump is fitted and the output of each engine exceeds 370 kW (500 shp).
8.2.2. The standby pump is to be of sufficient capacity to maintain the supply of oil for normal conditions with any one pump out of action. The pump is to be fitted and connected ready for immediate use, except that where the conditions referred to in (c) apply a complete spare pump may be accepted. In all cases satisfactory lubrication of the engines is to be ensured while starting and manoeuvring."

For lubricating oil filters [1]:

"*Where the lubricating oil for main propelling engines is circulated under pressure, provision is to be made for the efficient filtration of the oil. The filters are to be capable of being cleaned without stopping the engine or reducing the supply of filtered oil to the engine. Proposals for an automatic by-pass for emergency purposes in high speed engines are to be submitted for special consideration."*

The human element is also one of the most important contributory aspects to the causation and avoidance of system failures, and as the result of those failures - accidents. To produce valid results in reliability analysis it is necessary to assess the contribution of the human element to system failure. This contribution can be assessed using human reliability analysis (HRA) [2].

In a light of the above statement, the author decided to make approach to human reliability analysis in investigations.

2. Lubricating oil system for the MC – type diesel engine

The considered lubricating oil system, typical for the MC – type diesel engines, is shown on Fig. 1. Lubrication of engine bearings, camshaft bearings and piston cooling is carried out by the uni – lubricating oil system. Cylinder liners are lubricated by a separate cylinder lubricating oil system [3].

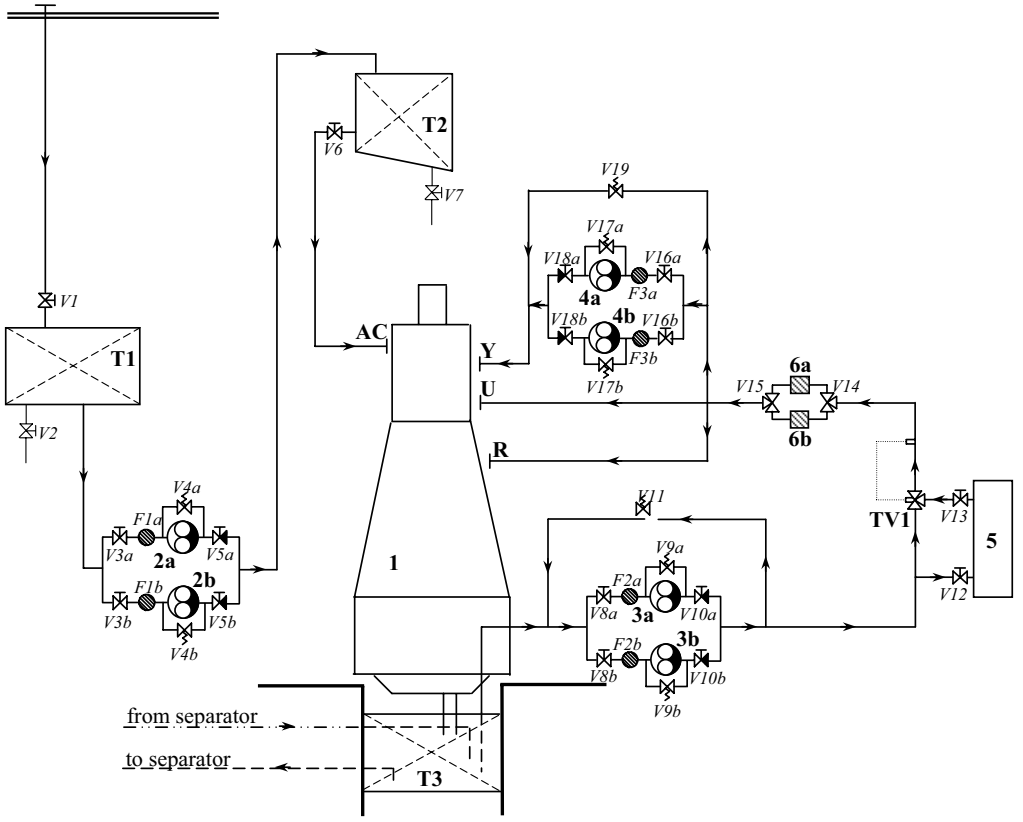

Fig. 1. Lubricating oil system for the MC – type diesel engine: 1 - diesel engine; 2a, 2b – cylinder lubricating oil transfer pumps; 3a, 3b - lubricating oil pumps; 4a, 4b – camshaft lubricating oil booster pumps; 5 – lubricating oil cooler; 6a, 6b – lubricating oil duplex filter; T1 – cylinder lubricating oil storage tank; T2 – cylinder lubricating oil service tank; T3 – lubricating oil bottom tank; TV1 – thermostatic valve; V… – valves; F… – suction filters

All the lubricating oil pups are of the screw wheel type. The lubricating oil cooler is of the plate type heat exchanger. The duplex lubricating oil filter is installed. It has sufficient capacity to allow the specified full amount of oil to flow through each side of the filter. The oil temperature control system can, by means of a three – way valve unit, by – pass the cooler totally or partly [3].

Only the external lubricating oil system is shown on Fig. 1. The rest of the system is supplied with the engine and is called the internal lubricating oil system. Treatment of the lubricating oil for bearings is carried out by self cleaning separators.

3. Reliability model of the lubricating oil system

Reliability of the lubricating oil system is the probability that the system will function properly. The continuous work of the diesel engine will be possible. The reliability is a function of time, beginning at zero time. To assess the reliability of the system the fault tree method and the minimal cut sets method have been used. The minimal cut sets method is a simplified method, so the results of calculations are approximate. This method gives the lower boundary of the system reliability.

The required reliability data for technical items have been adopted from [4, 5]. The data - failure rates of selected technical items λ [h^{-1}] are given in Tab. 1.

Tab. 1. Failure rates of technical items

Symbol	Item	Failure mode	Failure rate λ [h^{-1}]
1	Diesel engine	-	-
2a, 2b 3a, 3b 4a,4b	Cylinder lubricating oil transfer pumps, Lubricating oil pump, Camshaft lubricating oil booster pumps	_1 - low output, _2 - fail while running, _3 - fail to start, _4 - critical leakage,	5.87E-6 55.34E-6 26.66E-6 3.46E-6
5	Lubricating oil cooler	_1 - critical leakage, _2 - insufficient cooling,	0.46E-6 ~0E-6
6a,6b	Lubricating oil duplex filter	_1 - inadmissible pressure drop, _2 - damaged mesh, _3 - critical leakage,	4.53E-6 0.12E-6 0.19E-6
T1 T2 T3	Cylinder lubricating oil storage tank, Cylinder lubricating oil service tank, Lubricating oil bottom tank,	_1 - critical leakage,	2.34E-6
TV1	Thermostatic valve	_1 - critical leakage, _2 - insufficient temp. control,	0.76E-6 2.43E-6
F1a, F1b F2a, F2b F3a, F3b	Suction filters	_1 - inadmissible pressure drop, _2 - damaged mesh, _3 - critical leakage,	4.53E-6 0.12E-6 0.16E-6
V11, V19	Regulating valves	_1 - critical leakage, _2 - insufficient pressure control,	0.76E-6 0.16E-6
V4a, V4b V9a, V9b V17a, V17b	Safety valves	_1 - critical leakage, _2 - fail to open, _3 - opens under to low pressure,	0.76E-6 0.16E-6 2.02E-6
V1, V2 V6, V7 V12, V13 V3a, V3b V8a, V8b V16a, V16b	Stop valves	_1 - critical leakage, _2 - plugged in open/close position,	0.76E-6 0.56E-6
V5a, V5b V10a, V10b V18a, V18b	Non - return stop valves	_1 - critical leakage, _2 - plugged in open/close position, _3 - back flow,	0.76E-6 0.56E-6 2.02E-6
V14, V15	Three way valves	_1 - critical leakage, _2 - plugged,	0.76E-6 0.56E-6
Pl	Pipeline including sealing	_1 - critical leakage,	9E-6

The failure rates, given above, refer to calendar time. For redundant items it is necessary to take account that their active working time is only a part of the time (approximately 50 %).

The statistical reliability data in Tab.1. are mostly adopted from offshore installations. They are not fully representative for ship systems. The data have been used because it is extremely hard to get such data for ships. The achieved results of calculations based on the data are then of tentative character. Due to the data character - the exponential distribution has been used in the reliability calculations.

Technical state of system (reliability of the system) depends on human behavior. Avoiding of the machinery systems failures, especially in the sea, is a machinery crew task. Unfortunately a human being makes mistakes. That is why we should take into account a human error probability (HEP) in system reliability analysis.

Human Reliability Analysis (HRA) was developed primarily for the nuclear industry. Using HRA in other industries requires that the techniques be appropriately adapted. For example, because the nuclear industry has many built-in automatic protection systems, consideration of the human element can be legitimately delayed until after consideration of the overall system performance. Onboard ships, the human has more degrees of freedom to disrupt system performance. Therefore, a high-level task analysis needs to be considered at the outset of an Formal Safety Assessment (FSA). There are two main HRA quantitative techniques (HEART and THERP). As the data from all of these sources are based on non-marine industries, they need to be used with caution. A good alternative is to use expert judgement and one technique for doing this is Absolute Probability Judgement (APJ) [2].

The above mentioned techniques are very advanced. The preliminary human error probability assessment can be made using a very simple method ASEP - HRAP (Accident Sequence Evaluation Program - Human Reliability Analysis Procedure) published in 1987 by Swain [6]. Adaptation of the method in shipping one can find in [7]. The same method has been used in this study.

In the ASEP - HRAP technique the Basis Human Error Probability (BHEP) equals 0.03. BHEP contains both: human error of omission and human error of commission. If a potential for the error to be recovered exists, then the value of BHEP is multiplied by so called recovery factor (f) (mostly equals 0.1 or 0.01 depending on situation) [7]. Human error probabilities, taken account in model of lubricating oil system reliability, are shown in Tab. 2.:

Tab. 2. Human error probabilities in the lubricating oil system manning

Symbol	Human error	Human error probability
HEP_1	- no reaction or to late reaction to stop degrade of the system elements	0.03
HEP_2	- no reaction or to late reaction to an inadmissible pressure drop on a filter, (equipped with a pressure drop alarm device)	~ 0
HEP_3	- no reaction or to late reaction to inadmissible pressure drop on a filter, (not equipped with a pressure drop alarm device)	0.03
HEP_4	- no reaction or to late reaction to oil level low in a tank, (equipped with a level low alarm device)	~ 0

Three levels of crew qualification have been assumed in the model: high, average and low. According to TESEO (it. Tecnica Empirica Stima Errori Operatori) method [8, 9] the following assumptions have been made:

- for high crew qualification level the probability of human error equals 50 % of the value given in Tab. 2.,
- for low crew qualification level the probability of human error is three times higher then the value given in Tab. 2.

Additional assumptions to the model:

- the electric power supply is provided,
- the lubricating oil treatment system is efficient,
- all stop valves and non - return stop valves are opened (except V2, V7),
- all tanks are equipped with level low alarm devices,
- the lubricating oil duplex filter is equipped with a high pressure drop alarm device,
- all suction filters are not equipped with high pressure drop alarm devices,
- critical leakage means the engine has to be stopped immediately.

Lubricating oil system reliability with redundancy can be expressed as follows:

$$R_r(t) = 1 - \{ HEP\_4_{T1} + \{[1-\exp(-\lambda_{V2\_1}\cdot t)] + [1-\exp(-\lambda_{T1\_1}\cdot t)]\}\cdot HEP\_1 + HEP\_4_{T2} + \{[1-\exp(-\lambda_{V7\_1}\cdot t)] + [1-\exp(-\lambda_{T2\_1}\cdot t)]\}\cdot HEP\_1 + [1-\exp(-\lambda_{V6\_1}\cdot t)] \cdot HEP\_1 + \{[1-\exp(-\lambda_{V3a\_1}\cdot t)] + [1-\exp(-\lambda_{V3b\_1}\cdot t)] + [1-\exp(-\lambda_{V5a\_1}\cdot t)] + [1-\exp(-\lambda_{V5b\_1}\cdot t)]\} \cdot HEP\_1 + \{[1-\exp(-\lambda_{F1a\_1}\cdot t)] \cdot HEP\_3 + [1-\exp(-\lambda_{2a\_1}\cdot t)] \cdot HEP\_1 + [1-\exp(-\lambda_{2a\_2}\cdot t)] \cdot HEP\_1 + [1-\exp(-\lambda_{V4a\_3}\cdot t)] \cdot HEP\_1\} \cdot \{[1-\exp(-\lambda_{F1b\_1}\cdot t)] \cdot HEP\_3 + [1-\exp(-\lambda_{2b\_1}\cdot t)] \cdot HEP\_1 + [1-\exp(-\lambda_{2b\_2}\cdot t)] \cdot HEP\_1 + [1-\exp(-\lambda_{2b\_3}\cdot t)] \cdot HEP\_1 + [1-\exp(-\lambda_{V4b\_3}\cdot t)] \cdot HEP\_1\} + \{[1-\exp(-\lambda_{F1a\_3}\cdot t)] \cdot HEP\_1 + [1-\exp(-\lambda_{V4a\_1}\cdot t)] \cdot HEP\_1 + [1-\exp(-\lambda_{2a\_4}\cdot t)] \cdot HEP\_1 \} \cdot \{[1-\exp(-\lambda_{V3a\_2}\cdot t)] \cdot HEP\_1 + [1-\exp(-\lambda_{V5a\_3}\cdot t)] \cdot HEP\_1\} + \{[1-\exp(-\lambda_{F1b\_3}\cdot t)] \cdot HEP\_1 + [1-\exp(-\lambda_{V4b\_1}\cdot t)] \cdot HEP\_1 + [1-\exp(-\lambda_{2b\_4}\cdot t)] \cdot HEP\_1 \} \cdot \{[1-\exp(-\lambda_{V3b\_2}\cdot t)] \cdot HEP\_1 + [1-\exp(-\lambda_{V5b\_3}\cdot t)] \cdot HEP\_1 \} + HEP\_4_{T3} + [1-\exp(-\lambda_{T3\_1}\cdot t)] \cdot HEP\_1 + \{[1-\exp(-\lambda_{V11\_1}\cdot t)] + [1-\exp(-\lambda_{V11\_2}\cdot t)]\} \cdot HEP\_1 + \{[1-\exp(-\lambda_{V19\_1}\cdot t)] + [1-\exp(-\lambda_{V19\_2}\cdot t)]\} \cdot HEP\_1 + \{[1-\exp(-\lambda_{F2a\_1}\cdot t)] \cdot HEP\_3 + [1-\exp(-\lambda_{3a\_1}\cdot t)] \cdot HEP\_1 + [1-\exp(-\lambda_{3a\_2}\cdot t)] \cdot HEP\_1 + [1-\exp(-\lambda_{V9a\_3}\cdot t)] \cdot HEP\_1\} \cdot \{[1-\exp(-\lambda_{F2b\_1}\cdot t)] \cdot HEP\_3 + [1-\exp(-\lambda_{3b\_1}\cdot t)] \cdot HEP\_1 + [1-\exp(-\lambda_{3b\_2}\cdot t)] \cdot HEP\_1 + [1-\exp(-\lambda_{3b\_3}\cdot t)] \cdot HEP\_1 + [1-\exp(-\lambda_{V9b\_3}\cdot t)] \cdot HEP\_1\} + \{[1-\exp(-\lambda_{F2a\_3}\cdot t)] \cdot HEP\_1 + [1-\exp(-\lambda_{V9a\_1}\cdot t)] \cdot HEP\_1 + [1-\exp(-\lambda_{3a\_4}\cdot t)] \cdot HEP\_1 \} \cdot \{[1-\exp(-\lambda_{V8a\_2}\cdot t)] \cdot HEP\_1 + [1-\exp(-\lambda_{V10a\_3}\cdot t)] \cdot HEP\_1\} + \{[1-\exp(-\lambda_{F2b\_3}\cdot t)] \cdot HEP\_1 + [1-\exp(-\lambda_{V9b\_1}\cdot t)] \cdot HEP\_1 + [1-\exp(-\lambda_{3b\_4}\cdot t)] \cdot HEP\_1 \} \cdot \{[1-\exp(-\lambda_{V8b\_2}\cdot t)] \cdot HEP\_1 + [1-\exp(-\lambda_{V10b\_3}\cdot t)] \cdot HEP\_1\} + \{[1-\exp(-\lambda_{F3a\_1}\cdot t)] \cdot HEP\_3 + [1-\exp(-\lambda_{4a\_1}\cdot t)] \cdot HEP\_1 + [1-\exp(-\lambda_{4a\_2}\cdot t)] \cdot HEP\_1 + [1-\exp(-\lambda_{V17a\_3}\cdot t)] \cdot HEP\_1\} \cdot \{[1-\exp(-\lambda_{F3b\_1}\cdot t)] \cdot HEP\_3 + [1-\exp(-\lambda_{4b\_1}\cdot t)] \cdot HEP\_1 + [1-\exp(-\lambda_{4b\_2}\cdot t)] \cdot HEP\_1 + [1-\exp(-\lambda_{4b\_3}\cdot t) \cdot HEP\_1] + [1-\exp(-\lambda_{V17b\_3}\cdot t)] \cdot HEP\_1\} + \{[1-\exp(-\lambda_{F3a\_3}\cdot t)] \cdot HEP\_1 + [1-\exp(-\lambda_{V17a\_1}\cdot t)] \cdot HEP\_1 + [1-\exp(-\lambda_{4a\_4}\cdot t)] \cdot HEP\_1 \} \cdot \{[1-\exp(-\lambda_{V16a\_2}\cdot t)] \cdot HEP\_1 + [1-\exp(-\lambda_{V18a\_3}\cdot t)] \cdot HEP\_1\} + \{[1-\exp(-\lambda_{F3b\_3}\cdot t)] \cdot HEP\_1 + [1-\exp(-\lambda_{V17b\_1}\cdot t)] \cdot HEP\_1 + [1-\exp(-\lambda_{4b\_4}\cdot t)] \cdot HEP\_1 \} \cdot \{[1-\exp(-\lambda_{V16b\_2}\cdot t)] \cdot HEP\_1 + [1-\exp(-\lambda_{V18b\_3}\cdot t)] \cdot HEP\_1\} + \{[1-\exp(-\lambda_{V12\_1}\cdot t)] + [1-\exp(-\lambda_{V13\_1}\cdot t)] + [1-\exp(-\lambda_{5\_1}\cdot t)] + [1-\exp(-\lambda_{5\_2}\cdot t)] \}\cdot HEP\_1 + \{[1-\exp(-\lambda_{TV1\_1}\cdot t)] + [1-\exp(-\lambda_{TV1\_2}\cdot t)]\} \cdot HEP\_1 + \{[1-\exp(-\lambda_{V14\_1}\cdot t)] + [1-\exp(-\lambda_{V15\_1}\cdot t)]\} \cdot HEP\_1 + \{[1-\exp(-\lambda_{6a\_1}\cdot t)] \cdot HEP\_2 + [1-\exp(-\lambda_{6a\_2}\cdot t)] \cdot HEP\_1 + [1-\exp(-\lambda_{6a\_3}\cdot t)] \cdot HEP\_1\} \cdot \{[1-\exp(-\lambda_{6b\_1}\cdot t)] \cdot HEP\_2 + [1-\exp(-\lambda_{6b\_2}\cdot t)] \cdot HEP\_1 + [1-\exp(-\lambda_{6b\_3}\cdot t)] \cdot HEP\_1 + [1-\exp(-\lambda_{V14\_2}\cdot t)] \cdot HEP\_1 + [1-\exp(-\lambda_{V15\_2}\cdot t)] \cdot HEP\_1\} + [1-\exp(-\lambda_{Pl\_1}\cdot t)] \cdot HEP\_1 \}, \quad (1)$$

Lubricating oil system reliability without redundancy can be expressed as follows:

$$R_s(t) = 1 - \{ HEP\_4_{T1} + \{[1-\exp(-\lambda_{V2\_1}\cdot t)] + [1-\exp(-\lambda_{T1\_1}\cdot t)]\}\cdot HEP\_1 + HEP\_4_{T2} + \{[1-\exp(-\lambda_{V7\_1}\cdot t)] + [1-\exp(-\lambda_{T2\_1}\cdot t)]\}\cdot HEP\_1 + [1-\exp(-\lambda_{V6\_1}\cdot t)] \cdot HEP\_1 + \{[1-\exp(-\lambda_{V3a\_1}\cdot t)] + [1-\exp(-\lambda_{V5a\_1}\cdot t)]\} \cdot HEP\_1 + [1-\exp(-\lambda_{F1a\_1}\cdot t)] \cdot HEP\_3 + \{[1-\exp(-\lambda_{2a\_1}\cdot t)] + [1-\exp(-\lambda_{2a\_2}\cdot t)] + [1-\exp(-\lambda_{V4a\_3}\cdot t)]\} \cdot HEP\_1 + \{[1-\exp(-\lambda_{F1a\_3}\cdot t)] + [1-\exp(-\lambda_{V4a\_1}\cdot t)] + [1-\exp(-\lambda_{2a\_4}\cdot t)]\} \cdot HEP\_1 + HEP\_4_{T3} + [1-\exp(-\lambda_{T3\_1}\cdot t)] \cdot HEP\_1 + \{[1-\exp(-\lambda_{V11\_1}\cdot t)] + [1-\exp(-\lambda_{V11\_2}\cdot t)]\} \cdot HEP\_1 + \{[1-\exp(-\lambda_{V19\_1}\cdot t)] + [1-\exp(-\lambda_{V19\_2}\cdot t)]\} \cdot HEP\_1 + [1-\exp(-\lambda_{F2a\_1}\cdot t)] \cdot HEP\_3 + \{[1-\exp(-\lambda_{3a\_1}\cdot t)] + [1-\exp(-\lambda_{3a\_2}\cdot t)] + [1-\exp(-\lambda_{V9a\_3}\cdot t)]\} \cdot HEP\_1 + \{[1-\exp(-\lambda_{F2a\_3}\cdot t)] + [1-\exp(-\lambda_{V9a\_1}\cdot t)] + [1-\exp(-\lambda_{3a\_4}\cdot t)]\} \cdot HEP\_1 + [1-\exp(-\lambda_{F3a\_1}\cdot t)] \cdot HEP\_3 + \{[1-\exp(-\lambda_{4a\_1}\cdot t)] + [1-\exp(-\lambda_{4a\_2}\cdot t)] + [1-\exp(-\lambda_{V17a\_3}\cdot t)]\} \cdot HEP\_1 + \{[1-\exp(-\lambda_{F3a\_3}\cdot t)] + [1-\exp(-\lambda_{V17a\_1}\cdot t)] + [1-\exp(-\lambda_{4a\_4}\cdot t)]\} \cdot HEP\_1 + \{[1-\exp(-\lambda_{V12\_1}\cdot t)] + [1-\exp(-\lambda_{V13\_1}\cdot t)] + [1-\exp(-\lambda_{5\_1}\cdot t)] + [1-\exp(-\lambda_{5\_2}\cdot t)]\}\cdot HEP\_1 + \{[1-\exp(-\lambda_{TV1\_1}\cdot t)] + [1-\exp(-\lambda_{TV1\_2}\cdot t)]\} \cdot HEP\_1 + \{[1-\exp(-\lambda_{V14\_1}\cdot t)] + [1-\exp(-\lambda_{V15\_1}\cdot t)]\} \cdot HEP\_1 + \{[1-\exp(-\lambda_{6a\_1}\cdot t)] \cdot HEP\_2 + [1-\exp(-\lambda_{6a\_2}\cdot t)] \cdot HEP\_1 + [1-\exp(-\lambda_{6a\_3}\cdot t)] \cdot HEP\_1\} + [1-\exp(-\lambda_{Pl\_1}\cdot t)] \cdot HEP\_1 \}, \quad (2)$$

where:

t [h] - time,
λ [h^{-1}] - failure rates according to Tab.1.,
HEP - human error probabilities according to Tab. 2.

3. Results of the model investigations

Reliability values of lubricating oil system with and without redundancy of pumps and filters have been calculated in function of time and crew qualification levels. The results are shown on Fig. 2., Fig. 3., Fig. 4.

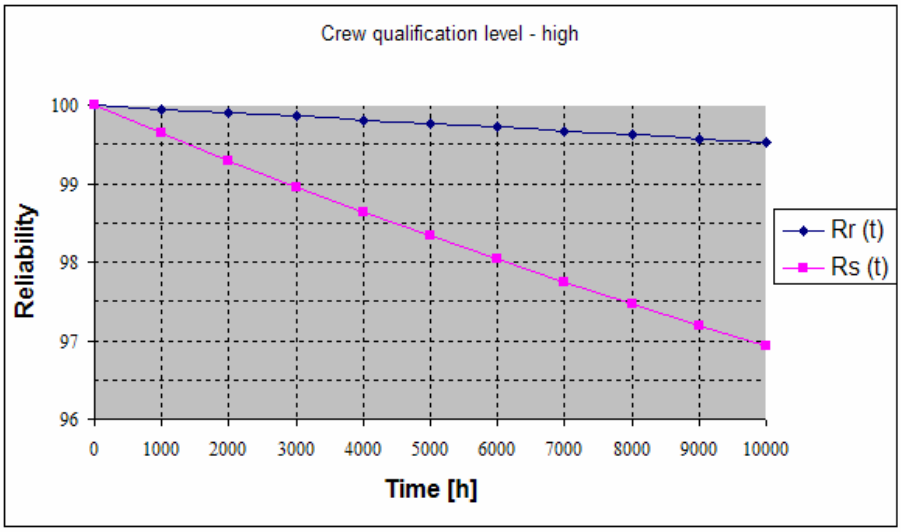

Fig. 2. Reliability function of lubricating oil system with redundancy Rr (t) and without redundancy Rs (t), crew qualification level is high

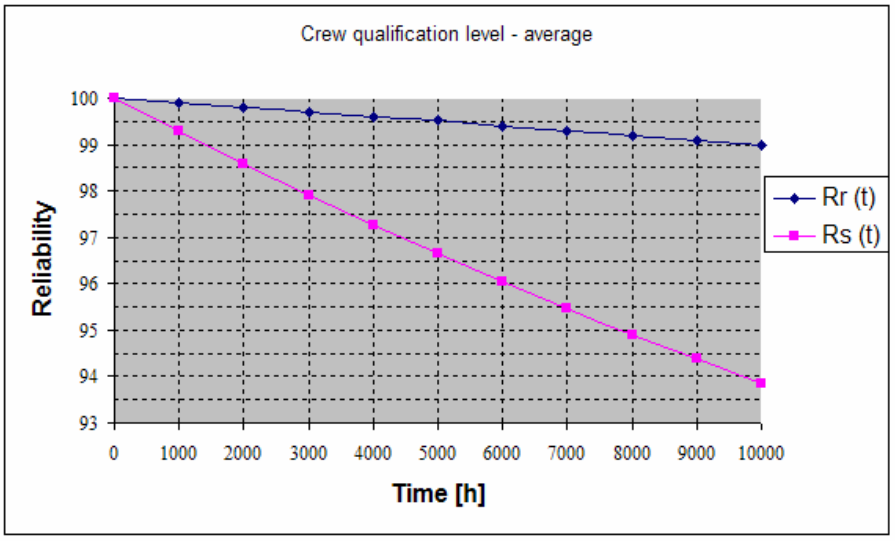

Fig. 3. Reliability function of lubricating oil system with redundancy Rr (t) and without redundancy Rs (t), crew qualification level is average

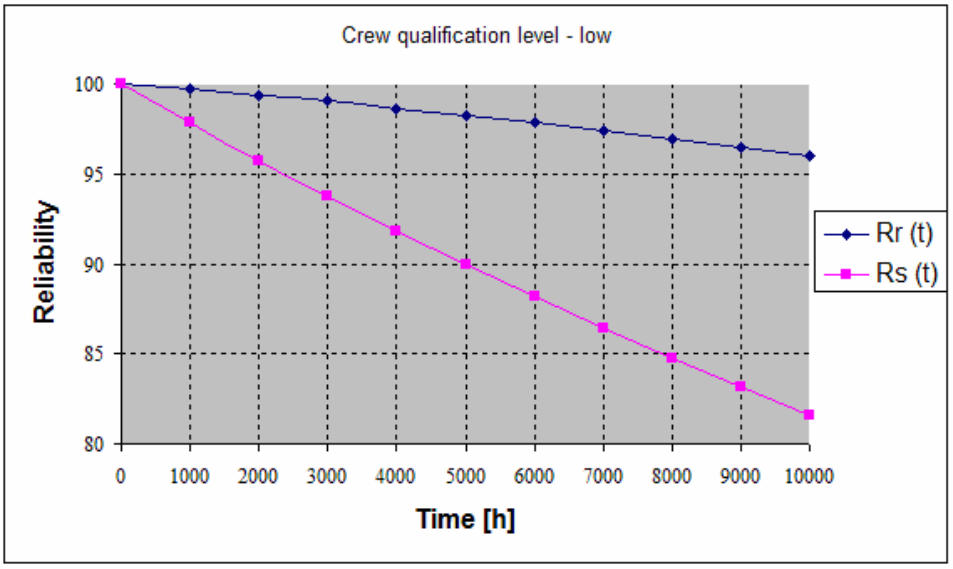

Fig. 4. Reliability function of lubricating oil system with redundancy Rr (t) and without redundancy Rs (t), crew qualification level is low

4. Conclusions derived from the model investigations

- Reliability of the lubricating oil system obviously depends on the reliability of relevant technical elements as well as on the crew qualification level – the reliability of human operator.
- The greater reliability of technical elements and human reliability the greater reliability of the system.
- Redundancy brings about the increase in the reliability of the lubricating oil system.
- The lower crew qualification level and lower reliability of technical elements the greater effect of redundancy to the reliability of the system.

Application of such models, like this one, is closely associated with data on reliability of technical elements used in shipbuilding. However they are unavailable in Poland. Perhaps they are saved in databases of classification societies like Det Norske Veritas or Lloyd Register. The other problem to solve is human error probabilities assessment. The first steps towards to deal with the problem have been already made by the author in [10].

References

[1] Lloyd Register of Shipping, *Lloyd's Register Rules and Regulations - Rules and Regulations for the Classification of Ships, July 2005, incorporating Notice No. 1 - Main and Auxiliary Machinery - Machinery Piping Systems - Lubricating oil systems,* London 2005.

[2] International Maritime Organization, *Guidelines for Formal Safety Assessment (FSA) for Use in the IMO Rule – Making Process,* MSC/Circ.1023 MEPC/Circ.392, London 2002.

[3] MAN B&W Diesel A/S, *Engine Selection Guide, Two – stroke MC/MC-C Engines*, 6th Edition, January 2002.

[4] OREDA, *Offshore Reliability Data*, 3rd Edition, DNV, Trondheim 1997.
[5] Liberacki, R., Nowak, P., *Wyniki symulacji bezpieczeństwa napędowego statków serii B 488*, opracowanie wewnętrzne, Politechnika Gdańska, Gdańsk 1998.
[6] Swain, A.D., NUREG/CR-4772, 1988.
[7] Kosmowski, K.T., *Ocena niezawodności operatora w realizacji wybranych funkcji w procesie sterowania na przykładzie instalacji wytwarzania energii elektrycznej statków serii B 488*, Politechnika Gdańska, Gdańsk, 1997.
[8] Radkowski, S., *Podstawy bezpiecznej techniki*, Politechnika Warszawska, Warszawa 2003.
[9] Safety and Reliability Directorate UK Atomic Energy Authority, *Human Reliability Assessors Guide*, 1988.
[10] Liberacki, R., *Modelowanie bezpieczeństwa środowiskowego statków*, rozprawa doktorska, Politechnika Gdańska, Gdańsk, 2005.

POSSIBILITIES TO BEARINGS DIAGNOSIS OF THE GAS TURBINE ENGINE LM 2500 ON THE BASIS OF OIL RESEARCH ON

Waldemar Mironiuk

Naval Academy
ul. Śmidowicza 69, 81-103 Gdynia, Poland
tel.: +48 58 6262731,
e-mail: wmiro@o2.pl

Abstract

While operation a gas turbine engine more modest method of research are brought into effect. But one of a basic method of estimate a technical condition of gas turbine engines bearing is oil analysis. To estimate a technical condition of gas turbine engines bearing systems on the basis of oil research on, an x-ray method of radio-isotope fluorescence was used. This method has been also satisfactorily used in aircraft engine diagnosis.

This paper presents the method of diagnosis bearings of marine gas turbines on the basis of studies of mechanical contamination in oil. Results of mechanical contamination research in oil vs time of engine work are presented. On the basis of experiments results the analytical function that makes calculating the future value of a process possible was chosen.

Keywords: *friction heat, operation, bearing, friction work, oil system, gas turbine engine*

1. Introduction

The looking for a new solution of propulsion system for the fast warship have conducted to apply in the power ships gas turbine engine. Such positive factors like a small mass and overall dimensions, a big power and a start speed have been used on warships of various classes. Gas turbine engines on warships operate in very difficult conditions. Exploitation of that propulsion systems in the sea condition need an ability to continue their operate during roll continues of ship. Results of influences on the gas turbine engine many outside and inside factors, technical condition of engine are changed, which uncontrolled develop can cause their destroy [3]. Their reliability depending to a great extent on oil installation ability. Throughout exploitation some friction elements including bearings whose consumption products are oil transported get worn and torn. Majority damages of ball-bearings of gas turbine engine depend on the conditions of oil system. Damages and get worn and torn of bearings during exploitation are showed grow of contents molecules of roll elements in the oil. Emitting of metallic parties by gas turbine friction elements give an overall view of these elements technical condition [6].

While operation a ship's gas turbine engine friction elements like engine bearings play a main role in. The good technical condition of bearings has influence on the reliability of the engine and a warship's combat readiness.

The reason of an engine's failures are very often bearings damage whose products are gathered in oil. The example of damaged bearings of gas turbine engines are shown in the Fig.1.

The direct reason of tribological system wear acceleration is always bad quality of lubricate. Hence a change of both physical and chemical characteristic of oil and concentration of mechanical contamination (a size and a morphology foreign body substance) included in oil can be index of the assessment of the oil useful characteristic. Therefore oil is a very valuable carrier of information about wear reasons and processes of both, the engine tribological system and oil.

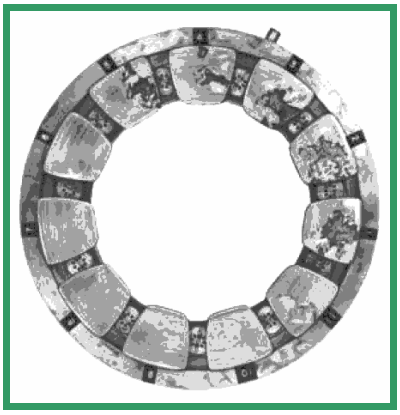

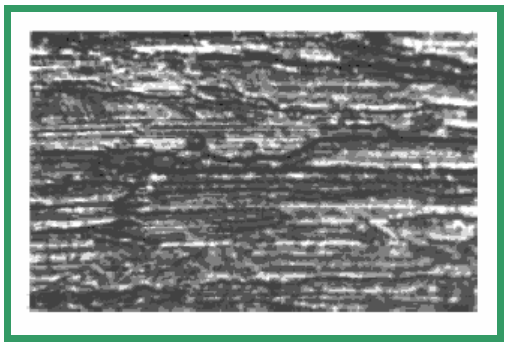

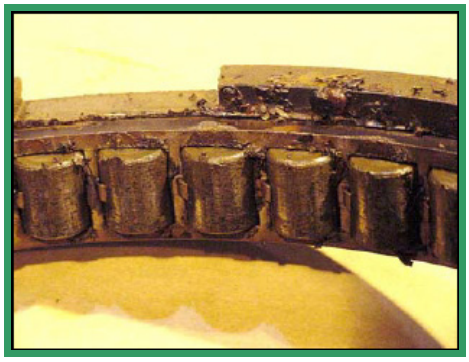

Fig. 1.The examples of bearings damage [7]

On the basis of the analysis of the chemical composition oil samples from the oil system, the monitor a change of mechanical contaminants and conduct assessment of the technical state of interact engine parts is possible.

2. The method of oil experimental research on

Using up of technical condition of bearings during exploitation is a continue process. The systematically control of mediation appears as the quantity metallic contamination in oil can estimate technical condition of bearings and find diagnostic symptoms which characterise damage threat of engine. The information of friction processes proceed include bearings or actual technical condition of elements are obtained from research of consumption products in oil.

The detection of the state before the damage of interact tribological system parts of gas turbine engine or an index of oil wear is possible on the basis of permanent or temporary contamination detection include in oil. The mechanical parts discharged from the engine tribological system gives the information about their technical state. The moving of both oil and contaminants can detect these contaminants direct in oil system or at the laboratory after taking oil sample from the engine. The research on contaminants in oil are conducted at the laboratory of The Naval Academy.

The X-ray radioisotope fluorescent method was used to estimate a quantity change of mechanical contaminants in oil. Thanks to induce and measurement of the characteristic intensity radiation, of this method, the chemical composition of oil samples was analyzed. The quantity

analysis, it means identification of element, was conducted on the basis of measurement energy radiation this element but quantity estimate was led on the basis of the intensity radiation energy line.

The characteristic radiation measurements are made by measuring system shown in the Fig. 2.

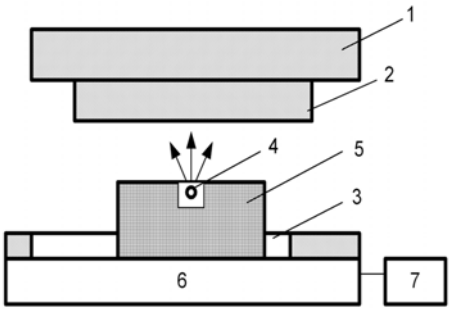

Fig. 2. XRF measuring device scheme:1 - filter, 2 - isotopic radiation source, 3 - Al or Co filter, 4 – detectors window, 5 – detector

There are filters used to reduce the influence of other elements on the results of the analysis:
- cobalt (Co) filters for determining of iron quantity,
- aluminium (Al) filters for determining of copper quantity.

3. Methodology of estimating the oil contamination

Oil samples for the analysis are collected after every return the ship from the sea. The scheme of the stand for mechanical impurities in oil analysis is shown in the Fig. 3.

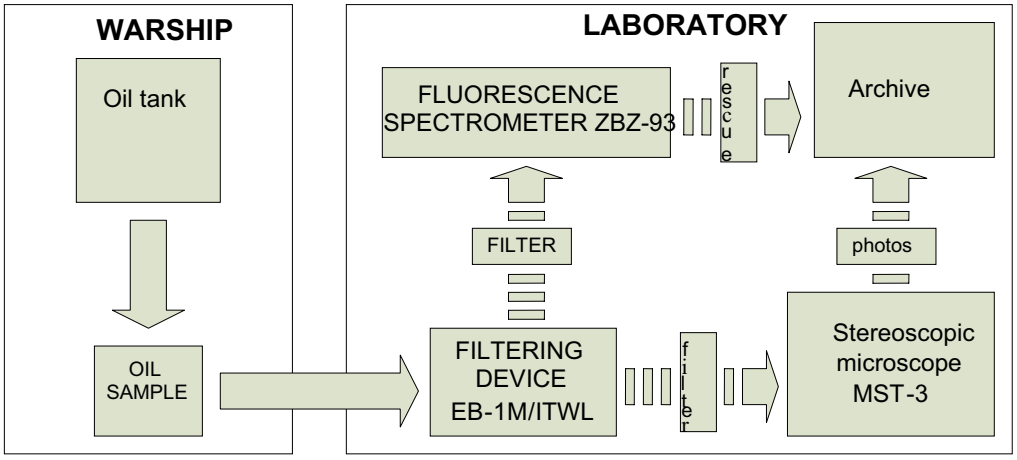

Fig. 3. The scheme of the stand for mechanical impurities in oil analysis

Two methods were adopted to determine quantity and quality of wear products in oil samples in the basic diagnostic system of marine gas turbine engines:
- stereoscopic microscopy,
- x-ray radioizotopic fluorescence.

Oil collected from the ship was filtered in filtering device EB-1M/ITWI using filters „coli-5". After twenty four hours it was watched under the stereoscopic microscope MST-3. Owing to that

types and sizes of wear particles and changes in their quantity were determined with high precision. Optical examination allows to estimate the contamination of oil with water, graphite and makes it possible to identify the type and place of wear arising. The photo of the contaminant in a oil drain is shown in the Fig. 4.

Fig. 4. The microscope view of the contaminant on the oil sample

.

The microscope observation of both a shape and a structure of contaminant element shows that majority part of contaminants from oil have a dimension to 5 μm with the shape like a grain of sand. Against the fine background there are some single and bigger particles with irregular shape. These particles have usually sharp edges and their dimension measurement approximately 30-50 μm but sometimes event to 100 μm. The majority of them are stopped by the oil filter.

Adding up the total number of particles on filter is very difficult. Therefore x-ray radioisotopic fluorescence (XRF) method was used to determine the quantitative changes. To determine the mechanical impurities concentration in oil the fluorescence spectrometer ZBZ-93 was used. It is appropriate to determine Fe and Cu concentrations in oil, which are the characteristic products of bearing wear process. The fluorescence spectrometer ZBZ-93 is presented below in the Fig. 5.

Fig.5. The fluorescence spectrometer ZBZ-93

The iron and the copper concentrations changing process, which is necessary to estimate engine bearings technical condition, was followed by analysing the chemical composition of periodically collected and properly prepared oil samples.

Each oil samples was researched on X-ray radioisotope fluorescent method three time to increase a rescue credibility and precision. The average rescue value of contaminants Fe and Cu each oil sample was given the content – related analysis.

The oil samples were taken from the four engines type LM 2500 which are propulsion of two warships.

Example of the results of Fe and Cu concentration changes in function of time of engine work is shown in the Fig. 6. Analysing the run of changes in Fe and Cu concentrations we can see that it is typical for attrition wear.

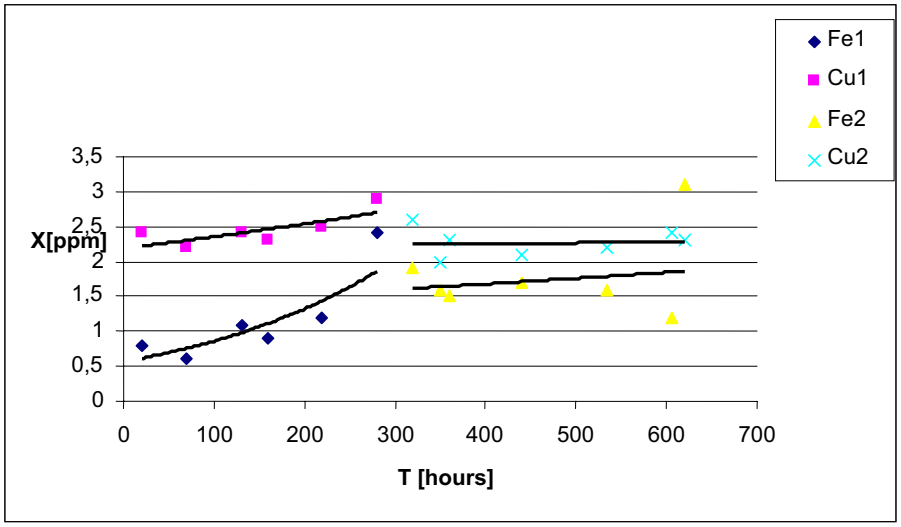

Fig.6. The graph of Fe and Cu impurities in oil in function of time of engine work

The methodology used to the assessment oil contaminants makes possible of changes following Fe and Cu concentration but it do not inform about the impurities value generated from the individual source. Therefore, the choice of the place to take oil samples from the oil system was the important stage of the research. After the carefully analysis of the oil system construction and take into consideration the possibility of bearings technical condition estimate two places were chosen:

- the bearings oil supply; from the oil supply filter,
- the bearings scavenge oil; from the oil pomp.

The scheme shown below in the Fig.7 presents the engine oil system with chosen places to take oil samples.

The value of Fe and Cu concentration in oil samples taken from marked places is shown as the form of graph in the Fig. 8.

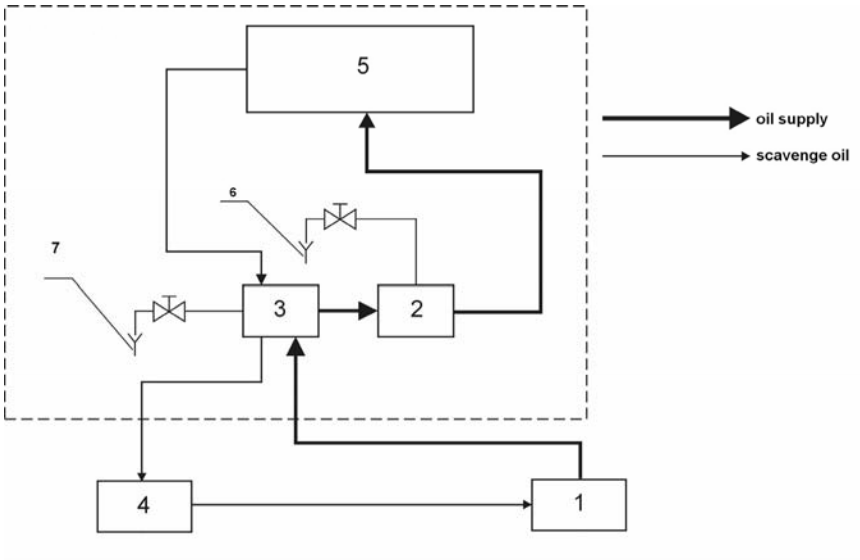

Fig.7. The lube oil system block diagram with the marked places to take oil samples;
1 – the oil tank; 2-the lube supply filters; 3-the oil pump; 4-the scavenge filters; 5-the gas turbine engine.

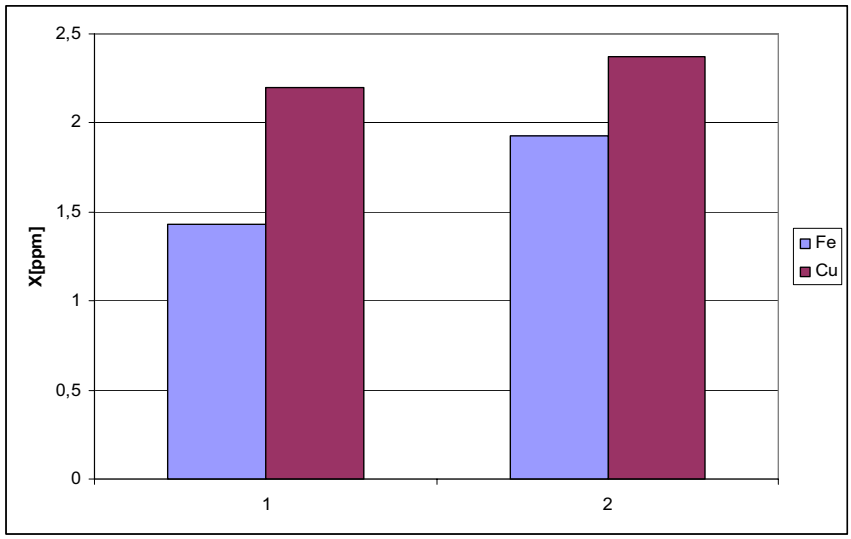

Fig. 8. The graph of Fe and Cu impurities in oil taken from chosen places of oil system:
1- oil sample taken from the lube supply filter, 2 – oil samples taken from the oil pump.

On the basis of the received results we can conclude that the main source of contaminants generation to oil are the engine's bearings. Hence, to estimate a technical condition of gas turbine engines bearings we should to observe a difference of both, Fe and Cu value, in the oil samples taken from the oil supply filter and the oil pomp. This difference marked as ΔX parameter and calculated from the mathematical formula (1) can be the diagnosis measure of the gas turbine engine bearing system [5].

$$\Delta X = X1 - X2 \tag{1}$$

where:

X1- the Fe and Cu concentration in oil taken from the lube supply filter;
X2- the Fe and Cu concentration in oil taken from the pomp.

On the basis of the research on Fe and Cu concentration in oil sample the example of ΔX parameter calculated according the mathematical formula (1) is shown in the Fig. 9.

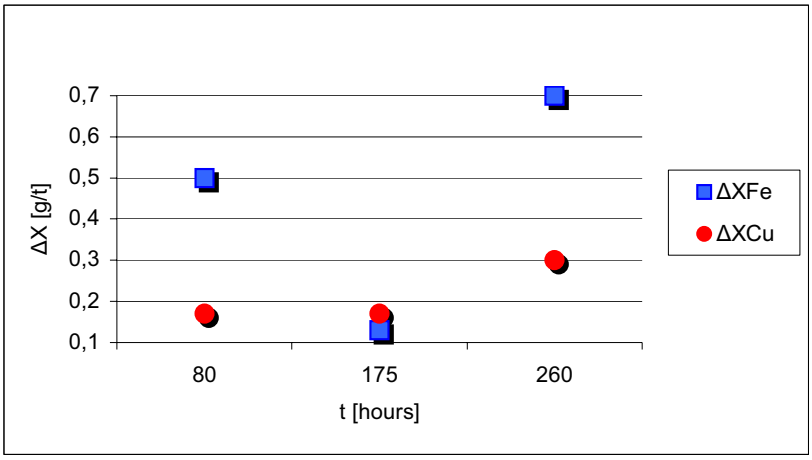

Fig. 9. The graph of ΔX parameters

To receive diagnosis results of engines bearings, contaminants oil research on ought to led on the basis of oil samples taken from the oil supply filter and oil pump. The observation of change of the diagnosis measure ΔX of gas turbine engine bearings, while exploitation the engines process, enables the assessment of technical condition its bearings. On the basis of experiments' results the analytical function that makes calculating the future value of a process possible can be worked out.

The conclusions

The results of experimental research confirmed the accuracy of measuring the Fe and Cu impurities concentrations levels in oil for diagnosis of marine gas turbine engines bearings.

The analysis of concentration of wear products in grease oil samples by x-ray radioisotopic fluorescence (xrf) enables the control of wearing away the rubbing parts of an engine smeared with oil.

The worked out mathematical formula of ΔX parameter changes properly corresponds to a run of wearing processes taking place in bearings. It enables to forecast the failures of the bearings.

The worked out methods compared with traditional methods make possible to estimate the technical condition of marine gas turbine engines bearings without with drawl of ships from exploitation and without disassembly of the engines.

References

[1] Charchalis, A., *Diagnozowanie okrętowych silników turbinowych*, AMW Gdynia, 1991.
[2] Baczewski, K., *Tribologia i płyny eksploatacyjne,* WAT Warszawa 1994.

[3] Korczewski, Z., *Identyfikacja procesów gazodynamicznych w zespole sprężarkowym okrętowego turbinowego silnika spalinowego dla potrzeb diagnostyki*, Gdynia: Zeszyty Naukowe AMW nr 138 A 1999. 163 str.
[4] Lewitowicz, J. & Ostapkowicz, M., *Ocena stanu łożysk na podstawie analizy oleju*, WPT nr 3 Warszawa, 1976.
[5] Łupina, E., *Możliwości diagnozowania wybranych elementów instalacji olejowej silnika LM2500 w oparciu o badania oleju smarującego*, Gdynia, 2004.
[6] Mironiuk, W., *Ocena stanów awaryjnych układów łożyskowych okrętowych silników spalinowych*, AMW Gdynia, 1995.
[7] www.navygasturbine.org

PISTON FAILURES OF MARINE TYPE 6RLD66 DIESEL ENGINES

Jan Monieta

Maritime University Szczecin, Institute of Marine Power Plant Operation,
Wały Chrobrego 2, 70-500 Szczecin, phone: (4891) 48-09-415; 48-09-479,
fax: (4891) 480-95-75, e-mail: jmonieta@am.szczecin.pl

Abstract

The paper presents results of operational research on the of reliability of pistons, which have bee often been subjected to critical damage, sudden and gradual. The low-speed marine diesel engines type 6RLB66 have been produced under Sulzer licence and used for main propulsion of bulk carriers (type B542). Sudden failures of pistons have caused bad operating troubles and large economic losses. Analysis of failures and wear was based on investigation of records ship's document, computer records and on observation of engines and their of sub-assemblies during ships' stays in ports and shipyards Selected functional and numerical coefficients of reliability were estimated by determining the relations between time of correct work and failures of combustion engines pistons.

Keywords: *marine engines, pistons, wear, sudden and gradual failures*

1. Introduction

The paper presents an analysis of failures of pistons of low-speed engines, type 6RLB66, used as the main propulsion of bulk carriers. In these engines pistons have been often [2, 3, 4]. Sudden failures of pistons, which eliminated engines from operation, are troublesome for shipowners. When the is a piston failure, it should be exchanged, piston rings replaced by spare ones or sometimes the engine runs with its speed reduced [2, 3, 5]. Such failures cause large economic losses due to the costs of a new piston, costs of delivering the spare piston and costs of the ship being not in operation.

The investigations of engines have been performed in the actual operating conditions, on the basis of collected information. The results of investigations should contribute to decreased frequency of failure occurrence and improvement of the readiness, effectiveness and reliability of marine engine units and subassemblies.

2. Object of researches

Investigated engines type 6RLB66 one manufactured under Sulzer licence in 1984 and 1985 years. They served for main propulsion of bulk carrier's type B-542, which have been manufactured by home shipyard in 1985 and 1986 year. Characteristic particulars of engines 6RLB66:

- diameter of cylinders – 660 mm,
- stroke – 1400 mm,
- horse power at 124 r. p. m. – 8160 kW.

The RL series engine is a single-acting, reversible two-stroke marine diesel engine with exhaust-gas turbocharging and loopscavenging for direct propeller drive. The cylinder jackets and frames are bolted onto the bedplate by means of tie rods.

The continuous part of the scavenge-air receiver serves as scavenging duct. The inner part is subdivided according to of the cylinders by transverse partitions. Small center longitudinal duct leads the air supplied by the auxiliary blower into the scavenging spaces of the cylinders.

The cylinder jackets, cylinder covers, turbocharger, pistons and fuel injection valves are cooled by fresh water. The scavenge-air cooler can either be supplied by sea or fresh water. The engine drives neither the lubricating oil nor the cooling water pumps.

The piston consists of the piston crown, the piston skirt and the piston rod. These three main parts are fastened together by waisted studs and their nits. The waisted bolt nuts are secured against slackening by locking discs.

The pistons crown, which contains the grooves for the compression rings is exposed to the highs temperature of the combustion gases and must therefore be cooled. The cooling of the piston crown is effected by fresh water enters and leaves trough telescoping pipes.

In the center of the piston crown a tapped hole is provided for fastening the piston suspension device. The lower three-compression piston ring grooves are chromed on one side the upper two ring grooves are hard chrome plated on both sides.

The piston skirt serves to guide in the cylinder liner and to keep the exhaust ports closed over turbocharger. It is equipped with bronze wearing rings, which are required particularly during the running in period, of the initial service.

The piston rod widens out at its upper end into a flange. Onto this flange the piston waisted trough studs and their nuts fasten skirt and crown.

3. Results of investigations

The paper formulates the following statement: *damage and wear of pistons and piston rings do depend on their working time.*

Type 6RLB66 engines has been examined: abrupt and gradual failures of pistons that had been replaced (Fig. 1). Such failures were signalled by the temperature rise of cooling water at the outlet from cylinder liners, leaks or loss of cooling water, fall of the peak firing pressure or compression pressure and knocks in cylinders. Some non-signalled failures were observed during periodical surveys, or special survey in a shipyard or by visual inspection. Same failures were not signalled because signalling aids were damaged.

In the investigation engines type 6RLB66 has been researched abrupt and gradual damages of pistons, which have been replaced (fig. 1). Such failures were signalled: temperature rise of cooling water on the departure from cylinder liner, leaks or loss of cooling water, fall of peak firing pressure or compression pressure and knocks in cylinder. Some not signalled failures have been stated during periodical survey, special survey in shipyard or visual inspection. Same failures have been not signalled because was damaged signalling aids.

Fig 1. View of a cracked of piston skirt

Fig. 2 shows that most of the failures were signalled by the values of compression pressure, maximum combustion pressure means and outlet temperature.

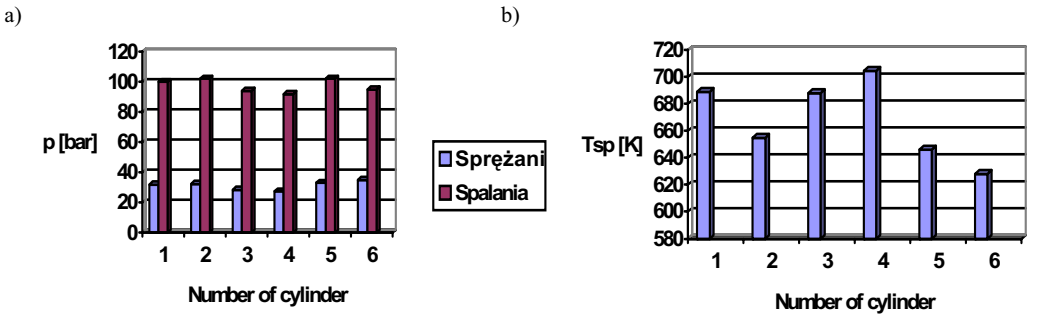

Fig. 2. Values of compression pressure and maximum combustion pressure a) and outlet temperature T_{sp} engine b) RLB66 at engine speed 188 rpm and load 76%: p – pressure

Figure 2 shows that in cylinders 3 and 4 there were low values of compression pressure and high values of outlet temperature of the engine. After a disassembly of pistons it was found that all piston rings suffered excessive wear over the limit values and there leakages of cooling water.

Three conditions of examined engines were distinguished: state of full ability, state of partial ability and state of disabilitto be operated. Investigations followed the plan *(n, R, t*), which embraced $n = 61$ pistons and $n = 41$ sets of piston rings. Damaged pistons were repaired (*R*), and the research was finished as soon as the correct time of piston reached the value *t*. Failures of pistons occurred mostly together with damage to cylinder liners.

The moment of failure one identified with his result, that is to say with consequently of state of unfitness, with exchange or with repair of piston. The well-ordered realisations of the correct time of work to instant failure of examined pistons are shown in Figure 3. Figure 4, in turn, shows well-ordered realizations of restoration time for the examined pistons. In the examined engine most pistons were exchanged on account of cracks in the piston skirt or piston crown. There were mostly long cracks of piston skirts.

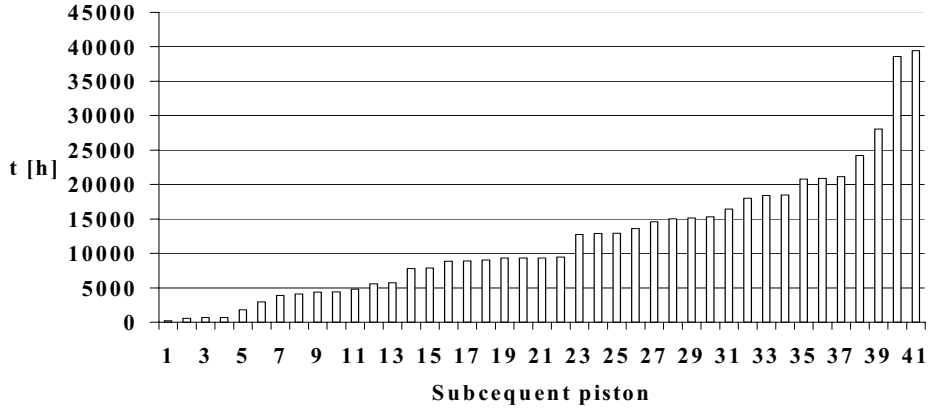

Fig. 3. Well-ordered realizations of time to failure of examined pistons engines, type 6RRLB66

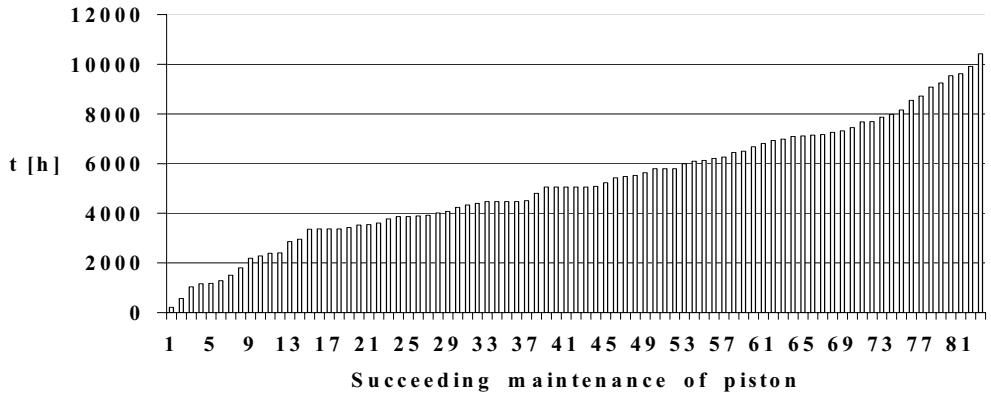

Fig. 4. Well-ordered realizations of time of restorations of examined pistons

The research also included the wear of pistons and piston rings. Changes in dimensions of pistons and pistons rings were determined by geometrical measurements. The sizes of pistons and piston rings are shown in Figures 5÷7.

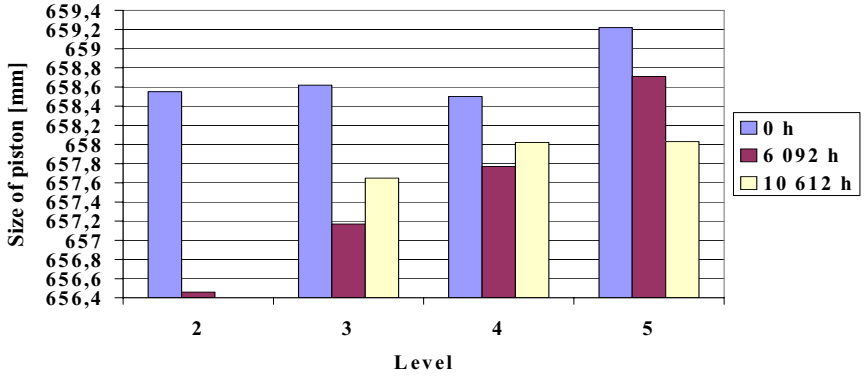

Fig. 5. Changes of piston dimensions in direction along the axis of engine for different times of work

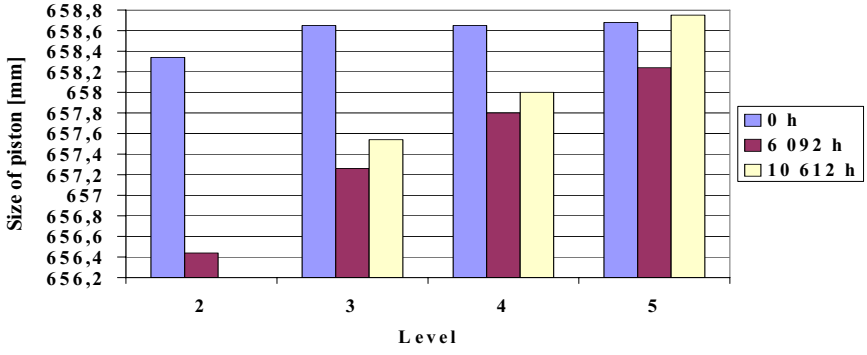

Fig. 6. Changes of pistons dimensions in the direction perpendicular to engine axis for different working times

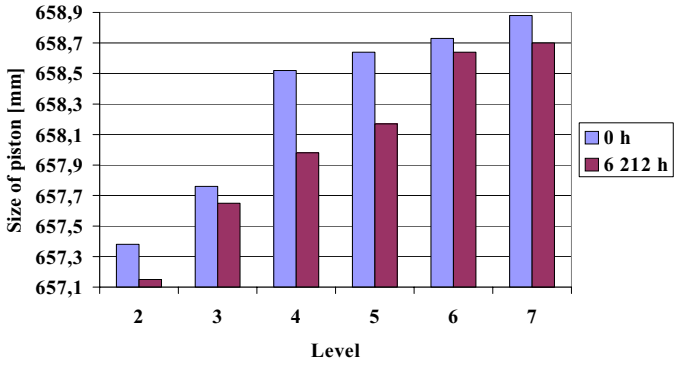

Fig. 7. Changes of pistons dimensions in the direction perpendicular to engine axis for different times of measurements

Figures 5÷7 imply that the wear of piston and piston rings is intensive in its top part.

From the available data quantitative coefficients of reliability were calculated for the examined; the compatibility between empirical and theoretical distributions were examined, too.

For renewable objects the basic functional characteristic of reliability is failure flux parameter $\omega^*(t)$:

$$\omega^*(t) = \frac{r}{n \cdot \Delta t} \tag{1}$$

where:

r – number of failures in researched sample in time $<t, t + \Delta t>$,
Δt – length of partition of time of research.

The results of calculations are given in Figure 8.

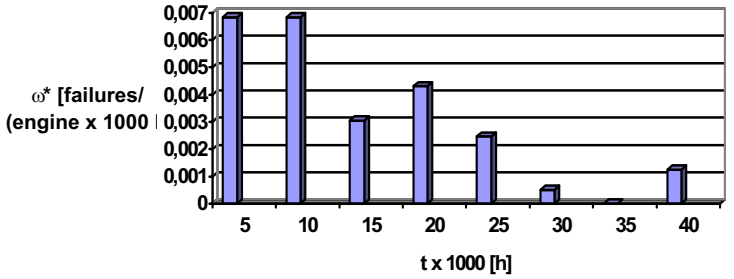

Fig. 8. Diagram of the flux failures parameter ω(t) of pistons of engines type 6RLB66*

The average durability of investigated pistons is described by this equation:

$$\bar{t} = \frac{1}{n}\sum_{i=1}^{n} t_i \tag{2}$$

where:

t_i – time of work i of piston (piston rings) to instant of failure,
n – number of pistons (piston rings) damaged.

Standard deviation time of correct work to the instant of failure is calculated from this formula:

$$\sigma_T^* = \sqrt{\frac{1}{n-1}\sum_{i=1}^{n}(t_i - \bar{t})^2} \tag{3}$$

The average value of correct work time to failures of investigated engine pistons was 12 109 h with a standard deviation of 9 308 h. The durability of piston rings amounted to 5 392 h of work with a standard deviation of 2 469 h.

4. Conclusions

In 65% of cases piston and cylinder liner damage were found in one unit. In 70% of failures of pistons wear or seizures of pistons rings were ascertained to cause blow-by of exhaust gases, increase of temperature and deterioration of lubrication conditions.

In 39% of cases defective injector valves were the cause of deposit formation: carbon deposits, lakes and cokes. In 70% of cases it was found that pistons suffered damage in the time interval 3500 ÷ 10 000 working hours. In the process of piston wear at first a decrease of sizes of pistons and piston rings was noted, then the operating time increase. It was a result of processes of adhesive wear and formed carbon deposits.

The durability of examined pistons was low and its scatter resulted from different conditions of operating and different trading regions.

The construction of examined pistons and cylinder liners with loop scavenging after modernisation is far from perfect. The producer of RLB engines has attempted recently to modernize the construction and production technologies and changes in the operational methods were introduced to minimize failures. Honing is used in final step of cylinder liner manufacturing.

References

[1] Grześkowiak, J., Kotkowski, K., Wołyńska-Mrowicka, E., Heppel, K., Nosal, S., *The efect of some selected factors on the running – in performance of a node modeling the marine engine cylinder liner – piston ring sliding pair*, EXPLO-DIESEL & GAS TURBINE ’01. Gdańsk – Międzyzdroje – Kopenhaga 2001, s. 115 – 122.

[2] Monieta, J., *Analysis of failures of cylinder liners of the low-speed marine diesel engines type 6RLB66*, Journal of KONES 2001, No. 1 – 2, s. 93 – 99.

[3] Monieta, J., *Failures of cylinder liners of the low-speed marine diesel engines Sulzer type RLB*. Collection of Research Papers of The Baltic Association of Engineering Experts No. 3 Kaliningrad 2003, p. 3 – 6.

[4] Monieta, J., *Metoda oceny eksploatacyjnego zużycia tulei cylindrowych okrętowych silników spalinowych napędu głównego*, Journal of KONES 2003 Vol. 10, No. 1 – 2, s. 209 – 216.

[5] Włodarski, J. K., *Eksploatacja maszyn okrętowych. Tarcie i zużycie*, Wyd. Wyższej Szkoły Morskiej w Gdyni, Gdynia 1998.

ANALYSIS OF RELIABILITY OF REDUNDANT SHIP POWER PLANTS

Jacek Rudnicki

Gdansk University of Technology
ul. Narutowicza 11/12, 80-950 Gdańsk, Poland
tel.: +48 58 3472430, fax: +48 58 3472430
e-mail:jacekrud@pg.gda.pl

Abstract

This paper presents possible applications of the theory of semi-Markovian processes to determination of reliability characteristics of complex propulsion systems of a given degree of redundancy. Based on a selected example system, a reliability model has been proposed in the form of a stochastic process of discrete states and continuous with time . On the basis of the limit distribution of the process practical aspects of using the reliability indices obtained from the model in question are shown.

Keywords: *reliability, redundancy, semi-Markovian processes, ship power plant*

1. Introduction

Regardless of the reliability level of every power plant, planned in its design stage and achieved in its manufacturing stage, various external and internal factors affect its functional subsystems ; the factors cause irreversible degradation processes which result in technical state changing and usually in gradual worsening operational characteristics. Hence in the subsystems failures of their components will appear, moreover the process of occurrence of the failures cannot be precisely described as the affecting factors are of random character [1, 2].

In the case of sea-going ship the above mentioned such change of technical state into that belonging to one of the subsets of unwanted states may cause a hazard not only to the power plant but also the whole ship which may meet with a serious casualty including sinkage - in the extreme case of loss of ability to motion and course-keeping in heavy weather conditions [3].

Intensive development of sea shipping, growing number of ships and ship traffic rate as well as variety of tasks performed by them create real hazards to man and the environment.

Scale of the hazards and trends in that domain can be observed in various reports and analyses published by special organizations worldwide. The institutions first of all deal with the entities a risk to which defined as [6]:

$$RI = FR \times CSQ, \tag{1}$$

where:

RI – risk,
FR - the *frequency* of a potential undesirable event is expressed as events per unit time, usually per year,
CSQ - c*onsequence* can be expressed as the number of people affected (injured or killed), property damaged, amount of spill, area affected, outage time, mission delay, dollars lost, etc.

is the greatest.

Many statistical reports published by IMO show that a great number of ship accidents take place , e.g. 119 accidents, including 26 serious ones, of passenger ships occurred in the years 1999 – 2006 [9] ; however the shipping of oil and its products seems to be the crucial issue today.

It can be exemplified by the reports of ITOPF Ltd *(The International Tanker Owners Pollution Federation)* dealing with the above mentioned problems on tankers. The data presented by the ITOPF (Fig. 1), which concern oil pollution from tankers , show that during about 30 years the average number of large spills decreased almost seven times, however the situation can be hardly deemed satisfactory

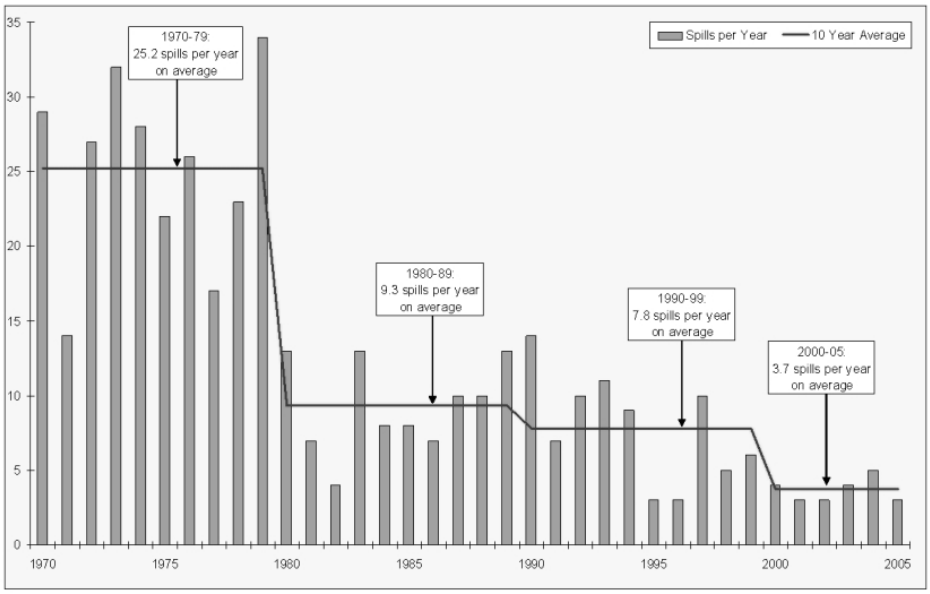

Fig. 1. Numbers of Spills over 700 tonnes [10]

Analyzing the causes of tanker accidents (Fig. 2) one can observe that about 20% of accidents have been still caused by power plant failures in spite of the obtained technological development.

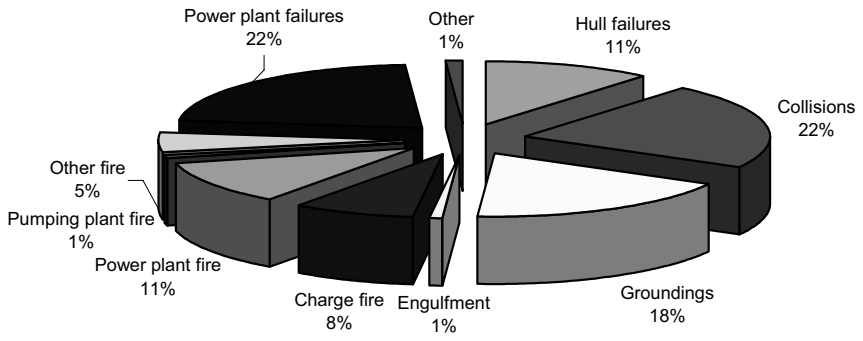

Fig. 2. Incidence of tankers by Causes [10]

The situation resulted in that ship classification societies introduced many stricter requirements for design solutions of propulsion systems on sea-going ships , which result - on the one hand - in risk lowering by decreasing occurrence probability of ship's disability, and - on the

other hand - in appearance of unusual design solutions of propulsion systems on ships of a given class.

2. Propulsion systems of a given redundancy degree

Tankers exemplify the type of ships to which the above described tendencies relate especially distinctly.

On tankers the direct propulsion system with one slow-speed diesel engine is most often applied. Most ships of the kind are still so built as to comply with a minimum of the requirements of legal acts in force (a.o. MARPOL 73/78 Convention), which first of all results from economical reasons [7].

However in recent years, often and often appear real and conceptual technical solutions in which the above presented principle is not obeyed any longer. It can be observed very distinctly in the case of propulsion systems on shuttle tankers. Their operation specificity consisting first of all in precise positioning the ship during oil loading operation at open sea, resulted in that multi-engine propulsion systems became prevailing design solution on such ships.

An example of the evolution of design solutions of propulsion systems on tankers is the unique solution applied on the VLCC tankers of STENA V-MAX type [8]. The propulsion system of the tanker of 333 m in length and design deadweight of 269 000 t is composed of two identical propulsion units located in separate engine rooms. The schematic diagram of the system is presented in Fig. 3.

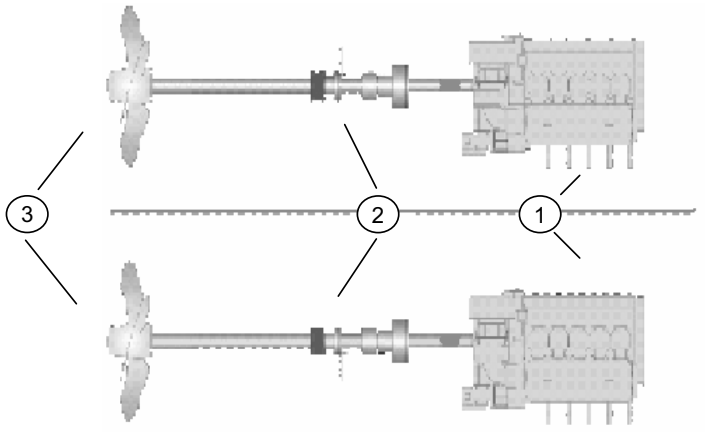

Fig. 3 Schematic diagram of the propulsion system of the crude oil tanker STENA V-MAX : 1 –7S60ME-C MAN B&W main engines, 2- shaft lines, 3 – screw propellers

Another example of the presented approach is the propulsion system installed on a series of tankers intended for operating in Arctic conditions, ordered by *the Sovcomflot*, a Russian shipowner, in the South Korean shipyard *Samsung Heavy Industries Shipbuilding & Offshore Division* [11].

Design solution of the propulsion system to be installed on each of 5 tankers of 257 m in length and design deadweight of 70000 t (presented in Fig. 4) is the typical diesel - electric propulsion system which consists of 4 electric generating sets and two azimuthing podded propellers developing 20 MW output power in total.

The design solution following that on the ships to which safety requirements are much more stringent, e.g. passenger cruisers or ice breakers , confirms the existing trends indirectly.

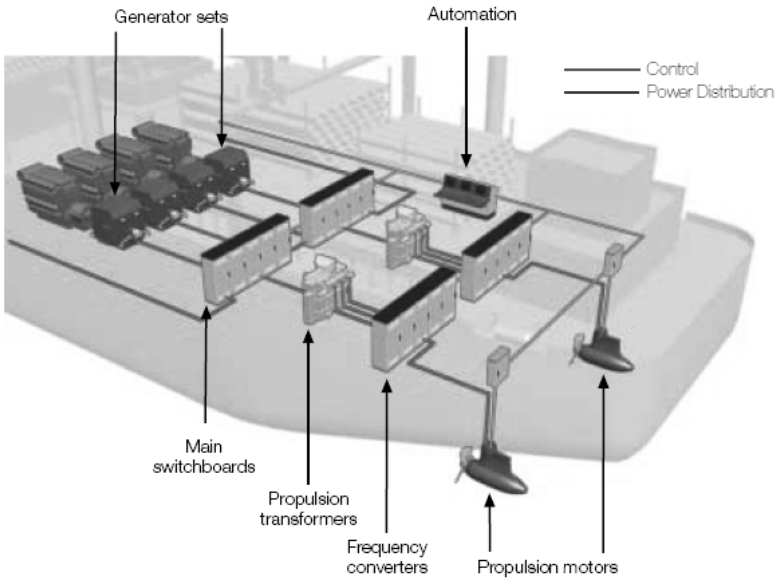

Fig. 4 Schematic diagram of the diesel-electric propulsion system on shuttle tanker [11]

3. Reliability analysis of redundant propulsion systems

Analysis of redundant propulsion systems becomes especially useful and effective when functional reliability models based on the theory of stochastic processes is applied.

Use of the theory of stochastic processes makes it possible to resign from the assumption on two-state character of the process of technical state changing of propulsion system's subsystems and elements , and on the splitting of the space S of possible states into a countable and finite number of subspaces differently distant from the extreme set of initial states [4].

Therefore the assumption on multi-state character is crucial in building functional reliability models. It makes it possible to separate , within the set of distinguished states, several states of different degree of serviceability as well as several unserviceability states (in contrast to most classical models) and to attribute renewability, an important feature which characterizes machines and mechanical devices, to the model .

It is specially important in the case of ship propulsion system of a given degree of redundancy as, being a complex technical object, it may fail in many ways, at different probability values and with various consequences corresponding with a given operational reliability.

In functional aspect the process of operation constitutes that of simultaneous changing both technical and operational states which, being mutually dependent, simultaneously occurr during phase of operation [2].

In that case the stochastic processes having discrete set of distinguished states and continuous duration time are suitable to model the technical state changing, crucial from the point of view of reliability and durability. Elements of the set of distinguished technical states, $S=\{s_i; i=1, 2, 3, ..., I\}$ are values of the process $\{W(t): t\geq 0\}$ which is formed by the successively occurring states $s_i \in S$, being in mutual cause-effect relationship [4].

Elaboration of a functional reliability model makes it possible to determine probabilistic characteristics of real reliability features of practical importance, e.g. for operational decision making with the use of statistical theory of decisions [2].

The above presented example of the shuttle tanker's propulsion system, shown in Fig. 4, has been taken into consideration in this work. Its simplified functional diagram is presented in Fig. 5.

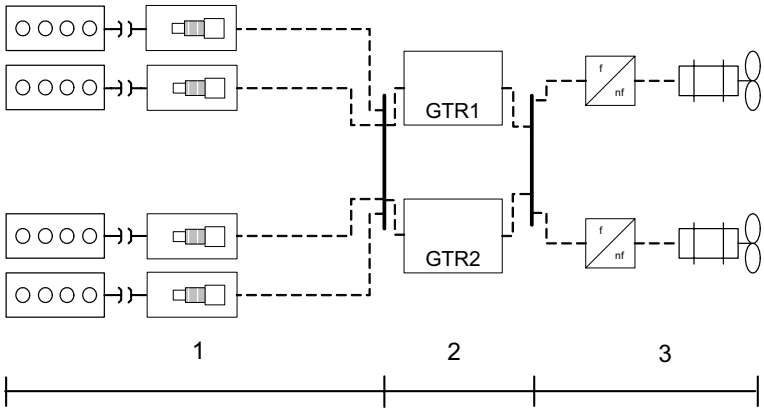

Fig. 5 Functional diagram of the diesel-electric propulsion system on shuttle tanker: 1 – electric power plant together with power transmission system, 2 – electric energy distribution system, 3 – units of podded azimuthing propellers

In can be assumed that for the presented propulsion system a model of technical state changing process – crucial for power plant reliability and durability - can be the stochastic process $\{W(t) : t \in T\}$ of discrete set and continuous duration time and of the following successively occurring distinguished states:

$$S = \{s_i ; i = 1, 2, 3, 4, 5, 6, 7\} \tag{2}$$

which can be interpreted as follows:

s_1 – full serviceability state of the system;
s_2 – partial serviceability state of the system due to not quite full serviceability of electric power plant (e.g. full unserviceability of one out of four electric generating sets);
s_3 – task unserviceability state of the system due to full unserviceability of electric power plant (full unserviceability of all four electric generating sets);
s_4 – partial serviceability state of the system due to not quite full serviceability of electric distribution system (e.g. full unserviceability of one out of two main switchboards);
s_5 – task unserviceability state of the system due to full unserviceability of electric power distribution system (full unserviceability of both main switchboards);
s_6 – partial serviceability state of the system due to not quite full serviceability of podded propellers system (e.g. full unserviceability of one out of two frequency converters);
s_7 – task unserviceability state of the system due to full unserviceability of podded propellers system (full unserviceability of both podded propellers).

The initial distribution of the process, p_i

$$p_i = P\{W(0) = s_i\},\ s_i \in S;\ i=1, 2, 3 \tag{3}$$

should be represented as follows:

$$p_1 = P\{W(0) = s_1\} = 1,\ p_i = P\{W(0) = s_i\} = 0 \ \text{ dla } i = 2, 3, \ldots, 7 \tag{4}$$

as assumed that at the initial instant of operation (t = 0) the system in question being a functional subsystem of the ship , has to be in the state s_1.

Since certain redundancy is applied to the system in question it can be assumed that from practical point of view the process of passing in one step from the full serviceability state s_1 to any of the distinguished states of full unserviceability, s_3, s_5 or s_7 , is not possible. Hence the functional matrix of the process , Q(t), whose elements are conditional probabilities of passing the process from the state *i* to state *j* during time not longer than *t* [4] can be expressed as follows:

$$Q(t) = \begin{bmatrix} 0 & Q_{12} & 0 & Q_{14} & 0 & Q_{16} & 0 \\ Q_{21} & 0 & Q_{23} & 0 & 0 & 0 & 0 \\ Q_{31} & Q_{32} & 0 & 0 & 0 & 0 & 0 \\ Q_{41} & 0 & 0 & 0 & Q_{45} & 0 & 0 \\ Q_{51} & 0 & 0 & Q_{54} & 0 & 0 & 0 \\ Q_{61} & 0 & 0 & 0 & 0 & 0 & Q_{67} \\ Q_{71} & 0 & 0 & 0 & 0 & Q_{76} & 0 \end{bmatrix} \tag{5}$$

In the case of ship main engine, for the above presented set of state classes, the graph of changing the states of the process {W(t): t ∈ T} can be drawn, as follows:

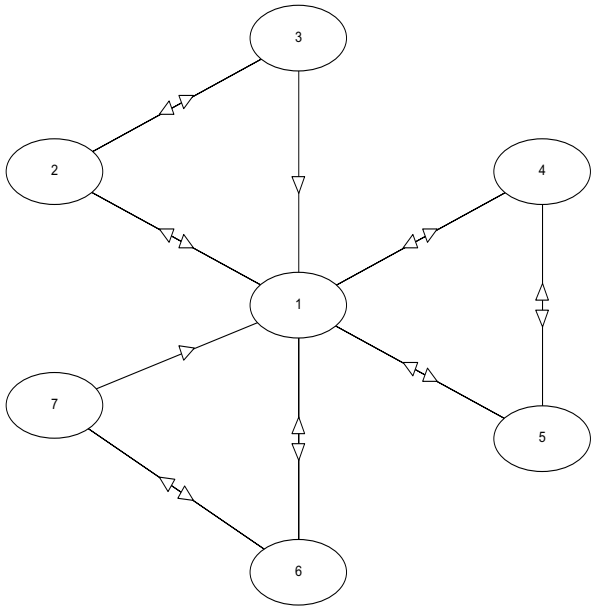

Fig. 6 The graph of changing the states of the process {W(t): t ∈ T}

The use of the relation [4]:

$$Q_{ij}(t) = p_{ij} \cdot F_{ij}(t) \tag{6}$$

where:

p_{ij} – probability of passing from the state s_i to the state s_j of Markovian chain inserted into semi-Markovian process, (i , j = 1, 2, …, 7 i≠j), whereas to assess the particular probabilities p_{ij}, is the most convenient to take the following value of the statistic P_{ij}^{*} (on the basis of empirical investigations):

$$p_{ij}^{*} = \frac{n_{ij}}{\sum_{j} n_{ij}} \tag{7}$$

where:

n_{ij} – number of transitions of the process from the state s_i to the state s_j $(i, j \in S, i \neq j)$,
$F_{ij}(t)$ – cumulative distribution function of the random variable T_{ij} which represents duration time of the process state s_i provided that the state s_j will be next one;
makes it possible to determine analytical function forms of particular elements of the functional matrix (5) of the process. Fulfillment of the showed conditions determines entirely the considered semi - Markovian process and thus enables to determine also all necessary reliability characteristics.

The limit distribution of the process $\{W(t): t \in T\}$ is undoubtedly one of the most important characteristics because of long time of realization of the propulsion system tasks.

The further part of this paper, as its volume is limited, concerns only the above mentioned distribution.

3. Limit distribution of the process $\{W(t): t \in T\}$

Knowing the 1st order moment of the random variables T_i (expected values) one is able to determine relatively easily the limit distribution of the process (not being forced to solve a set of Volterra's integral equations of 2nd kind , that appears very troublesome in some cases).

For the model in question the distribution interpreted by means of the formula [4]:

$$P_j = \lim_{t\to\infty} P\{W(t) = s_j\}; \quad s_j \in S, j = \overline{1,7} \tag{8}$$

can be determined from the following relationship [4]:

$$P_j = \frac{\pi_j E(T_j)}{\sum_{k=1}^{7} \pi_k E(T_k)}; \quad j = 1,2,3,4,5,6,7 \tag{9}$$

where the distribution π_j, $j = 1, 2, 3, 4, 5, 6, 7$ is limit one for the Markovian chain inserted into the process $\{W(t): t \geq 0\}$ $(j \in S)$. The limit distribution of the process $\{W(t): t \in T\}$ can be determined from the set of equations [4]:

$$\left.\begin{array}{l} \left[\pi_1\ \pi_2\ \pi_3\ \pi_4\ \pi_5\ \pi_6\ \pi_7\right]\begin{bmatrix} 0 & p_{12} & 0 & p_{14} & 0 & p_{16} & 0 \\ p_{21} & 0 & p_{23} & 0 & 0 & 0 & 0 \\ p_{31} & p_{32} & 0 & 0 & 0 & 0 & 0 \\ p_{41} & 0 & 0 & 0 & 0 & 0 & 0 \\ p_{51} & 0 & 0 & p_{54} & 0 & 0 & 0 \\ p_{61} & 0 & 0 & 0 & 0 & 0 & p_{67} \\ p_{71} & 0 & 0 & 0 & 0 & p_{76} & 0 \end{bmatrix} = \left[\pi_1\ \pi_2\ \pi_3\ \pi_4\ \pi_5\ \pi_6\ \pi_7\right] \\ \\ \pi_1 + \pi_2 + \pi_3 + \pi_4 + \pi_5 + \pi_6 + \pi_7 = 1 \end{array}\right\} \tag{10}$$

By solving the set of equations (10) the following relationships assessing the limit distribution of the process $\{W(t): t \in T\}$, can be achieved:

$$P_1 = \frac{(1 - p_{23}p_{32}) \cdot (p_{45}p_{54} - 1) \cdot (p_{67}p_{76} - 1) \cdot E(T_1)}{H} \tag{11}$$

$$P_2 = \frac{(p_{67}p_{76} - 1) \cdot (p_{45}p_{54} - 1) \cdot p_{12} \cdot E(T_2)}{H} \tag{12}$$

$$P_3 = \frac{(p_{67}p_{76} - 1) \cdot (p_{45}p_{54} - 1) \cdot p_{23}p_{12} \cdot E(T_3)}{H} \tag{13}$$

$$P_4 = \frac{(p_{67}p_{76} - 1) \cdot (p_{23}p_{32} - 1) \cdot p_{14} \cdot E(T_4)}{H} \tag{14}$$

$$P_5 = \frac{(p_{67}p_{76} - 1) \cdot (p_{23}p_{32} - 1) \cdot p_{14}p_{45} \cdot E(T_5)}{H} \tag{15}$$

$$P_6 = \frac{(p_{23}p_{32} - 1) \cdot (p_{45}p_{54} - 1) \cdot p_{16} \cdot E(T_6)}{H} \tag{16}$$

$$P_7 = \frac{(p_{23}p_{32} - 1) \cdot (p_{45}p_{54} - 1) \cdot p_{16}p_{67} \cdot E(T_7)}{H} \tag{17}$$

where:

$$\begin{aligned} H = {} & (p_{45}p_{54} - 1) \cdot (p_{67}p_{76} - 1) \cdot [E(T_1)(1 - p_{23}p_{32}) + E(T_2)p_{12} + E(T_3)p_{23}p_{12}] + \\ & + (p_{23}p_{32} - 1) \cdot (p_{67}p_{76} - 1) \cdot [E(T_4)p_{14} + E(T_5)p_{14}p_{45}] + \\ & + (p_{23}p_{32} - 1) \cdot (p_{45}p_{54} - 1) \cdot [E(T_6)p_{16} + E(T_7)p_{16}p_{67}] \end{aligned} \tag{18}$$

where:

$P_1, P_2, \ldots, \tilde{P_7}$ - probabilities that the process $\{W(t): t \in T\}$ will find itself in the states : $s_1, s_2, \ldots, s_7$, respectively ;
$E(T_1), E(T_2), \ldots, \tilde{E(T_7)}$ - expected values of duration time of the states : $s_1, s_2, \ldots, s_7$, respectively

The probabilities determined by the formulae (11), (12), (14), (16) are crucial for the operational subsystem (SU) as they characterize probabilistic possibilities of application of the system to a given operational system (SE) provided that it is in the state of full or partial serviceability.

Practical use of the probability values determined by the relations (11 ÷ 17) depends of course on a given decision situation. One of numerous possibilities of the kind is to apply the FTA method (Fault Tree Analysis) [5, 6] for determining the occurrence probability of an unwanted situation.

The example fault tree (no. 1) for the top event : „ limited ability to motion and manoeuvring ” is presented in Fig. 7.

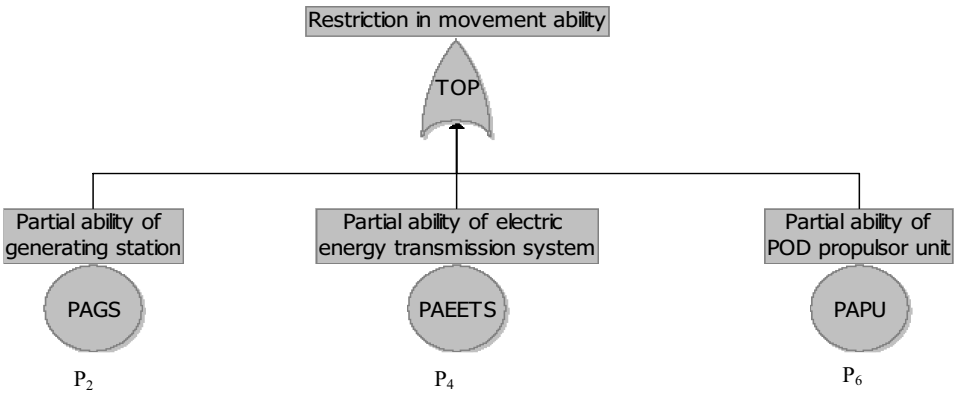

Fig. 7 Fault tree no. 1

To perform a quantitative analysis of the considered sequence of events leading to occurrence of the top event „TOP" is possible by making use of the probabilities P_2, P_4 and P_6 determined by the relations (12), (14 and (16).

Another example showing practical usefulness of the presented approach may be the situation in which occurrence probability of partial serviceability state together with limit conditions, is considered.

If the above presented top event is taken into consideration but under assumption that the full serviceability state of both azimuthing propeller systems is required then - by using the FTA method - the considered sequence of events can be expressed as follows (fault tree no. 2 – Fig. 8):

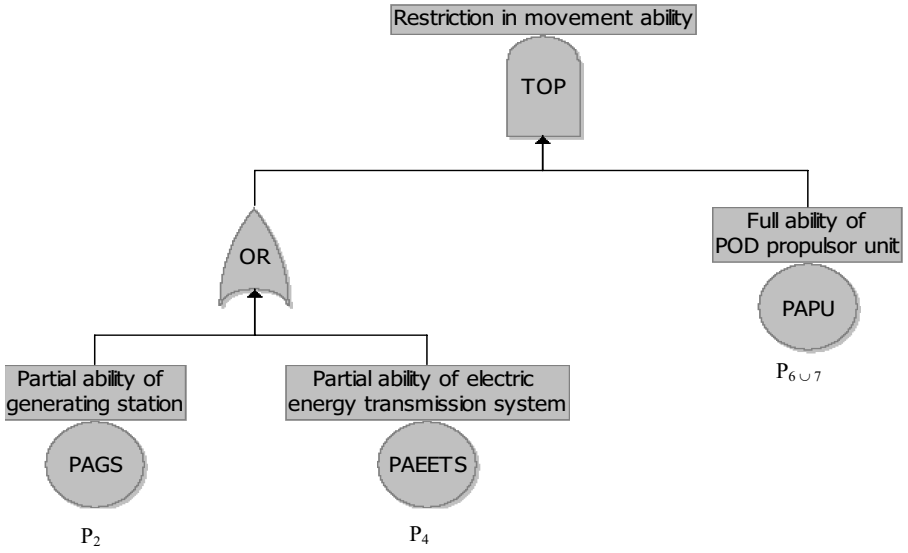

Fig. 8 Fault tree 2

The sequence of events can be quantitatively analyzed by using values of the probabilities P_2, P_4 determined by the relations (12) and (14) , as well as the probability $P_{6 \cup 7}$ which , under the probability feature, can be expressed as:

$$P_{6 \cup 7} = 1 - (P_6 + P_7) \tag{19}$$

where:

$P_{6 \cup 7}$ – probability of the event that the state s_6 or s_7 will not occur

4. Summary

The models elaborated with the use of the theory of stochastic semi-Markovian processes (in particular cases – theory of Markovian processes) seem to be very useful for investigating the reliability of complex technical systems such as the considered propulsion systems of a given degree of redundancy.

The fundamental assumption taken into account in designing such systems, that apart from the full serviceability state a few partial serviceability states must take place in them , indicates in a natural way that the described stochastic processes are equivalent to reliability models.

The practically useful complex description of reliability features of ship power plant (in the considered case – the propulsion system) can be made on the basis of one versatile model. Hence during modeling the process of ship power plant operation it would be usually not necessary to consider various models of a different structure and complexity, which is very important in an utilitarian aspect as it greatly facilitates elaboration of a ready- for- use tool for aiding the process of decision making by the operator..

References

[1] Birolini, A., R*eliability Engineering. Theory and Practice*, Springer – Verlag, Berlin – Heidelberg New York 1999.

[2] Girtler, J., *Możliwości zastosowania i przydatność procesów semimarkowskich jako modeli procesów eksploatacji maszyn,* Zagadnienia Eksploatacji Maszyn, Kwartalnik Z.3, Polska Akademia Nauk, Warszawa 1996.

[3] Girtler, J., Kuszmider, S., Plewiński, L., *Wybrane zagadnienia eksploatacji statków morskich w aspekcie bezpieczeństwa żeglugi*, Wyższa Szkoła Morska, Szczecin 2003.

[4] Grabski, F., *Teoria semimarkowskich procesów eksploatacji obiektów technicznych*, Zeszyty Naukowe Akademii Marynarki Wojennej, nr 75A, Gdynia 1982.

[5] Modarres, M., *What Every Engineer Should Know About: Reliability and Risk Analysis*, Marcel Dekker, New York 1993.

[6] Smith, D. J., *Reliability, Maintainability and Risk. Practical Methods for Engineers*, Butterworth –Heinemann Linacre House, Oxford 2001.

[7] Waters, J.K., Mayer, R.H., Kriebel, D.L., *Shipping Trends Analysis*, Department of Naval Architecture and Ocean Engineering United States Naval Academy, Annapolis 2000.

[8] http://www.concordia-maritime.se/eng/fleet/vmaxmicrosite/tech/

[9] http://gisis.imo.org/Public/ISPS/Default.aspx

[10] http://www.itopf.com/stats.html

[11] http://www.sovcomflot.ru/

ESTIMATION OF CATALYTIC CONVERTER EFFICIENCY WITH THE ASSISTANCE OF NOx SENSOR IN LIGHT OF FUNCTION OF OBD SYSTEM IN VEHICLES WITH CI ENGINES

Marcin Rychter

Motor Transport Institute
80 Jagiellońska St., 03-301 Warszawa
phone: + 48-22-811-32-31; fax: +48-22-811-09-06
e-mail: rychter@poczta.fm

Abstract

One of the methods to reduce emission of toxic components is continuous control over engine elements that are directly or indirectly responsible for level of emission of these components. Introduction of these requirements caused creation of the self-diagnostic definition and utilising innovation definition self-diagnostic - self-diagnostic system comparing value of signals from circuit of electronic control device with control values. If the real signal value does not comply with control value, the memory of the control devices records the error code.

This paper include basic terms and rules of function European On Board Diagnostic in light of large quantity of vehicles in Europe and in the whole world, level of pollution environment and one of method of prevention degradation environment and basic rules according to built and monitoring of catalytic converters.

The development of a catalytic converter required an analysis of selected physical parameters of the supports. This resulted from the necessity to assume given parameters of the supports applied in the tests in exhaust gas environment in the CI engines. An analysis of ionic conductors which constitute the basic solution in voltage sensors providing signals through NO_x electrocatalysis.

The aim of this paper is to determine the basis for the monitoring of catalytic converters in compression ignition engines by the emission level of a selected exhaust gas component as a diagnostic signal. The emission of NO_x has been taken as the basis. This required the development of a specialized system allowing the reduction of NO_x and obtaining of a diagnostic signal reflecting the level of the said reduction.

Those paper include same results of testing and possibilities monitoring of prototype catalytic converter on the test bad.

Keywords: *monitor, OBD II, EOBD, sensor, temperature, pressure, catalytic converter.*

1. Introduction

The OBD system (*On Board Diagnostic* system; known in the United States as the OBD II system and in Europe as the EOBD one) is a set of diagnostic tests and calculation and decisive procedures which are performed in a real time and are intended as a measure for evaluation of the emission efficiency and the efficiency of elements responsible for the passive and active safety of a vehicle. The OBD system is an integral part of the vehicle connected with the engine control system. Nowadays the investigation on the on board diagnostic systems in their different applications is one of the basic problems that the OBD method is concerned with. The implementation of the investigation method for the OBD system efficiency is one of the main questions of the matter in hand.

In order to satisfy such postulates the realization of the implemented diagnostic procedures during the real operation of vehicles and in the possible shortest time is necessary. Thus the evaluation of the operating efficiency OBDE (*On Board Diagnostic Efficiency*) of the OBD system is also necessary.

2. Tested station

The engine research work presented in this paper was carried out in the laboratory of the Institute of Combustion Engines and Transport at Poznań University of Technology. For the research needs an exhaust system of the tested engine was adequately adapted. The engine test stand consisted of the following elements [4]:

- 4CT90 compression-ignition engine manufactured by WSW Andoria,
- AMX-210/100 eddy-current brake with water cooling,
- reducing catalytic converter *(catalyst*) equipped with carriers of 200 cpsi density,
- HORIBA MEXA 7100 exhaust emission analyser,
- temperature sensors,
- pressure sensor.

For determining the efficiency of the applied catalyst, and NO_x probe as well, on the adapted test stand under the engine test bench conditions (fig. 1), some preliminary tests were carried out according to the obligatory ESC (*European Stationary Cycle*) test.

A special catalytic converter equipped with carriers of 200 cpsi density was built for the test needs. It consists of five blocks with dimensions of 125×50 mm. The catalyst casing enables performing the tests for a variable number of catalytic blocks and taking the measurements behind each block.

A chemical composition of the catalytic converters was developed (*selected*) in the Institute of Internal Combustion Engines at Poznań University of Technology in cooperation with the Department of Inorganic Chemistry at AGH University of Science and Technology in Kraków. The catalytic layers were produced by means of the USPD (*Ultra Spray Pyrolysis Deposition*) and sol-gel methods for CeO_2-ZrO_2/PtPd and CeO_2-ZrO_2/PtRu components [5].

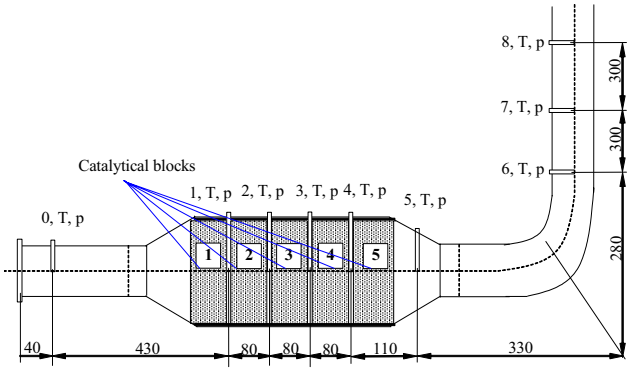

Fig. 1. Diagram of modification exhaust pipe with installed catalytically converter *in test bed and present of measurement points [3]; 0-8 – measurement points:(T) – temperature, (p) – pressure*

3. Analyses of temperatur dissolution in exhaust pipe

The temperature is a basic parameter affecting the ability of generating voltage signals by the sensors produced in the „*sensor to sensor*" technology. Owing to the design of sensors and the constructional materials used for the execution of electrodes in the individual areas, as shown in papers [3, 4, 5], it was necessary to provide an additional reheating to reach the temperatures which enable starting the oxygen pumps. Taking into consideration the operating parameters of the engine examined on the engine test bed the exhaust gas temperatures during the realization of the ESC test could reach the range in which generating the diagnostic signals by the sensors was

possible. Overheating the measuring probe of a sensor caused by too high temperatures of exhaust gas while supplying a system of heaters with an external voltage can result in a degradation of electrodes. Therefore the developed laboratory system requires a manual selection of the voltage for supplying a sensor in a way eliminating a risk of exceeding the threshold voltage value for given engine operating conditions. To complete the gathered knowledge on the possibilities of delivering the supply voltage depending on the temperature in the exhaust engine system an analysis of the temperature distribution was carried out in the measuring points of the exhaust system, provided for the NO_x sensors (fig. 2 – 3) [3].

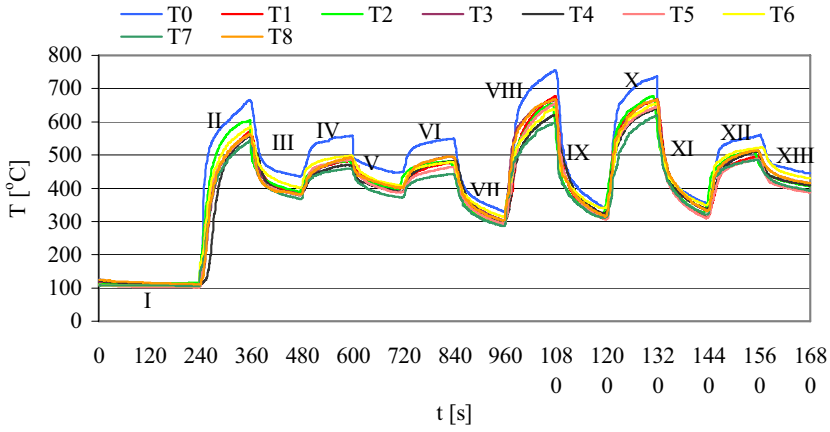

Fig. 2. Distribution of temperature in measurement point T0-T8 exhaust pipe of testing engine without catalytically converter during realization ESC test [3]

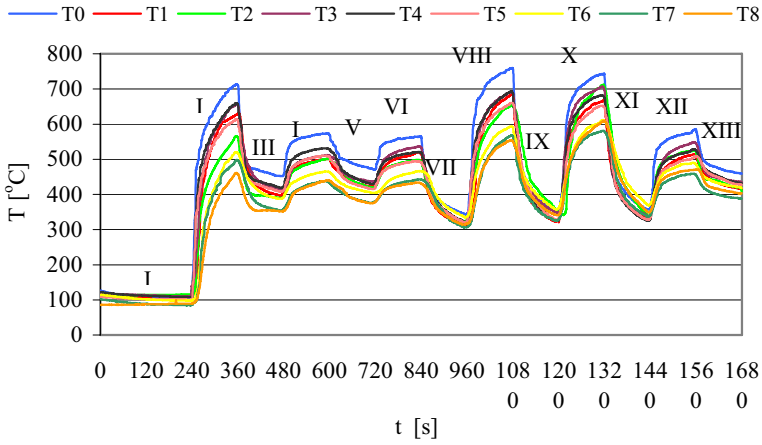

Fig. 3. Distribution of temperature in measurement point T0-T8 exhaust pipe of testing engine with 200 cpsi catalytically converter during realization ESC test [3]

The performed analysis indicates that with regard to the exhaust gas temperatures the phases II, VIII and X are most critical. It concerns both temperatures measured without and with the catalyst provided. In case of phase II the highest temperature of 710°C was reached at the T0 point of the exhaust system equipped with a catalyst with a carrier of 200 cpsi density.

In case of phases VIII and X the exhaust gas temperature were reaching the values ranging from 737°C to 759°C. These are temperatures at which the sensors, owing to their design and

constructional materials for electrodes, are able to generate voltage signals without necessity of reheating. For all other test phases the highest temperatures were reached at the T0 point and the recorded temperatures were not exceeding the value of 600°C.

This analysis indicates that in case of phases VIII and X, during a realization of the engine test bed examinations, the applied sensors will be most sensitive to the controlled supply voltage value. The obtained temperature distribution suggests that for these phases the sensor reactions should be fastest as the optimum sensor temperatures can be reached without necessity of reheating. However, the above applies to the sensor installed at T0.

4. Analyses of pressure dissolution in exhaust pipe

The rate of chemical reactions is a function of the reactive exhaust gas components, exhaust gas temperature, type of the applied catalyst and pressure. For reactions proceeding in a gaseous phase the concentrations and pressures are interdependent. However, the pressure can independently affect the reaction rate values, thereby the response times of the sensor in the considered system. In order to find the importance of these variables the experiments should be carry out in a way which makes possible a simultaneous change of the smallest number of parameters. It is impossible to perform such experiments in case of examination being realized under the engine test bed conditions. For this reason the importance of pressure is limited to its effect on the sensor response time with regard to the exchange of exhaust gas present in the sensor's probe.

The pressure in the exhaust system affects the intensity of the gas exchange in a sensor by affecting the pressure present in a measuring probe, as shown in papers [3, 4, 5]. When an increase in pressure in a measuring area is faster the speed of the gas exchange in the individual regions of the NO_x increases and thereby a frequency of the voltage signals should be greater.

With reference to the classic catalyst the engine exhaust system pressure results in a number of the molecules adsorbed within a catalytic layer. Regarding it to the sensor conditions a number of the collisions of oxygen molecules with the electrode *Pt* should be also higher what can directly result in the sensor response time value.

In the phase I of the test, in which the engine was operating at idling speed, the average overpressure in the exhaust system without the catalyst was of $0{,}03 \cdot 10^{-4}$ Pa (fig. 4). In case of the exhaust system equipped with the catalysts with the 200 cpsi carriers such same overpressure values of $0{,}03 \cdot 10^{-4}$ Pa were recorded. From the considered research point of view such values do not allow to get information necessary for the realisation of the next assumed examination.

Analysing a distribution of pressure in the exhaust system without the catalyst it can be found that for all phases of the test the pressure differences between the p0–p5 points are small (fig. 4). In points p6–p8 which are distant from the point p5 by 60 cm the pressure values are also similar. In every phase, depending on the overpressure values, the measuring points can be separated into two groups of points p0–p5 and p6–p8. In points p6–p8 the overpressure values in every phase are smaller what results from their greater distance from the exhaust collector. The differences in the overpressure values measured in the measuring points of the individual groups can be explained by the pressure fluctuation in the engine exhaust system and an indication error of the applied pressure measuring sensors (fig. 5).

As the distance from the exhaust collector increases the pressure value decreases. In case of measuring points before (p0), in (p1 – p4) and just after the catalysts (p5), the differences in the overpressure values are caused by the exhaust gas flow resistance in the individual catalytic blocks. For every test phase in points distant from the catalyst (p6 – p8) the pressure values are much lower and continue their falling tendency depending on the distance in relation to the exhaust collector.

In case of the catalyst the highest overpressure values were recorded for the phase X at the point p0 and they were of $6{,}3 \cdot 10^{-4}$ Pa for the catalyst equipped with the 200 cpsi carrier.

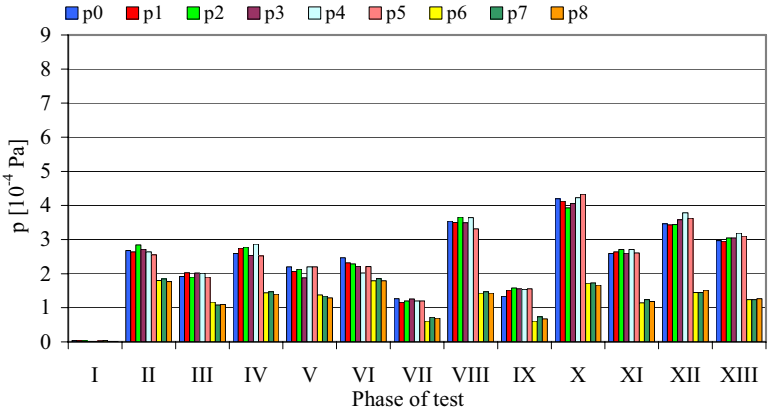

Fig. 4. Distribution of pressure in measurement point p0-p8 exhaust pipe of testing engine without catalytically converter during realization ESC test [3]

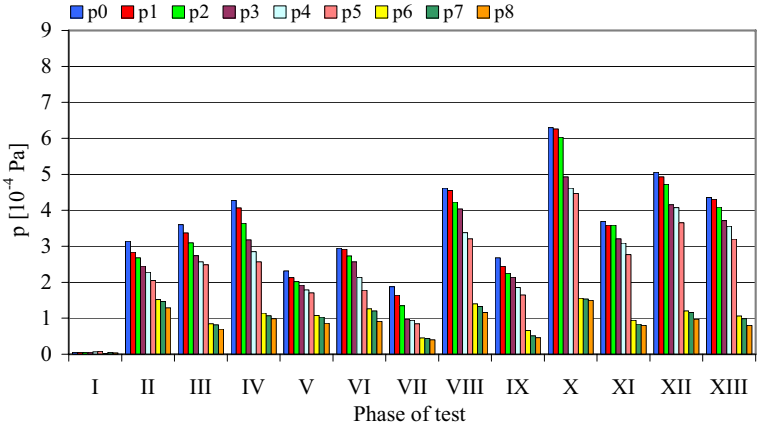

Fig. 5. Distribution of temperature in measurement point T0-T8 exhaust pipe of testing engine with 200 cpsi catalytically converter during realization ESC test [3]

5. Analyses of tested catalytic converter with 200 cpsi

In order to determine the effectiveness of the applied catalytic converter for the reduction of the NO_x emission according to the obligatory official certification test ESC some preliminary examinations of its efficiency under the engine test bend conditions were performed. Taking the operation nature (character) into consideration the NO_x emission in each phase of the test was analysed [3].

To determine the reduction in the NO_x emission the emission measurements were taken after each catalytic block. The presented results are referred to the NO_x concentration values before the catalytic converter**.** The efficiency for the individual catalytic blocks was determined from the relation:

$$k_r = \frac{C_p - C_z}{C_p} \cdot 100\,[\%],$$

where:

C_p –concentration NO_x before catalytic converter, C_z –concentration NO_x after catalytic converter.

Due to the diversified parameters characterising the catalytic converters, which are being built with the use of the catalytic carriers with different cell densities, the examinations were performed for the catalytic blocks based on the carriers with a cell density typical for the compression-ignition engines of 200 cpsi (fig. 6). The application of the catalytic carriers with higher cell densities was considered inadvisable because of a high resistance of flow of exhaust gases intensified by the PM emission.

The operation performance of the catalytic converter with the 200 cpsi carrier is similar in each phase of the test (fig. 7). In phases II-XIII the catalytic converter was characterized by an effectiveness of the reduction in the NO_x emission of 15%. The analysis of the measuring points shows that from the point c3 on the reduction in the NO_x emission level was constant. That means that the catalytic reactor volume is sufficient with reference to the assumed amount of the active layer deposited on each catalytic block. The ratio of that volume to the engine displacement volume was 0.76. The analysis of the bibliographic data shows that this ratio values are in the 0.75-1.3.range.

Fig. 6. Metallic enclosure of tested catalytic converter [3]

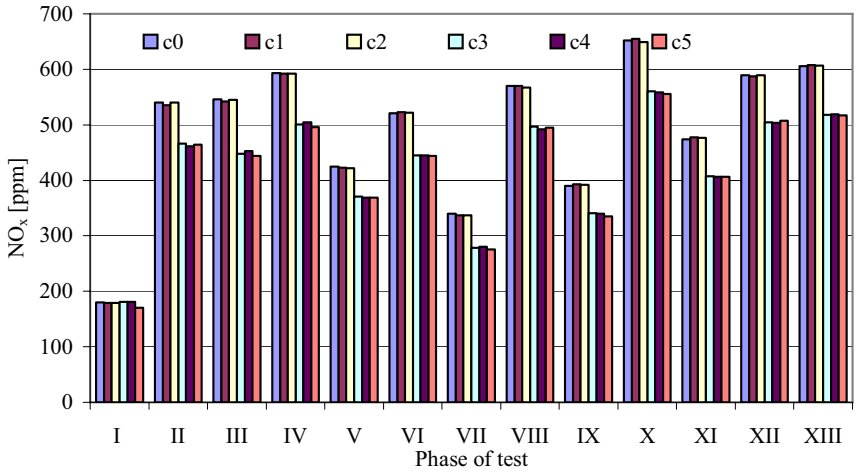

Fig. 7. *Value of NO_x concentration during ESC test of catalytically converter with 200 cpsi [3]*

The emission measurements in points *c6–c8* are considered close to the emission measured in the point *c5*. For the discussed points the difference in the NO_x concentration was at the indication error level of the measuring exhaust gas analyser.

The performed analysis shows that the catalytic converter with the 200 cpsi carrier allows to obtain a satisfactory difference in the voltage signals basing on the NO_x concentration after the third catalytic block. However, it should be noted that the obtained effectiveness of the catalytic converter for the NO_x reduction is unsatisfactory. The average percentage effectiveness of the discussed catalytic converter in the measuring point c5 was 14% (table 1).

Table 1. *Efficiency of limit NO_x concentration [%] behind ever catalytically blocks in light of concentration before catalytically converter (200 cpsi) [3]*

No phase	I	II	III	IV	V	VI	VII	VIII	IX	X	XI	XII	XIII
Point c1	0,3	0,8	0,1	-0,3	2	0,3	-1	1	0,3	-10	0,3	10	0,3
Point c2	0,4	-0,1	-0,5	-0,3	2	0,4	-1	1	0,4	-9	0,4	10	0,4
Point c3	-0,8	13	17	15	14	15	16	14	13	5	15	23	14
Point c4	-0,8	14	16	14	15	15	16	14	13	6	15	23	14
Point c5	5	14	18	16	15	15	17	14	15	6	15	22	15

Conclusions

On the basis of the performed examinations and obtained test results the following conclusions can be drawn:

1. The analysis of the NO_x concentrations in exhaust gas from the compression-ignition engine can be based on the indications of the voltage probes with the modified electrodes of the oxygen pump;
2. The application of the reduction conditions in the voltage probes using the nitrogen oxides reduction by the electro-catalytic way depends on the exhaust gas parameters, the values of which change depending on the rotational crankshaft speed and engine load. For this reason obtaining the diagnostic signal for the whole engine operation range is impossible. The control of the correctness of the catalyst operation regarding the nitrogen oxides reduction can be realised for the defined operating parameters of the tested engine;
3. For phases VIII and X of the ESC test the reheating the test probe installed before the catalyst was unnecessary owing to the high exhaust gas temperature (737–759^{o}C).

References

[1] Merkisz, J., Mazurek, S., *Pokładowe systemy diagnostyczne pojazdów samochodowych*; WKiŁ, Warszawa, 2002.

[2] Merkisz, J., Rychter, M., *Monitorowanie sprawności reaktora katalitycznego pod kątem diagnostyki pokładowej EOBD II*, Warszawa, Kones, 2002.

[3] Rychter, M., *Monitorowanie silnika o zapłonie samoczynnym w systemie OBD na podstawie emisji spalin w kontekście poprawy właściwości ekologicznych silnika*, Rozprawa doktorska, Politechnika Poznańska, Poznań, 2004.

[4] Rychter, M.: *Analiza warunków panujących w układzie wylotowym silnika o ZS w aspekcie zastosowania sond pomiarowych określających stężenie NO_x*, Transport Samochodowy 1/2006, str. 53–73, 2006.

[5] Rychter, M.: *Wykorzystanie przewodników jonowych w budowie czujników stężenia składników gazów wylotowych w celu monitorowania reaktora katalitycznego w silnikach o ZS w aspekcie systemu OBD II/EOBD*, Kongres PTNSS, 25–28.09.2005,Szczyrk, Polska, CD-R, 2005.

Abbreviations

cpsi	*cells per square inch*
EOBD	*European On Board Diagnostic*
ESC	*European Stationary Cycle*
NO_x	*Nitrogen oxides*
OBD II	*On Board Diagnostic II*
OBD	*On Board Diagnostic*
OBDE	*On Board Diagnostic Efficiency*
USPD	*Ultra Spray Pyrolysis Deposition*

OPERATIONAL AVAILABILITY OF THE TECHNICAL OBJECT

Sergiusz Szawłowski

Polish Navy HQ - Logistics
ul. Pułaskiego 7, 81-912 Gdynia, Poland
tel.: +48 58 263428, fax: +48 58 263167
e-mail: sergszaw@mw.mil.pl

Jan Borgoń

Air Force Institute of Technology
ul. Księcia Bolesława 6, 01-494 Warsaw, Poland

Sylwester Gładyś

Warsaw University of Technology
Plac Politechniki 1, 00-661 Warsaw, Poland

Abstract

The most important issue for each system is its effectiveness E_f, which depends on reliability, availability and maintainability (RAM). The operational availability (A_o) even for mature systems usually has large improvement capabilities. One of the most critical parameter of A_o is ALDT (Administrative and Logistic Delay Time). The article presents most important aspects of operational availability, taking into account the helicopter operating from frigate as the object for analyzing. In spite of the fact that such helicopter is specific, the presented topic is common, and useful for each system, including ship propulsion system, its accessories and their reliability.

Keywords: *reliability, technical object availability, operational availability*

1. Introduction

The goal of each system designer is that his or her system will perform its functions in any conditions, independently to any kind and intensiveness of any impact of inner and outer factors. The real world with practical conditions of system working guarantee that the system will meet problems in the future, hard to predict during design process, which could disturb or even stop its work eventually. The question is: how prepare the system to protect it from disturbances.

The effectiveness measure of the system is the probability performing the job by the system successfully. This is presented by below equation:

$$E_f = R \cdot G \cdot O \tag{1}$$

where:

E_f - probability that the system will perform the mission successfully;
R - probability that the system will perform its intended functions for a specified intervals,
G - probability that the system will be available to perform its intended functions in required time,
O- probability that the system will be suitable for its intended functions and specified conditions.

Each of the elements mentioned above has crucial importance for entire system performance.

This paper is focused on readiness, or more precisely, on operational availability (A_o) of the technical object – the item (TO), which could represent any object or system, including propulsion system, single engine, and its accessories.

The maritime helicopter performing its missions from middle class ship has been chosen as the object for the analysis. Despite to its specific functions and missions, it could be good example to present the A_o and the way for modeling its value.

2. Technical object (TO) availability index

One of the most important parameters of the maintenance of the TO is its availability.
Availability is a function which characterizes its ability to start to perform specified task(s), in specified conditions just after, or previously determined time after, when it is called.
The measure of the availability is „K" index, which determines the probability of the event, that the item will be at UP state at random moment of time [18].

$$K_g = \frac{E(T_k`)}{E(T_k`) + E(T_n)} \tag{2}$$

where:

$T_k`$ – random variable- determining UP time of the item between failures,
T_n – random variable- determining the time of the repair.

Practically in most cases we use simplified relation, which describes steady value of K - index, assuming that the time of using (operating) and the time of recovery have both exponential distribution..

$$K_g = \frac{MTBF}{MTBF + MTTR} \tag{3}$$

where:

MTBF – Mean Time Between Failure,
MTTR – Mean Time to Repair.

All military forces maintain the enormous number of systems, which are to be used when it is needed, so they must have high level of availability.
The availability of systems is widely described in NATO and US Department of Defense standardization documents: [10, 11, 12, 13, 14, 17].

There are few availability indexes:
A_i – (Inherent Availability) - (designed),
A_a – (Achieved Availability) - (technological),
A_o – (Operational Availability) - (practical).

The equation (3) for K_g index is true as well as for A_i index - inherent availability

$$A_i = \frac{MTBF}{MTBF + MTTR} \tag{4}$$

The A_i is calculated during design process (it includes reliability parameter - MTBF and connected with it the time of repair - MTTR). This shows that A_i does not include all parameters which are met during real operation conditions of TO. Specially it does not include the time which is necessary to perform preventive or any scheduled maintenance and time for logistic system response.

Next index - A_a (availability achieved technologically) includes preventive maintenance already but still ignores the delay of the logistic system.

$$A_a = \frac{MTBM}{MTBM + MMT} \tag{5}$$

where:

MTBM - Mean Time Between Maintenance on the object,
MMT - Mean Maintenance Time on the object.

In the real operation the most important is the real level of availability of TO, which is described by operational availability A_o. This index includes all real time factors, which have impact on availability of the item (TO).

The general relation for A_o is:

$$A_o = \frac{Tup}{Tup + Tdown} \tag{6}$$

where:

T_{up} – Up time of the object
T_{down} - Down time of the object
Up time – time that the item is in the customer's possession and works
Down time – total time that the item is not operable / not usable
The sum of times: T_{up} and T_{down} – gives us the TT (Total time of considered item operation period).

US Navy [17] definition for operational availability (A_o): probability that the system will be ready to perform its specified function, in its specified and intended operational environment, when called for at a random point in time.

$$A_o = \frac{MTBM}{MTBM + MMT + MLDT} \tag{7}$$

where:

MTBM – Mean Time Between Maintenance,
MMT – Mean Maintenance Time (for all type of maintenance: preventive-scheduled, corrective – non scheduled),
MLDT - Mean Logistic Delay Time.
A_o is determined by reliability (MTBM), maintainability (MMT) and supportability (MLDT – Mean Logistic Delay Time).

Slice different definition of operational availability is presented in the NATO standard document [11]: the probability that an equipment / system at any instant in the required operating time will operate satisfactorily under stated conditions where the time considered includes: operating, corrective and preventive maintenance, administrative delay time and logistic delay time.

I order to be closer a little bit to the real conditions of item operation, for more precise determination of Ao, is easier to apply below relation:

$$A_o = \frac{OT + ST}{OT + ST + TPM + TCM + ALDT} \tag{8}$$

where:

OT - Operating Time,
ST - Standby Time,

TPM - Total Preventive Time,
TCM - Total Corrective Time,
ALDT - Administrative and Logistic Delay Time.

TPM – dependent on the item maintenance system, item maintainability, personnel skill level, maintenance material package – taken with the item for operation period, properly calculated for range and depth,
TCM – dependent on the item reparability, spare parts package properly calculated for range and depth and support equipment (SE) set all taken with the item (i.e helicopter spares and SE stored on the ship), skills of maintenance personnel, availability of additional (non organic for item) repair facility, etc.

There is unbroken link between TCM and ADLT, because in most cases the logistic system is alerted and run when the item failure occurred and the spares or material package does not cover the needed material, or there is no proper specialist, or equipment or data on hand to perform the Corrective Maintenance.

$$ALDT(wg.NATO) \equiv MLDT(wg.USNavy) \tag{9}$$

ALDT includes:
MSRT - Mean Supply Response Time,
$M_{adm}DT$ - Mean Administrative Delay Time) – for obtaining necessary data, publications, documents, special support equipment, personnel, training.

I would like to focus your attention on the fact, that among of these three measures: TPM, TCM, ADLT, which determine the Time UP, the ADLT measure has definitely the most significant impact on A_o value, because it dominates the others. The estimated range of ALDT is from several to hundreds of hours, or even (but very rarely) up to few thousand of hours.

3. Shipboard helicopter

In order to fulfill the requirement of the contemporary maritime operation theatre the shipboard helicopter is operationally integrated with the ship weapon system. Thanks to this the helicopter increases the offensive and defensive capabilities of the ship. Practically it increases the chance of the ship to survive on the modern sea battle field.
For this paper the SH-2G type helicopter operating form the Oliver Hazard Perry class frigate was chosen as the object for the analysis.
The SH-2G Super Seasprite helicopter was designed according to US Navy LAMPS (Light Airborne Multi Purpose System) Mk. I concept [7]. The main goal of LAMPS is to increase the combat capability of the single ship by improving capabilities of her own helicopter.
According to LAMPS Mk. I the helicopter must be ready to perform following tasks:
1. primary missions:
   - ASW – Antisubmarine Warfare,
   - ASST - Anti-Ship Surveillance and Targeting)

Present conflicts for War on Terror have added to primary missions also the asymmetric missions – ship antiterrorist protection.
2. secondary mission:
   - VERTREP – Vertical Replenishment,
   - SAR - Search and Rescue,
   - MEDEVAC - Medical Evacuation,
   - COMREL – Communications Relay.

Additionally LAMPS required that the shipboard helicopter must have the HIFR (Helicopter In Flight Refueling) capability.

The operation of the maritime helicopters (performing tasks from costal bases or ships) is definitely more complicated than the land base helicopters operation, due to specific maritime weather conditions: increased level of humidity and salt of water and atmosphere, and rapid changes of the weather conditions (wind, fog, precipitation).
For the shipboard helicopters the above phenomena level are multiplied by open ocean conditions, and appears additional problems unique for maritime deployment.

4. Availability of helicopter on ship

Taking into account the equation (1), the operating model of aircraft (ME) could be presented in categories of probability [4, 5]:

$$ME(t,\tau,\theta) = R(t_o,\tau)\cdot G(t_o,t_1,\tau,\theta,ZL)\cdot O(\tau,\theta,ZL) \tag{10}$$

where:

ME - probability of performing the aviation task (ZL) at the operating model of aircraft,
R (t_o, τ) - reliability of aircraft,
G(t_o, t_1, τ, θ, ZL) - availability to perform the task ZL, after the θ time and maintained during the aircraft mission time - τ,
O (τ, θ, ZL) - suitability as function of technical means and measures necessary to perform the ZL task,
t - current time,
θ - time of achieving the availability G(θ), where $\theta = t_1 - t_o$,
τ - time of aircraft mission.

The above aircraft model which realizes the air task (ZL) could be presented on graphic form. Besides mentioned parameters as: availability (G), reliability (R) i suitability (O), the ME model considers such elements as: Flight Safety (BL), Durability (T_R), Survivalability (Ż), Maintainability (P_E) and Logistics (L).

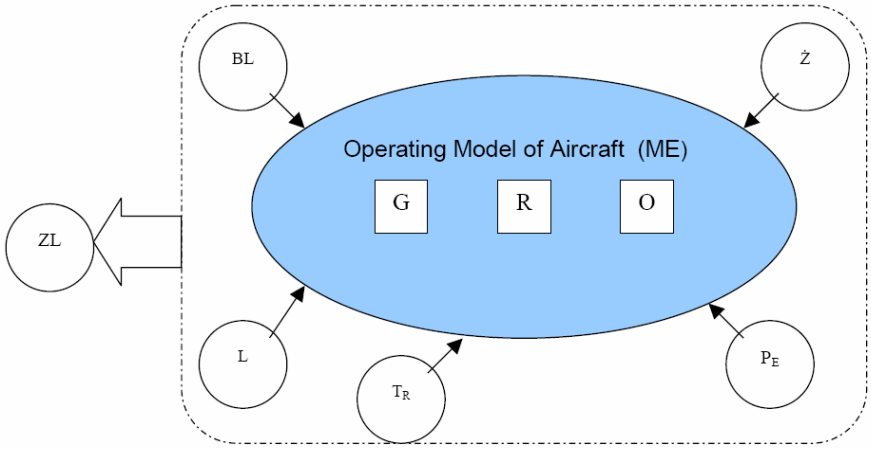

Fig.1 Operating Model of Aircraft conducting the Air Task

Based on above model, in similar way we can describe the Operating Model of Ship conducting the Sea Task (ZO).

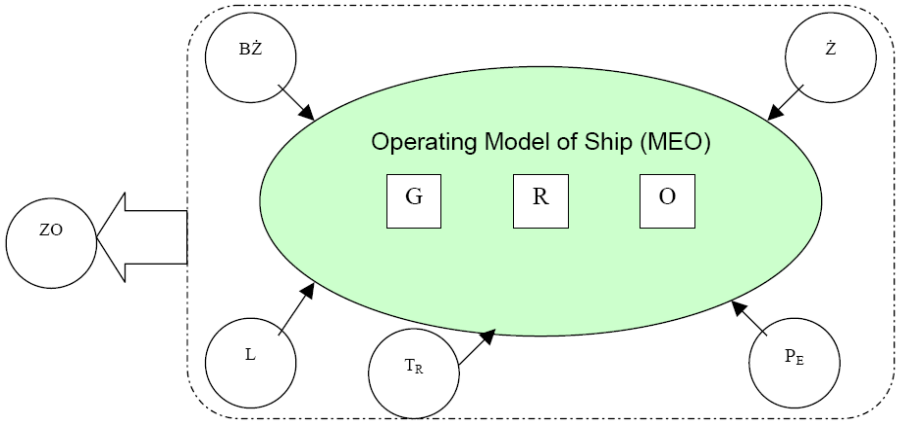

Fig 2. Operating Model of Ship conducting the Sea Task

The components of the MEO model depend on parameters of particular subsystems of the ship or those which have impact on the MEO. In spite of the fact that aviation detachment is onboard of the ship during the maritime mission, and it is integrated with ship weapon system, the Operating Model of Shipboard Helicopter (MEŚP) should be separated from Operating Model of the Ship (MEO) because of its specific operation, maintenance in reference to ships systems.

Having analyzed the MEŚP, we need to remember that Air Task (ZL) is subordinate to Sea Task (ZO) and that MEŚP and MEO models have close relationships in range of: availability, dependability and suitability. Moreover between these two models there is the a sphere, where MEŚP elements are included in MEO model structure as well. This is for instance: food, accommodation, medical assistance ship services and common supply channel of the logistic system. This intersection is eliminated when the helicopter performs the mission for non host ship (i.e. other ship from own Task Group).

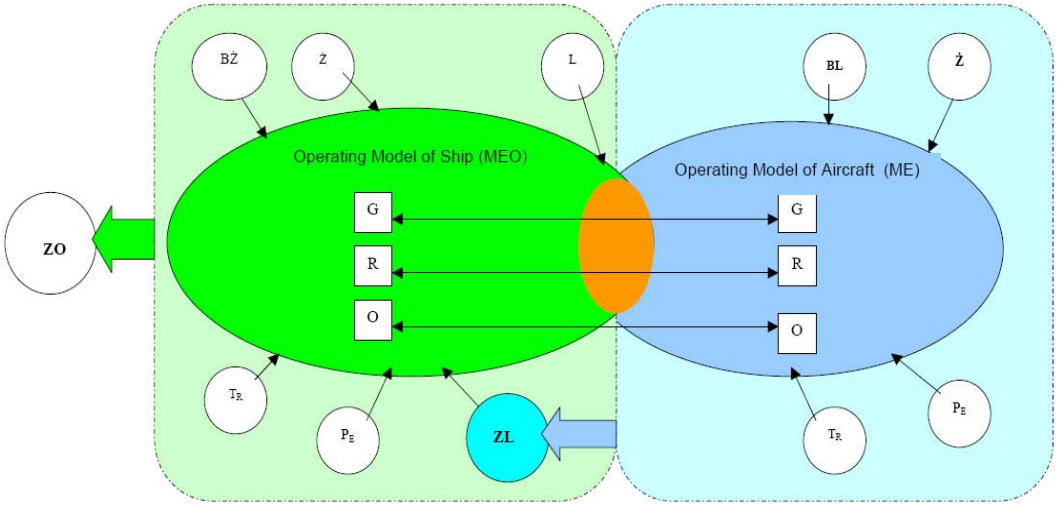

Fig 3. Operating Model of Deck Helicopter conducting the Air Task for home ship.

The set of factors having influence on helicopter maintenance process during deployment we can divide into 3 groups:

- I - requirements;
- II - limitations;
- III – operational – environmental conditions.

Group I - ship mission requirements for helicopter operations
Group II – set of limitations of the ship and helicopter (aviation detachment), which reflects the capability to fulfill the requirement of the Group I,
Group III -describes the outside conditions, which generally no ship, neither aviation detachment have influence on, but must be considered during the mission as well.
Group I requirements includes:

- the basic - priority of the ship mission,
- requirement of helicopter multipurpose usage (multipurpose missions),
- requirement of availability of the helicopter for the total time of the ship mission (deployment) readiness for 24 hours a day , 7 days a week,
- requirement of availability far away from home base and supply channels,
- requirement of all weather i climate conditions readiness,

Group II – limitations includes:

- ship class which determines her dimensions and autonomy:
    - limited dimensions of the landing deck on the ship,
    - limited maintenance and storage space,
    - limited accommodation and food services capabilities,
- capability of aircraft facility on the ship,
- ship repair shops capabilities,
- operational limitations of the helicopter:
    - frequency and duration of Preventive Maintenance (PM),
    - frequency and duration of Corrective Maintenance (CM),
    - limitation of available of flight hours (due to higher level of maintenance requirement or time components status)
    - limitation of performing the air mission (ZL) because of safety of helicopter operation (usage and maintenance)
- limited number of helicopter maintenance personnel embarked on ship,
- health limitation (psycho and physical) of the ship crew and aviation detachment,
- lack of the spare helicopter on the ship;
- limited access to spares and PM material, based on taken packages and effectiveness of supply channel of the logistic system,
- limitation of the logistic system (especially delay of it reaction).

Group III includes:

- region of operation (distance from home base and supply pipes),
- time of the mission (deployment),
- climate – weather conditions,
- composition and capabilities of the other ships of the Task Group,
- the goe – political conditions (peace, war),
- the combat capability of the enemy.

5. Conclusion

Presented above set of factors show us, how many elements have influence on keeping the helicopter on the ship during deployment time ready to use when it's needed. Because of limitations and parameters impact, there is no possibility to achieve the 100% of A_o for his helicopter during several months deployment. Based on experience of the US Navy and Doutche Marine the available asymptotic level of A_o (for 1 embarked helicopter) is 90%. Taking into

account presented before examples the biggest potential for improvement had Group II – limitations. Searching the better Ao we should focus the attention on ALDT parameter. Similar method for Ao improvement could be chosen for other than helicopter systems, for instance a ship and her subsystems.

This article shows that during analysis the effectiveness of any system, including ship propulsion system, there is necessary to deeply consider of the system availability, which is modeling by both: its subsystems and outside parameters.

References

[1] Borgoń, J., Szawłowski, S., *Eksploatacja śmigłowca na okręcie*, V Międzynarodowa Konferencja „Perspektywy i rozwój systemów ratownictwa, bezpieczeństwa i obronności w XXI wieku" AMW Gdynia, 2005.

[2] Girtler, J., Kitowski, Z., Kuriata, A., *Bezpieczeństwo okrętu na morzu ujecie systemowe*, WKŁ, Warszawa, 1995.

[3] Konieczny, J., *Podstawy eksploatacji urządzeń,* Wydawnictwo MON, Warszawa, 1975.

[4] Lewitowicz, J., *Podstawy eksploatacji statków powietrznych. Cz.I Statek powietrzny i elementy teorii,* Wydawnictwo ITWL, Warszawa, 2001.

[5] Lewitowicz, J., Kustroń, K., *Podstawy eksploatacji statków powietrznych. Cz.II Własności i właściwości eksploatacyjne statku powietrznego,* Wydawnictwo ITWL, Warszawa, 2003.

[6] Olearczuk, E., Sikorski, M., Tomaszek, H., *Eksploatacja samolotów - elementy teorii* Wydawnictwo MON, Warszawa, 1978.

[7] Szawłowski, S., *Śmigłowiec pokładowy SH-2G jako element systemu uzbrojenia okręt,* Materiały VI Forum Śmigłowcowego. Instytut Lotnictwa, Warszawa, 2006.

[8] Żurek, J., *Problemy gotowości techniki lotniczej,* Wydawnictwo ITWL, Warszawa, 1993.

[9] APP2/MPP2, *Helicopter Operations From Ships Other than Aircraft Carriers (HOSTAC*).

[10] ARMP-1, *NATO requirements for reliability and maintainability*.

[11] ARMP-4, *Guidance for writing NATO R&M requirements documents, 2003*.

[12] ARMP-7, *NATO R&M terminology applicable to ARMPs, 2001*.

[13] *DoD guide for achieving Reliability, Availability, and Maintainability (RAM),* 2005.

[14] DoD 3235.1-H, *Test & evaluation of system reliability, availability and maintainability. A primer. Director test and evaluation*.

[15] MIL-HDBK-338B, *Electronic reliability design handbook,* 1998.

[16] NWP 3-04.1M, „*Helicopter operating procedures for air – capable ships*.

[17] OPNAVINST 3000.12.A, *Operational Availability handbook,* Washington, 2003

[18] Polska Norma PN-77/N-04005, *Wskaźniki niezawodności. Nazwy, określenia i symbole*.

[19] Polska Norma PN-77/N-04010, *Wybór wskaźników niezawodności*.

[20] Polska Norma PN-90/04041/09 "*Zapewnienie niezawodności obiektów technicznych. Modele wzrostu niezawodności".*

[21] TM 5-698-1 "*Reliability / Availability of electrical & mechanical systems for command, control, communications, computer, intelligence, surveillance, and reconnaissance (C4ISR) facilities,* 2003.

[22] TM 5-698-2, *Reliability – Centered Maintenance (RCM) - for command, control*, *communications, computer, intelligence, surveillance, and reconnaissance facilities*, 2003.

[23] Norma Obronna NO-07-A025 „*Wspólne działanie okrętów i lotnictwa,*2002.

[24] DMW, *Tymczasowa instrukcja wykonywania operacji lotniczych z pokładów fregat*, Gdynia, 2003.

[25] DMW, *Tymczasowa instrukcja przemieszczania oraz kotwiczenia śmigłowca SH-2G na pokładzie okrętu*, Gdynia, 2003.

INFLUANCE OF CHANGES OF AXIAL COMPRESSOR VARIABLE STATOR VANES SETTING ON GAS TURBINE ENGINE WORK

Paweł Wirkowski

The Polish Naval Academy
ul. Śmidowicza 69, 81-103 Gdynia, Poland
tel.: +48 58 6262756, fax: +48 58 6262963
e-mail: pawir@o2.pl, p.wirkowski@amw.gdynia.pl

Abstract

The paper deals with problem influence of changes settings variable stator vanes axial compressor of gas turbine engine on work parameters of compressor and engine. Incorrect operation of change setting system of variable vaness could make unstable work of compressor and engine. This situation is unacceptable because of mechanical overloads which could demage the engine. This paper presents theoretical analysis of situation described above and presents results of own researches done on real engine.

Keywords: *gas turbine engine, axial compressor, variable stator vanes*

Parameters, abbreviations and subscripts:

α_1	- air stream outlet angle with stator vanes,
α_{KW}	- setting angle of variable stator vanes,
β_1, β_2	- air stream inlet and outlet angles in rotor vanes,
c_a	- axial component of air stream absolute speed,
c_{1a}	- axial component of air stream absolute speed on rotor blades inlet,
$c_{1a\,cal}$	- calculating value axial component of air stream absolute speed on rotor blades inlet,
CCS	- space between high pressure compressor and combustor,
CS	- space between low pressure compressor and high pressure compressor,
CO	- combustor,
HPC	- high pessure compressor,
HPT	- high pressure turbine,
η^*_S	- compressor efficiency,
i	- air stream inlet angle on rotor blades,
LPC	- low pressure compressor,
LPT	- low pressure turbine,
LPTPTS	- space between low pressure turbine and power turbine,
$\dot{m}$	- air mass flow,
n	- compresssor rotor speed,
p_{fuel}	- fuel pressure,
P_{nom}	- nominal engine power,
π^*_S	- compression ratio,
TS	- space between high pressure turbine and low pressure turbine,
u	- circumferential speed,
w_1, w_2	- air stream relative speed on inlet and outlet rotor blades,
Δw_u	- air stream whirl in rotor,
z	- number of inlet guide stator vanes,

1. Introduction

A compressor is a part of gas turbine engine especially sensitive on change their technical state during operation process. Polluted atmospheric air flowing in compressor caused permanent change of interblades ducts shape, rise of blades surface roughness and change of compressor rotor mass. It exerts an important influance on compressor stable work, change their characteristic and engine performance and efficiency. In compressor construction is assembled system of setting change of variable stator vanes its task is made optimal cooperation engine units during permanent improvement of compressor characteristic. Perturbations in operation of this system could cause changes in work of compressor and engine similar like changes of rotational speed or polluted interblades ducts of compressor.

2. Purpouse of researches

Purpouse of investigations made on real engine was determination influance of incorect operation of axial compressor inlet guide variable stator vanes control system of gas turbine engine on parameters of compressor and engine work.

Compressor characteristic is relationship between compression ratio π^*_S, compressor efficiency η_S and air flow mass $\dot{m}$ and compressor rotational speed n. It makes possible to determine the best condition of compressor and another engine units mating. Characteristic is using to select optimal conditions of air flow regulation and assessment of operational factors on compressor parametres.

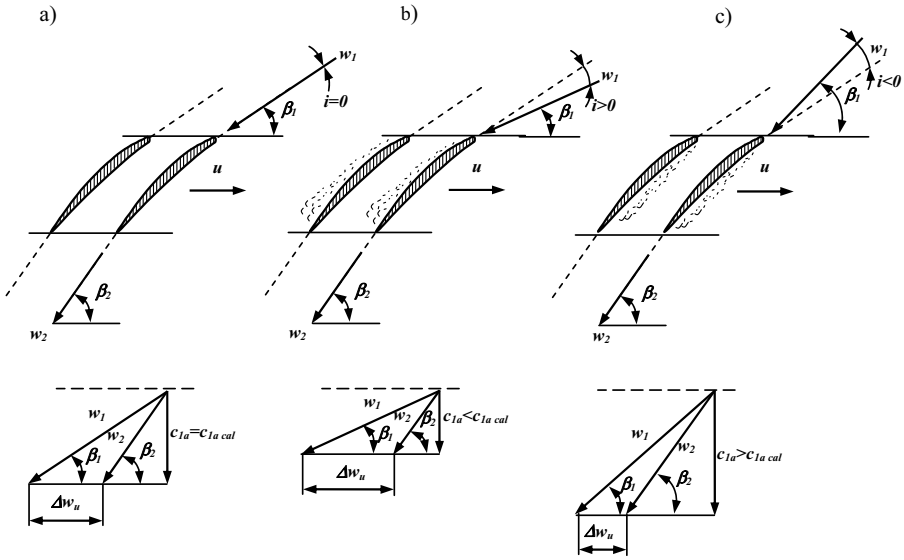

Fig. 1. Schema of flow round of axial compressor rotor blades during constant rotor speed and variable air stream inlet angles: a) calculating inlet angle, b) positive inlet angle, c) negative inlet angle

Compressor unstable work is explained on Fig. 1. This Fig. presents schema of flow round of axial stage compressor rotor blade which is moving with constant rotational speed n. For this stage is made change of air flow intensity $\dot{m}$. Fig. 1a presents schema of flow round for optimal stage efficiency. Relative speed vectors w_1 and w_2 have parallel direction to center line of blade profile. It causes laminar flow of air stream in interblades ducts. Decrease of air flow intensity (Fig. 1b) for constant circumferential speed u causes decrease axial component of air stream absolute speed c_a.

It takes effect increase of air stream inlet angle *i* on rotor blades. This situations favours tearing off laminary boundary layer on convex blades surfaces and forming vortex regions.

Similar effect takes place on concave blades surfaces (Fig. 1c) when air flow intensity $\dot{m}$ increases during constant circumferential speed *u*.

For critical values of air stream inlet angle *i* by formated vortex regions of lower pressure, can occure air stream back off in inlet compressor direction. It could cause rapid rise of stream fluctuations transmited on engine construction. This situation is undesirable and dengerous on account of mechanical and thermal overload of engine construction [2].

Therefore compressor should be so controlled in operational range of rotational speed that the compressor and engine mating line has a stock of stable work. The main rule of compressor control during change of their rotational speed or flow intensity is to keep up the stream inlet angles *i* values near zero. One of the most popular ways of axial compressor control is changing their flow duct geometry by application of inlet guide stator vanes or variable stator vanes of several first compressor stages [2].

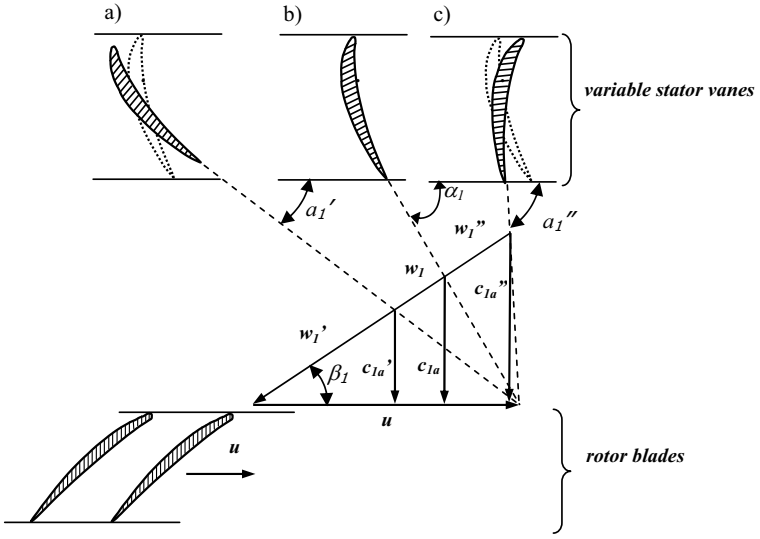

Fig. 2. Axial compressor stage control by change of setting angle of stator vanes during changing speed of flow stream: decreasing axial speed, b) calculating axial speed, c) increasing axial speed

This solution makes possibile to change of air stream inlet angle on rotor baldes of compressor stages by change of stator vanes setting angles during change of compressor rotational speed. Fig. 2 illustrates, on example one stage of compression, rule of regulation of variable stator vanes.

For average values of operational range of compressor rotor speed is situation on Fig. 2b – speed values and directions with subscript *1*. In this situation is intermediate angle setting of stator vanes. Air stream inlet angle on rotor blades do not cause disturbance of stream flow by interblades ducts. For lower values of compressor rotor speed and in consequence lower values of absolute axial component speed c_{1a}', it is necessary to reduce the stream outlet angle of variable stator vanes α_1 (Fig. 2a). The angle reduction range should allow keeping the same value of stream inlet angle on rotor blades. Analogical situation takes place during work of compressor with higher rotational speed. For higher rotational speed absolute axial component speed c_{1a}'' increases. In this situation for keeping stable work of compressor and in consequence constant value of stream inlet angle on rotor blades, it is necessary to increase the stream outlet angle of variable stator vanes – Fig. 2c.

Application in gas turbine engine construction of control system of flow ducts geometry has a bearing on run of unstable processes [3].

3. Object and course of researches

The object of researches is type DR 77 marine gas turbine engine. It is three-shafts engine with can-ring-type combustor chamber and reversible power turbine. Fig. 3 illustrates block diagram of DR gas turbine engine with marked control sections of flow duct and measuring parameters.

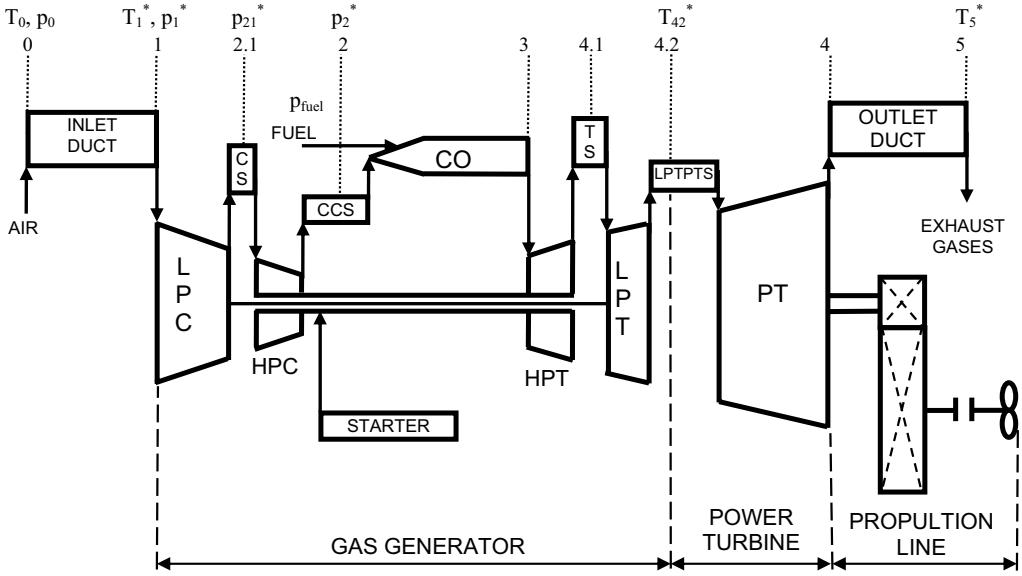

Fig. 3. Block diagram of DR gas turbine engine

In compressor construction configuration of this engine there are used inlet guide stator vanes which make possibilities to change setting angle incidance (change of compressor flow duct geometry) in depend on engine load. This process is operated by control system which working medium is compressed air received from last stage of high pressure compressor. On Fig. 4 are presented elements of control system of variable stator vanes.

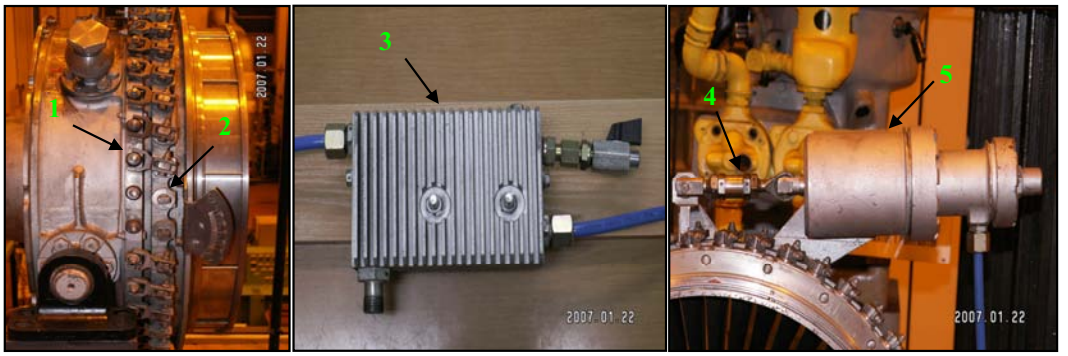

Fig. 4. Elements of control system of variable stator vanes DR type engine
1 – moving ring, 2 – stator vane, 3 – cleaning and cooling block, 4 – strand, 5 – control actuator

Block diagram of flow control signal is presented on Fig. 5. Compressed air from last stage of high pressure compressor is supllied to working space of control actuator by cleaning and cooling block. Compressed air exerts pressure on control actuator elements. It causes moving of control piston which is connected with moving ring. This ring moves on circumference of compressor body. Ring is connected with stator vanes by levers. When the ring is moving stator vanes realize rotational motion changing the air stream outlet angle α_1.

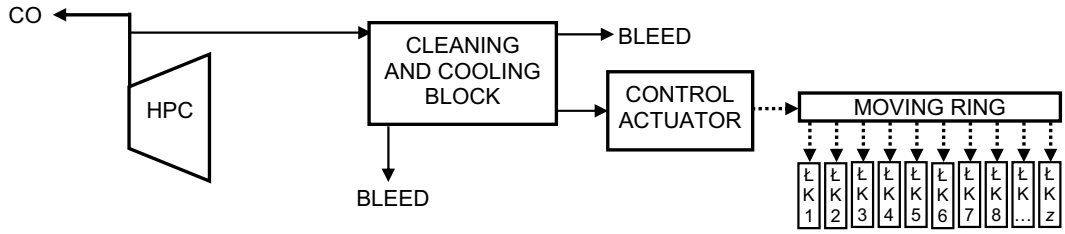

Fig. 5. Block diagram of stator vanes change setting mechanism;
CO – combustor, HPC – high pressure compressor, ŁK – variable stator vane

In cleaning and cooling block are holes. During researches air stream was bleeded by holes and less air was supplied to actuatir. It caused change of setting angle α_{KW} of variable stator vanes and in consequence of that change of flow duct geometry.

Experiment was carry out an engine load $0{,}5P_{nom}$. For this load setting angle α_{KW} of variable vanes takes value - 4^o. During change engine load in whole range from idle to full load setting angle α_{KW} of variable vanes changes in range from -18^o to $+ 18^o$. Realizing experiment a few parameters of engine work was measured and registered for three different setting angle α_{KW} of variable vanes: A —α_{KW} = - 4^o, B —α_{KW} = - 11^o, C —α_{KW} = - 18^o. Tab. 1 presents measured and registered parameters of engine work.

Tab. 1. Parameters of engine DR work measured during researches

Parameter	Measurement range	Parameter name
n_{LPC}	0 ÷ 20000 [min^{-1}]	low pressure rotor speed
n_{HPC}	0 ÷ 22000 [min^{-1}]	high pressure rotor speed
n_{PT}	0 ÷ 10000 [min^{-1}]	power turbine rotor speed
p_1	-0,04 ÷ 0 [MPa]	subatmospheric pressure on compressor inlet
p_{21}	0 ÷ 0,6 [MPa]	air pressure on low pressure compressor outlet
p_2	0 ÷ 1,6 [MPa]	air pressure on high pressure compressor outlet
p_p	0 ÷ 10,0 [MPa]	fuel pressure before injectors
T_1	-203 ÷ 453 [K]	air temperature on compressor inlet
T_{42}	273 ÷ 1273 [K]	exhaust gases temperature on inlet power turbine

4. Results of researches

Fig. 6 presents results of experiment. Prameters are depend on time of mesure and setting angle of variable stator vanes. On Fig. 6 are presented those parameters which are the most sesitive on change of vanes setting angle. Change vanes setting from position A to position C caused increase air flow resistance by stator vanes. In consequence of that subatmospheric pressure on compressor inlet p_1 decreases (Fig. 6c). It causes pressure decrease in next parts of compressor and engine flow duct (rys. 6de). In this way reduced air density flowing by compressor, for stable quantity of stream fule supllied to combustor, causes increase of compressors rotor speed. The most visible

is increase of low pressure compressor rotor speed (rys. 6a) caused by directly influence on this compressor incorectly setting variable stator vanes. Range of change this parameter is above 2% value of rotational speed for undisturbed angle setting of vanes.

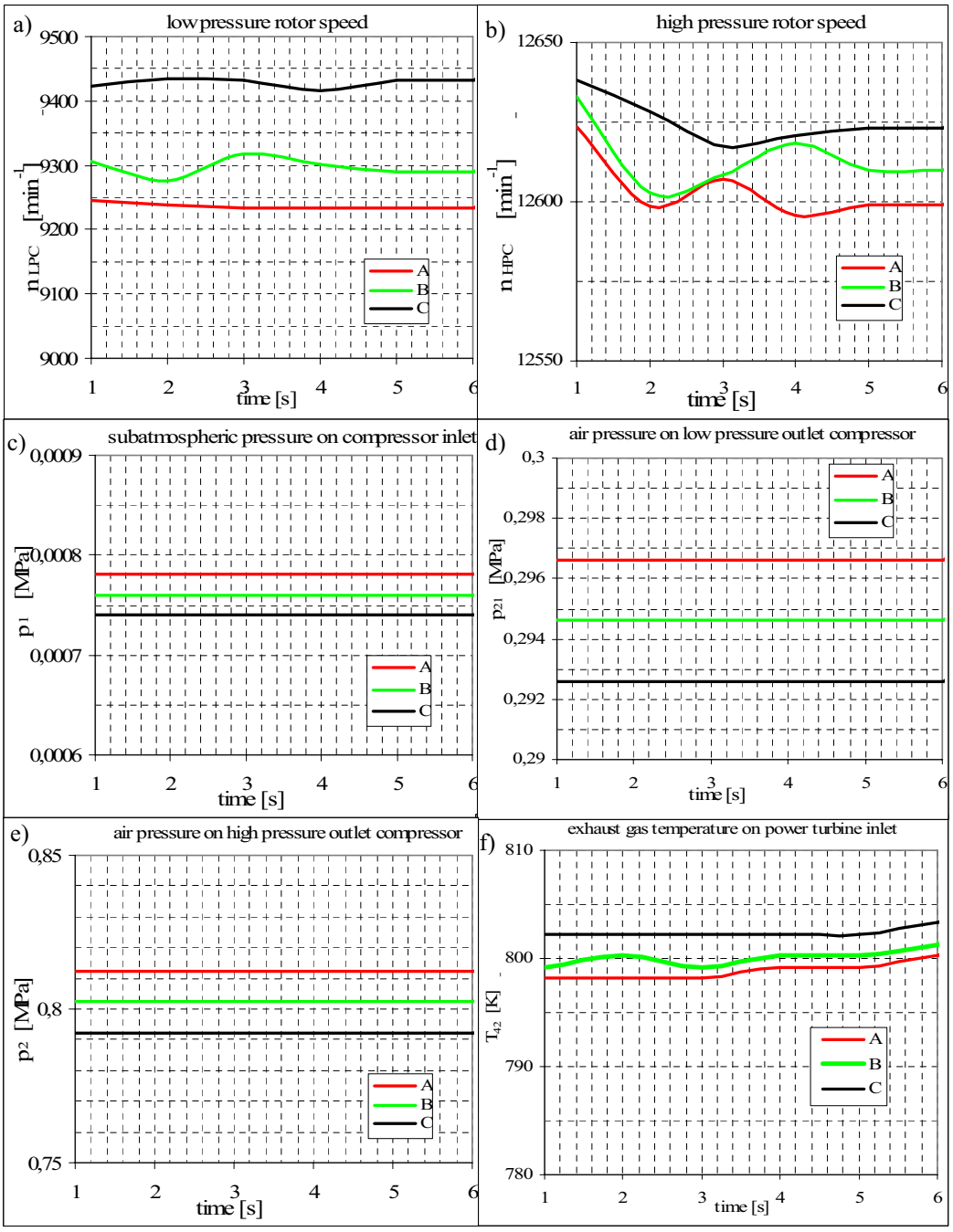

Fig. 6. Change of engine DR work parameters in function of variable inlet guide stator vanes setting angle:
A — α_{KW} = - 4°, B — α_{KW} = - 11°, C — α_{KW} = - 18°

Gasodynamical conection between low pressure compressor and high pressure compressor absorbs disturbances work of low pressure compressor which are transferred on high pressure compressor. Therefore range of change high pressure compressor rotor speed is lower than low pressure compressor. In this experimental it is below 1% and it is in measuring error of sensor range.

Change of subatmospheric pressure is above 5% undisturbed value of this parameter. Changes of low and high pressure compressor outlet presure are adecuately above 1,3% and above 2,4% undisturbed value of angle setting α_{KW} = - 4°.

Changes of pressure and air mass flow intensity values accompanied disturbing work of compressor, during constant fuel mas flow intensity in combustor, caused enrichment of fuel mixture. As a result of that, temperature combustor outlet gases increases. In experiment was confirmed tendency changes of gases tempertaure values even though range of thoses changes is in measuring error of sensor range.

5. Conclusions

On the base realised theoretical consideration and experimental researches we can draw a conclusion that incorrect operation of control system of inlet guide variable stator vanes or first stages stators vanes gas turbine engine compressor exerts negative influence on compressor work and engine performances.

Multi-shaft construction of gas turbine engine reduces effects of incorrectly setting of variable vanes. Therefore compressors of three-shaft gas turbine engine do not require variable stators vanes as many stages as compressor of two-shaft engine with the same achivements.

Preliminary researches confirme necessity for making inspection of correct operation of variable stator vanes system control. It makes possibility of elimination this factor from group of factors informing about technical state of engine which are identified during diagnostic inspections.

References

[1] Balicki, Wł., Szczeciński, St., *Diagnozowanie lotniczych silników turbinowych*, Wydawnictwo Biblioteka Naukowa Instytutu Lotnictwa, Warszawa 1997.

[2] Dżygadło, Z., *Napędy Lotnicze. Zespoły wirnikowe silników turbinowych*, Wydawnictwa Komunikacji i Łączności, Warszawa 1982.

[3] Korczewski, Z., *Identyfikacja procesów gazodynamicznych w zespole sprężarkowym okrętowego turbinowego silnika spalinowego dla potrzeb diagnostyki*, AMW, Rozprawa habilitacyjna, Gdynia 1998.

[4] Korczewski, Z., Wirkowski, P., *Modelling gasodynamic processes within turbine engines' compressors equipped with variable geometry of flow duct*, IV International Scientifically-Technical Conference "Explo-Diesel & Gas Turbine '05", Gdańsk-Międzyzdroje-Kopenhaga, Wyd. Politechnika Gdańska, str. 227÷236, Gdańsk 2005.

[5] Marschal, D.J., Muir, D.E., Saravanamuttoo, H.I.H., *Health Monitoring of Variable Geometry Gas Turbines for the Canadian Navy*, The American Society of Mechanical Engineers 345 E, 47 St., New York, N.Y.10017.

A METHOD TO DETERMINE FUNCTIONAL AVAILABILITY OF TECHNICAL OBJECTS

Józef Żurek [1], Jarosław Ziółkowski [2]

[1] *Instytut Techniczny Wojsk Lotniczych*
(Air Force Institute of Technology)
skr. poczt. 96, ul. Księcia Bolesława 6, 01-494 Warszawa, Poland
tel.: +48 22 6852173, fax: +48 22 6852163,
e-mail: jozef.zurek@itwl.pl

[2] *Wojskowa Akademia Techniczna*
(Military University of Technology)

Abstract

The intended aim of the paper is to present a problem of reaching engineering maturity by a technical object being introduced into service and designed for emergency activities. These are objects and systems associated with those of basic performance. Failures to the latter ones are hazardous to safety. Models of availability analysis, in particular of servicing by teams of specialists have been based on the theory of Markov/semi-Markov processes. The method of analysis has been introduced using a ship-helicopter as an example.

Keywords: *maritime systems, safety, reliability, maintenance, service*

1. Introduction

The question of reaching engineering maturity of objects newly introduced into service usually consists in coming up to the nominal level of availability, starting however from the underrated one.

The underrated level of availability results from both higher failure rate and longer servicing and repair times throughout initial stage of operational phase. From this standpoint, particular attention should be paid to emergency/rescue vehicles. Any ship-helicopter exemplifies such objects.

When consideration is given to such technical objects, prior to formulating a model of availability estimation, some simplifying assumptions should be made:

- all transitions from the state $i \in E$ to the state $j \in E$ show discrete nature (are described with a discrete random variable),
- mean time of the object's staying in the state *'i'* before transition thereof to the state *'j'* is described with a random number or function,
- both operational states $S = \{1, 2 \ldots r\}$ and duration thereof t_{ij} are mutually independent, i.e. they cannot occur simultaneously,
- all possible transitions can be described with an operation/maintenance graph that does not change its form throughout the time of examining the problem, i.e. T_0.

If the operational phase of these objects satisfies all the above-mentioned assumptions, a model of a Markov/semi-Markov process of some finite number of states can prove a proper analytical model.

2. A model to calculate functional availability of technical objects

2.1. Determination of boundary probabilities for the Markov chain

On the grounds of analyses of the operational phase of any technical object that performs indivisible tasks (sea voyages, flights) within emergency and rescue systems it has been found that such an object can remain in one of the following states:
S_1 – being on duty (waiting for a task),
S_2 – operating, and
S_3 – emergency object under refurbishment (becoming replaced with a capable one).

Furthermore, the following assumptions have been made to formulate a mathematical model of the operational phase from the point of view of availability analysis:

- any technical object can remain at any time instance in only one of possible states,
- in the course of performing tasks, the objects fail at random time instances,
- time needed for the object's refurbishment (replacement with a capable one) is strictly determined,
- duration of the process T_0 has been pre-set.

A diagraph representing the operational process (Fig. 1) is a representation thereof. There are interrelations between all the states (they 'communicate' with each other), thus generating a reducable chain [3, 4].

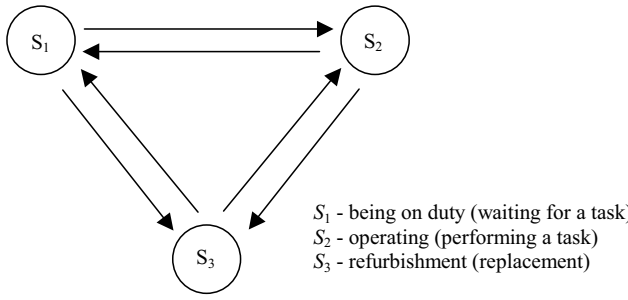

Fig. 1. A graph illustrating the technical object's operation

Presented in Fig. 1 is a 3 x 3 square matrix of transitions of the process; all transitions from the state *'i'* to the state *'j'* are possible for this matrix:

$$M_1=[p_{ij}]_{3x3} = \begin{bmatrix} 0 & p_{12} & p_{13} \\ p_{21} & 0 & p_{23} \\ p_{31} & p_{32} & 0 \end{bmatrix}. \tag{1}$$

Ergodic probabilities p_j can be calculated from the boundary of the matrix of transition in n steps $M_n = M_1^n$ by means of solving either a system of linear equations or an equivalent matrix equation [3]:

$$\underset{j}{\wedge} p_j = \lim_{n\to\infty} p_{ij}(n) = \sum_i p_i p_{ij} \Leftrightarrow M_1^T \left[p_j\right] = \left[p_j\right], \text{ when } \sum_j p_j = 1, \tag{2}$$

where:

M_1^T - transpose of the transition matrix M_1,
p_j - boundary probability,
p_{ij} - probability of transition from state 'i' to state 'j'.

$$M_1^T(p_{ij}) = \begin{bmatrix} 0 & p_{21} & p_{31} \\ p_{12} & 0 & p_{32} \\ p_{13} & p_{23} & 0 \end{bmatrix}. \tag{3}$$

According to both the relationship $M_1^T \cdot [p_j] = [p_j]$ and the normalisation condition $\sum_j p_j = 1$, in the matrix notation the boundary (ergodic) probabilities p_j are calculated according to (4) and the system-normalisation condition (5):

$$M_1^T(p_{ij}) = \begin{bmatrix} 0 & p_{21} & p_{31} \\ p_{12} & 0 & p_{32} \\ p_{13} & p_{23} & 0 \end{bmatrix} \cdot \begin{bmatrix} p_1 \\ p_2 \\ p_3 \end{bmatrix} = \begin{bmatrix} p_1 \\ p_2 \\ p_3 \end{bmatrix}, \tag{4}$$

$$\sum_{j=1}^{3} p_j = 1, \tag{5}$$

or as the forms of linear equations (6):

$$\begin{cases} p_{21} \cdot p_2 + p_{31} \cdot p_3 = p_1 \\ p_{12} \cdot p_1 + p_{32} \cdot p_3 = p_2 \\ p_{13} \cdot p_1 + p_{23} \cdot p_2 = p_3 \\ p_1 + p_2 + p_3 = 1 \end{cases}. \tag{6}$$

After having solved the system of equations (6), the following formulae to find boundary probabilities are arrived at:

$$p_1 = \left(\frac{1 - p_{12} \cdot p_{21} - p_{23} \cdot (p_{12} \cdot p_{31} + p_{32})}{(p_{12} \cdot p_{31} + p_{32}) \cdot p_{13}} \right) \cdot p_2, \tag{7}$$

$$p_2 = \frac{1}{1 + \dfrac{1 - p_{12} \cdot p_{21}}{p_{12} \cdot p_{31} + p_{32}} + \dfrac{1 - p_{12} \cdot p_{21} - p_{23}(p_{12} \cdot p_{31} + p_{32})}{(p_{12} \cdot p_{31} + p_{32}) \cdot p_{13}}}, \tag{8}$$

$$p_3 = \left(\frac{1 - p_{12} \cdot p_{21}}{p_{12} \cdot p_{31} + p_{32}} \right) \cdot p_2. \tag{9}$$

Table 1 gives estimates of probabilities p_{ij} that the object remains in a particular state found for a real operational process:

Tab.1. Probabilities p_{ij} that the object remains in particular operational states

$S_{i/j}$	S_1	S_2	S_3
S_1	0	0,91	0,09
S_2	0,95	0	0,05
S_3	0,5	0,5	0

After having substituted the assumed values of p_{ij} from Tab. 1 into eqs (7) – (9), the boundary probabilities for the Markov chain are arrived at (Fig. 2).

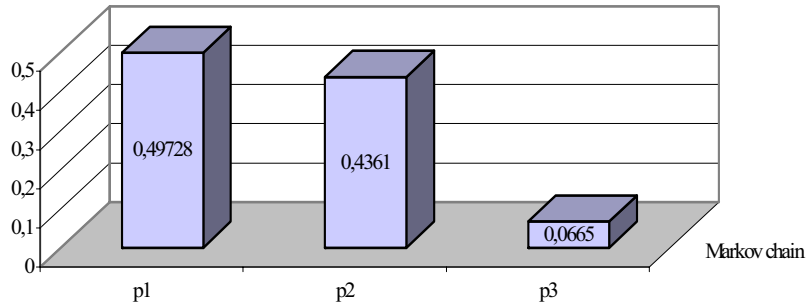

Fig. 2. Boundary probabilities for the Markov chain

2.2. Finding boundary probabilities for the Markov/semi-Markov process

Technical objects under operation are featured throughout their whole life cycles with different times of performing servicing and/or repairs. Fig. 3 shows characteristics of changes in servicing time and of coming up to the nominal time.

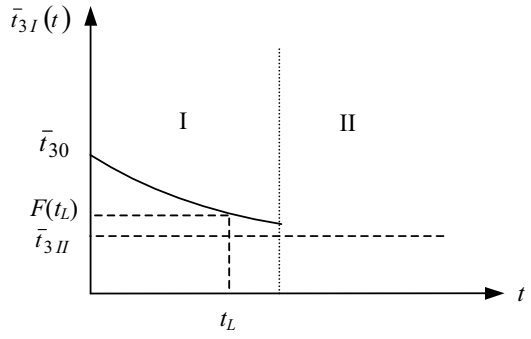

Fig. 3. Characteristics of changes in servicing time and of coming up to the nominal time

Interval I – the time of learning, featured with relatively long and gradually decreasing servicing and repair times. This is an effect of coming up to the engineering maturity in production and operational phase, including the teaching/learning of the staff expected to provide new objects introduced into service with maintenance (getting rid of errors in maintenance procedures and techniques, acquiring new habits).

Interval II – a 'plateau' period, i.e. time of proper operation/maintenance, in the course of which the failure rate keeps constant or nearly constant. It usually results from random failures and errors made by servicing personnel.

For Interval I (Fig. 3), a model of the semi-Markov process might prove a proper mathematical apparatus to describe operational phase. The semi-Markov process is a Markov process, throughout which mean times of the emergency object's staying in the state '*i*' prior to transition to the state '*j*' are random functions of time.

In phase I, mean time of transition from the state of refurbishment $\bar{t}_{3I}(t)$ to other states for $t = 0$ reaches maximum and decreases down to reach the mean time of refurbishment calculated in Phase II (Fig. 3). The time dependence can be described with the exponential function as:

$$\bar{t}_{3I}(t) = (\bar{t}_{30} - \bar{t}_{3II}) \cdot \exp^{-t/\tau} + \bar{t}_{3II}, \tag{10}$$

where:

$\bar{t}_{3I}(t)$ - time of transition from the state of refurbishment to other states within Interval I,
$\bar{t}_{30}$ - assumed maximum time of performing the refurbishment,
$\bar{t}_{3II}$ - the expected value of time of performing the refurbishment in phase II (Fig. 3).

Operational data show that the maximum time of 'learning' (t_L) how to provide new emergency objects with servicing amounts to 7 days. Since usually $t_L = t_{90\%}$, the learning constant can be found (Fig. 3):

$$\frac{F(0) - F(t_L)}{F(0) - F(\infty)} = 0{,}9 \quad \text{therefore,} \quad \frac{\bar{t}_{30} - \bar{t}_{3\,II\,(90\,\%)}}{\bar{t}_{30} - \bar{t}_{3\,II}} = 0{,}9, \tag{11}$$

$$\ell^{-\frac{t_L}{\tau}} = 0{,}1, \tag{12}$$

$$\ell^{\frac{t_L}{\tau}} = \ln 10 \cong 2{,}303, \tag{13}$$

$$\tau = \frac{t_L}{2{,}303} = \frac{7}{2{,}303} = 3{,}04 \approx 3 \text{ days.} \tag{14}$$

Hence, the form of time dependence for the learning period is as follows:

$$\bar{t}_{3I}(t) = 20 \cdot \ell^{-\frac{t}{3}} + 10, \tag{15}$$

where:

$\bar{t}_{3I}$ - random function of time of staying in the state of refurbishment at stage I,
$t = \{0,1,...,7\}$ - random variable of physical time of 'learning' measured with days.

Mean times of staying in the state of refurbishment are what is arrived at after having substituted possible values of t in eq (15) for stage I. Then, transition rates are found according to (18) and (19) and substituted in the system of equations (21); values of probabilities p_j (Tab. 2) are calculated for variable rates of transition λ_{3j} from the state of refurbishment to other states.

Tab.2. Expected values of time of staying in the state of refurbishment for stage I

t [days]	$\bar{t}_{3I}(t)$	$\lambda_{3I}(t)$	$p_{1I}(t)$	$p_{2I}(t)$	$p_{3I}(t)$
0	30	44	0,735216	0,248457	0,016327
1	24,3804	54,1427	0,737471	0,249219	0,013309
2	20,3397	64,8975	0,739102	0,24997	0,011128
3	17,3605	76,0368	0,740309	0,250178	0,009513
4	15,2764	86,4077	0,741155	0,250464	0,008381
5	13,8053	95,6161	0,741754	0,250666	0,00758
6	12,7089	103,88	0,742138	0,250797	0,00698
7	11,9477	110,4824	0,742511	0,250922	0,006567
∞	10	132	0,7427	0,25081	0,00552

at:

$$\bar{t}_{3I}(t) = \bar{t}_{31}(t) + \bar{t}_{32}(t), \tag{16}$$

where:

$\bar{t}_{3I}(t)$ - function of time of refurbishment at stage I,
$\bar{t}_{31}(t)$ - function of time of refurbishment prior to transition to the state of being on duty,
$\bar{t}_{32}(t)$ - function of time of refurbishment prior to transition to the state of operation.

Figs 4 – 6 illustrate probabilities $p_j(t)$ throughout the period of learning.

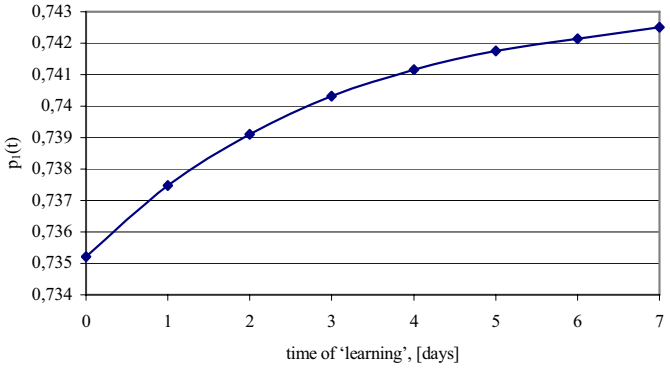

Fig. 4. Values of probabilities $p_1(t)$ for the semi-Markov process, the state of being on duty

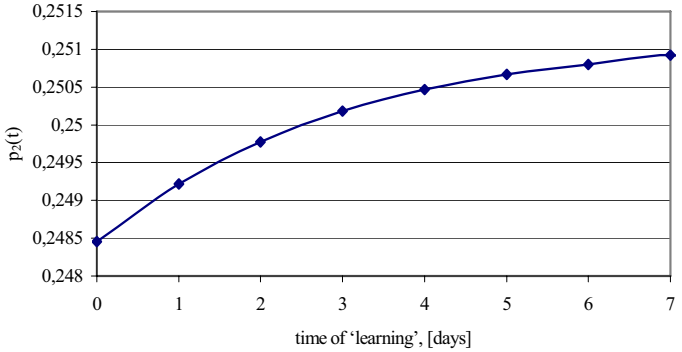

Fig. 5. Values of probabilities $p_2(t)$ for the semi-Markov process, the state of operation

Figs 4 and 5 prove that for both the state of being on duty and the state of performing the task, respectively, values of probabilities p_1 and p_2 gradually increase in the real time, whereas for the state of refurbishment decrease is observed (Fig. 6).

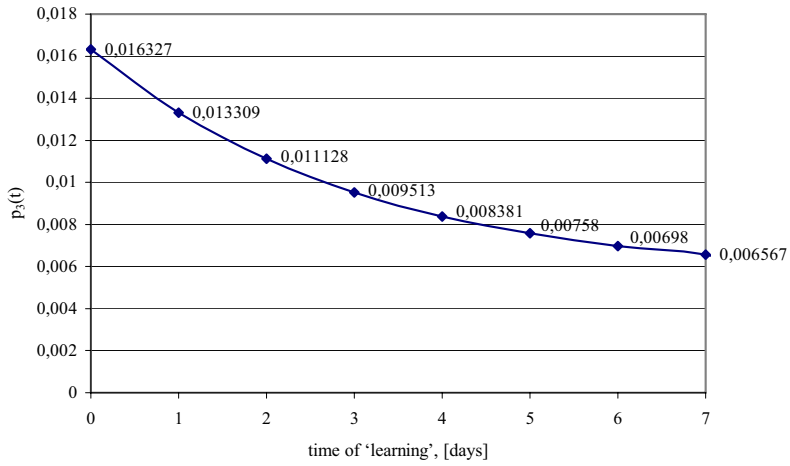

Fig. 6. Values of probabilities $p_3(t)$ for the state of refurbishment

As time passes by, i.e. time for progress in learning how to service new devices/systems, the number of errors made by the staff who operate/provide maintenance of objects recently introduced into service decreases, which means lower and lower probability that a failure occurs due to incorrect operational use and maintenance.

$$K_I = \frac{p_1(t) + p_2(t)}{\sum_{j=1}^{3} p_j(t)} = 0{,}983 \div 0{,}993 .$$

For stage II (Fig. 3) featured with constant failure rates it has been assumed that the Markov process $X(t)$ of finite phase space $\Omega = \{S_1, S_2, S_3\}$ is a model of operating/servicing technical objects.

If:
$X(t) = 1$, at time instance t the object is in the state of being on duty (waiting for a task),
$X(t) = 2$, at time instance t the object is in the state of performing a task,
$X(t) = 3$, at time instance t the object is in the state of refurbishment.

The stochastic process $X(t)$, i.e. the Markov process of some finite set of states S can be completely determined by means of the following:

- initial distribution of the process $X(t) = [1,0,0]$,
- matrix M of probabilities of changes of the states for the Markov chain,
- matrix of intensities of transitions Λ of the process.

The Λ matrix has been built on the basis of the digraph shown in Fig. 1:

$$\Lambda = \begin{bmatrix} -\lambda_{11} & \lambda_{12} & \lambda_{13} \\ \lambda_{21} & -\lambda_{22} & \lambda_{23} \\ \lambda_{31} & \lambda_{32} & -\lambda_{33} \end{bmatrix}. \tag{17}$$

Intensities λ_{ij} and λ_{ii} of the states $S_1 - S_3$ for the Markov process under consideration, calculated by test, have been given in Table 3.

Tab. 3. Matrix of intensities of transitions while operating a technical object throughout stage II

$\lambda_{ij}/\lambda_{ii}$	λ_1	λ_2	λ_3
λ_1	-34,879	32,154	132
λ_2	100,32	-98,0392	66
λ_3	132	132	-132,15

with λ_{ij} calculated according to the relationship:

$$\lambda_{ij} = \frac{1}{\bar{t}_{ij}}, \tag{18}$$

where:

$\bar{t}_{ij}$ - mean time of staying in the state *i* before transition to the state *j*.

Diagonal rates have been found as:

$$\lambda_{ii} = 1/\bar{t}_i = \frac{1}{\frac{\sum_{j \in J_{ij}} t_{ij}}{n_i}} = \frac{1}{\frac{\sum_{j \in J_{ij}} n_{ij} \cdot \bar{t}_{ij}}{n_i}} = \frac{1}{\sum_{j \in J_{ij}} \omega_{ij} \cdot \frac{1}{\lambda_{ij}}}, \tag{19}$$

where:

ω_{ij} - frequency of transitions from the state *i* to the state *j*,

λ_{ij} - rate of transitions from the state *i* to the state *j*.

According to the theory of Markov processes, for ergodic processes the matrix equations are satisfied [3]:

$$\Lambda^T \cdot [p_j] = 0, \tag{20}$$

where:

$\Lambda = [\lambda_{ij}]$ - matrix of rates for diagonal λ_{ii} and non-diagonal elements λ_{ij}.

According to eq (20) for the matrix notation with the normalisation condition, the following is arrived at:

$$\begin{bmatrix} -\lambda_{11} & \lambda_{21} & \lambda_{31} \\ \lambda_{12} & -\lambda_{22} & \lambda_{32} \\ \lambda_{13} & \lambda_{23} & -\lambda_{33} \end{bmatrix} \cdot \begin{bmatrix} p_1 \\ p_2 \\ p_3 \end{bmatrix} = \begin{bmatrix} 0 \\ 0 \\ 0 \end{bmatrix}, \tag{21}$$

$$\sum_{i=1}^{3} p_i = 1,$$

i.e.

$$\begin{cases} -\lambda_{11} \cdot p_1 + \lambda_{21} \cdot p_2 + \lambda_{31} \cdot p_3 = 0 \\ \lambda_{12} \cdot p_1 - \lambda_{22} \cdot p_2 + \lambda_{32} \cdot p_3 = 0 \\ \lambda_{13} \cdot p_1 + \lambda_{23} \cdot p_2 - \lambda_{33} \cdot p_3 = 0 \\ \sum_{i=1}^{3} p_i = 1 \end{cases} . \tag{22}$$

After having solved the above-shown system of equations the following formulae for boundary probabilities of the Markov process are arrived at:

$$p_1 = \left[\frac{\lambda_{21}(\lambda_{11} \cdot \lambda_{31} + \lambda_{32} \cdot \lambda_{11})}{\lambda_{11}(\lambda_{11} \cdot \lambda_{22} + \lambda_{12} \cdot \lambda_{21})} + \frac{\lambda_{31}}{\lambda_{11}} \right] \cdot p_3, \tag{23}$$

$$p_2 = \left[\frac{\lambda_{11} \cdot (\lambda_{31} + \lambda_{32})}{\lambda_{11} \cdot \lambda_{22} - \lambda_{12} \cdot \lambda_{21}} \right] \cdot p_3, \tag{24}$$

$$p_3 = \frac{1}{\frac{\lambda_{11} + \lambda_{31}}{\lambda_{11}} + \frac{\lambda_{21} \cdot \lambda_{11} \cdot (\lambda_{31} + \lambda_{32})}{\lambda_{11}(\lambda_{11} \cdot \lambda_{22} - \lambda_{12} \cdot \lambda_{21})} + \frac{\lambda_{11} \cdot (\lambda_{31} + \lambda_{32})}{\lambda_{11} \cdot \lambda_{22} - \lambda_{12} \cdot \lambda_{21}}} . \tag{25}$$

With values taken from Tab. 3 and substituted into eqs (23) – (25), boundary probabilities (Fig. 7) are obtained for the Markov process (stage II).

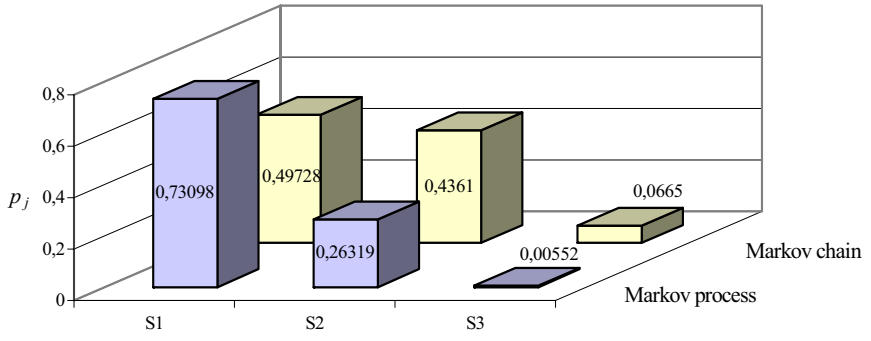

Fig.7. Boundary probabilities pj at stage II for an emergency object

The calculated rate of functional availability for stage II is:

$$K_{II} = \frac{p_1(t) + p_2(t)}{\sum_{j=1}^{3} p_j(t)} = 0{,}993.$$

3. Conclusion

The paper has been intended to introduce a method of determining functional availability of technical objects introduced into service, in particular, within rescue systems. The required characteristics of such objects are availability and readiness to perform tasks that arise at random time instances during the duty. Hence, the objects usually perform tasks, or keep waiting in the fit-for-use state.

A three-state Markov/semi-Markov model has been used for analysis; the object's lifetime has been divided into three stages. The first one: for objects of a new type recently introduced into service, the rate of failures due to servicing errors gradually decreases. The second one is the time of constant failure rate and constant functional availability. For the first stage (Fig. 3) the semi-Markov process has been assumed., for which mean times of refurbishment have been described with the exponential function. The second stage has been described with the Markov process. The effect is that, on the basis of data, rates of functional availability have been calculated, according to the following relationship:

$$K = \frac{p_1(t) + p_2(t)}{\sum_{j=1}^{3} p_j(t)}.$$

The rates for particular stages are as follows:

1) stage I, for which some increase in the rate of availability $K_I = 0.983 \div 0.993$ is observed; this results from the improvement in quality of performing services,
2) stage II of constant availability $K_{II} = 0.993$, in the course of which constant errors are made

References

[1] Brzeziński J., *Zintegrowany system bezpieczeństwa człowieka* (*An integrated system of human's safety*), Bobrowisk XXI wieku-piramida równoboczna, http://www.zabezpieczenia.com.pl

[2] Bobrowski D., *Modele i metody matematyczne teorii niezawodności* (*Mathematical models and methods of the theory of reliability*), WNT, Warszawa 1985.

[3] Fisz M., *Rachunek prawdopodobieństwa i statystyka matematyczna* (*Probability calculus and mathematical statistics*), PWN, Warszawa 1967.

[4] Kubik L. T., Krupowicz A., *Wprowadzenie do rachunku prawdopodobieństwa i jego zastosowań* (*Probability calculus and applications thereof – introductory remarks*), PWN, Warszawa 1982.

[5] Ziółkowski J., *Analiza systemu logistycznego bazy lotniczej w aspekcie gotowości* (*Analysis of the air-base system of logistics from the standpoint of availability*), Rozprawa doktorska, ITWL, Warszawa 2004.